A PETROGRAPHICAL AND MINERALOGICAL INVESTIGATION OF THE ROCKS OF THE BUSHVELD IGNEOUS COMPLEX IN THE TAUTESHOOGTE-ROOSSENEKAL AREA OF THE EASTERN TRANSVAAL

by

GERHARD VON GRUENEWALDT

Submitted in partial fulfilment of the requirements
for the degree of
DOCTOR OF SCIENCE
in the Faculty of Science,
University of Pretoria.

October, 1971.

ABSTRACT

This study comprises a petrographical and mineralogical investigation of rocks from an area 850 sq. km in size, situated about 80km northeast of Middelburg. Roughly half of the area is occupied by rocks of the epicrustal phase of the Bushveld Complex, and consists largely of Rooiberg Felsite and granophyre as well as leptite, microgranite and granodiorite. Numerous veins of fine-grained granite traverse the leptite which is considered to be highly metamorphosed felsite. These veins of fine-grained granite probably owe their origin to the melting of the leptite. The coalescence of these products of melting gave rise to the thick sheet of granophyre between the leptite and the felsite.

Rocks of the Layered Sequence occupy the eastern half of the area and consist of the Main and Upper Zones which were subdivided into various subzones on the basis of characteristic rock types and marker horizons. Mineralogical investigations are restricted to the minerals from rocks of the Layered Sequence, namely orthopyroxene, plagioclase, apatite and the sulphides of the Upper Zone.

In Subzone A of the Main Zone, the orthopyroxene is present as cumulus crystals, but it changes in texture to ophitic in the lower half of Subzone B where small discrete grains of inverted pigeonite are also developed. Inverted pigeonite is present in the upper half of Subzone B and in rocks of the Upper Zone, whereas the orthopyroxene-pigeonite relationships in Subzone C of the Main Zone are a repetition of those observed in the underlying rocks. The phase-change from orthopyroxene to pigeonite takes place over a transition zone in which both phases crystallized from the magma. It is envisaged that the first pigeonite to have crystallized from the magma at high temperatures had a lower Fe/Mg ratio than the hypersthene precipitating at slightly lower temperatures, with the result that the early formed pigeonite was unstable and reacted with the magma to form hypersthene. This caused the formation of groups of grains of hypersthene which are optically continuous over large areas and which may contain a few blebs of augite exsolved from the original pigeonite. A few pigeonite grains were effectively trapped in other minerals, mostly augite, and consequently escaped reaction with the liquid. These inverted to hypersthene at the appropriate temperature and contain numerous exsolution-lamellae of augite. As fractional crystallization of the magma continued, it moved further into the stability

field of pigeonite and out of the stability field of hypersthene with the result that the formation of hypersthene by the reaction of pigeonite with magma was replaced by inversion of pigeonite to hypersthene. This inverted pigeonite is also present as groups of grains optically continuous and contains pre-inversion exsolution-lamellae of augite orientated at random, and post-inversion exsolution-lamellae which are orientated parallel to the (100) plane of the orthopyroxene throughout a unit. The inverted pigeonite is orientated in such a way that its crystallographic c-axis lies close to or in the plane of layering. This is explained as being due to the load pressure of the superincumbent crystal mass during the inversion.

Textural features of the plagioclase revealed interesting information on the postcumulus changes in the rock. Reversed zoning, interpenetration and bending of plagioclase crystals as well as the presence of myrmekite are described. These are considered to be due to increased load pressure prior to and during crystallization of the intercumulus liquid. It is considered that the various types of pegmatoids may have originated by an increase in pressure on the intercumulus liquid which was concentrated to form pipe-like bodies by lateral secretion or filter pressing.

Cumulus apatite is developed in the olivine diorites of Subzone D of the Upper Zone. From unit cell dimensions it seems as if it changes in composition from a fluor-rich hydroxyapatite at the base of this subzone to a relatively pure hydroxyapatite 70m below the roof. There seems to be a substantial increase in the fluor content of the apatite in the topmost 70m of the intrusion.

Rocks of the Upper Zone contain considerably more sulphides than those of the Main Zone. This is ascribed to an increase in the sulphur content of the magma owing to fractional crystallization. The magma reached the saturation point of sulphur when rocks of Subzone D of the Upper Zone started to crystallize with the result that these rocks contain numerous small droplets of sulphide which constitute on an average about 0,5 per cent by volume of the rocks. A concentration of the sulphides in these rocks would not yield a deposit of economic interest because of the unfavourable composition of the sulphide phase, which consits of more than 90 per cent pyrrhotite. Sulphides in the rocks below this subzone are intercumulus and a concentration could be of economic importance because the sulphide phase contains appreciable amounts of chalcopyrite and pentlandite. Although no economic concentration of sulphides are known from the

Upper Zone, this study has revealed the presence of a mineralized anorthosite below Lower Magnetitite Seam 2 which contains in places up to 1 per cent Cu, 0,18 per cent Ni and 1,6g/ton platinum metals.

Continuous, slow convection and bottom crystallization probably gave rise to the homogeneous rocks of the Main Zone. Injection of a considerable amount of fresh magma took place at the level of the Pyroxenite Marker which resulted in a compositional break and gave rise to a repetition in Subzone C of the rocks of the Main Zone below this marker. The oxygen pressure during crystallization of the magma was probably low, causing a gradual enrichment in iron in the magma and gave rise to the appearance of magnetite at the base of the Upper Zone. Intermittent increase in the oxygen fugacity is considered to be important in the formation of magnetitite seams.

As a result of fractional crystallization the volatile content of the remaining magma gradually increased. This is seen firstly, by the appearance of biotite secondly by the appearance of cumulus apatite and droplets of sulphide and lastly by hornblende in the rocks of the Upper Zone. Some water-rich residual liquids apparently also intruded the overlying leptite, causing additional melting of the latter and the formation of irregularly shaped veins and pockets of granodiorite.

A lateral change in facies of the rocks of the Layered Sequence in a souther ly direction is described. This is considered to be due to crystallization of the magma at slightly lower temperatures because of the more effective heat loss where the magma chamber was thinner.

Two parameters of differentiation for layered intrusions are proposed, viz. a modified version of the differentiation index and a modified version of the crystallization index. The former seems more applicable for intrusions such as the Bushveld Complex, whereas the latter seems to be more applicable for intrusions in which there is a considerable development of ultramafic rocks. These two parameters can also be used to indicate the differentiation trend if they are plotted against height in the intrusion.

SAMEVATTING

Die studie behels 'n petrografiese en mineralogiese ondersoek van gesteentes afkomstig van 'n gebied 800 vk. km in grootte wat ongeveer 80km noordoos van Middelburg geleë is. Die epikrustale fase van die Bosveldkompleks word in die westelike helfte van die gebied aangetref en bestaan grootendeels uit Rooibergfelsiet en granofier, asook leptiet, mikrograniet en granodioriet. Talle are van fynkorrelrige graniet sny oor die leptiet wat as 'n hoogs gemetamorfoseerde felsiet beskou word. Hierdie are van fynkorrelrige graniet het waarskynlik ontstaan weens die opsmelting van leptiet. Samevloeiing van die opsmeltingsprodukte het vermoedelik oorsprong gegee aan die dik plaat van granofier wat tussen die leptiet en die felsiet aangetref word.

Die oostelike helfte van die gebied word beslaan deur die Hoof- en Bosone van die gelaagde opeenvolging wat onderverdeel is in verskeie subsones op grond van kenmerkende gesteentetipes en merkerlae. Mineralogiese ondersoeke is beperk tot minerale van gesteentes van die gelaagde opeenvolging, naamlik ortopirokseen, plagioklaas, apatiet en sulfiede van die Bosone.

Ortopirokseen is in gesteentes van Subsone A van die Hoofsone teenwoordig as kumulus kristalle, terwyl dit in die onderste helfte van Subsone B groot ofitiese kristalle vorm. In laasgenoemde gesteentes word ook klein korrels van ortopirokseen aangetref wat deur inversie van pigeoniet ontstaan het (inversie-pigeoniet). Inversie-pigeoniet is die Ca-arm pirokseen in die boonste helfte van Subsone B van die Hoofsone en in gesteentes van die Bosone, terwyl die ortopirokseen-pigeoniet verhouding in Subsone C van die Hoofsone 'n herhaling is van die wat in die onderliggende Subsones A en B waargeneem is. Die faseverandering van ortopirokseen na pigeoniet vind plaas in 'n oorgangssone waarin altwee minerale gelyktydig aangetref word. Dit word veronderstel dat die eerste pigeoniet wat uit die magma gekristalliseer het, 'n laer Fe/Mg verhouding gehad het as hipersteen wat by 'n effens laer temperatuur gekristalliseer het met die gevolg dat die vroeë pigeoniet onstabiel was en met die magma gereageer het om hipersteen te vorm. Dit het die vorming van groepe van hipersteenkorrels tot gevolg gehad wat in dunseksie opties kontinu is oor groot gebiede (ofities) en wat 'n paar spikkels ougiet mag bevat wat uit die oorspronklike pigeoniet ontmeng het. 'n Paar van die pigeonietkorrels is vasgevang deur ander minerale, meesal ougiet, en het gevolglik reaksie met die vloeistof vrygespring. Hulle is omgesit

in hipersteen by 'n laer temperatuur en bevat talryke ontmengingslamelle van ougiet. Met verdere fraksionasie het die magma uit die stabiliteitsveld van hipersteen en in die stabiliteitsveld van pigeoniet beweeg, met die gevolg dat reaksie van pigeoniet met die magma vervang is deur inversie van pigeoniet om hipersteen te vorm. Korrels van hierdie inversie-pigeoniet is ook teenwoordig as groepe wat opties kontinu is en bevat voor-inversie ontmengingslamelle van ougiet wat 'n willekeurige oriëntasie besit en na-inversie ontmengingslamelle wat parallel aan die (100) vlak van die ortopirokseen georienteer is. Hierdie hipersteen wat van pigeoniet ontstaan het, is so georiënteer dat sy kristallografiese c-as na aan of in die vlak van die gelaagdheid lê. Dit word toegeskryf aan belastingsdruk tydens die inversie vanweë die oorliggende massa kristalle.

Dit is gevind dat veral teksture wat deur plagioklaaskristalle geopenbaar word belangrik is by afleidings aangaande die na-kumulus veranderinge in die gesteentes. Omgekeerde sonebou, deurdringingsverskynsels en gebuigde plagioklaaskristalle asook die teenwoordigheid van mirmekiet word toegeskryf aan 'n toename in die belastingsdruk voor en tydens kristallisasie van die interkumulus vloeistof. Die verskillende tipes pegmatoïede mag hulle oorsprong ook te danke hê aan 'n toename in druk op die interkumulus vloeistof wat deur laterale afskeiding en uitpersing gekonsentreer is om pypvormige liggame te vorm.

Kumulus apatiet word aangetref in die oliviendioriete van Subsone D van die Bosone. Van eenheidseldimensies is afgelei dat die samestelling verander van 'n fluoorryke hidroksielapatiet aan die basis van die subsone na 'n relatief suiwer hidroksielapatiet 70m vanaf die top van die intrusie. In die boonste 70m is daar blykbaar weer 'n aansienlike toename in die fluoorinhoud van die apatiet.

Die gesteentes van die Bosone bevat aansienlik meer sulfiede as die van die Hoofsone, wat toegeskryf kan word aan 'n toename in die swaelinhoud van die magma weens fraksionele kristallisasie. Die magma was tydens kristallisasie van die gesteentes van Subsone D van die Bosone versadig aan swael met die gevolg dat talle klein druppels van sulfiede wat ongeveer 0,5 volume-persent van die gesteentes uitmaak, hierin aangetref word. 'n Konsentrasie van die sulfiede in die gesteentes sal nie 'n ekonomies belangrike afsetting vorm nie vanweë die ongunstige samestelling van die sulfiedfase, wat uit meer as 90 persent pirrotiet bestaan. Sulfiede in gesteentes onder hierdie subsone is interkumulus maar omdat hulle heelwat meer chalkopiriet en pentlandiet bevat, sou konsentrasies daarvan van ekonomiese waarde wees. Alhoewel tot nog toe geen ekonomiese konsen-

trasie van sulfiede in die Bosone gevind is nie, word 'n gemineraliseerde anortosiet onder die Onderste Magnetitietband No. 2 beskryf wat op plekke tot 1 persent Cu, 0,18 persent Ni en 1,6g/ton Pt-groep metale bevat.

Onafgebroke, stadige konveksie en kristallisasie naby die vloer het vermoedelik oorsprong gegee aan die homogene gesteentes van die Hoofsone. Inplasing van 'n aansienlike hoeveelheid vars, ongedifferensiëerde magma het plaasgevind na kristallisasie van gesteentes van Subsone B van die Hoofsone wat 'n onderbreking in die differensiasieverloop tot gevolg gehad het, en gelei het tot 'n herhaling in Subsone C van die gesteentes onderkant die Piroksenietmerker. Die suurstofdruk tydens die kristallisasie van die magma was waarskynlik redelik laag en het 'n geleidelike verryking van yster in die magma tot gevolg gehad wat oorsprong gegee het aan die verskyning van magnetiet aan die basis van die Bosone. Magnetitietbande het vermoedelik ontstaan weens 'n verhoging in die suurstoffugasiteit wat met tussenposes plaasgevind het.

'n Toename in die vlugtige bestanddele in die magma weens fraksionele kristallisasie kan gesien word aan die verskyning van, eerstens, biotiet, tweedens, apatiet en druppels van sulfiede, en derdens, horingblende in die gesteentes. Van die laaste waterryke vloeistowwe het vermoedelik ook die dakgesteentes geïntrudeer en addisionele opsmelting van die leptiet veroorsaak wat gelei het to die vorming van onreëlmatige are en liggame granodioriet.

'n Laterale fasiesverandering van die gesteentes van die gelaagde opeenvolging in 'n suidwaartse rigting word beskryf. Dit word toegeskryf aan kristallisasie van die magma by effens laer temperature weens die meer effektiewe hitteverlies waar die magmakamer dunner was.

Twee parameters van differensiasie vir gelaagde intrusies word voorgestel, naamlik, 'n gemodifiseerde differensiasie-indeks en 'n gemodifiseerde kristallisasie-indeks. Eersgenoemde blyk meer doeltreffend te wees vir intrusies soos die Bosveldkompleks terwyl laasgenoemde meer doeltreffend blyk te wees vir intrusies waarin meer ultramafiese gesteentes ontwikkel is. Hierdie twee parameters kan o.a. ook gebruik word om die differensiasieverloop aan te dui as hulle teen hoogte in die intrusie geteken word.

CONTENTS

LIST OF TABLES AND FIGURES IN THE TEXT

I. INTRODUCTION AND ACKNOWLEDGEMENTS

Over the past few decades, post-graduate students and staff of the Department of Geology of the University of Pretoria have been actively engaged in the study of rocks of the Bushveld Complex. In the course of these investigations practically all the aspects of this complex have been covered, such as structure, metamorphism, the Layered Sequence, acid rocks, and minerals of economic importance. These investigations left an area of approximately 850 sq. km in the vicinity of Tauteshoogte and Roossenekal (Fig. 1) where little or no work has been done during the past 20 to 30 years. It was consequently decided to investigate this area as part of a scheme of the Geological Survey whereby Geology Departments at Universities are invited to participate in its mapping programme with the aim of expediting publication of geological sheet maps of the Republic on a scale of 1:125 000.

Mapping of the area was done on aerial photographs (scale 1:36 000) during the winter months of 1968 and the information obtained was transferred on to 1:50 000 topocadastral maps from which the final geological map was compiled (Folder I).

Petrographical and mineralogical investigations of the collected specimens were undertaken at the Geology Department of the University of Pretoria from 1968 to 1971. The laboratory studies were mostly confined to rocks of the Layered Sequence and special attention was given to orthopyroxene, plagioclase, apatite and the sulphides in the Upper Zone. Detailed accounts of the mineragraphy of the magnetite are given by Molyneux (1964, p. 41-56; 1970a, p. 51-114; 1970b, p. 231-240), Groeneveld (1968, p. 125-154) and Willemse (1969b) which obviated the necessity of an investigation of this mineral. Some attention was given to the textures of the rocks of the Layered Sequence which yielded interesting information on the postcumulus changes. In addition, two parameters, plotted against height in the intrusion, are proposed by which the trend of differentiation in layered intrusions can be illustrated graphically.

The terminology to describe magmatic sediments has evolved from the work of Wager and Deer (1939, p. 271) on the Skaergaard Intrusion and Hess's (1960) as well as Jackson's (1961) work on the Stillwater Complex. Reviews and definitions of terms are given by Wager et al. (1960) and modified by Jackson (1967, p. 22). In the present study it was deemed advisable to retain the term

FIG. 1: PLAN SHOWING ADJACENT AREAS MAPPED BY VARIOUS AUTHORS, AND LOCALITY MAP (INSET)

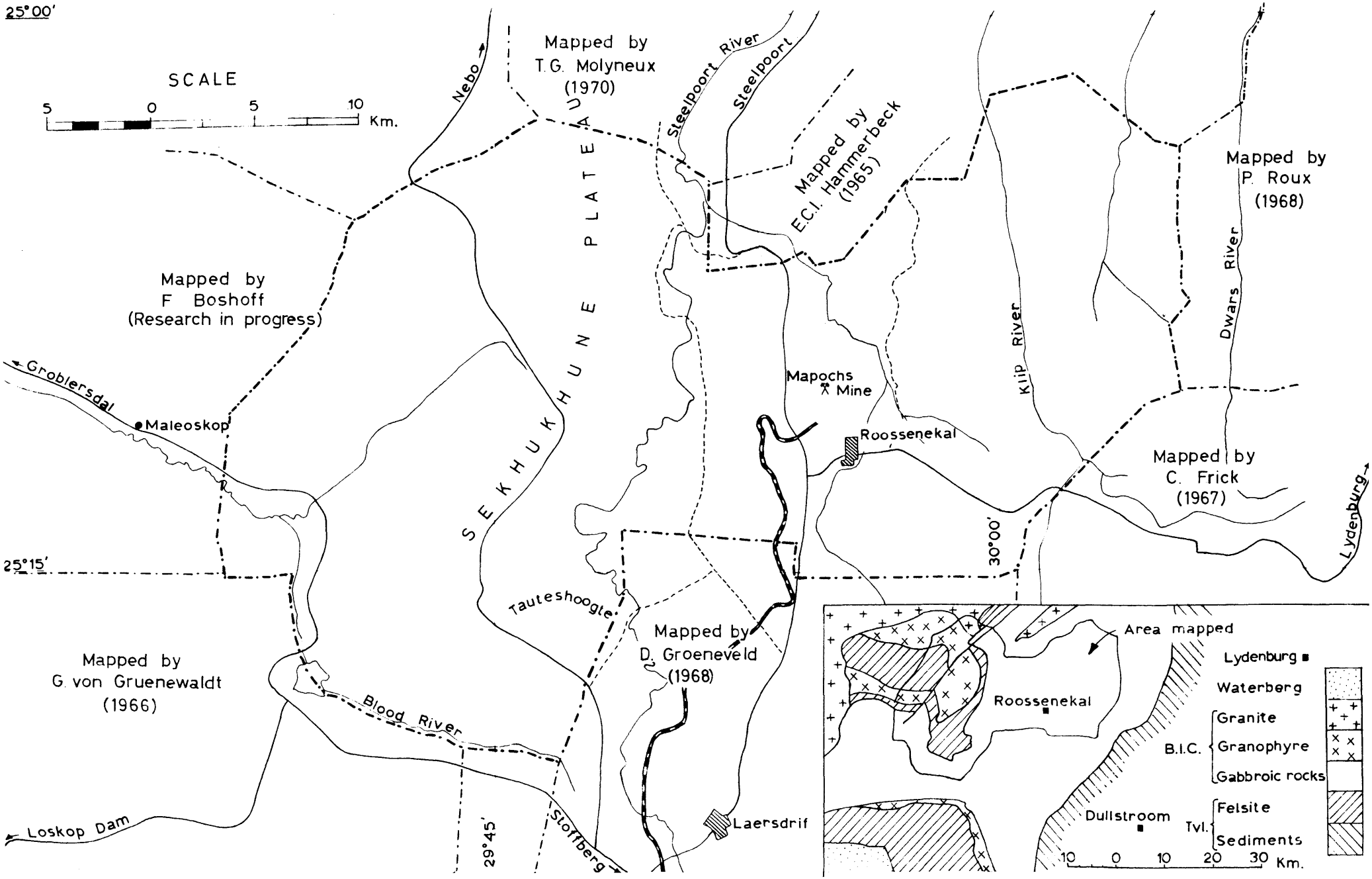

"adcumulus growth" because it was originally coined by Wager et al. (1960, p. 77) for the extension of the cumulus crystals by material of the same composition. Jackson's term "postcumulus growth" (Jackson, 1967, p. 23) is not restricted to material of the same composition and zoned crystals may be the result. As most of the plagioclase of the Layered Sequence shows only slight zoning, and where present, only at the outermost rims of the crystals, the term "adcumulus growth" is considered to be more appropriate. Other terms used in this treatise are "intercumulus material" which are the minerals formed by the filling of the spaces after adcumulus enlargement, and "intercumulus liquid", i. e. the liquid that occupied the interstices between the cumulus crystals before and after adcumulus enlargement.

Previous work in this area was done by Boshoff (1942) who investigated the relationships between the various rocks east and north of Tauteshoogte and by A. F. Lombaard (1949) who undertook a similar study of a large area west of Tauteshoogte. The purpose in remapping these areas was largely to determine whether the relationships between the various rock types conform to the latest conceptions regarding the origin of these rocks. B. V. Lombaard (1934) analysed various specimens collected by him along a traverse east and west of Roossenekal, with the purpose of determining the trend of differentiation of the Layered Sequence.

During the course of the investigation, numerous persons and organisations rendered valuable assistance, without which this study would not have been possible.

Financial assistance in the form of honoraria to cover expenses of mapping was rendered by the Geological Survey of the Department of Mines and by the Anglo American Corporation of South Africa Limited. A large number of the laboratory investigations were done during 1970 while the author was the recipient of a bursary from the National Institute for Metallurgy.

Rand Mines Limited made available the core of a 1340m deep bore-hole of the lower part of the Main Zone and Anglo American Corporation of South Africa Limited gave access to the core of two shallow bore-holes on the farm Doornpoort 171 JS.

The Director of the Geological Survey accepted samples of rocks and minerals for chemical analyses by the National Institute for Metallurgy.

Drs D. R. Bowes and T. G. Molyneux made available chemical analyses

and CIPW norms of rocks from the Main and Upper Zones prior to publication.

Accommodation while field work was being undertaken was provided by Messrs. J. G. van den Heever and J. J. du Toit, as well as by the Management of the Mapochs Mine of Highveld Steel and Vanadium Corporation Limited.

Miss P. S. Martin did the final draughts for most of the diagrams in the text.

The Transvaal Board for the Development of Peri-Urban Areas granted permission to use information contained in a report on the mineral potential of the Roossenekal townlands, which was compiled for the board by the late Prof. J. Willemse.

Last, but by no means least, thanks are due to my promoters, Dr C. P. Snyman and Dr E. B. Förtsch for their many helpful suggestions and discussions and to my wife for her patience and encouragement as well as for the typing of the manuscript.

II. GENERAL DESCRIPTION OF THE AREA

1. Field-relationships (Folder I)

Apart from dykes and a few small sedimentary inclusions, the whole area is occupied by rocks of the Bushveld Igneous Complex. Good exposures of the Main and Upper Zones made a study of most of the constituting rock types possible. The roof-rocks outcrop on the slopes and on top of the prominent Sekhukhune Plateau which is incised along its edges by tributaries of the Steelpoort and Blood Rivers and thus lends itself perfectly to the investigation of the complex roof-relationships.

The roof-rocks extend from the higher slopes of the escarpment surrounding the Sekhukhune Plateau, and occupy the whole of the tableland in the western part of the area. At the base, they consist of highly metamorphosed felsite, generally referred to as leptite, which is about 350m thick but remarkably consistent along the strike at the edge of the plateau from Tauteshoogte in the south to Signal Hill in the north (Molyneux, 1970, Plate I). They are traversed by numerous veins of fine-grained granite and granodiorite, which, as will be seen, are considered to have originated by the melting of the leptite. The leptite is separated from less altered felsite by a thick sheet of granophyre, very homogeneous in appearance over the larger part of the area with microgranophyre and a granitic variety only locally developed at Paardekop and on Groothoek 139 JS. A conspicuous, thin layer of granodiorite or melanogranophyre is associated with the granophyre and could be followed at its base over the whole area. The overlying Rooiberg Felsite consists of a relatively homogeneous succession of black and red, mostly porphyritic felsite, more than 2500m thick of which only a small portion consists of agglomerate and amygdaloidal or flow-banded varieties.

The remaining area, i. e., south and east of the Sekhukhune Plateau, consists of rocks of the Layered Sequence which is subdivided according to the scheme proposed by Molyneux (1970, Plate II). Rocks of the Main Zone are present in the area east of longitude 29° 56' E on which the village of Roossenekal is situated, whereas the Upper Zone extends up to the Sekhukhune Plateau but is also encountered in the low-lying country of the Blood River valley except on the southern portion of the farm Buffelsvallei 170 JS where there are some outcrops of the Main Zone. Subzone A of the Main Zone consists of a

variety of anorthositic and gabbroic rocks of which only the top 600m are developed along the eastern and north-eastern boundary of the area. Subzone B is separated from the underlying rocks by the Upper Mottled Anorthosite (Folder I) and, apart from a fine-grained norite at the top, consists of a thick succession of homogeneous gabbroic rocks. These are overlain by the Pyroxenite Marker at the base of Subzone C, but with the exception of some spotted gabbroic rocks and mottled anorthosites in the lower half of this subzone, the rocks are very similar in appearance to those of Subzone B.

The base of the Upper Zone is a mottled anorthosite which is characterized by the presence of intercumulus magnetite. It is overlain by a differentiated succession of magnetite gabbro, mottled anorthosite and magnetitite seams of Subzones A, B and C of this Zone. Olivine makes its appearance at the base of Subzone C about 1 km west of the main road from Middelburg to Burgersfort. Subzone D, at the top of the Upper Zone consists mainly of olivine-bearing diorites, but olivine tends to be absent in the rocks associated with magnetitite seams. Hornblende, K-feldspar and quartz become more abundant only in the topmost differentiates of the intrusion and are considered, as published previously (Von Gruenewaldt, 1968, p. 169) to be partially due to assimilation of some of the roof-rocks by the Bushveld magma.

Over the greater part of the area, the layering of the mafic rocks is remarkably persistent and most of the horizons can be correlated accurately with those described by Molyneux (1964 and 1970) from the Leolo Mountains and Magnet Heights to the north. In the valley of the Blood River to the south, a remarkable change in this generally persistent layering takes place. This is especially noticeable in rocks of Subzone D of the Upper Zone and although the constituting rock types remain the same, the number of magnetitite seams differs considerably.

Inclusions of sedimentary material in the Layered Sequence are relatively scarce. Two very small occurrences of cordierite hornfels (G414 and G258)*, the presence in which of orthopyroxene places them in the pyroxene hornfels facies, were encountered in the Upper Zone north of the Mapochs Mine and on Duikerskrans 173 JS, respectively. Larger occurrences of original calcareous sediments are present on Luipershoek 149 JS and Mapochsgronde 500 JS.

---

* Numbers in brackets refer to specimens collected in the field, and are indicated on Folder I.

Mineral assemblages developed in these correspond to those described by Willemse and Bensch (1964, p. 33 and 71) from the Upper Zone in the vicinity of Magnet Heights. These occurrences are presently being investigated in detail by Mr J. Joubert (research in progress).

A number of small quartzite xenoliths are present in the diorite of the Upper Zone close to or on the contact with the roof-rocks (Folder I). The largest one of these is on Duikerskrans 173 JS where rheomorphic breccia which consists of fragments of quartzite in a quartzitic matrix, is also developed. All these xenoliths are pure quartzite and there is no evidence that any granitization has taken place. They probably represent disrupted fragments from the floor which drifted to the top of the intrusion.

The Bushveld Granite has intruded the leptite and the granophyre in the extreme northern part of the area. Smaller intrusions of granite porphyry and some aplitic and pegmatitic veins are considered to be related to the Steelpoort Park Granite.

Post-Bushveld intrusive rocks consist of a few fine-grained porphyritic dykes and sills, probably related to the Spitskop Alkaline Intrusion, and of numerous dolerite dykes of Karroo age. These rocks were not investigated in this study.

2. Topography and drainage

Broadly, the area can be subdivided into three distinct topographic regions, namely, the Sekhukhune Plateau in the west, the valleys of the Steelpoort and Blood Rivers, and a rugged mountainous terrain east of Roossenekal.

The Sekhukhune Plateau has an average elevation of more than 1600m above sea-level. It forms a gently undulating tableland which is deeply incised along its edges by tributaries of the Blood and the Steelpoort Rivers. In a northerly direction the elevation gradually increases and reaches its maximum of 1900m at the prominent Paardekop, the highest point for many kilometres.

The edge of the plateau is well defined and the transition to the low-lying surrounding country is in the form of steep slopes along which the contact of the hard, resistant, acid rocks and the underlying gabbroic rocks of the Upper Zone is situated. This sudden drop in elevation is about 330m in the south, but increases northwards along the eastern edge to about 600m where prominent cliffs of leptite enhance the beauty of the landscape.

Short, but deeply incised rivers drain the plateau region. The rivers often

follow zones of weakness, as for instance along the Steelpoort Fault and where dolerite dykes intruded the acid rocks.

Rocks of the Upper Zone occupy the low-lying country which surrounds the plateau. The elevation is about 1300m in the south and drops to 1100m above sea-level in the north. These low-lying areas are drained by the Steelpoort and Blood Rivers, east and south of the plateau respectively. The Blood River, a small and insignificant rivulet, can hardly be held responsible for the wide valley in which it flows, whereas the much more significant Steelpoort River is characterized by deeply incised meanders. Willemse and Frick (1970, p. 161-171) who investigated the drainage pattern of the Steelpoort River concluded (p. 162) that the headwaters of the Blood River were captured by a tributary of the Swartspruit (south of the area mapped), which is considered by them to represent the southern continuation of the Sekwati River (north of the area mapped). These headwaters of the Sekwati River, characterized by a mature stage of development, were captured by the Steelpoort River owing to headward erosion along the Steelpoort Fault (p. 169). This caused rejuvenation of the captured upper course of the Sekwati River and would thus explain the deeply incised meanders of the Steelpoort River (ex Sekwati) in this area.

East of Roossenekal, the relatively homogeneous rocks of the Main Zone offer more resistance to weathering than the differentiated rock types of the Upper Zone, and consequently the elevation of the country rises to above 1800m. This high mountainous region, the southern continuation of the Leolo Mountains, is drained by the Klip and the Dwars Rivers, which have cut deep valleys into the gabbroic rocks. The presence of high-lying marshes (1750m above sea-level) on Draaikraal surrounded by mountain peaks of up to 2300m, is ascribed by Willemse and Frick (1970, p. 166) to a complex history of the drainage system. They are of the opinion that the headwaters of the Klip River were captured by the Klein Dwars River and that the recapturing by the Klip River of its head-waters caused the elbow in this river on Draaikraal 48 JT and the windgap on the border of this farm and Uysedoorns 47 JT.

III. THE ROOF-ROCKS

The roof-rocks are restricted to the western half of the area and form the high-lying region generally referred to as the Sekhukhune Plateau. A great variety of acid volcanic and intrusive rocks is developed here, previously described in some detail by Boshoff (1942) and A. F. Lombaard (1949). The aim in remapping these rocks was to establish whether the relationships between the various roof-rocks at the southern extremity of the Sekhukhune Plateau could be correlated with the proposed origin of similar rocks from west of Bothasberg (Von Gruenewaldt, 1968). Consequently, the description of these rocks in the following pages is based mostly on the observed relationships in the field, as microscopic re-investigation would probably only confirm the work of Boshoff (1942) and Lombaard (1949).

1. The Rooiberg Felsite

a) Field-relationships

Rocks which are considered as belonging to this volcanic sequence, occupy a large basin in the western half of the area. They are intruded discordantly by a thick sill of granophyre which separates the highly metamorphosed rocks at the base from relatively little altered types at the top. Owing to the Steelpoort Fault, only the lower, metamorphosed rocks of this sequence are developed to the east, whereas the bulk of these acid volcanics which lie above the granophyre outcrop to the west of the fault. From dip measurements of the banding and from intercalated sediments, the thickness of the volcanic rocks was calculated as being close to 3000m of which more than 2500m are preserved above the granophyre.

Recently, the author (1968, p. 159) has subdivided the Rooiberg Felsite west of Bothasberg into three zones on the basis of different rock types developed in the sequence. The Lower Felsite Zone, (ibid., p.154-159) which consists of black felsitic rocks recrystallized to micrographic felsite and leptite, is separated from the Upper Felsite Zone of mostly red porphyritic rock types, by a thick middle zone of predominantly amygdaloidal felsite. This threefold division can also be applied to this area, although there are pronounced differences, especially between the upper two zones of these two areas.

i) The Lower Felsite Zone

The rocks of this zone have a sharp, undulating contact with the rocks of

the Layered Sequence (Fig. 2) and are highly altered to a variety of recrystallized and partially remelted rock types collectively referred to as leptite. As a result, it is practically impossible to determine the original nature of these rocks, but because of the relatively homogeneous appearance of this leptite, and the presence of plagioclase phenocrysts, they were probably uniform, dark, glassy porphyritic felsites. Seeing that felsites of the higher zones are also involved in this high-grade metamorphism, the leptites are described collectively under a separate heading below.

In the extreme west of the area, on the farm Bankfontein 158 JS some of the rocks of this zone are present above the granophyre and are less altered than their counterparts from lower horizons. They consist, for the greater part, of alternating brown and black, very fine-grained, slightly recrystallized, porphyritic and non-porphyritic felsite.

Amygdaloidal felsite is extremely scarce in this zone and was observed between Doornpoort 171 JS and Drievoet 182 JS, on Kafferskraal 181 JS and on Buffelsvallei 170 JS. Recrystallized rocks which still display flow-banding and also some agglomeratic textures are found in association with the first-mentioned occurrence of amygdaloidal felsite.

On the north-eastern side of the hill on which the trigonometrical beacon 121 south of Tauteshoogte is situated, fine-grained dark grey to black amygdaloidal lavas are developed. A thin section (G17) of these rocks revealed the presence of large amounts of small plagioclase crystals (An_{41}) as well as a few grains of garnet. These rocks may represent uplifted Dullstroom Volcanics, the garnets probably having originated from material in the amygdales.

ii) The Middle Felsite Zone

This zone, some 1700m thick west of Bothasberg (ibid., p. 159), has its counterpart in this area in one thin layer of amygdaloidal felsite about 150m thick. It occurs above the granophyre on the farm Bankfontein 158 JS where it consists of a black amygdaloidal felsite, and also below this granophyre on the eastern side of the Steelpoort Fault. Here it could be followed from Zaaiplaats 157 JS in the north to Uitkyk 172 JS in the south, where it seems to peter out, although the amygdaloidal rocks on Duikerskrans 173 JS and The Wedge 175 JS may also belong to this zone.

iii) The Upper Felsite Zone

Rocks of this zone form the bulk of the Rooiberg Felsite in this area. They

Fig. 2. Sharp, undulating contact between diorite of the Upper Zone (light) and leptite (jointed, dark). Quarry north of the main road on Buffelsvallei 170 JS

consist mostly of homogeneous porphyritic and non-porphyritic black or red felsite. Black varieties are especially common in this zone and were not found by the author west of Bothasberg. Near the middle of the succession is a thin layer of quartzite which could be followed for 4,5km along strike. On Paardenfontein 159 JS, strange asterisk-shaped patterns are developed on the weathered surface of these rocks (Fig. 3), but were not investigated. Some agglomerate is developed below and above the quartzite on the western portion of this farm. The top of the zone shows some variation in this respect that flow-banding is well developed along the western boundary of Holnek 153 JS (Fig. 4) and that the highest exposed horizons consist of a prominent black agglomerate (Fig. 5) underlain locally by a red tuff which contains a few volcanic bombs. Apart from fragments of felsitic material, the agglomerate also contains fragments of quartzite (Fig. 6).

The noticeable differences between successions of Rooiberg Felsite from the Sekhukhune Plateau and Bothasberg do not make regional correlations of certain horizons feasible at this stage, as was done recently by the author (1968, Table 1, p. 159. See also Coetzee, 1970, p. 324).

It is generally believed (Hall, 1932, p. 242-250; B. V. Lombaard, 1932, p. 163 and Willemse, 1969a, p. 6) that the Rooiberg Felsite represents lavas, but owing to the homogeneous nature of the greater portion of the succession, no clarity exists as to the mode of emplacement of these rocks, and Willemse (1964, p. 115) even mentioned the possibility that the rocks could be a composite product of magmatic differentiation, anatexis and palingenesis.

An ignimbritic origin for the agglomerates west of Naboomspruit was postulated by Menge (1963, p. 7-12). A similar origin for the massive, homogeneous porphyritic and non-porphyritic felsite north of Nylstroom was rejected by Coetzee (1970, p. 322-323) on account of a lack of textural evidence in these rocks and he suggested that (p. 324) "the felsites themselves are fused and mobilized Pretoria Series sedimentary rocks". Such a theory is hardly acceptable because of the presence, although not abundant, of amygdaloidal rocks, flow-banding, agglomerates and tuffs. The author would favour a volcanic origin for these rocks, whether as separate lava-flows or as thick accumulations of ignimbrites. Very detailed mapping, microscopic investigation and chemical analyses may throw some light on the thicknesses and lateral extent of the individual flows and also on the mode of emplacement of these rocks.

Fig. 3. Asterisk-shaped patterns in quartzite interbedded in Rooiberg Felsite. Paardenfontein 159 JS.

Fig. 4. Flow-banded felsite in the Upper Felsite Zone on Holnek 153 JS.

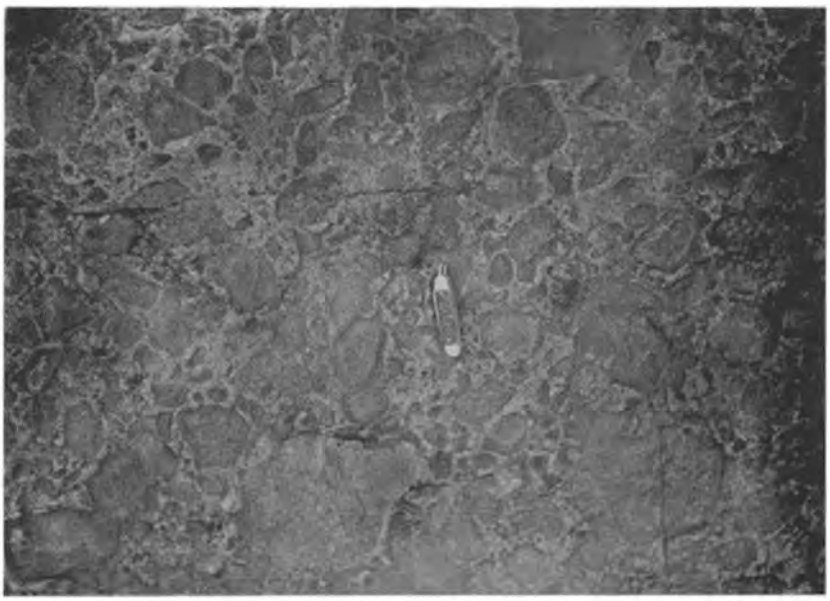

Fig. 5. Agglomerate of the Upper Felsite Zone on Holnek 153 JS.

Fig. 6. Black agglomerate containing fragments of quartzite. Upper Felsite Zone, Holnek 153 JS.

b) Leptite

As stated above, rocks of all the three zones are developed below the thick transgressive sheet of granophyre and are collectively referred to as leptite. The author (1968, p. 156) considers these fine-grained acid rocks to be recrystallized, metamorphosed Rooiberg Felsite. They were subdivided (p. 155-156) into leptite, (i.e. fine-grained, granular quartz-feldspar rocks) at the base and micrographic felsite (i.e. those rocks which display an intergrowth of quartz and K-feldspar (ibid., Plate I, Fig. 1)) above the leptite. Microgranites were described as occurring on the same stratigraphical horizon as the leptite and the micrographic felsite and are considered to have originated by partial melting of these rocks.

All three these rocks are present in the Tauteshoogte area and although an effort was made to distinguish between them in the field, it was found to be very difficult owing to the irregular relationships and gradual variations between them. The macroscopic characteristics and distribution of the various rocks are broadly as follows:

i) The micrographic varieties are usually dark in colour, i.e. dark grey to dark brown, but red where coarser grained. Leptite is usually brown to red in colour but where these rocks grade into microgranites the colour is usually red to light red.

ii) In the fine-grained varieties, original plagioclase phenocrysts can clearly be seen on weathered surfaces as small, white angular spots. Original amygdales are sporadically found in these rocks and consist either of quartz or of spherical concentrations of hornblende. In the microgranites, these textures were not observed.

iii) Micrographic felsite is present only in the southern area i.e. on the farms Doornpoort 171 JS, Uitkyk 172 JS, Kafferskraal 181 JS and Paardekloof 176 JS where they usually overlie leptite or microgranite. They were hardly ever observed to be in direct contact with the topmost differentiates of the Layered Sequence, the only place being locally along the new road in the valley south of Tauteshoogte.

iv) Microgranite is developed between the Layered Sequence and the overlying micrographic felsite on the southern half of Doornpoort 171 JS, for some distance along the southern edge of the Sekhukhune Plateau on Kafferskraal 181 JS and also on the south-eastern portion of Uitkyk 172 JS.

v) Leptite, on the other hand, is present over the whole area, but is the only rock type along the eastern and southern scarps of the plateau north of The Wedge 175 JS and eastwards from Buffelsvallei 170 JS, respectively.

Under the microscope, the textures of these rocks are very similar to those described by the author (1968, p. 155-157) from the Kruis River area and need not be repeated here. It is sufficient to say that variations in the grain size are common and that it is difficult to draw a line between leptite and microgranite. Rocks of which the grain size is about 1mm or more were usually considered as microgranites and the finer-grained rocks as leptites.

The distribution of amygdaloidal rocks, agglomerates and those which display flow-banding has already been described and these rocks may therefore be termed "amygdaloidal leptite", "agglomeratic leptite" and "flow-banded leptite", respectively.

In a few localities grey, banded rocks were encountered in the leptite on the south-eastern part of the plateau. In hand-specimens, these rocks closely resemble hornfels, but in thin section they display the same fine granular texture as leptite. They differ, however, from the latter in that they contain larger amounts of hornblende and clinopyroxene and in some specimens also contain larger grains of quartz irregularly distributed throughout the ground-mass (G192, G225). Seeing that the composition and the texture of these rocks militate against a sedimentary or intrusive origin, they are provisionally considered to be interlayered tuffs, slightly more mafic than the associated leptite.

Throughout the whole area, the leptite is traversed in an irregular manner by three types of rocks, namely, veins of red, fine-grained granite, granodioritic rocks and larger patches of granophyre. The fine-grained granite closely resembles the coarser-grained varieties of the larger masses of microgranite and is present in the leptite as thin veins to small irregularly shaped pockets, a few cm in diameter. Contacts are mostly gradational into the leptite (Figs. 7 and 8) although sharp contacts with thin rims of mafic minerals (basic fronts, Reynolds, 1947, p. 209) are also developed.

The granodiorite is generally found as larger veins and pockets, a few metres in diameter, but also as thin irregularly anastomosing veins in the leptite (Fig. 9). The larger occurrences usually have sharp, unchilled contacts

Fig. 7. Veins of fine-grained granite cutting irregularly across leptite (dark). Zaaiplaats 157 JS.

Fig. 8. Gradational contacts between leptite (dark) and fine-grained granite. Zaaiplaats 157 JS.

Fig. 9. Irregular veins of granodioritic composition produced by melting of the leptite. Duikerskrans 173 JS.

Fig.10. Close-up of Fig. 9 to illustrate gradational contacts between leptite (fine-grained) and granodiorite (coarser-grained). Duikerskrans 173 JS.

with the latter and often contain numerous inclusions of leptite whereas the contacts of the smaller veins are gradational into the leptite (Fig. 10). Of interest is the fact that, apart from appreciable amounts of quartz, K-feldspar, plagioclase and hornblende, these granodiorites also contain small amounts of fayalite. These rocks were described in detail by Boshoff (1942, p. 60-64) as sub-acid granodiorite and sub-acid granite, and by A. F. Lombaard (1949, p. 365-366) as granodiorite.

2. Granophyre and the basal granodiorite

The bulk of the granophyre is present as a thick, discordant sheet-like intrusion in the Rooiberg felsite. It has a thickness of about 2000-2500m on Buffelsvallei 170 JS and Bankfontein 158 JS but may be thicker in the vicinity of Paardekop in the north. The northern contact with the felsite on Goedgedacht 152 JS seems to be steep and cross-cutting so that dips of rocks in which it is intrusive cannot be used for calculation of its thickness, as was done in the south. The difference in elevation between the top of Paardekop and the lowest occurrence of granophyre on Groothoek 139 JS is about 1000m and this value is therefore an absolute minimum of its thickness in this area.

On the eastern side of the Steelpoort Fault, the granophyre seems to be essentially flat-lying and relatively thin, judging from the low dip of the contact with the underlying rocks in the deeply incised rivers. In the vicinity of Tauteshoogte the granophyre is also present as irregularly shaped pocket-like, sometimes granitic, intrusions in the leptite.

Throughout the greater part of the area, the granophyre varies only slightly in appearance. There are small differences in the colour, but it is homogeneous in composition in that it consists essentially of intergrown quartz and microcline perthite (see also descriptions by Boshoff, 1942, p. 39-40 and A. F. Lombaard, 1949, p. 367). Variations are microgranophyres, the most conspicuous of which is developed at Paardekop. B. V. Lombaard (1934, p. 11) referred to these rocks as felsite, and both he and Daly (1928, p. 718) consider them to be a chilled phase of the granophyre. These rocks are even more fine-grained than the microgranophyre described by the author (1968, p. 160) as cross-cutting sill-like intrusions in the Middle Felsite Zone west of Bothasberg. In thin section, the rock consists almost exclusively of an extremely fine intergrowth of quartz and K-feldspar which closely resembles spherulites in lavas. Lower down in the sequence, the granophyric intergrowth becomes gradually

coarser, but on the larger part of the farm Dwars-in-de-Weg 137 JS the granophyre is finer-grained than its counterpart farther south. A. F. Lombaard (1949, p. 367) describes similar fine-grained spherulitic "felsites" which also display gradational contacts with the normal granophyre on the portion of the farm Haakdoorndraai 169 JS outside the area mapped. Finer-grained granophyres are also developed directly north of Baviaansnek on the farm Elandslaagte 155 JS.

A coarse-grained granitic variety of the granophyre is locally developed at the lowest exposed horizon on the farm Groothoek 139 JS (Folder I). In grain size it corresponds closely to the Bushveld Granite near by, but differs from the latter in this respect, that it contains some granophyric intergrowth, less hornblende and accessory minerals and no allanite. This granitic phase of the granophyre seems to be more common farther north, where sheets of granite intrusive into the granophyre and also various stages in the alteration of granophyre to Bushveld Granite were found by Molyneux (1970, p. 10). Granitic varieties were also found by the author (1968, p. 161) in similar rocks west of Bothasberg, where no Bushveld Granite is developed and it seems possible that some of the granite associated with granophyre in the area described by Molyneux may in fact be related to the granophyre.

On aerial photographs of the farms Goedgedacht 152 JS and Dwars-in-de-Weg 137 JS an interesting concentric pattern is observed in the granophyre (dotted lines Folder I). Seeing that the "spherulitic" microgranophyre occurs at the topographically highest point, i. e. at Paardekop close by, it seems as if the granophyre lies relatively flat or has a shallow dip to the west, to conform with the regional dip of the rocks of the Layered Sequence. If this is so, then the observed concentric patterns cannot be due to layering in the granophyre and may represent steeply dipping ring fractures. The fractures are however only developed in the granophyre and do not continue into the adjoining felsite.

The upper contact of the granophyre with the felsite was always found to be sharp, but at the lower contact it is separated from the leptite by a thin layer of granodiorite termed "porphyritic granophyre" by Boshoff (1942, p. 40). It differs from the granophyre in this respect that it contains appreciable amounts of hornblende and plagioclase, but it may also contain granophyrically intergrown quartz and K-feldspar and could therefore be termed "melanogranophyre". The contact with the overlying granophyre is gradational but sharp and un-

chilled against the underlying leptite. The melanogranophyre differs slightly in appearance from one locality to the next which is mainly due to small variations in the content of hornblende and plagioclase. In several localities it closely resembles the granodiorite which occurs as pockets and veins in the leptite, a feature also noted by A. F. Lombaard (1949, p. 367). Numerous small inclusions of leptite are present in these rocks, but are never observed in the overlying granophyre.

Of interest is the presence of veins of red granophyric granite which are intrusive in the diorites of the Upper Zone in the vicinity of Tauteshoogte. They were found in two deep valleys on the northern portion of Kafferskraal 181 JS, close to the main road, and also in the deep valley at the boundary between Uitkyk 172 JS and The Wedge 175 JS (Fig. 11). Although these rocks were not investigated under the microscope, they closely resemble the pocket-like intrusions of granophyre in the leptite. Their probable mode of origin is given below.

In his treatise on the geology of the Bushveld Complex in the Blood River area, A. F. Lombaard (1949, p. 358-361) describes a gradual transition from the olivine diorite of the Upper Zone to the overlying granophyre. These unusual transitional relationships are to be found along the slopes of two prominent hills which stand apart from the Sekhukhune Plateau and on which the western and southern beacons of the farm Drievoet 182 JS are situated (Folder I). As described by Lombaard, the rocks grade upwards from olivine diorite to fayalite-bearing diorite to fayalite-bearing melanogranophyre to granophyre. He (ibid., p. 369) considers this transition to be due to magmatic differentiation, but a different hypothesis by which such relationships may originate is postulated below.

3. The origin of the various roof-rocks

Any hypothesis on the origin of the various roof-rocks must account for the complicated relationships which have been described above, and are briefly summarized below.

a) The presence of various rock types which traverse the leptite and display gradational contacts with it, i. e. fine-grained granite and granodiorite, as well as the larger pockets of granophyre and granophyric granite.

b) The presence of granodioritic rocks, which contain small inclusions

Fig. 11. Veins of granitic material cutting across diorite of the Upper Zone. Uitkyk 172 JS.

Fig. 12. Breccia of the Steelpoort Fault on Groothoek 139 JS.

of leptite, at the base of the thick sheet of granophyre and its gradation into this granophyre at the top.

c) The relatively thin sheet of leptite wedged between granophyre above and the Layered Sequence below. This leptite can be followed at the scarp of the Sekhukhune Plateau as far north as Signal Hill (Molyneux, 1970, Plate I).

d) The gradual transition from diorite of the Upper Zone to granophyre on Drievoet 182 JS and vicinity.

e) The presence of "spherulitic" microgranophyre in the normal granophyre.

f) Veins of granophyre which cut across the diorites of the Upper Zone in the Tauteshoogte area.

Boshoff (1942, p. 50-51) considers the various acid roof-rocks (granophyre, microgranite and leptite) to represent the most differentiated of successive surges of magma, from a deep-seated chamber, which gave rise to the Layered Sequence of the Complex. The discontinuity in composition between the topmost diorites of the Layered Sequence and the acid rocks is explained as being due to a considerable interval between the successive intrusions and that the composition of the magma which was generated at depth had changed in composition towards the final residual liquid during this interval, and (p. 51) "the Bushveld granophyre was emplaced after the differentiation in depth had finally attained the composition of the favoured residual magma". The inclusions of leptite in the melanogranophyre (porphyritic granophyre, p. 42) are considered by him to represent "schlieren developed locally in the lowest horizon of the porphyritic marginal phase of the granophyre" (ibid., p. 44). He also noted (p. 65) that the granodiorite and granite which occur as veins and pockets in the leptite have a composition intermediate between that of the topmost differentiates of the Layered Sequence and the Bushveld granophyre. He is of the opinion (p. 67) that owing to differentiation in situ of the pulse of magma which gave rise to the olivine diorites residual liquids of granodioritic composition were formed and injected into the overlying fine-grained rocks of the succeeding heave.

A. F. Lombaard (1949, p. 364) recognised the felsitic character of the fine-grained acid rocks (leptites) and did not include them in the Upper Zone of the Layered Sequence because of lack of evidence as to their position in time and because of the sharp contacts between these rocks and the over and under-

lying granophyre and olivine diorite respectively. Owing to the observed transition from olivine diorite to granodiorite and to granophyre and because both the granodiorite and the granophyre occur as pockets in the leptite, he considers (p. 366) these rocks to be part of the Layered Sequence. The sheet of granophyre which is separated from the Layered Sequence by the leptite is considered by him (p. 369) to have originated by magmatic differentiation below the roof and subsequent injection of the residual liquid into these fine-grained acid rocks.

Recently the author (1968, p. 156 and 162) summarized various other hypotheses concerning the origin of leptite and granophyre. He came to the conclusion (p. 156) that the leptite west of Bothasberg represents highly metamorphosed, recrystallized felsite, whereas the microgranophyre and granophyre are palingenetic products of the felsite.

If the concept of Jackson (1961) of bottom crystallization and convective overturn is accepted for the origin of the Layered Sequence, then the largest amount of heat lost by the gabbroic magma was through the roof. He (ibid., p. 97) states that "convective overturn thus would have raised the temperature of the magma near the upper contact and maintained it at high values. High temperatures resulted in (1) a high rate of conductive heat loss at the top and (2) virtual cessation of crystallization there, because the adiabatic magma temperature exceeded the melting point temperature for pressures at that depth".

Recently Irvine (1970) calculated the heat transfer during solidification of layered intrusions. He is of the opinion (p. 1046-1049) that a high-temperature magma, such as a basalt, could melt a considerable amount of granitic material which has a melting temperature of 200-300^{o}C lower than that of the magma. He calculated (p. 1059) that the time of accumulation of the Layered Sequence of the Bushveld Complex was about 200 000 years, and if the temperature of the magma was 1050^{o}C it could melt about 1000m of the roof-rocks if melting of these rocks took place at 800^{o}C.

Tilley et al. (1963, p. 81 and 1968, p. 458) investigated melting relations of samples from the chilled border-phases of layered intrusions and found that crystallization of liquids which gave rise to these rocks commenced at temperatures above 1200^{o}C. These temperatures are based on dry measurements at one atmosphere and would therefore be slightly lower at higher water pressures under natural conditions. Tuttle and Bowen (1958) and Von Platen (1965, p. 342-

380) on the other hand have done a considerable number of experiments to determine the temperatures necessary to produce melts of granitic composition. From their data it is evident that at a depth of about 4km a felsite will begin to melt at about 700°C if the concentration of volatiles is high, whereas complete melting with 2 per cent of water will take place at temperatures slightly above 800°C. The available evidence therefore points to even larger differences in the melting temperature of the roof-rocks and the magma temperature of the intrusion. Consequently Irvine's conclusion that 1000m of roof-rocks could have been melted by the intrusion may even be considered as a minimum value.

Furthermore, it is of interest to note that the melting of a felsite would produce an initial liquid of a composition on the cotectic line close to the isobaric minimum in the system Ab-Or-Q-H_2O (Tuttle and Bowen, 1958, p. 75) and that subsequent cooling of this liquid necessitates simultaneous crystallization of quartz and microcline perthite, thus favouring granophyric intergrowths.

With the above experimental evidence in mind there can be little doubt that a considerable amount of melting of roof-rocks did take place and the following sequence of events, diagrammatically shown in Fig. 13, is therefore proposed to explain the observed relationships between the various rocks developed in the roof.

Emplacement of the gabbroic magma of the Bushveld Complex caused a gradual increase in the temperature of the overlying felsite which resulted in the recrystallization of these glassy rocks to micrographic felsite and leptite (Fig. 13A). As crystallization of the Layered Sequence commenced, the temperature of the metamorphic aureole gradually rose until melting started at an appropriate temperature. It is envisaged that these liquids concentrated as pockets in the leptite and gradually moved to higher levels where they spread out laterally to form, initially, thin, sheet-like intrusions in the felsite (Fig. 13B). As a large amount of the water in the felsite is probably contained in biotite and hornblende, the temperature of melting depends to some extent on the temperature at which these hydrated phases react to form pyroxene and magnetite thus releasing water for melting (Brown and Fyfe, 1970, p. 313-314). These early granophyric liquids were probably emplaced in a still fairly cool environment, resulting in rapid crystallization, thus forming sheets of microgranophyre in the Bothasberg area and the microgranophyre and "spherulitic felsite" in the Tauteshoogte-Paardekop area. As the metamorphic aureole became wider, and

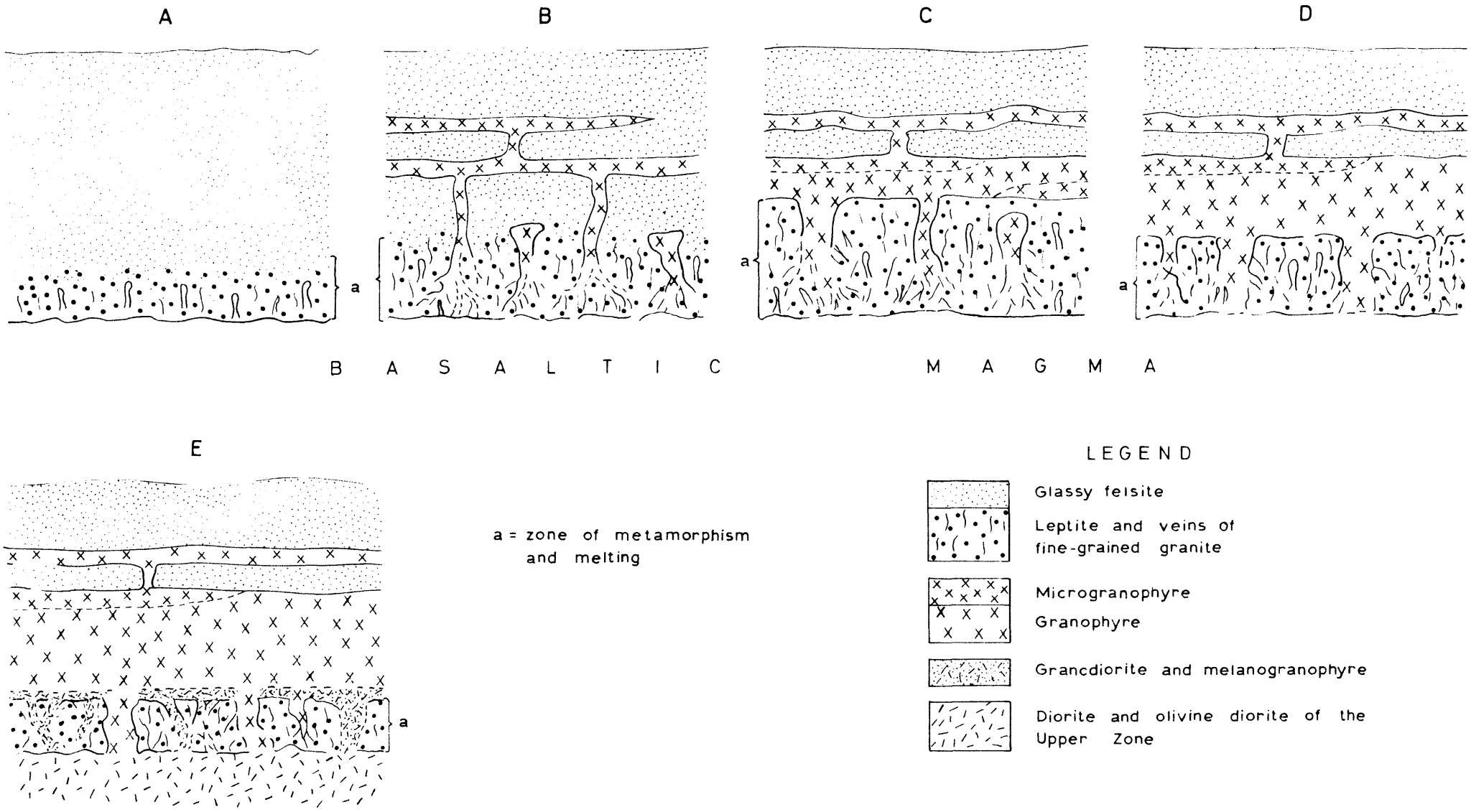

FIG. 13. STAGES IN THE DEVELOPMENT OF THE VARIOUS ROOF-ROCKS (For explanation see text)

the temperature in the roof-rocks gradually increased (Irvine, 1970, Fig. 12, p. 1047) these granophyric liquids remained fluid and were replenished by continued melting of leptite close to the contact with the basaltic magma (Fig. 13C). As stated above, some of the water for melting was probably derived from biotite and hornblende due to the reaction to form pyroxene and magnetite at high temperatures. The scarcity of biotite and hornblende in the granophyre indicates that after reaction the refractory residues remained in the leptite and were probably pushed outwards from the points of melting as basic fronts which are sometimes observed in these rocks. When the melt migrated to higher levels, the mafic constituents remained behind and were eventually assimilated by the gabbroic magma. Continuous addition of more liquid to the granophyric magma resulted in a thickening of the sheet. This thickening was in a downward direction, thus causing gradually higher horizons of the leptite to be melted (Fig. 13C and D).

This process continued until the greater part of the Layered Sequence had accumulated. At this stage, the sequence consisted therefore of a thick sheet of fluid granophyre, separated from the remaining magma of the Layered Sequence by a few hundred metres of leptite which displayed all stages of melting. This is seen as veins of granitic material cutting irregularly across the leptite and coalescing in places to form conduits which were connected to and "fed" the granophyre sheet. These conduits are preserved as the large number of pockets of granophyre and granophyric granite in the vicinity of Tauteshoogte.

The melting process so far must be considered as relatively "dry", the only water or volatiles being derived from the original felsite itself. Basaltic magmas which give rise to layered intrusions and show enrichment in iron in the later differentiates, are considered to be dry, (Hamilton and Anderson, 1967, p. 474-475) and as a result no, or very little water was added to enhance the melting of the roof-rocks. As fractional crystallization of this magma proceeded, the remaining magma became gradually enriched in volatiles, so much so that first biotite, then apatite and lastly hornblende appear as constituents in ensuing rock types.

The residual liquids of the Bushveld magma were probably enriched in water and it is considered (as also proposed by Boshoff, 1942, p. 67) that they invaded the leptite in the final stages of crystallization of the Layered Sequence.

These water-rich liquids, in composition probably similar to the topmost differentiates (diorites), caused additional melting of the leptite and were consequently hybridized to granodioritic liquids. These are now found to traverse the leptite as veins and pockets with gradational as well as sharp contacts and to contain numerous inclusions of leptite. The hybrid granodioritic liquids moved upwards through the leptite until they encountered the sheet of granophyre magma, at the base of which they were concentrated as a thin sheet (Fig. 13E). Although mixing of these two liquids took place, this was limited and the rocks display now, in the solid state, a transition from melanogranophyre or granodiorite to granophyre. This late-stage addition of granodioritic liquid to the granophyre magma may be considered as basal contamination of the latter by the former.

As gradual cooling set in after solidification of the topmost diorites, the sheet and pockets of granophyric material still remained liquid for some time and thin, dyke-like downward injections of this liquid may therefore be present in the topmost differentiates of the Layered Sequence as encountered at a few places near Tauteshoogte.

It seems very likely that large pockets or conduits of granophyre came into contact with the last differentiates of the intrusion. Limited mixing of these two liquids at the contact would result in the gradual transition from olivine diorite to granophyre as observed in the vicinity of Drievoet 182 JS.

The above hypothesis would seem to account for all the various relationships observed in the roof, as briefly summarized at the beginning of this chapter.

In Table I a few chemical analyses of rocks from the Tauteshoogte-Paardekop area are listed. Of these, the first four analyses are new, whereas the last four analyses have been published previously. These analyses show that the granophyres of this area all have essentially the same composition (G511, 3622, 3627) and that the microgranophyre from Paardekop (3627) does not differ appreciably in composition from the other granophyres. Analyses of leptite vary somewhat from one locality to the next (G328, Lieb-13 and 2(b)) and if these rocks are recrystallized felsite then such variations are to be expected (Von Gruenewaldt, 1968, p. 165). Although the composition of granodiorite G329 is very similar to that of leptite 2(b), the former sample is from a vein of granodiorite which has a gradational contact with the leptite G328. The difference in composition between G328 (leptite) and G329 (granodiorite) seems to indicate

TABLE I FOUR NEW AND FOUR PUBLISHED CHEMICAL ANALYSES OF ACID ROCKS FROM THE VICINITY OF TAUTESHOOGTE AND PAARDEKOP

Sample No.	G328	G329	G374B	G511	LIEB-13	2(b)	3622	3627
SiO_2	70,49	68,22	66,43	74,09	69,00	68,25	74,15	74,00
TiO_2	0,55	0,66	0,90	0,39	0,40	0,50	0,37	0,48
Al_2O_3	11,76	12,50	13,17	11,64	12,17	11,15	12,61	12,45
Fe_2O_3	1,91	1,41	1,70	1,65	3,35	1,95	0,90	0,47
FeO	4,54	5,98	5,74	2,02	3,80	6,50	2,39	1,88
MnO	0,13	0,17	0,22	0,14	0,11	n. d.	0,32	0,17
MgO	0,10	0,13	0,15	0,06	0,68	0,50	0,03	0,37
CaO	2,24	2,90	2,45	0,80	2,11	3,40	0,82	0,99
Na_2O	3,20	3,84	4,04	3,05	3,53	3,00	2,87	3,09
K_2O	4,14	3,74	3,92	5,07	4,30	4,05	4,86	4,93
H_2O^+	0,20	0,33	0,92	0,62	0,83	0,05	0,40	0,39
H_2O^-	0,31	0,23	0,23	0.19		0,05	0,17	0,13
P_2O_5	n. d.	n. d.	n. d.	n. d.	1,39	0,35	0,14	0,09
	99,57	100,11	99,87	99,72	101,67	99,75	100,03	99,44

G328 Leptite, Steynsdrift 145 JS

G329 Granodiorite, same locality as G328

G374B Granodiorite north of Baviaansnek, Elandslaagte 155 JS

G511 Normal granophyre, Elandslaagte 155 JS

Analyses by the National Institute for Metallurgy, Johannesburg.

Lieb-13 Leptite, Tauteshoogte, C. J. Liebenberg, 1961, p. 72-73.

2(b) Dark, greyish felsite, Tauteshoogte. B. V. Lombaard, 1934, Table 2(b), p. 12.

3622 Granophyre, ½ mile west of Paardekop, R. A. Daly, 1928, Table II, p. 717.

3627 Felsite (microgranophyre) from Paardekop. R. A. Daly, 1928, Table II, p. 717.

that melting of G328 was accompanied by the introduction of some mafic constituents, and as postulated above, they were probably derived from the residual liquids of the magma which gave rise to the Layered Sequence. It is considered that granodiorite G374B has originated in a similar way. This specimen was collected close to the contact of the leptite and the overlying granophyre in the northern road cutting at Baviaansnek, and contains, among others, a few crystals of fayalite.

4. The Bushveld Granite

Bushveld Granite is only developed in the northern part of the area where it is present as a few isolated outcrops on the farms Steynsdrift 145 JS and Tigerhoek 140 JS and as a tongue which projects outwards on Groothoek 139 JS from the large pluton north of Paardekop (Molyneux, 1970, Plate I). The isolated occurrences consist of granite porphyry which would seem to suggest that they are small stock-like intrusions of Bushveld Granite. In comparison, the larger masses on Groothoek 139 JS and on Steelpoort Park 366 KT (Hammerbeck, 1970, p. 301) to the southeast, are homogeneous coarse-grained granites.

The composition of the Bushveld Granite (G333) and the granite porphyry (G321, G332) is very similar: quartz, microcline perthite and hornblende are the major constituents, whereas apatite, zoned zircon and allanite are the most abundant accessory minerals.

A few dykes of fine-grained acid rocks are present on the farm Luipershoek 149 JS. Their strike is similar to that of the close by Steelpoort Park Granite and they are probably related to this intrusion.

IV. THE LAYERED SEQUENCE OF THE BUSHVELD COMPLEX

1. General

The portion of the Layered Sequence of the Bushveld Complex investigated includes the Main and Upper Zones. The lower portion of the Main Zone was not included in this mapping project as it had recently been undertaken by P. Roux (1968). However, the generous assistance of Rand Mines, who kindly provided core from a bore-hole 1300m deep, drilled on the farm Pietersburg 44 JT (Folder I), made it possible to investigate rocks of the complete succession of the Main Zone.

In subdividing the rocks of these two zones, the author adhered to the scheme as proposed by Molyneux (1970, Plate II), except for the division between the lower two subzones of the Upper Zone which is taken at the base of the Main Magnetitite Seam. The thicknesses of the various zones and subzones are given in Table II and these are also compared with those given by Molyneux (1970, p. 14) from the area north of the Steelpoort River. A more detailed schematic profile of the various subzones and the characteristic rock types is given in Folder II.

In the general descriptions of the field characteristics of the various rock types, the cumulus terminology of Wager et al. (1960, p. 73) and/or Jackson (1967, p. 22 and 1970, p. 392) cannot be used, as it is extremely difficult to distinguish the various cumulus phases in hand-specimen. For the same reason, subdivision of rocks into gabbro, hypersthene gabbro, hyperite and norite (Raal, 1965, p. 3) cannot be made in the field. Rocks are therefore generally referred to as gabbros in the Main Zone and magnetite gabbros in the Upper Zone. Where reference is made to specific horizons in the Layered Sequence, descriptive rock names such as fine-grained norite, norite, mottled anorthosite, spotted anorthosite, porphyritic norite etc. are used. For a general description of the last three terms, see Willemse (1969a, p. 14).

Names, according to relative abundances of pyroxenes (illustrated diagrammatically by Raal, 1964, p. 3) are given in Appendix I for rocks on which modal analyses were made. Cumulus phases, where evident, are indicated by an asterisk next to the volumetric percentage of the particular mineral.

2. The Main Zone

The Main Zone extends from Roossenekal in the west to the Dwars River

TABLE II SUBDIVISION AND THICKNESS OF THE UPPER AND MAIN ZONES IN THE ROOSSENEKAL AREA

Zone	Subzone	Rock types	Thickness in metres	Magnet Heights (Molyneux 1970 p. 14)
UPPER ZONE	Subzone D	Magnetitite Seams 15-21, olivine diorite, anorthosite, diorite	990	650
		Appearance of cumulus apatite		
	Subzone C	Magnetitite Seams 8-14, troctolite, magnetite gabbro, olivine gabbro, anorthosite	600	500
		Appearance of olivine (Sisal Marker)		
	Subzone B	Magnetitite Seams 1-7 above the Main Magnetitite Seam, anorthosite, magnetite gabbro, feldspathic pyroxenite	540	450
		Main Magnetitite Seam		
	Subzone A	Lower Magnetitite Seams 1-3, anorthosite, magnetite gabbro	140	190
		Appearance of magnetite		
		Thickness of Upper Zone	2270	1790
MAIN ZONE	Subzone C	Pyroxenite, anorthosite, gabbroic rocks	690	660
		Pyroxenite Marker		
	Subzone B	Homogeneous gabbroic rocks, fine-grained norite	1985	1000
		Upper Mottled Anorthosite		
	Subzone A	Pyroxenite, noritic and gabbroic rocks, mottled and spotted anorthosite	1265	1200
		Merensky Reef		
		Thickness of Main Zone	3940	2860
		Total thickness	6210	4650

in the east. It occupies a rugged, mountainous region which can be regarded as the southern continuation of the Leolo Mountains. The thickness was calculated as being 3940m, which is about 1000m more than that calculated by Molyneux north of the Steelpoort River and may in part be due to possible strike-faults in Subzone B of this zone. This faulting is extremely difficult to evaluate as the rocks of this subzone are very homogenous in appearance and also show very little variation in composition of the cumulus phases (Folder III).

a) Subzone A

All the specimens investigated from this subzone are from a bore-hole drilled by Rand Mines on the farm Pietersburg 44 JT. The top of this subzone is taken at the so-called "Upper Mottled Anorthosite" which could be followed for some distance along strike close to the eastern boundary of the area mapped. Only in the extreme north-eastern corner are rocks below this horizon present on the farm Hebron 5 JT (Folder I).

No specimens were available from the Merensky Reef, but this reef has been described in some detail by several authors from various localities of the Bushveld (Cousins, 1964, p. 227-229, and 1969, p. 239; Van Zyl, 1970, p. 91-93; Liebenberg, 1970, p. 181-189) as well as by Roux (1968, p. 69-74) east of this area.

Thirty-five metres above the Merensky Reef is the well known Bastard Reef, which is a feldspathic pyroxenite (orthopyroxene-plagioclase cumulate). It is separated from the Merensky Reef by alternating mottled anorthosite and spotted noritic to anorthositic rocks. The most common rock type for 100m above the Bastard Reef is mottled anorthosite which in turn is succeeded, after some normal gabbroic rocks, by the prominent "porphyritic norite". These porphyritic rocks are about 200m thick and contain large crystals of orthopyroxene which constitute on an average about 20 per cent by volume of the rock and are characterized by numerous small inclusions of plagioclase laths. Directly underlying this porphyritic norite is a fine-grained plagioclase-orthopyroxene cumulate, some 20m thick, which corresponds to the height of the needle-norite in other localities. Although no typical needles of orthopyroxene as described by Willemse (1969a, p. 15) were found in these rocks, some of these crystals tend to have a pronounced prismatic habit.

The Main Mottled Anorthosite of Subzone A is approximately 50m thick, 700m above the Merensky Reef. It forms a prominent exposure on the face of a

cliff on Hebron 4 JT in the extreme north-eastern corner of the area. Mottled anorthosite is however developed intermittently in the overlying 80m and the underlying 60m and consequently this whole zone of 200m is often referred to as the Main Mottled Anorthosite (Molyneux, 1970, p. 15).

The top 400m of this subzone consists of fairly uniform gabbroic rocks which contain a few thin layers of spotted and porphyritic rocks as well as three layers of mottled anorthosite at the top. The upper two of these are about 10m apart (Upper Mottled Anorthosite) and mark the top of Subzone A of the Main Zone. Apart from separating the variable rock-types of Subzone A from the fairly uniform overlying gabbroic rocks, this anorthosite is situated in the sequence close to the first appearance of inverted pigeonite and also close to a small compositional break of the cumulus phases in the sequence (Folder III).

b) Subzone B

Practically the whole of Subzone B consits of monotonous gabbroic rocks which show hardly any variation from top to bottom. This subzone is close to 2000m thick in this area, although two faults may possibly have caused duplication of parts of the sequence. The most characteristic textural feature of the rocks of this subzone, is that the orthopyroxene is optically continuous over large areas with the result that, in hand-specimen, cleavage planes reflect the sunlight over large areas (Fig. 35).

At the top of this subzone is a fine-grained norite, about 100m thick, which could be followed for 20km along strike directly underlying the Pyroxenite Marker at the base of the next subzone. In the south, these fine-grained rocks contain large quantities of cumulus magnetite and also more cumulus clinopyroxene than in the north (G453 and G450). Rocks of the same stratigraphical horizon, east of Stoffberg and also farther south, contain, apart from magnetite, dark gray to black plagioclase crystals, the colour of which is caused by numerous inclusions of tiny rods of magnetite, (Groeneveld, 1970, p. 39). These dark gabbroic rocks are not developed in the Roossenekal area. This lateral change in composition of the rock types in one correlated layer suggests that the composition of the magma was not uniform throughout the chamber and that it was probably more iron-rich in the south than in the north.

In the west of the area, on the farm Buffelsvallei 170 JS gabbroic rocks of the Main Zone outcrop south of the Blood River. The highest exposed rocks contain small amounts of magnetite and these rocks are therefore correlated with the top of Subzone B east of Roossenekal.

c) Subzone C

The base of Subzone C is taken at the contact between the fine-grained rocks of the previous subzone and the overlying Pyroxenite Marker of the Main Zone. This pyroxenite, first described by Lombaard (1934, p. 7) was found to be an excellent marker and was followed for more than 80km along strike by Molyneux (1970, p. 22) and the author, north and south of the Steelpoort Park Granite respectively. The Pyroxenite Marker does not seem to be present in the area to the south, but Groeneveld (1970, Fig. 1, p. 38) recorded a compositional break of the cumulus phases in the sequence above the black gabbroic rocks.

The thickness of the Pyroxenite Marker could not be determined in the field. It usually outcrops as a few boulders in a slight depression between parallel dipslopes east of Roossenekal. On the northern portions of Mapochsgronde 500 JS and on the adjoining farms a slightly coarser-grained pyroxenite is developed, a few metres below or sometimes directly below the Pyroxenite Marker. No sulphides were found to be present in this pyroxenite.

The rocks of the lower half of Subzone C can easily be recognized in the field in that they contain primary cumulus orthopyroxene in contrast with the large units of similarly orientated grains of this mineral in the over- and underlying rocks. In appearance they are similar to the rocks of Subzone A. Spotted varieties are characteristic owing to large crystals (up to 5mm in diameter) of orthopyroxene. Some of the "porphyritic" rocks of this subzone differ, however, from those of Subzone A as they contain larger amounts of clinopyroxene which is present as long needles orientated parallel to the plane of layering. The character and appearance of these clinopyroxene needles (up to 8mm long and 1mm wide) is very similar to that of the orthopyroxene in the needle-norite described by Willemse (1969a, p. 15) from Subzone A.

Two layers of mottled anorthosite are present about halfway up in this subzone, the upper one of which could be followed for some distance along the strike to the west of and parallel to the road to Steelpoort Park. Above this anorthosite, the rocks are very similar to those of Subzone B.

3. The Upper Zone

This zone, 2270m thick, occupies the area from Roossenekal in the east to the foot of the Sekhukhune Plateau in the west, as well as the low-lying region south and west of Tauteshoogte. The division between the Upper and the Main

Zone is taken at the appearance of magnetite in the rocks. This is generally in a fairly prominent mottled anorthosite in which some of the mottles are caused by intercumulus magnetite (Molyneux, 1970, p. 22).

a) Subzone A

The top of this subzone is taken at the base of the Main Magnetitite Seam in contrast to the subdivision by Molyneux (1970, p. 24) who considers the boundary to be at the base of an olivine gabbro some 50m below the Main Seam. This olivine gabbro was not found in the Roossenekal area, but may possibly be concealed by the large amount of magnetitite rubble up-dip from the Main Seam. Because of the large amount of magnetitite rubble (Folder I), the author has resorted to river-sections to determine the sequence of this subzone. In most cases, however, it was found that where rivers traverse the massive and resistant Main Magnetitite Seam, the courses follow lines of weakness in the rocks, i.e. where faults and folds are developed. This, together with the low dips of the rocks, made mapping and reconstruction of the sequence difficult, and consequently some uncertainty still exists about the succession of rock types of this subzone.

Above the mottled anorthosite, which forms the base of the Upper Zone, follows some magnetite gabbro which contains the first of the lower magnetitite seams. About 30m above Lower Seam 1 is a mottled anorthosite, about 1,5m thick which contains disseminated sulphides. This is overlain by Lower Seam 2. Lower Seam 3 follows only a few metres above and was only observed on Zwartkop 142 JS.

The magnetite gabbros above these two seams are succeeded after a short distance by a very fine-grained magnetite-bearing gabbroic rock. At its upper contact, big xenoliths of the latter were found in the overlying magnetite gabbro (Fig. 14) in an outcrop in a tributary of the Mapochs River, north-east of the Mapochs Mine. This magnetite gabbro is fairly homogeneous, about 60m thick, and contains two layers of mottled anorthosite in which a few specks of intercumulus sulphides were observed. At the base of the Main Seam is the well-known mineralized anorthosite which was found to be about 3m thick in this area.

In an effort to obtain a clearer picture of the sequence of rocks in Subzone A, the author investigated outcrops in a tributary of the Mapochs River near the southern boundary of Zwartkop 142 JS. It was, however, found that the

sequence differs in several respects from that to the south, e. g. :

i) The mottled anorthosite at the base of this subzone contains very little or no magnetite. The contact with the underlying gabbro of the Main Zone is irregular and large inclusions of the one are often encountered in the other.

ii) The first magnetitite seam is followed by about 6-7m of magnetite gabbro and is overlain by 12m of mottled anorthosite which seems to cut across the lower horizons in places.

iii) The mottled anorthosite below Lower Seam 2 is exceptionally rich in sulphides in this locality.

iv) Above the very fine-grained gabbro is a prominent mottled anorthosite, about 3m thick.

(v) A magnetitite plug is situated below these fine-grained rocks. This plug is surrounded by anorthositic rocks which contain little veinlets and nodules of magnetitite (Hammerbeck, 1970, p. 308).

The sequence of rocks in this river section is by no means clear. The abundance of anorthositic rocks which seem to cut across the normal layering, the presence of a magnetitite plug and shearing, seems to indicate that considerable disturbance took place during and after consolidation of the rocks. Much more detailed mapping in this area is necessary to unravel these complex relationships.

b) Subzone B

The Main Magnetitite Seam at the base of this subzone differs very little in appearance from that in the Magnet Heights area, as described by Molyneux (1964, p. 58). Only Upper Seams 1 and 2 were found in this area, directly above the Main Seam, because of poor exposures of the greater part of Subzone B. In the valley of the Mapochs River, at the boundary between Mapochsgronde 500 JS and Zwartkop 142 JS, two mottled anorthosites are developed above these seams. The lower one of these two is slightly more than 1, 5m thick and could be followed for some distance along strike (Folder I). This anorthosite is correlated with the one directly underlying Seam 3 in the Magnet Heights area (Molyneux, 1964, p. 67). In the same valley, fairly good exposures of the overlying magnetite gabbros as well as Magnetitite Seams 6 and 7 are present. The only outcrop of the feldspathic pyroxenite some distance below Seam 6 is present east of the Erts Railway Station, close to the vermiculite-bearing pegmatoid (Folder I).

Owing to poor exposures, the sequence of rocks at the top of this subzone is not quite clear. The appearance of olivine is generally taken as being the beginning of Subzone C. These olivine-bearing rocks usually form a fairly prominent ridge west of, and parallel to, the main road from Middelburg to Steelpoort. However, one specimen collected some distance below this ridge (G658) was found to contain some olivine, whereas some of the rocks from this scarp contain very little (G365, G351) and sometimes no olivine at all. Underlying this scarp there seem to be some magnetite gabbro and anorthosite which outcrop intermittently along strike and the presence of magnetitite rubble associated with these rocks seems to indicate the presence of an additional magnetitite seam at the top of Subzone B.

c) Subzone C

The basal 150m of this subzone seems to consist of alternating layers of olivine gabbro, magnetite gabbro, anorthosite and troctolite. The Sisal Marker, a magnetite-bearing troctolite about 30m thick, was taken by Molyneux as the base of this subzone, but it is developed about 40m above the first olivine-bearing rocks in this area. The top of this olivine-rich basal unit of Subzone C is taken at a characteristically fine-grained norite which contains, apart from large amounts of cumulus inverted pigeonite, also a few cumulus crystals of olivine (G314). On Onverwacht 148 JS two layers of these fine-grained rocks are developed.

Magnetitite Seam 8 follows directly on this olivine-bearing norite and marks the appearance of seven seams which succeed each other at short distances at the base but at greater intervals higher up. Interlayered rocks are magnetite gabbro, which tend to be anorthositic at the base of the seams, and two thin layers of olivine gabbro above and below Seam 11. Seam 13 is followed by a prominent mottled anorthosite some 5m thick, which is characterized in that the lower 1,5m contains smaller mottles than the upper 3,5m. Owing to differential weathering of the alternating rock-types in this subzone the layering is clearly visible in the field (Fig. 15).

d) Subzone D

The rocks of this subzone contain andesine and consequently most authors (Boshoff, 1942, p. 24; Wager and Brown, 1968, p. 376; Willemse, 1969, p. 10; Groeneveld, 1970, p. 40, and Molyneux, 1970, p. 26) have termed these rocks either olivine diorite or ferrodiorite. If olivine is present in these rocks, it

Fig. 14. Large inclusion of very fine-grained magnetite gabbro in ordinary magnetite gabbro. Subzone A of the Upper Zone, Mapochsgronde 500 JS

Fig. 15. Layering of the rocks of Subzone C of the Upper Zone. Luipershoek 149 JS.

should be more iron-rich than about Fo_{40} according to the definition of ferrodiorite (Wager and Brown, 1968, p. 78) and for the Bushveld, the usage of this term is therefore justified. It must however, be borne in mind that the majority of olivine diorites contain fair amounts of cumulus apatite (Folder IV), usually between 4 and 8 per cent by volume, which indicates that the magma was still rich in Ca and would probably have precipitated labradorite if the concentration of phosphorus did not reach saturation at the level where andesine appears in the sequence. Furthermore, where apatite is not present in these rocks, as for instance between Seams 17 and 21, the Ca-content of the plagioclase increases noticeably and attains values of above An_{50} (Folder III). The appearance of all these rocks is very similar to the magnetite gabbros from lower horizons and for the same reason Wager and Deer (Wager and Brown, 1968, p. 78) originally decided to refer to the ferrodiorite of Skaergaard as ferrogabbro. For the above reasons the author would favour the term olivine gabbro, but in order to avoid further confusion in terminology, the name olivine diorite (ferrodiorite) is retained for the majority of rocks in this part of the sequence.

The term "diorite" is used in this treatise for the topmost 100m of the intrusion, because of the large amount of hornblende present in these rocks. Olivine is very subordinate, but as it has an extremely iron-rich nature, the term "fayalite diorite" is often used by other authors (Boshoff, 1942, p. 29, and Groeneveld, 1970, p. 41). The name "granodiorite" (Molyneux, 1970, p. 26) for rocks which constitute the uppermost part of the Layered Sequence, is not recommended as this term defines more closely the hybrid rocks which are associated with the overlying acid roof of the complex.

Olivine diorite is the most common rock type of Subzone D and constitutes about 70 per cent of this sequence. Olivine-free rocks are characteristically developed where magnetitite seams are present (Folder IV). The first of these olivine-free rocks are developed above and below Seam 15 and consist of mottled anorthosite which underlies this seam and magnetite gabbro which overlies it. Directly above this magnetite gabbro is the ovicular olivine diorite, characterized by the presence of numerous elongated inclusions which consist exclusively of plagioclase (Fig. 16). The rocks between Seams 17 and 21 are mostly olivine-free "anorthositic diorites" alternating with magnetitite seams and thin layers of olivine diorite. A peculiar rock which contains numerous perfectly spheroidal

Fig. 16. The ovicular olivine diorite, Subzone D of the Upper Zone. Onverwacht 148 JS.

Fig. 17. Spheroidal inclusions of anorthosite in magnetite diorite. Luipershoek 149 JS.

inclusions of anorthosite (Fig. 17) outcrops a small distance below Seam 21 on Luipershoek 149 JS. In appearance it is analogous to the "Boulder-anorthosite" below the Merensky Reef (Cousins, 1964, p. 228) and the "Tennis-ball Marker" of the Main Zone in the Kruis River area (Von Gruenewaldt, 1966, p. 50) in which the inclusions are spheres of pyroxenite. No satisfactory explanation for the origin of these rocks can be offered at this stage.

4. The Magnetitite Seams of the Upper Zone

The magnetitite seams of the Upper Zone were described in detail by Molyneux (1964, p. 57-77) in his investigation of the rock types at Magnet Heights. Not all the seams are exposed in the Roossenekal area, but those which are present are strikingly similar to those at Magnet Heights. The nature of most of the magnetitite seams developed in the Roossenekal area are diagrammatically illustrated in Fig. 18.

a) Magnetitite Seams of Subzone A

The magnetitite seams of this subzone differ slightly from those described by Molyneux (1964, p. 57-58). Lower Seam 1 usually consists of 5cm of solid magnetitite at the base, followed by about 75cm of feldspathic magnetitite. The upper contact is usually gradational into the overlying magnetite gabbro. This seam is exceptionally thick on the farm Zwartkop 142 JS where it consists of massive and plagioclase-rich magnetitite alternating with magnetite gabbro over a thickness of 2,5 to 3 metres.

Lower Seam 2 is very similar to Lower Seam 1, and is about 80cm thick and composed of feldspathic magnetitite with lenticular patches of solid magnetitite near its base. Lower Seam 3 was only observed on Zwartkop 142 JS where it consists of about 1m of feldspathic magnetitite.

An additional thin magnetitite seam was found on Zwartkop in the magnetitite gabbros about half-way between Lower Seam 3 and the Main Magnetitite Seam. This seam consists of 4cm of solid magnetitite at the base and 11cm of feldspathic magnetitite at the top.

b) Magnetitite Seams of Subzone B

i) The Main Magnetitite Seam is the most prominent of all the seams of the Upper Zone, and owing to its thickness and its solid nature, it outcrops practically everywhere in the Bushveld Complex where this zone is developed. It forms prominent pavements east of the main road from Middelburg to Steelpoort and is currently being mined north of Roossenekal by Highveld Steel and

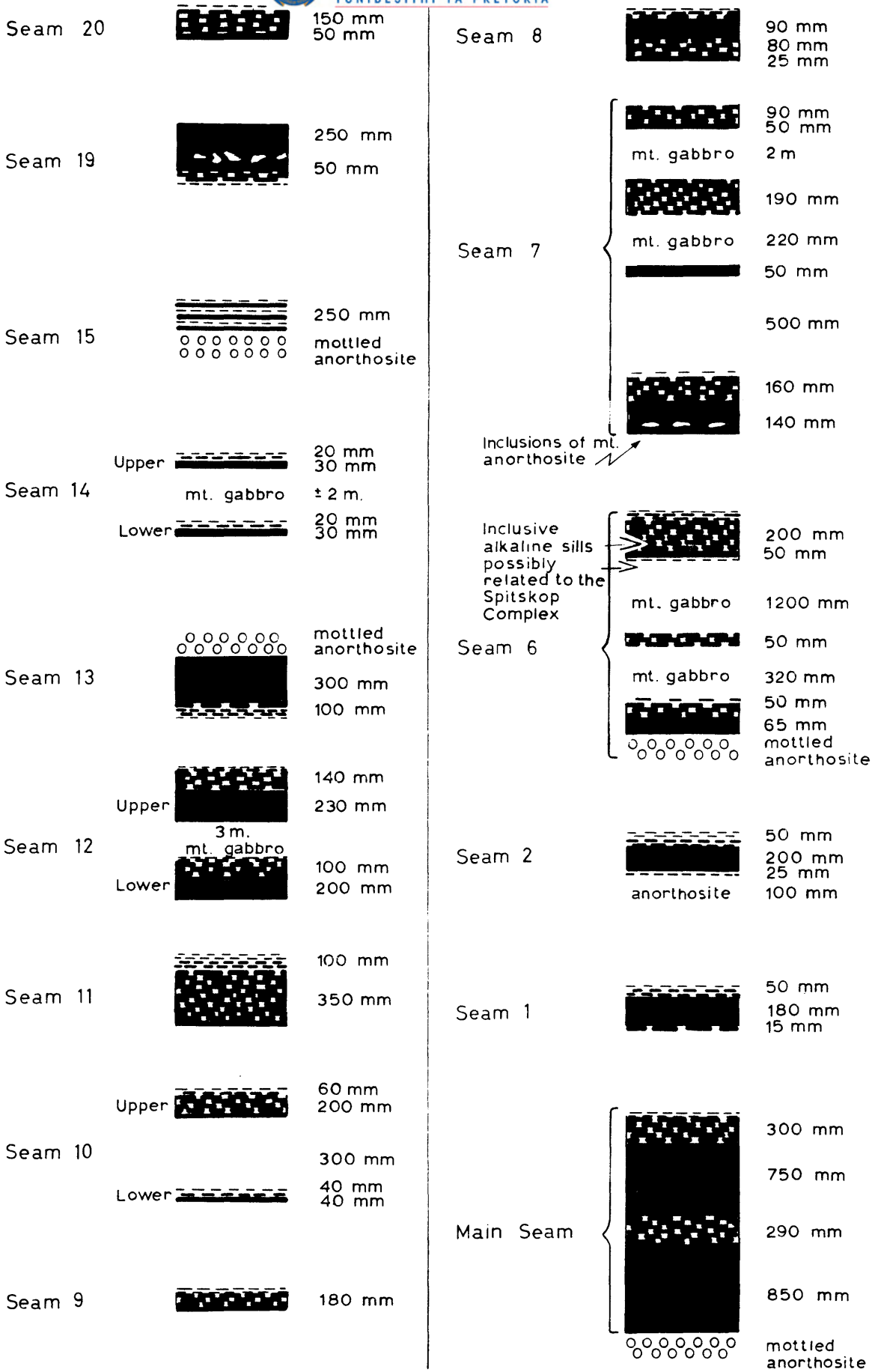

FIG. 18. SCHEMATIC REPRESENTATION OF SOME OF THE MAGNETITITE SEAMS OF SUBZONES B, C AND D OF THE UPPER ZONE. SOLID - PURE MAGNETITITE, DOTTED - FELDSPATHIC MAGNETITITE. STRIPED - GRADATION INTO MAGNETITE GABBRO.

Vanadium Corporation Limited (Fig. 19). Up-dip from these pavements, large areas are covered by a thick layer of magnetitite rubble, owing to dislocation of the seam caused by the weathering of the underlying anorthosite (Folder I).

ii) Only the first two of the five magnetitite seams which are present within 30m above the Main Seam at Magnet Heights (Molyneux, 1964, p. 65-67) were found in this area. This may in part be due to poor outcrops as especially Seams 3 and 5 are friable and feldspathic and only mappable in areas of good exposure (ibid., p. 67).

iii) Seams 6 and 7 are exposed in the Mapochs River at the boundary between Mapochsgronde 500 JS and Zwartkop 142 JS. Both consist of several seams over thicknesses of 2 and 3, 5m respectively (Fig. 18). In the remainder of the area they form small, rubble strewn scarps which run parallel to each other for several kilometres along strike.

c) Magnetitite Seams of Subzone C

i) The lower three seams, Nos 8, 9 and 10, of this subzone succeed one another at short intervals and consist mostly of feldspathic magnetitite. They usually tend to weather to rubble composed of small fragments and outcrops are to be seen only in river sections, except in the case of Seam 8 which forms a few pavements overlying the fine-grained olivine-bearing norite. Seam 10 consists of two thin seams, approximately 30cm apart. (Figs. 18 and 20).

ii) Although feldspathic, Seam 11 could be followed along strike for many kilometres, and is usually found at the base of a fairly resistant olivine gabbro. It is the thickest of the seams of Subzone C and forms pavements on Onverwacht 148 JS and Luipershoek 149 JS.

iii) Seam 12 consists of two seams, very similar in nature and about 3m apart. (Fig. 18).

iv) Seam 13 is unusual in so far as it has a sharp upper contact with the overlying mottled anorthosite and a gradational lower contact with the underlying magnetite gabbro. This seam, together with the overlying mottled anorthosite is an excellent marker and its nature and appearance is similar to that at Magnet Heights (ibid., p. 75).

v) Seam 14 consists of two thin seams about 2m apart and outcrops only sporadically. On Luipershoek 149 JS the upper one is locally much thicker and consists of 50cm of feldspathic magnetitite.

Fig. 19. One of the quarries on the Main Magnetitite Seam at the Mapochs Mine, Roossenekal.

Fig. 20. Outcrop of Magnetitite Seam 10 on Luipershoek 149 JS. Note the thin lower seam about 30 cm below the more prominent upper seam.

d) Magnetitite Seams of Subzone D

i) The lowest seam of this subzone, No. 15, is usually not well developed, but a perfect exposure is on Onverwacht 148 JS where it is seen together with underlying mottled anorthosite and the overlying magnetite anorthosite and magnetite gabbro on a steep cliff on the south side of the Steelpoort River. The seam is very thin, and consists of a few thin magnetitite bands, alternating with magnetite anorthosite.

The presence of this seam is also indicated by rubble on the southern portion of Onverwacht 148 JS and also on Steynsdrift 145 JS. In the case of the latter occurrence, the magnetitite fragments are fairly large, about 10cm in diameter, which indicates a local thickening of the seam.

ii) The only indication of a magnetitite seam which could correspond to Seam 16 of the Magnet Heights area is the presence of a small amount of magnetitite rubble associated with a thin layer of magnetite gabbro near the common beacon of the farms Onverwacht 148 JS, Duikerskrans 173 JS and Mapochsgronde 500 JS.

iii) Seam 17 is close on 60cm thick and is well developed on the farm Onverwacht 148 JS. Its presence is usually indicated by large blocks of magnetitite, but nowhere could exposures be found to indicate contact-relationships with the over- and underlying rocks. This seam is considerably thinner at the boundary between Duikerskrans 173 JS and Mapochsgronde 500 JS where it consists of a few thin stringers of magnetitite in magnetite anorthosite.

iv) Seams 18 and 19 occur close to each other in a river section on Luipershoek 149 JS, only a small distance above Seam 17. Seam 18 is a thin feldspathic magnetitite, whereas Seam 19 is about 30cm thick and has a gradational lower contact and a sharp upper contact (Figs. 21 and 22). These seams peter out gradually in a southerly direction and in the valley of the Steelpoort River on Duikerskrans 173 JS only one of these was observed as a thin concentration of magnetite in the gabbroic rocks.

v) Seam 20, seldom seen in outcrop, is about 20cm thick. The lower 5cm of the seam are fairly solid and the upper 15cm feldspathic. It rests with a sharp lower contact on magnetite anorthosite.

vi) The giant of all the magnetitite seams is undoubtedly Seam 21. It is almost 10m thick, but owing to a large number of lenses of anorthosite, it is friable and seldom forms prominent outcrops (Fig. 23). Small cumulus crystals

Fig. 21. Banded magnetite gabbro below Seam 19 (at hammer). The banding is caused by varying amounts of magnetite Onverwacht 148 JS.

Fig 22. Magnetitite Seam 19, characterized by a sharp upper contact, gradational lower contact and irregularly shaped inclusions of anorthositic material at its base. Onverwacht 148 JS.

of olivine are distributed evenly throughout the magnetitite seam. The presence of the seam can clearly be noticed on aerial photographs as a low ridge which runs parallel to the foot of the Sekhukhune Plateau. It could be followed for about 20km along strike, from Paardekloof 176 JS in the south, where a few outcrops are present in the dongas below Tauteshoogte, up to the boundary of Steynsdrift 145 JS in the north where it disappears under a thick covering of talus at the foot of the plateau. Six kilometres farther north, it reappears at a topographical level much lower than to the south, approximately in line with Seam 15 on Steynsdrift 145 JS. Hammerbeck (1970, Fig. 1, p. 300) considers this to be due to faulting. In the west of the area, it outcrops in a few places on Doornpoort 171 JS and it was also intersected in a bore-hole (DDH2, Folder I) drilled by the Anglo American Corporation on this farm.

5. Pronounced lateral variation of facies in the Layered Sequence

The sequence of rock types in Subzone D of the Upper Zone between Bothasberg and Tauteshoogte differs considerably from that described above. This lateral "facies change" takes place over a distance of about 10km, but owing to poor exposures south-east of Tauteshoogte, it could not be studied in detail. Outcrops in the upper reaches of the Blood River are, however, slightly better and it is therefore possible to attempt a correlation between the two sequences.

When the rocks of Subzone D are followed southwards from Onverwacht 148 JS, a noticeable increase in the amount of olivine diorite between Seams 17 and 21 can be observed. The former seam gradually becomes thinner and disappears on Paardekloof 176 JS, whereas olivine-free rocks below Seam 21 make way for olivine-bearing rocks. Olivine diorite was also intersected above and below this magnetitite seam in bore-hole DDH2 on Doornpoort 171 JS, which indicates that the change in sequence also takes place in a westerly direction.

Farther to the south, in the valley of the Blood River, the lowest horizon exposed along the road from Stoffberg to Groblersdal consists of apatite-free olivine gabbro which contains plagioclase of composition An_{51}. It is overlain by a prominent magnetitite seam which could be followed intermittently in the Blood River and its tributaries from Rhenosterhoek 180 JS in the east to Grootkop 185 JS in the west (Folder I and Fig. 32). On the farm Rhenosterhoek 180 JS it consists of one massive seam, about 1-1,5m thick, characterized by a

Fig. 23. Numerous lenticular inclusions of anorthosite in Magnetitite Seam 21. Onverwacht 148 JS.

Fig. 24. The magnetitite seam on Kafferskraal 181 JS.

15cm feldspathic parting in the middle, but on the south-eastern portion of Kafferskraal 181 JS, it locally splits into three seams of variable thicknesses (Fig. 24). In the northern tributaries of the Blood River, on the farm Kafferskraal 181 JS, it consists of two seams. The lower one is 60 cm thick and is separated by 1m of weathered magnetite gabbro from the upper seam which is about 45cm thick. On Grootkop 185 JS only one seam, 1m thick, was observed. A mottled anorthosite, the plagioclase of which has a composition of An_{52} overlies this seam on the south-eastern portion of Kafferskraal 181 JS. The mottles in the lower metre of this anorthosite are smaller than those in the upper portion of the anorthosite, thus, in appearance, closely resembling those which overlie Seam 13 to the north.

A thin magnetitite seam, a few centimetres thick with a sharp lower and gradational upper contact, outcrops in the Blood River a short distance to the west of the above-mentioned occurrence. The over- and underlying rocks of this seam are very weathered and it could not be determined whether they are olivine-bearing or not. Overlying the mottled anorthosite is olivine-free magnetite diorite (plagioclase An_{48}) in which a magnetitite seam, 10cm thick, is present on Blaauwbank 179 JS.

The overlying olivine diorite (Folder I, Fig. 32) could be followed in several stream beds from Blaauwbank 179 JS in the east to Grootkop 185 JS in the west. Along these river sections and on the slopes of Grootkop, fairly continuous outcrops are present right up against the roof and no additional magnetitite seam was observed. This olivine diorite contains plagioclase with a composition of An_{42} or lower which corresponds to that above Seam 21 farther north. Apatite is present in appreciable quantities in these rocks in contrast with the olivine gabbros lower down in the sequence.

The composition of the plagioclase of the rocks over- and underlying the prominent magnetitite seam in the Blood River valley, corresponds to that of Subzone C in the north. This is also borne out by the absence of cumulus apatite in the olivine gabbro. The overlying olivine-free rocks fall in the diorite field of composition on the grounds that the plagioclase is andesine and may therefore be correlated with the olivine diorite at the base of Subzone D farther north.

The sequence of rocks exposed in the Blood River valley is similar to that described by Groeneveld (1970, Fig. 3, p. 70) from south of Stoffberg. A considerable number of faults seem to be present between Bothasberg and

Tauteshoogte and this, together with relatively poor exposures, (Fig. 32), makes it impossible at this stage to calculate thicknesses accurately. For the construction of this sequence (Fig. 25) the diagrammatic section by Groeneveld (1970, Fig. 3) was therefore used. The sequence of rocks in the Stoffberg area (ibid., Figs. 1 and 3) and also that in the Blood River valley are referred to in the ensuing discussion as the southern section, whereas the sequence of the Tauteshoogte-Roossenekal area will be referred to as the northern section (Fig. 25). To illustrate lateral cryptic variation of some of the cumulus phases, compositions of these are added in both sections on Figure 25.

Groeneveld (1970, Fig. 3) correlates the prominent magnetitite seam in the Blood River valley and also to the east of Bothasberg with Magnetitite Seam 21 east of Tauteshoogte (ibid., p. 44) but notes the distinct differences between the two. The magnetitite seams between this seam and the Main Seam in the Stoffberg area are correlated with those of Subzone C farther north. On the basis of this correlation, the whole sequence between the Main Seam and Seam 21 is reduced by about 50 per cent, i.e. from 1870m to about 900m, whereas the olivine-diorites above Seam 21 in the northern section have a fourfold increase in thickness in the south. These tremendous variations in thicknesses between the various parts of the Upper Zone take place over a distance of only 10km whereas the total thickness of the Upper Zone decreases by only about 15 per cent over the same distance.

On the grounds of this rather small difference in total thickness, the author attempted a correlation based on certain marker horizons in both sequences and also on the appearance of certain cumulus phases (Fig. 25).

The magnetitite seams of Groeneveld's Subzone C occur about 200m above the Main Seam in the Stoffberg area, at a height which corresponds closely to Magnetitite Seams 6 and 7 in the northern section. Olivine appears in both sequences between 500-600m above the Main Seam, and the prominent magnetitite seam in the Blood River valley corresponds to a position of Seam 13 to the north. As already mentioned above, the mottled anorthosite which overlies this magnetitite seam in the south is very similar in appearance to that above Seam 13 to the north. In both sections, cumulus apatite appears about 250m above these seams.

If the composition of cumulus phases in the two sections, above and below horizons which can be correlated with certainty, as for instance the Main

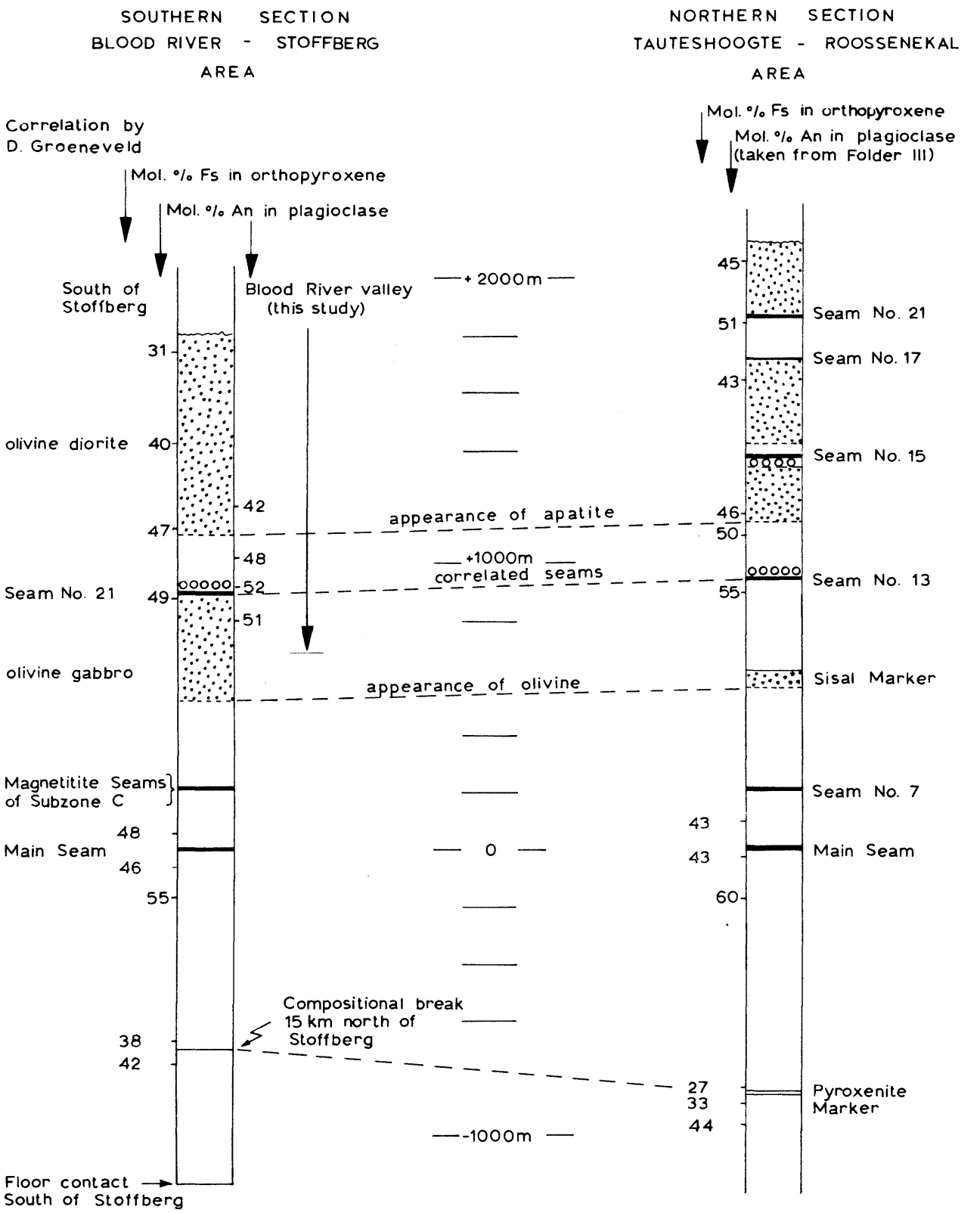

FIG. 25. DIAGRAMMATIC REPRESENTATION OF THE FACIES CHANGE IN THE BUSHVELD COMPLEX. LEFT-HAND COLUMN AND COMPOSITION OF CUMULUS PHASES FROM AREA SOUTH OF STOFFBERG AFTER GROENEVELD (1970, FIG. 1, 2 AND 3)

Magnetitite Seam and the compositional break at the Pyroxenite Marker are compared, an increase in the less refractory components of these phases from north to south is noted.

The thickness of the complete succession of rocks of the Layered Sequence south of Stoffberg is given by Groeneveld as being about 3000m (ibid., Figs. 2 and 3) which is considerably thinner than the Layered Sequence farther to the north. This is probably due to lateral extension of the magma chamber during crystallization which may have been caused by an influx of large quantities of fresh, undifferentiated magma. Lateral extension caused the magma to be emplaced in relatively cool environments and consequently conductive heat loss was more effective in the south than in the north where an extensive metamorphic aureole was already established in the over- and underlying rocks. It is therefore envisaged that a lateral temperature gradient existed in the magma, resulting in differences in composition of cumulus phases which settled simultaneously in the two areas.

Lateral cryptic variation of cumulus phases has been described by Hughes (1970, p. 323) from the Great Dyke. He found that in the lower rhythmically layered sequence of the Hartley Complex, the orthopyroxene in correlated layers changes in composition from the centre to the margin of the complex. In the marginal areas the orthopyroxene contains on an average, between 4-6 per cent less of the En molecule than in the central portion some 120km away. This is considered by him to be due to a more rapid decrease in temperature in a thinner body of basic magma that gave rise to a condensed sequence in the marginal areas of the complex compared to the central area.

Another explanation for the observed lateral cryptic variation in the Bushveld Complex is the influx of fresh, undifferentiated magma in the central portion of the chamber, thus pushing the existing differentiated magma outwards into the marginal areas. This would result in a change in composition of the magma from north to south, a possibility already mentioned in the section dealing with the rock types at the top of Subzone B of the Main Zone. The appearance of cumulus apatite at the same height in the intrusion in both sequences militates against such differences in composition. If the magma in the south were more differentiated than that in the north, cumulus apatite would be expected to appear at a lower position in the southern sequence. As this is not the case, the phosphorus concentration in the magma is considered to be the decisive

factor in the proposed correlation. Fractional crystallization caused a gradual enrichment of the phosphorus content in the remaining magma which reached saturation at the top of Subzone C. Cumulus apatite is therefore present in the overlying rocks in both sections, but owing to differences in temperature during crystallization of correlated horizons in the two sequences, apatite is associated with lower-temperature phases in the south and with higher-temperature phases in the north.

This difference in temperature and consequent crystallization of less refractory phases in the south also had a pronounced effect on the succession of rock types in the two sequences. Crystallization of lower-temperature phases extracted more iron from the magma in the south than in the north with the result that the crystallizing magma in the north was enriched in iron. Small periodic increases in the oxygen pressure (Osborn, 1962, p. 221-225) gave rise to the lower magnetitite seams of Subzone C in the north, but did not cause the formation of magnetitite seams in the cooler, less iron-rich magma in the south. Crystallization of the ferromagnesian silicates, although Fe-rich, probably also led to some increase in the Fe-content of the magma in the south, so that the upper magnetitite seams of Subzone C are developed in both areas. The absence of magnetitite seams of Subzone D in the south may possibly also be due to extraction of sufficient iron from the magma during crystallization of the ferromagnesian silicates.

6. Mafic pegmatoids in the Layered Sequence

a) Magnetitite pipes

A striking feature of the area is the presence of numerous magnetitite pipes of which more than 100 were encountered in the field. Most of these are shown on the map (Folder I) and many occurrences indicated by one pipe actually consist of a cluster of a few small pipes (Fig. 26). The largest one is situated 100m east of Mapochsgronde 500 JS on the farm Klipbankspruit 76 JT (Fig. 27) and measures about 30m in diameter. The majority of pipes are however considerably smaller and the presence of some is indicated only by a few large boulders of magnetitite in the field. They are mostly circular in outline, but one elongated dyke-like pipe, 7m wide and 35m long is situated about 0,5km west of Galgkop on Mapochsgronde 500 JS.

The magnetitite pipes are encountered from the middle of Subzone B of the Main Zone up to Subzone D of the Upper Sone. The lowest occurrence consists

Fig. 26. A cluster of several small magnetitite pipes in the Upper Zone on Onverwacht 148 JS. Rocks in foreground are magnetite gabbro of Subzone C. Prominent ridge in middle distance is olivine-diorite at the base of Subzone D. Sekhukhune Plateau in background.

Fig. 27. A prominent magnetitite pipe on Klipbankspruit 76 JT. In the distance on the left are sediments of the Pretoria Series and on the right gabbros of the Main Zone.

of a cluster of small pipes, not far south of the beacon CH-IN 11 on the farm Uysedoorns 47 JT, whereas the highest plug is situated on the horizon of Magnetitite Seam 21 on the farm Steynsdrift 145 JS.

According to Willemse (1969b, p. 192) diallagite pegmatoid is sometimes found associated with these magnetitite pipes, but owing to the extensive magnetitite rubble which surrounds these pipes, no such rock type was observed in this area.

The distribution of the magnetitite pipes, most of which occur in two well-defined zones in the sequence, is of interest. The lower concentration of pipes is situated in Subzone C of the Main Zone, east of Roossenekal, whereas the upper concentration of pipes is at a horizon above and below Magnetitite Seam 8 in the Upper Zone. This distribution of the pipes would seem to favour the contention of Willemse (1964, p. 118) that their magma could have originated by a process such as filter-pressing or lateral secretion leading to a concentration of iron-rich fluids. Such a process would depend on the amount and composition of intercumulus liquid present in the crystal cumulate, and the forces by which these liquids were concentrated to escape to higher levels in the form of pipes. On a relatively small scale such a process could have given rise to single pipes, or, on a more regional scale, a concentration of pipes at certain horizons, as described above, could have originated.

The distribution in the sequence of the majority of magnetitite pipes in this area contradicts Coertze's (1962, p. 256) hypothesis that their emplacement was controlled by fault-zones, as no such faulting, with which the pipes could be associated, was observed.

b) Vermiculite-bearing pegmatoids

Two vermiculite-bearing pegmatoids are located in this area. One is situated close to the Erts Railway Station on the horizon of the feldspathic pyroxenite of the Upper Zone, whereas the other one occurs 3km south of Roossenekal, in the middle of Subzone B of the Main Zone (Folder I). According to the residents of the area, three additional pipes are known, all of which fall outside the area mapped. Of these, two are apparently situated north of Laersdrif and one north of the Mapochs Dam.

The first mentioned occurrence was investigated in some detail by Willemse (1953, p. 3-9). He considers it to be pipe-like in form and to transgress the layering of the country-rocks. Associated coarse-grained pyroxene

crystals suggest, according to him, pegmatitic affinities of the rocks and a possible genetic relationship to diallagite pegmatoids which occur widely in the Bushveld Complex. Investigation of the physical properties of the vermiculite (ibid., p. 5-6) revealed it to be of a quality inferior to that from Phalaborwa, owing to an exfoliation factor which is only about half of that of the latter occurrence.

Gossans carrying chalcopyrite and malachite were also described by him (ibid., p. 7) from this locality. Analyses of the ore showed that it contains, apart from Cu, small quantities of Au and Ag, but negligible amounts of Pt and Ni.

Prospecting operations which started a few months ago, revealed additional interesting information about the pipe. For the greater part it seems to consist of intensely brecciated country-rock (Fig. 28). Unfortunately the big chunks of gabbroic rock are strongly weathered and it was not possible to determine the composition of cumulus phases in order to decide whether they were derived from lower horizons. Their angular nature would, however, indicate that they were not derived from any great depth, as is the case with the perfectly rounded inclusions in a similar pipe on Tweefontein 360 KT, close to the famous chromite occurrence at the Dwars River bridge (Ferguson and McCarthy, 1970, p. 75).

The large boulders of gabbroic rocks are embedded in diallagite pegmatoid which is mostly altered to brown amphibole. Occasional green malachite staining of this amphibole indicates that the pegmatoidal liquids also contained some copper and sulphur. On surface this gives rise to the Cu-bearing gossan described by Willemse. Crystals of magnetite and vermiculite are present in this amphibole-rock, but the bulk of the vermiculite occurs as large pockets, a few metres in diameter in the zone of brecciation (Fig. 29).

On the northern side of the present prospecting pit, an extremely magnetite-rich, vermiculite-bearing pegmatoid cuts across the zone of brecciation (Fig. 30). This pegmatoid contains, apart from books of vermiculite approximately 30cm in diameter, also smaller plates of this mineral in the magnetite. The magnetite of this pipe is extremely coarse-grained and forms crystals of up to 3cm in diameter, which indicates that it is not part of a magnetitite seam as previously believed by Willemse (1953, p. 4) but part of the pegmatoid.

The observed relationships point towards a forceful injection of the peg-

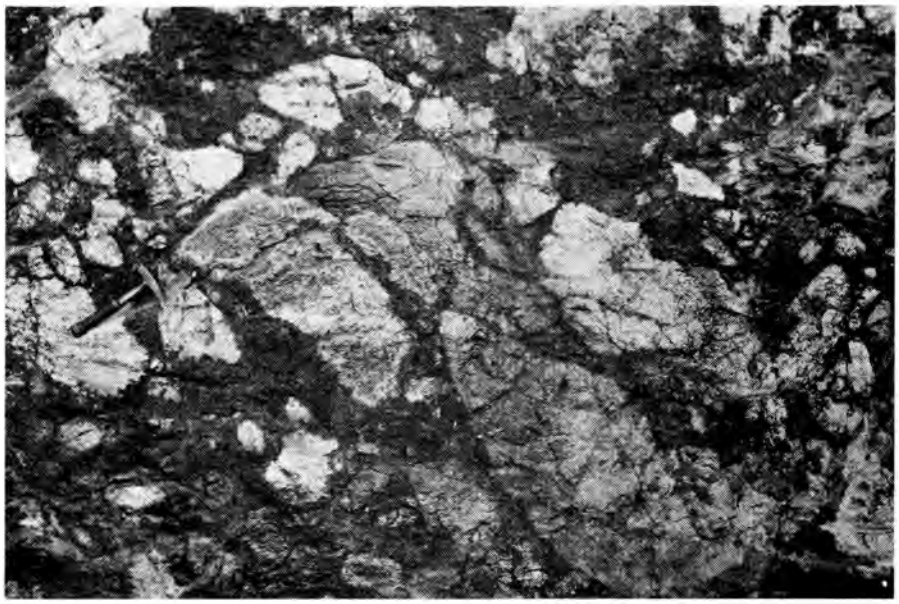

Fig. 28. Brecciated country-rock of the vermiculite-bearing pegmatoid west of Roossenekal. The matrix is amphibolized vermiculite-bearing diallagite pegmatoid.

Fig. 29. A large pocket of very coarse-grained vermiculite (bottom). Vermiculite-bearing pegmatoid west of Roossenekal.

matoid. It is envisaged that aggregation of volatile-rich intercumulus liquids took place at a lower horizon. The pressure of these liquids must have been higher than the load pressure and they probably intruded the overlying rocks in a pipe-like vent, simultaneously brecciating the country-rocks. The pipe itself is now filled with vermiculite and diallagite-bearing magnetitite whereas large pockets of vermiculite also crystallized in the surrounding zone of brecciation.

Only portions of this pipe have so far been opened up by exploration, and the actual shape is therefore not yet known, as it does not outcrop on surface. The width has been traversed by a wide trench, about 25m long. Excavation parallel to its major axis has not exceeded 30m at the time of writing, but the pipe seems to be elongated in a N-S direction.

The presence of the vermiculite pipe south of Roossenekal is indicated by small dumps of this mineral. No further information about this pipe could be obtained as prospecting operations ceased a long time ago and the pits have since fallen in.

The association of magnetitite with vermiculite and diallagite pegmatoid in these pipes clearly indicates that a genetic relationship exists between the various pipe-like bodies frequently encountered in the Bushveld Complex, as was envisaged by Willemse (1970a, p. 11).

c) Anorthositic pegmatoid

Coarse-grained anorthositic rocks are occasionally encountered in Subzones C and D of the Upper Zone. They usually outcrop as fairly large boulders over areas a few metres in diameter and have no preferred orientation with regard to the layering of the complex, or any preferred concentration with respect to position in this part of the Layered Sequence. In the field they are easily recognised by their light colour and large, anhedral crystals of plagioclase which may attain a length of 1cm or more.

Two specimens, G318 and G232 from close to the base of Subzone C on Onverwacht 148 JS and from the vicinity of Magnetitite Seam 20 on Duikerskrans 173 JS respectively, were investigated. In both occurrences the rocks consist of between 80-90 per cent of plagioclase, the core of which has a composition of about An_{62} whereas the mantle has an anorthite content of 52 per cent. The intercumulus minerals are, in order of decreasing abundance, green pleochroic hornblende, which in places contains small patches of clinopyroxene, quartz, magnetite and apatite.

Fig. 30. Magnetite-vermiculite-diallage pegmatoid (dark) cutting across brecciated country-rock (left). Shiny material at hammer and centre right is vermiculite. Vermiculite-bearing pegmatoid west of Roossenekal.

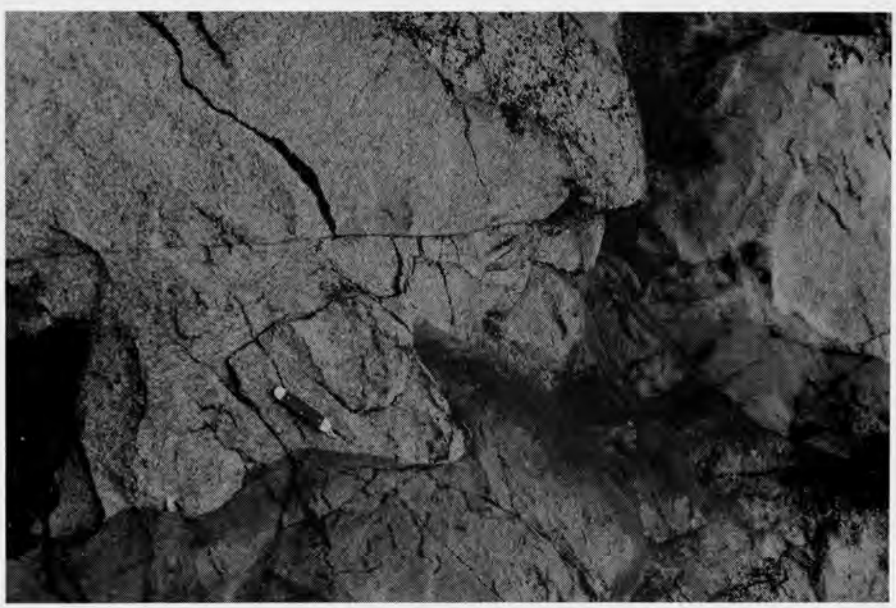

Fig. 31. Anorthositic pegmatoid (white) on Duikerskrans 173 JS. Note the coarse-grained nature of the pegmatoid and its sharp contact with the magnetite diorite (dark).

Of interest is the fact that the composition of the plagioclase in the pegmatoid is a few mol. per cent higher in anorthite than that of the surrounding country-rocks, and that they are often bent and saussuritized. The occurrence on Duikerskrans 173 JS has an irregular but sharp contact with the surrounding magnetite diorite (Fig. 31). Boshoff (1942, p. 53-55) also noted the presence of these rocks and found some of the plagioclase crystals to have a composition as high as An_{70-80}.

If these anorthositic rocks are pegmatoids of similar origin to the various other types in the Layered Sequence (Willemse, 1964, p. 118 and 1969a, p. 11) i.e. that they originated as a result of a concentration of volatile-rich intercumulus liquids and the emplacement of these into higher horizons, then the plagioclase is expected to be enriched in the albite molecule. However, as pointed out by Bowen and Tuttle (Wager and Brown, 1968, p. 387) the crystallization of a melt with moderate amounts of dissolved water, would, under sufficient load pressure, result in an increase in water and pH_2O in the remaining liquid and this in turn would have the effect of lowering the liquidus-solidus temperatures of the anorthite-albite system (Yoder et al., in Wager and Brown, 1968, p. 387). If, therefore, volatile-rich intercumulus liquid is expelled from the interstices of a pile of cumulus crystals, owing to an increase in the load pressure, and this liquid moves under pressure to higher levels in the intrusion, the plagioclase which crystallizes from it may have a higher anorthite content than that in the surrounding rocks. The bent plagioclase crystals and the associated hornblende indicate that the former were subjected to pressure and that the liquid from which they crystallized was enriched in water.

d) Diallagite pegmatoids

Two diallagite pegmatoids are located near the northern boundary of the farm Pietersburg 44 JT (Folder I) but were not investigated.

V. STRUCTURE

The Layered Sequence of the Bushveld Complex generally strikes north-south and dips at low angles to the west. In the Leolo Mountains the dip is about 9-10° (Molyneux, 1970, Plate I) and it increases to between 12° and 15° in the Tauteshoogte-Roossenekal area and to 25° in the Stoffberg area (Groeneveld, 1970, p. 37). Owing to doming in the Marble Hall-Dennilton area, a shallow syncline was formed which is occupied in its central portion by the acid roof-rocks at Tauteshoogte in the north and Bothasberg in the south. Dips of the Layered Sequence west of Tauteshoogte are therefore to the east, but they swing to south-east in the direction of the Kruis River.

In order to obtain more information on the structural relationships and the sequence of rock types, the author mapped an additional small area between Tauteshoogte and Bothasberg. This has revealed that the two synclinal basins of Tauteshoogte and Bothasberg are separated by two shallow pitching anticlines (Fig. 32). The structure is complicated by several parallel faults which strike WNW - ESE. The downthrow side of the northern faults is to the south, whereas that of the southern faults is to the north. This has given rise to a graben parallel to the axes of the two pitching anticlines. These faults are situated along the continuation of, and have the same strike as the prominent Laersdrif Fault (Groeneveld, 1970, p. 38), the downthrow side of which is to the north. To the west they may possibly join up with the fault on Mineral Range 190 JS (Von Gruenewaldt, 1966, p. 95) which has the same strike and a downthrow to the south.

The most prominent fault of the area is the southward continuation of the Steelpoort Fault. Its downthrow side is to the north, and it has a horizontal displacement of about 2km in the north and about 3km in the south. Its throw is difficult to calculate because of the difficulty in obtaining dip measurements in the granophyre and leptite. The fault has a maximum horizontal displacement of about 9km farther north, where Molyneux (1970, p. 31) calculated its throw to be about 1000m. Its smaller horizontal displacement of only 2km on Groothoek 139 JS makes it doubtful whether it has a throw in excess of 500m. A prominent fault-breccia is developed on this farm (Fig. 12) on the lower slopes of Paardekop. Farther south, on Zaaiplaats 157 JS its presence is indicated by a prominent quartz vein which contains fragments of the surrounding country-rock. It dis-

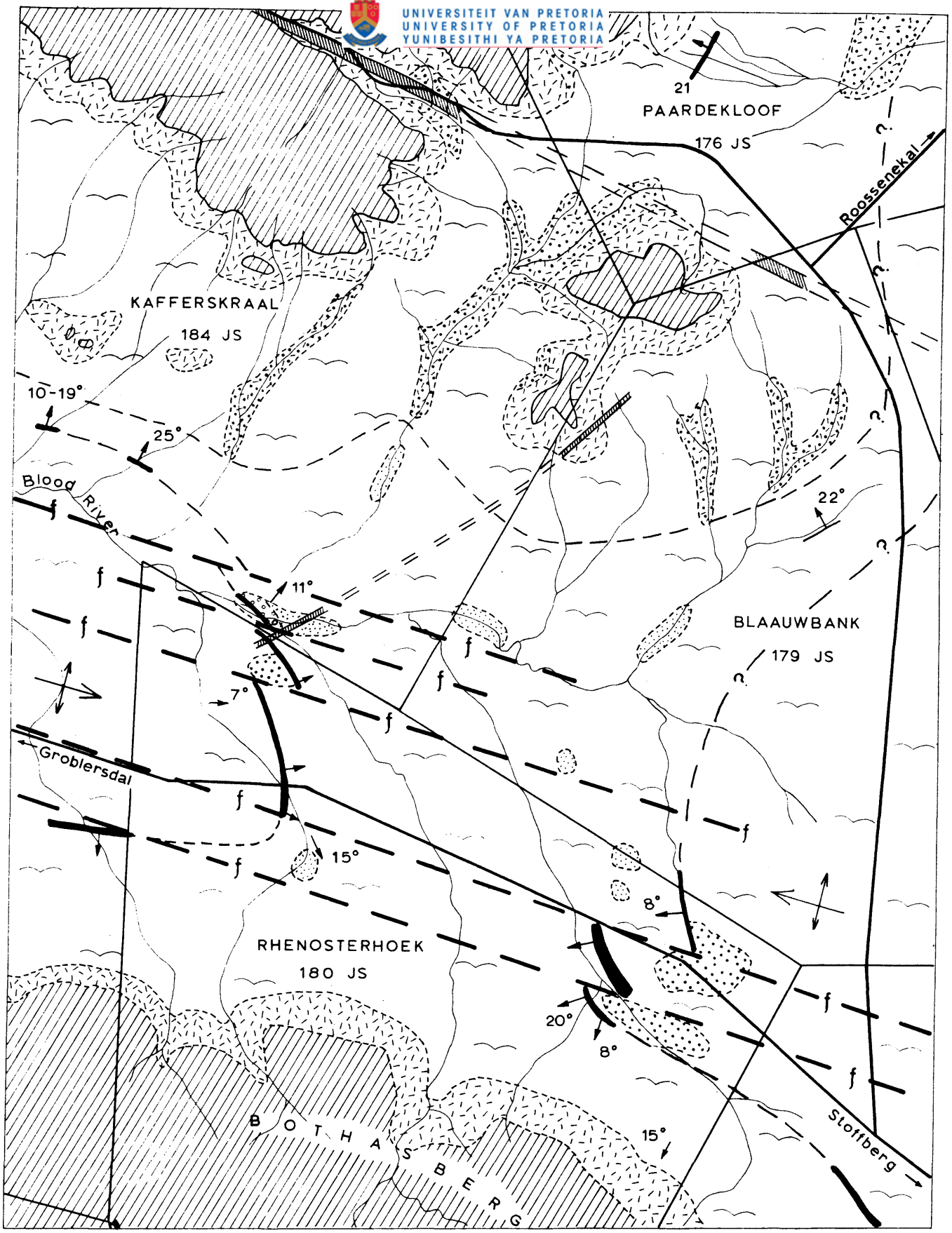

FIG. 32. STRUCTURAL MAP OF THE AREA BETWEEN TAUTESHOOGTE AND BOTHASBERG

LEGEND

Inferred fault —f—

Karroo dolerite

Roof-rocks

UPPER ZONE
- Diorite
- Olivine diorite
- Magnetite diorite
- Mottled anorthosite
- Magnetitite Seam
- Olivine gabbro

SCALE
1:50 000

0 1 2 3 4 5 km.

appears below a thick cover of alluvium on Buffelsvallei 175 JS where it is probably cut off at right angles by another fault (Von Gruenewaldt, 1966, p. 96) which strikes WNW - ESE. This latter fault was inferred by the author (ibid., p. 95) because the roof rocks north of the Blood River dip to the north, whereas rocks of the Main Zone occur south of it and have an easterly dip.

A number of smaller faults, all with their downthrow sides to the south are present on Mapochsgronde 500 JS where they displace the Main Magnetitite Seam and the over- and underlying rocks. All these faults strike parallel to the Steelpoort Fault and the Steelpoort Park Granite. A fault with similar strike, but with its downthrow side on the north, is present on Steynsdrift 145 JS where it displaces the uppermost magnetitite seam.

Some folding seems to be associated with the faults where the Mapochs River cuts across the Main Magnetitite Seam. The structure of this area is not clear, but it seems as if a shallow syncline and anticline are developed both of which dip at low angles to the north-west, i.e. perpendicular to the strike of the faults.

Duplication of parts of Subzone B of the Main Zone has already been mentioned previously as a possible explanation for its abnormal thickness of 1950m (Table II) which is about twice that in the area mapped by Molyneux. A possible strike-fault is indicated by the presence of a quartz vein on Draaikraal 48 JT, the continuation of which may be in the valley of the Klein Dwars River. The possible duplication due to this fault cannot be more than 350m because inverted pigeonite appears 350m upwards in the sequence west of the fault, whereas it is absent to the east of it.

Another possible fault could be situated in the valley of the Klip River as suggested by Willemse and Frick (1970, p. 164). Hammerbeck (1970, p. 299) reports shearing of the Steelpoort Park Granite where it is traversed by the Klip River but could find no evidence of any displacement. The very straight course of this river and the fact that its valley cuts obliquely across the strike of the Layered Sequence, seems to indicate the presence of a fault. Rocks to the east and west of the Klip River valley contain inverted pigeonite and seeing that the composition of the cumulus phases in rocks of Subzone B of the Main Zone do not change much with height in the intrusion (Folder III) it is impossible to determine whether any displacement has taken place. However, if a fault is developed, the maximum duplication may amount to about 300m. North of the

Steelpoort River, Molyneux (1970, p. 31) has located several strike-faults, the most prominent one of which is the Sekhukhune Fault. The downthrow side of this fault is to the west and it has a maximum throw of 2100m at Sekhukhune. To the south the effect of this fault decreases rapidly and at the Steelpoort River its throw is only 30m. The continuation of this fault south of the Steelpoort Fault coincides with the Klip River valley, although, if the Sekhukhune Fault does continue along this valley then its downthrow side must be to the east to cause duplication of the sequence.

These two postulated faults would still result in about 350m being unaccounted for if it is assumed that the thicknesses of the succession in the area north and south of the Steelpoort River remained the same. The thicknesses of Subzones A and C of the Main Zone agree very closely with those determined by Molyneux (Table II) and this would also favour faulting in this area, but until such time as more concrete evidence for faulting becomes available, the thickness of the Main Zone east of Roossenekal will be taken as 3940m.

A prominent joint system is clearly discernible on the aerial photographs of rocks of the Layered Sequence. The more prominent set strikes north-east to south-west, i.e., parallel to the majority of faults in this area, whereas the other set is developed at right angles to it.

VI. THE MINERALOGY OF THE LAYERED SEQUENCE

A. ORTHOPYROXENE

1. Introduction

An interest in the orthopyroxene-pigeonite relationships was stimulated by a study of rocks from the Main Zone of the Bushveld Complex in the Kruis River area (Von Gruenewaldt, 1966). Consequently, prior to the mapping of the area under consideration in this treatise, detailed investigations of the Ca-poor pyroxenes were started on specimens from different localities, especially from Dsjate 249 KT in Sekhukhuneland and from Bon Accord north of Pretoria. These earlier investigations have been supplemented by the results of the study of specimens from the Tauteshoogte-Roossenekal area. This has made it possible to reconstruct the sequence of events leading to the crystallization of pigeonite from the Bushveld magma. Portions of the results were published recently (Von Gruenewaldt, 1970).

2. Determinative methods

The composition of the orthopyroxene was determined from 2V measurements and by refractive index determinations of n_z. $2V_x$ measurements were made on grain-mounts of separated orthopyroxene and the values given in Appendix I represent the average values of between 8 and 10 direct readings of both optical axes under conoscopic illumination. The measurements were corrected for the set of hemispheres used with the aid of the diagrams constructed from the nomogram by Tröger (1959, p. 124) and the composition was evaluated by using the graph of Hess (Tröger, 1959, p. 59). Judging from the scatter of points on this graph (Deer et al., 1963, Fig. 10, p. 28) the accuracy of this method is probably greater than $\pm$ 5 mole per cent. In the compositional range Fs_{45-55} use was made of refractive index determinations by the immersion method. The liquids used were mixtures of monobromonaphthalene and methylene iodide, and the index of refraction of these mixtures was determined with a Leitz-Jelley refractometer. The accuracy of this method is considered to be $\pm$ 0,002 which corresponds to $\pm$ 3 mole per cent.

Five samples of separated orthopyroxene from Dsjate 249 KT were submitted for chemical analyses to the National Institute for Metallurgy. Separation to a purity of above 98,5 per cent was achieved with the Franz Isodynamic Separator, the only impurity being augite. The analyses given in Table III were

corrected for impurities by determining optically the composition of the co-existing augite. The analyses differ therefore slightly from those published recently (Von Gruenewaldt, 1970, p. 68) although the published Fe:Mg:Ca ratios are based on the corrected analyses. From the corrected analyses the structural formulae (Table III) were calculated using the method outlined by Hess (1949, p. 625).

3. Compositional Variations (Folder III)

No samples of the Merensky Reef were available from bore-hole PB1, but Roux (1968, p. 70) found that the orthopyroxene of this reef, directly east of the mapped area, has a composition of approximately Fs_{20}. The orthopyroxene in samples from the first 90m above the reef varies in composition between Fs_{20} and Fs_{25}. At 93m the composition rises abruptly to Fs_{34} and from the abundance of thick exsolution-lamellae of augite in the orthopyroxene, it is concluded that this is the first inverted pigeonite in the sequence. The presence of inverted pigeonite at this level in the intrusion is highly anomalous and no explanation for its presence can be offered at this stage. Plagioclase also changes in composition from An_{76} to An_{68} in these rocks. This zone is only a few metres thick and at its top the Fe-content of the orthopyroxene decreases gradually to Fs_{25}, 150m above the Merensky Reef. A similar break in the compositional trend was observed by Molyneux (1970, Fig. 12) about 300m above this reef on the Dsjate traverse.

From here onwards the composition of the orthopyroxene changes very gradually, apart from a small break about 1150m above the Merensky Reef (Folder III), to Fs_{44} below the fine-grained norite which underlies the Pyroxenite Marker of the Main Zone. The orthopyroxene of this fine-grained norite, although considerably enriched in the En molecule (Fs_{32-33}) is still inverted pigeonite but at the base of the Pyroxenite Marker the magma moved back into the field of crystallization of primary orthopyroxene with composition of Fs_{27}. These low Fs values are maintained upwards in the succession for about 300m from where the composition changes fairly rapidly to Fs_{44} below the Main Magnetitite Seam.

For the greater part of Subzones B and C of the Upper Zone, the composition of the orthopyroxene fluctuates between Fs_{40} and Fs_{46} and the iron content only increases to Fs_{50} in the topmost 100m of Subzone C. According to Molyneux (1970, p. 41) the erratic variation in composition of the orthopyroxene

in these two subzones may possibly be ascribed to the periodic extraction of iron from the magma during crystallization of the magnetitite seams. The pyroxenite of the Upper Zone (G649) in this area was found to contain inverted pigeonite (Fs_{43}) in contrast to the correlated horizon at Magnet Heights where it contains primary orthopyroxene (Molyneux, 1970, p. 41). The rocks of Subzone D only contain orthopyroxene for short distances above and below Seam 21. The composition of this orthopyroxene is Fs_{53} below the seam and changes rapidly to Fs_{62} (G368) about 40m above the seam. Molyneux (1970, p. 41) found orthopyroxene, 210m above Seam 21, to have a composition of Fs_{71}, which corresponds to the most Fe-rich intercumulus orthopyroxene in this area (Atkins, 1969, p. 241, ferrodiorite from Duikerkrans, S. A. 1143). Samples collected at higher levels than G368 and used in this investigation, did not contain any orthopyroxene.

4. Textural Features

a) General description of the textural variations

For the greater part of Subzone A of the Main Zone, the orthopyroxene is present as cumulus crystals, varying in size from about 1,6 x 0,7mm in the normal gabbroic rocks to 4,7 x 3,0mm in the so-called "porphyritic norites". The larger orthopyroxene grains usually contain small laths of plagioclase (Fig. 33) which would indicate that the latter was the first mineral to crystallize, and that the orthopyroxene had a higher growth rate. The size of the enclosed plagioclase laths may vary considerably, apparently depending on the time lapse between the onset of crystallization of the plagioclase and the onset of crystallization of the orthopyroxene.

There is an important textural change 1000m above the Merensky Reef, where the orthopyroxene changes from cumulus to intercumulus. The term "ophitic" would be more fitting for this texture because the orthopyroxene (Fs_{32}) forms units optically continuous over large areas which may completely enclose numerous plagioclase crystals (Fig. 34). In the field these units are readily recognizable because the parallel cleavage planes reflect the sunlight over areas up to 30cm in diameter on large boulders (Fig. 35). One hundred and fifty metres above the first appearance of ophitic orthopyroxene there is a compositional break (Folder III) and for 50m upwards typical cumulus orthopyroxene (Fs_{27}) is again encountered. Where the composition changes back to Fs_{32}, about 1200m above the Merensky Reef, the orthopyroxene is again "ophitic".

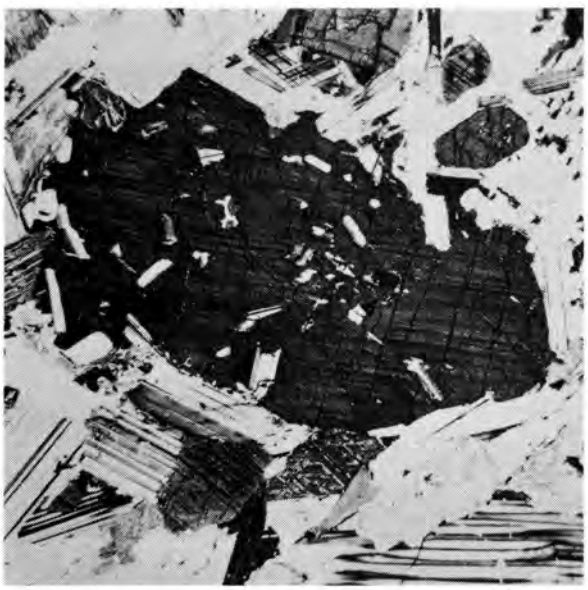

Fig. 33. Large orthopyroxene crystal which contains small inclusions of plagioclase. PB 3051. Crossed nicols, x12.

Fig. 34. Primary ophitic orthopyroxene. Specimen PB 717. Crossed nicols, x20.

Fig. 35. A large unit of similarly orientated orthopyroxene crystals which reflect the sunlight. Chieftains Plain 46 JT.

Almost simultaneously with this textural change of the hypersthene, the first inverted pigeonite appears in the sequence. This is characterized by the presence of numerous exsolution-lamellae of augite, which are considerably thicker than the fine striae common in primary orthopyroxene. The term "inverted pigeonite" is generally used for orthopyroxene which has originated from pigeonite owing to inversion of the latter (Brown, 1967, p. 349). This inverted pigeonite is present as small, irregularly shaped grains, usually enclosed in or surrounded by augite. It is very seldom found close to the primary ophitic orthopyroxene in thin sections. Two Ca-poor pyroxenes coexist for 1125mof the sequence in this area, i.e. up to the level in the intrusion where inverted pigeonite is the only Ca-poor pyroxene present. The change in composition of the orthopyroxene over this height is from Fs_{32} to about Fs_{37}.

Of interest is the observation that the level in the intrusion where inverted pigeonite becomes the only Ca-poor pyroxene, seems to rise from north to south. On the Dsjate traverse this level is taken at 1400m above the Merensky Reef (Molyneux, 1970, p. 33; Von Gruenewaldt, 1970, p. 69). On Mooimeisjesfontein, 50km south of Dsjate, Molyneux (1970, p. 33) records the appearance of inverted pigeonite 1900m above the Merensky Reef, whereas in this area, 40km south of Mooimeisjesfontein inverted pigeonite proper appears at 2325m above the Merensky Reef. In all three localities, the composition of this inverted pigeonite is about Fs_{36-37}. On Dsjate 249 KT, however, the first small grains of inverted pigeonite appeared at 1100m above the Merensky Reef with a composition of Fs_{33} for the primary hypersthene (Von Gruenewaldt, 1970, p. 69). This corresponds very closely to the appearance of inverted pigeonite in this area.

Inverted pigeonite is the only Ca-poor pyroxene up to the level of the Pyroxenite Marker, where primary cumulus orthopyroxene takes its place. From the Pyroxenite Marker up to the base of the Upper Zone there is a repetition of the observed textural features in the lower 3250m of the Main Zone. Cumulus orthopyroxene is present for 450m above the marker, where it is replaced by the ophitic variety. Simultaneously, small grains of inverted pigeonite, associated with clinopyroxene, make their appearance. Over the next 190m these two phases coexist, and from 50m below the Upper Zone inverted pigeonite (Fs_{37}) is the only Ca-poor pyroxene present in the remainder of the intrusion.

Characteristic of all the rocks in the sequence where cumulus inverted

pigeonite is developed, is the fact that they are present as groups of grains which possess similar orientations. This feature, together with the observed exsolution textures is discussed in detail in the following section.

In the rocks of the "orthopyroxene-pigeonite transition" (Folder III) there is a gradual change in the character of the ophitic hypersthene upwards in the succession. As mentioned already, at the base of this "transition zone", the orthopyroxene is typically ophitic. In this hypersthene the plagioclase has well developed crystal faces (Fig. 34), but at succeedingly higher levels the boundaries between the plagioclase and the ophitic orthopyroxene become more and more irregular. Gradually the ophitic hypersthene takes on the shape of separate cumulus crystals, although still optically continuous over large areas. This is termed "granular ophitic orthopyroxene" in Appendix I. Simultaneous with this gradual change in the texture of the hypersthene there is an increase in the amount of exsolved blebs of augite (Fig. 36), but this amount remains considerably less than in the inverted pigeonite at higher levels. The texture of this hypersthene corresponds closely to the typical units of similarly orientated cumulus grains of inverted pigeonite (to be discussed in the ensuing section) except for the difference in the amount of exsolved augite. Small quantities of inverted pigeonite persist in these rocks. Only at about 2300m above the Merensky Reef does the exsolved augite in the hypersthene correspond to the quantities typical of inverted pigeonite.

From the observed textural relationships it seems as though there is a gradual transition from ophitic primary hypersthene to inverted pigeonite. This is apparent from the gradually increasing amounts of exsolved augite. Over this entire transition zone, pigeonite also crystallized from the magma. A possible explanation for the coexistence of inverted pigeonite and primary hypersthene, as well as for the observed textural features in this "transition zone" is given further below (p. 83).

b) Units of similarly orientated grains of inverted pigeonite

All the gabbroic rocks of the Bushveld Complex which contain cumulus grains of inverted pigeonite are characterized by the occurrence of this mineral as groups of grains which possess similar orientations over large areas. These grains of inverted pigeonite usually contain two sets of exsolution-lamellae of augite. One set has the same orientation in each grain throughout the group or unit of inverted pigeonite grains, whereas the orientation of the second set of

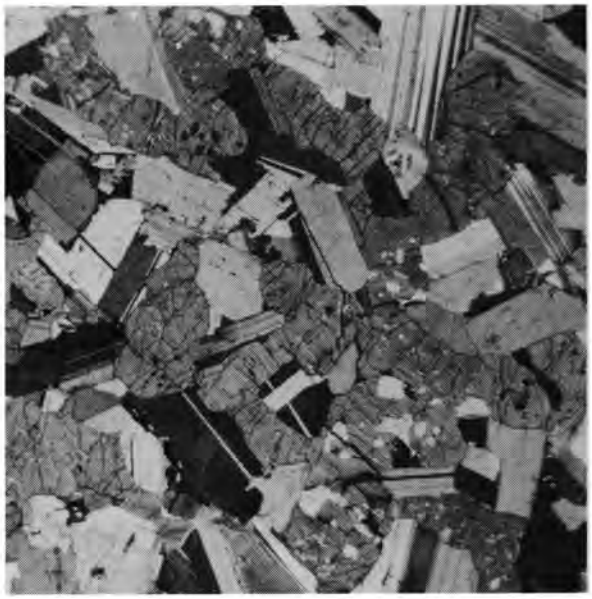

Fig. 36. Similarly orientated crystals of orthopyroxene (grey) which contain a few blebs of exsolved augite. G589, Uysedoorns 47 JT. Crossed nicols, x20.

Fig. 37. Several grains of orthopyroxene (in extinction) which together contain five sets of pre-inversion exsolution-lamellae of augite orientated at random and one set of post-inversion exsolution-lamellae of augite parallel to the (100) plane of the orthopyroxene. L13, Mineral Range 190 JS, Crossed nicols, x35. (Taken from Von Gruenewaldt, 1970, Fig. 1, p. 67).

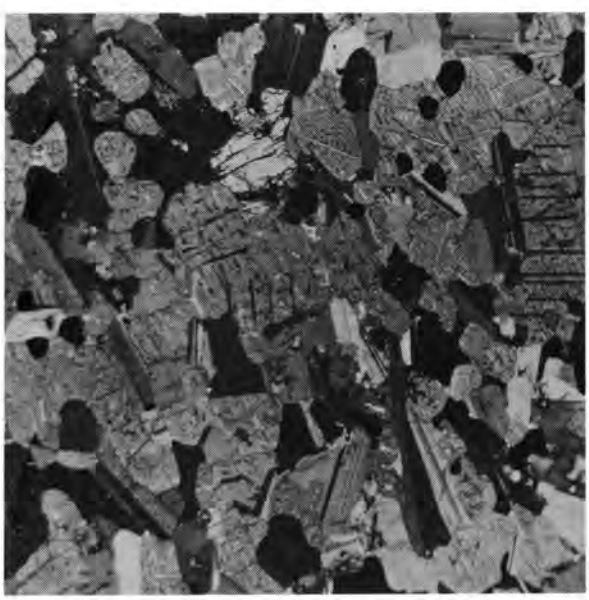

Fig. 38. A group of similarly orientated grains of orthopyroxene (grey) which contain pre- and post-inversion exsolution-lamellae of augite. G314, Luipershoek 149 JS. Crossed nicols, x20.

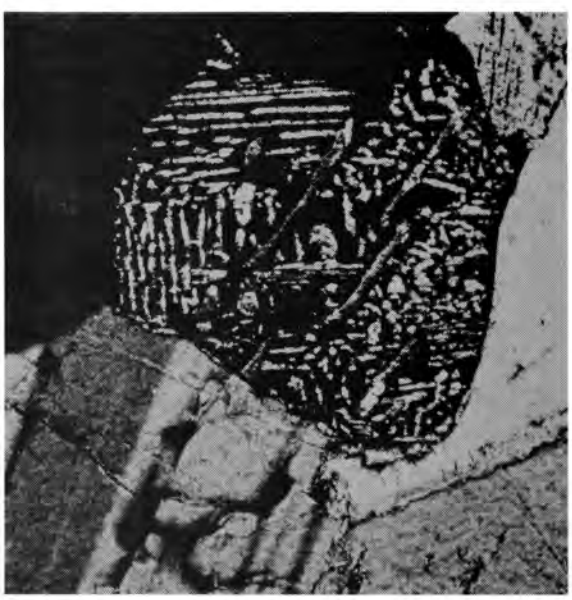

Fig. 39. A grain of inverted pigeonite (in extinction) which contains two sets of post-inversion exsolution-lamellae of augite. Horizontal lamellae parallel to (100), vertical lamellae parallel to (001), diagonal lamellae exsolved prior to inversion. G460, Mapochsgronde 500 JS. Crossed nicols, x75.

exsolution-lamellae differs from grain to grain in the same unit (Fig. 37). It was found without exception that the former set of exsolved lamellae of augite is orientated parallel to the (100) plane of the orthopyroxene host and that the latter set of exsolution-lamellae, which are usually much broader, is orientated at random in the orthopyroxene.

Augite usually exsolves as lamellae parallel to the (001) plane in pigeonite. According to Poldervaart and Hess (1951, p. 482), these lamellae are retained after inversion to orthopyroxene along a relict (001) plane, a plane near to (101) in the orthopyroxene. Bruynzeel (1957, p. 509) found that these pre-inversion exsolution-lamellae lie closer to the (102) plane of the orthopyroxene. This was not observed in the thin sections investigated from the Bushveld Complex, where most of the pre-inversion exsolution-lamellae of augite are orientated at random in the orthopyroxene.

Fortunately, the author had at his disposal the sections which were prepared for petrofabric analyses by Van den Berg (1946, p. 155). Two different types of stereographic plots were made from the majority of his sections. Firstly, the pre-inversion exsolution-lamellae were plotted with respect to the igneous layering (Fig. 40) and secondly, with respect to the orthopyroxene host (Fig. 41).

From Fig. 40, a compilation of a-, b- and c- petrofabric diagrams (see Van den Berg, 1946, p. 160), it can be seen clearly that the majority of the pre-inversion exsolution-lamellae have an orientation nearly perpendicular or perpendicular to the plane of igneous layering. Taking into consideration that these lamellae exsolved parallel to the (001) plane in pigeonite it is evident that most of the pigeonite grains represent settled crystals which came to rest on the magma floor with their major crystallographic axis (c-axis) parallel to the igneous layering.

Fig. 41 represents a compilation of a number of stereograms on which the pre-inversion exsolution-lamellae were plotted together with the optical orientation of the orthopyroxene host. This figure illustrates the random orientation of the pre-inversion exsolution-lamellae of augite in the inverted pigeonite. The tendency of these lamellae to be concentrated along a certain zone in the orthopyroxene cannot be ascribed to rules governing the inversion of pigeonite to orthopyroxene. Seeing that these plots represent the poles of the exsolution-lamellae, which, as stated in the previous paragraph, are orien-

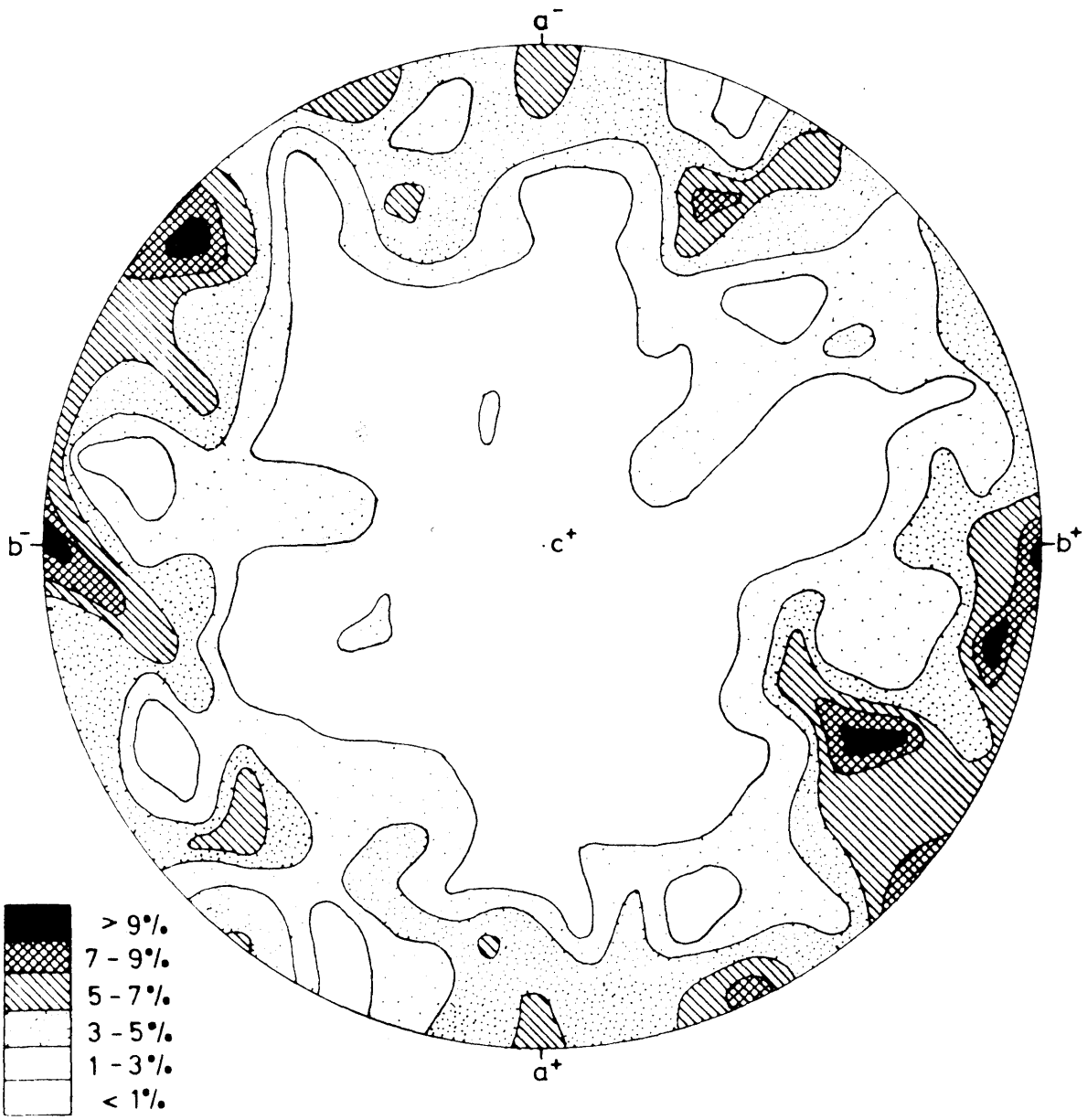

Fig. 40. Contoured distribution diagram of 227 pre-inversion exsolution-lamellae of augite in orthopyroxene, from Van den Berg's thin sections cut perpendicularly to the a, b and c fabric axes, a^+-a direction of dip, b^+-b^- strike, c^+-perpendicularly to layering.

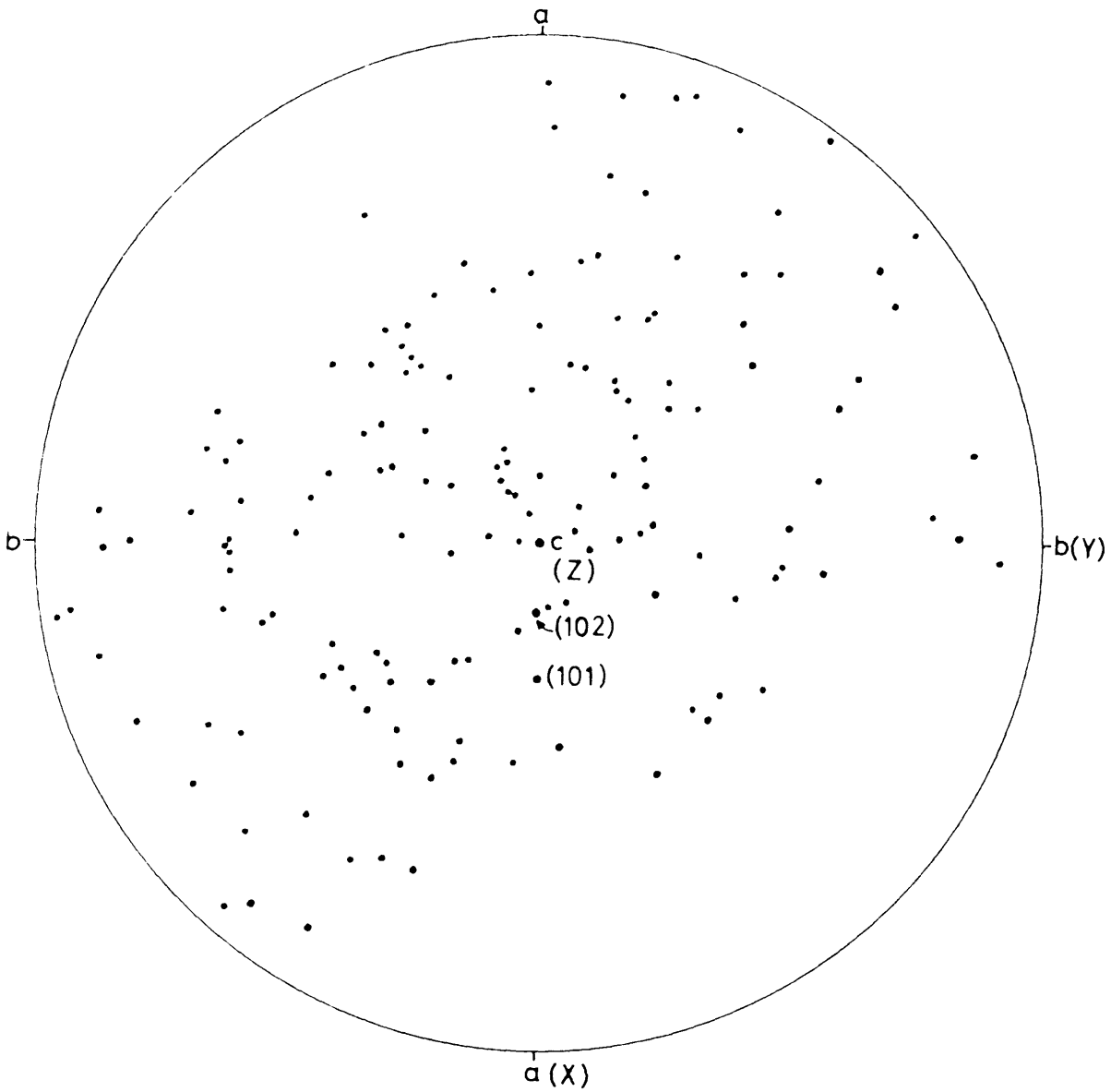

Fig. 41. Orientation of 149 pre-inversion exsolution-lamellae of augite in orthopyroxene from a number of Van den Berg's thin sections.

tated nearly perpendicular or perpendicular to the plane of layering, and seeing that the inverted pigeonites, although in groups, are orientated so that their major crystallographic axis lies close to or in the plane of layering (Van den Berg, 1946, p. 176, Fig. 18) a concentration of lamellae along a certain zone in the orthopyroxene is to be expected.

According to Poldervaart and Hess (1951, p. 482) the inversion of pigeonite to orthopyroxene develops in such a way that the b and c crystallographic axes of the parent-pigeonite are retained in the orthopyroxene. They do, however, describe exceptions to this rule. From Fig. 37 and from several other sections investigated from all over the Bushveld Complex, it seems as though the orientation of the inverted pigeonite bears no relation to that of the primary phase. This is not peculiar to the Bushveld Complex; it has been recorded from the Skaergaard Intrusion (Brown, 1957, p. 532-534), from Insizwa (Bruynzeel, 1957, p. 513) and from Ingeli (Maske, 1964, p. 61).

The same phenomenon was observed by Bowen and Schairer (1935, p. 151) who investigated the inversion relationship of orthopyroxene on heating. They found that orthopyroxene approaching the two end-members of the $MgSiO_3$-$FeSiO_3$ series are transformed readily into the monoclinic modification, whereas the intermediate members are only transformed with the aid of a flux and that "in general, a single crystal or crystal fragment of the orthorhombic pyroxene is transformed into an aggregate of several grains of monoclinic pyroxene of random orientation with respect to each other and to the original orthorhombic substance" (ibid., p. 169). They ascribe the sluggishness of the inversion of the intermediate members to structural complexities and to the steady decline in the inversion temperature with enrichment in iron.

Brown (1967, p. 351), who investigated experimentally the inversion relationship of pigeonite and orthopyroxene on natural, inverted pigeonites, found that in the absence of a flux the inversion was sluggish and that the reaction took place over a long period of time at elevated temperatures. In the presence of a liquid of composition similar to that of the magma from which the investigated natural pyroxenes had crystallized, the inversion took place readily, and at much lower temperatures than in the absence of liquid.

As mentioned previously, the groups of grains of inverted pigeonite possess the same optical orientation over large areas (Fig. 38). The grains of each group extinguish simultaneously or very nearly so, but differ in orientation

from grains of another group. This was previously observed in gabbroic rocks from the Bushveld Complex by B. V. Lombaard (1934, p. 26), Van den Berg (1946, p. 176), A. F. Lombaard (1949, p. 353), Raal (1965, p. 16) and Von Gruenewaldt (1966, p. 84) as well as by Maske (1964, p. 61) in similar rocks from the Ingeli Mountain Range. The size of these units varies considerably, but may attain a diameter of a few centimetres. Van den Berg (1946, p. 178) counted as many as 80 individual grains, in one thin section, all belonging to the same group.

To explain the random orientation of the pre-inversion exsolution-lamellae of augite in inverted pigeonite groups from Ingeli, Maske (1964, p. 61) suggests that, owing to the sluggishness of the structural rearrangement, inversion did not take place at the appropriate temperature. He is of the opinion that primary hypersthene was one of the first minerals to be precipitated from the interstitial liquid around the grains of pigeonite below the inversion temperature and thus formed rims free from lamellae. This stable orthorhombic phase would then start the inversion of the pigeonite in such a manner that the orientation of the secondary orthopyroxene would be continuous with the mantles of late hypersthene. This explanation is not applicable to the units of inverted pigeonite in the Bushveld Complex because of the absence of mantles of orthopyroxene free from lamellae, and because the units seem to have common orientations with their crystallographic c-axes parallel to the plane of igneous lamination.

It seems obvious that before inversion the orthopyroxene units consisted of several cumulus crystals of pigeonite. On cooling, lamellae of augite were exsolved parallel to the (001) plane of each pigeonite grain. When the inversion temperature was reached, directed pressure due to the accumulating superincumbent mass developed, and the first pigeonites to invert were probably those which, after inversion, produced an orthopyroxene with an orientation most stable under the prevailing conditions of pressure. This was not difficult to achieve, because many of the pigeonite crystals were favourably orientated (Fig. 40). All the grains with different orientations would take longer to invert owing to the sluggishness of inversion which probably took place in the absence of a flux, i. e. after most of the intercumulus liquid had already crystallized. As the pigeonite grains were probably in contact with one another, the first-formed orthopyroxene could set off the inversion in the adjoining grains, which would adopt an orientation continuous with that which started the reaction. This

process would then continue until all the pigeonite grains were inverted and this would result in groups of similarly orientated grains of inverted pigeonite which contain pre-inversion lamellae of augite orientated at random. On further cooling, more augite was exsolved parallel to the (100) plane of the inverted pigeonite. These post-inversion exsolution-lamellae of augite therefore have the same orientation throughout a unit. In a few sections a second set of post-inversion exsolution-lamellae was observed (Fig. 39) and is exsolved parallel to the (001) plane of the inverted pigeonite.

A. F. Lombaard (1949, p. 353 and Fig. 2) describes several adjacent grains of inverted pigeonite of different orientation. They contain parallel pre-inversion exsolution-lamellae of augite with the same optic orientation, which pass from one grain into another. In this case, a single grain of pigeonite evidently produced on inversion several grains of orthopyroxene of different orientation. This has also been observed in some of the thin sections investigated by the author, but is not very common. It seems as though the inversion was not always influenced by directed pressure from the accumulating crystal mass which might be due to a very stable framework of feldspar crystals.

5. The phase-change from orthopyroxene to pigeonite

The application of the experimentally observed relationships in the pyroxene quadrilateral to natural pyroxenes revealed important information on the crystallization trends during fractionation of a basaltic magma. In this regard, the early work of Hess (1941) and of Poldervaart and Hess (1951) is noteworthy. These authors showed that particular exsolution textures in the pyroxenes could be related to various stages of fractional crystallization, and Brown (1957, p. 527) related these exsolution textures to the cooling history of the Skaergaard magma.

Hess (1941, p. 583 and 1960, p. 40) and Brown (1957, Fig. 5, p. 530) related the inversion curve of Bowen and Schairer (1935) to crystallization temperatures of natural pyroxenes in the Bushveld, Stillwater and Skaergaard Intrusions. Yoder and Tilley (1962, p. 390-391) and Yoder and others (1963, p. 90) have shown that, owing to the uncertainty of the nature of the inversion, inversion temperature, pressure effects and the uncertainty of the influence of the $CaSiO_3$ component, magma temperatures cannot be estimated from the orthopyroxene-clinopyroxene inversion.

Recently, Brown (1967, p. 451) has reinvestigated the inversion relation-

ships of natural pyroxenes in the presence of andesitic liquid. He found that a pigeonite from the Bushveld Complex with composition $En_{40}Fs_{60}$ (wt. per cent) crystallized from a liquid of ferrodioritic composition at between 1050^{o} and $1060^{o}C$ at atmospheric pressure. This inverted pigeonite (S. A. 616) was collected by Atkins (1969, p. 232) from Subzone B of the Upper Zone, probably at a horizon between the uppermost magnetitite seam (No. 7) of Subzone B and the base of Subzone C. Inversion of this pigeonite to the orthorhombic phase took place at $1000^{o}C$, at atmospheric pressures and would correspond to an inversion temperature of $\pm$ $1025^{o}C$ at a pressure of 3-4 Kb (Brown, 1967, Fig. 10, p. 350) which is an estimate for this level in the intrusion.

Owing to the uncertainty which prevailed prior to detailed studies of the Main Zone (Molyneux, 1970 and this investigation) about the composition and the height in the intrusion at which pigeonite appears in the sequence, a number of specimens was collected by the author early in 1968 along a road which traverses the Main Zone on Dsjate 249 KT in the Leolo Mountains (Fig. 42). These samples were supplemented by those collected by Dr. L. Liebenberg along the same road.

Five samples of orthopyroxene from the Dsjate traverse were analysed by the National Institute for Metallurgy. The results as well as the structural formulae and the Fe:Ca:Mg ratios are given in Table III. The Fe:Ca:Mg ratios of these new analyses, as well as those of previously published analyses (Table IV) are plotted on Fig. 43 on which the trend of crystallization of Ca-poor pyroxenes was inferred from these analyses and from optical determinations of orthopyroxenes which were not analysed. The thin dotted lines on this diagram are not tie-lines between coexisting pairs of Ca-poor pyroxenes, but are the minimum and maximum Fe/Mg ratios at which primary hypersthene and inverted pigeonite were found to coexist in the rocks from Dsjate and from the area investigated in this study. The Fe/Mg ratio was derived in both instances from the more abundant primary hypersthene.

The results obtained from the study of the rocks from Dsjate were substantiated by the study of the rocks from the Roossenekal area (see p. 68). On Dsjate cumulus orthopyroxene (G10) is replaced by ophitic orthopyroxene (G9) about 750m above the Merensky Reef.

Ophitic orthopyroxene was found to be the only Ca-poor pyroxene up to a Mg:Fe ratio of 63:37, but at a higher Mg:Fe ratio small crystals of inverted

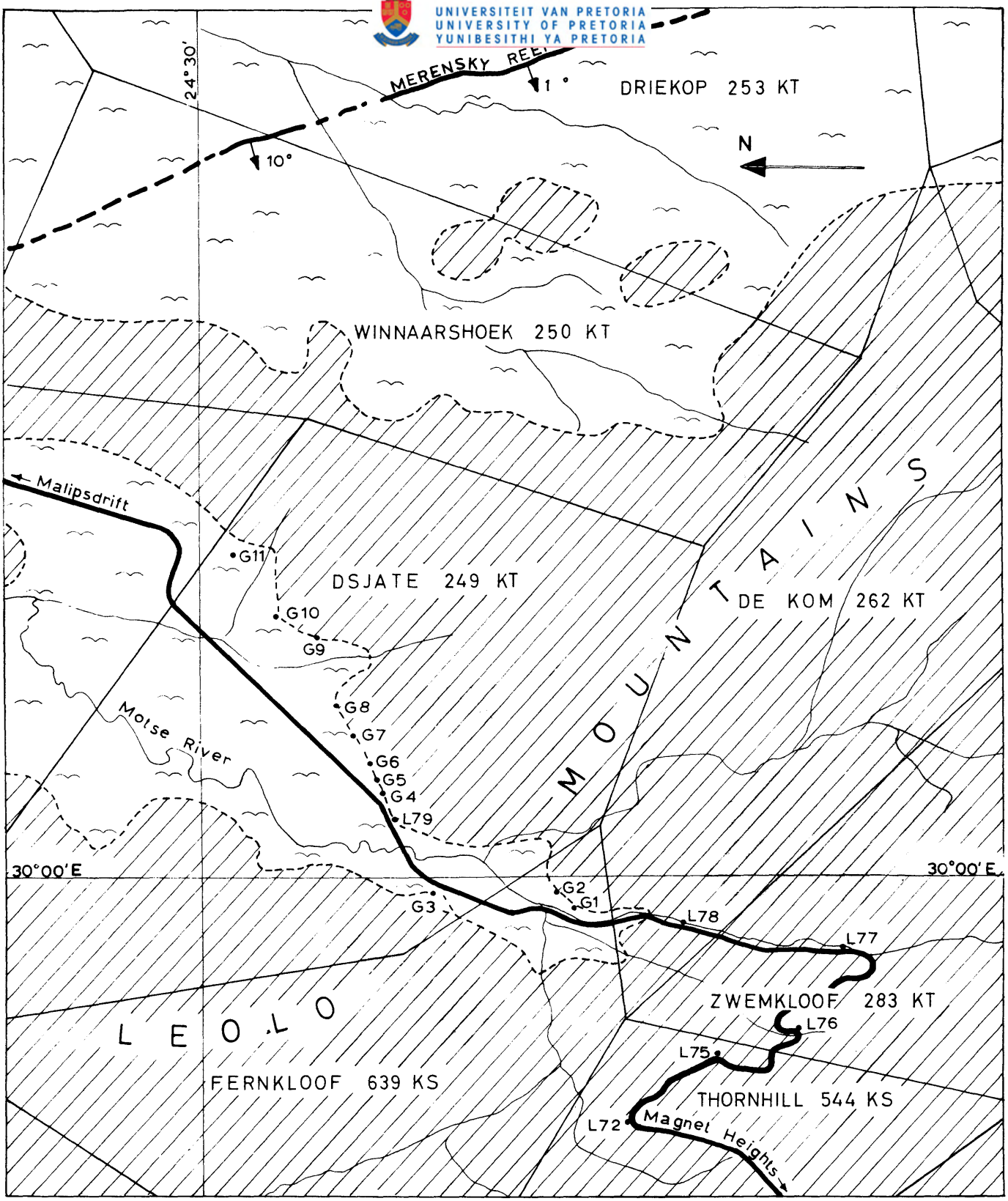

FIG. 42. MAP SHOWING LOCALITIES OF SAMPLES COLLECTED ON DSJATE 249 KT AND VICINITY

SCALE 1:50 000

TABLE III CHEMICAL ANALYSES AND STRUCTURAL FORMULAE OF ORTHOPYROXENE FROM THE EASTERN TRANSVAAL

		G10	G8	G7	G6	L77
	SiO_2	53, 71	53, 93	53, 04	52, 83	53, 34
	TiO_2	0, 25	0, 42	0, 30	0, 30	0, 30
	Al_2O_3	1, 33	1, 30	1, 38	1, 41	1, 52
	Fe_2O_3	1, 37	1, 31	1, 71	1, 52	1, 69
	FeO	16, 05	15, 43	17, 05	18, 12	16, 23
	MnO	0, 36	0, 40	0, 43	0, 44	0, 46
	MgO	25, 03	25, 06	24, 15	23, 20	23, 14
	CaO	1, 10	1, 39	1, 19	1, 35	2, 60
	Na_2O	0, 47	0, 55	0, 39	0, 43	0, 54
	K_2O	0, 10	0, 09	0, 09	0, 08	0, 08
	H_2O	n. d.	n. d.	n. d.	n. d.	n. d.
		99, 77	99, 88	99, 73	99, 68	99, 90
	Atomic per cent					
	Ca	2, 3	2, 8	2, 4	2, 7	5, 3
	Mg	70, 0	70, 4	67, 6	65, 7	65, 6
	*Fe	27, 7	26, 8	30, 0	31, 6	29, 1
	Numbers of ions on the basis of 6 oxygens					
Z	Si	1, 959	1, 961	1, 948	1, 953	1, 956
Z	Al	0, 037	0, 036	0, 049	0, 044	0, 044
WXY	Al	0, 021	0, 021	0, 012	0, 018	0, 022
WXY	Fe^{3+}	0, 038	0, 035	0, 048	0, 041	0, 048
WXY	Fe^{2+}	0, 489	0, 469	0, 524	0, 560	0, 497
WXY	Mn	0, 014	0, 013	0, 014	0, 014	0, 014
WXY	Mg	1, 360	1, 358	1, 322	1, 277	1, 264
WXY	Ca	0, 044	0, 054	0, 046	0, 053	0, 101
WXY	Na	0, 032	0, 039	0, 026	0, 029	0, 039
WXY	K	0, 004	0, 004	0, 004	0, 004	0, 004
WXY	Ti	0, 008	0, 011	0, 009	0, 009	0, 009
	Z	1, 996	1, 997	1, 997	1, 997	2, 000
	WXY	2, 010	2, 004	2, 005	2, 005	1, 998

*Fe = Fe^{3+} + Fe^{2+} + Mn

TABLE III (continued)

G10 Hypersthene from norite, 700m above Merensky Reef. Dsjate 249 KT, Lydenburg district.

Analysis corrected for 1,5% augite of composition $Wo_{41}En_{44}Fs_{15}$.

G8 Hypersthene from norite, 850m above Merensky Reef. Dsjate 249 KT, Lydenburg district.

Analysis corrected for 1,18% augite of composition $Wo_{41}En_{44}Fs_{15}$.

G7 Hypersthene from hypersthene gabbro, 950m above Merensky Reef, Lydenburg district.

Analysis corrected for 0,87% augite of composition $Wo_{40,5}En_{42}Fs_{17,5}$

G6 Hypersthene from norite 1000m above Merensky Reef, Lydenburg district.

Analysis corrected for 0,57% augite of composition $Wo_{41,5}En_{41,5}Fs_{17}$

L77 Pigeonite inverted to hypersthene from fine-grained norite 1600m above Merensky Reef, Zwemkloof 283, KT, Lydenburg district. No impurities.

Analyses by the National Institute for Metallurgy, Johannesburg.

TABLE IV Ca:Mg:Fe RATIOS OF BUSHVELD ORTHOPYROXENE FROM PREVIOUSLY PUBLISHED ANALYSES

	1a	2a	3a	4a	5a	6a	7a	8a
Ca	2,8	3,1	2,3	2,8	2,2	2,9	8,4	7,6
Mg	85,0	83,3	75,0	77,7	72,0	60,4	55,4	40,7
Fe	12,2	13,6	22,7	19,5	25,8	36,7	36,2	51,7

1a Cumulus bronzite from bronzitite (7666) of the Basal Zone, Jagdlust. (Hess, 1960, p. 25).

2a Cumulus bronzite from bronzitite (S. A. 685) of the Basal Zone, Jagdlust (Atkins, 1969, p. 231).

3a Cumulus bronzite from gabbro (S. A. 660) of the Critical Zone, Jagdlust (Atkins, 1969, p. 231).

4a Cumulus bronzite from gabbro (S. A. 722) of the Critical Zone, Jagdlust (Atkins, 1969, p. 231).

5a Cumulus bronzite from gabbro (S. A. 733) of the Main Zone, Middelpunt (Atkins, 1969, p. 231).

6a Cumulus inverted pigeonite (S. A. 738) of the Main Zone, Blauwbloemetjeskloof (Atkins, 1969, p. 231)

7a Cumulus inverted pigeonite (7493) of the Main Zone, Pretoria district (Hess, 1960, p. 28)

8a Cumulus inverted pigeonite from ferrogabbro (S. A. 616), Upper Zone near Magnet Heights (Atkins, 1969, p. 231).

pigeonite are also developed. These two phases were found to coexist in specimens G2-G4, over 300m, and at a Mg:Fe ratio of approximately 65:35, pigeonite is the only Ca-poor phase present.

Although the position of L77 in Fig. 43 seems anomalous as this rock is from a stratigraphical position some 300m above the level at which primary hypersthene disappears, it indicates that pigeonite with a Mg:Fe ratio of 69:31 was precipitated from the magma and also that the more magnesian pigeonites contain less of the $CaSiO_3$ component than the more iron-rich varieties. This low Fe/Mg ratio for pigeonite may be explained in a similar way as that of the fine-grained norite underlying the Pyroxenite Marker in the Roossenekal area (see p. 88).

6. Coexisting inverted pigeonite and primary hypersthene

It has been recorded above that in parts of Subzones B and C of the Main Zone inverted pigeonite coexists with primary ophitic hypersthene. This association seems anomalous because experimental studies in the $CaSiO_3$ - $MgSiO_3$ - $FeSiO_3$ system on synthetic as well as natural pyroxenes (Bowen and Schairer, 1935, Yoder et al., 1963, p. 88-91; Brown 1967, p. 347) have shown that an inversion relationship exists between pigeonite and hypersthene. The temperature of this inversion drops with increase in the Fe-content of the Ca-poor pyroxene, and as a result of fractional crystallization of a basaltic magma the crystallization curve of the Ca-poor pyroxenes intersects the inversion curve at a specific Mg:Fe ratio which depends on the composition of the magma. If the magma is therefore in equilibrium with the crystallizing phases, as is generally assumed for slowly cooling intrusions like the Bushveld, then either primary hypersthene or pigeonite coexists with augite, but not both. Where non-equilibrium conditions prevailed, as during rapid crystallization in basaltic or andesitic lavas as well as in dolerites and diabases, primary orthopyroxene and pigeonite may be present in the same rock.

Recently, however, Nakamura and Kushiro (1970a, p. 275 and 1970b,

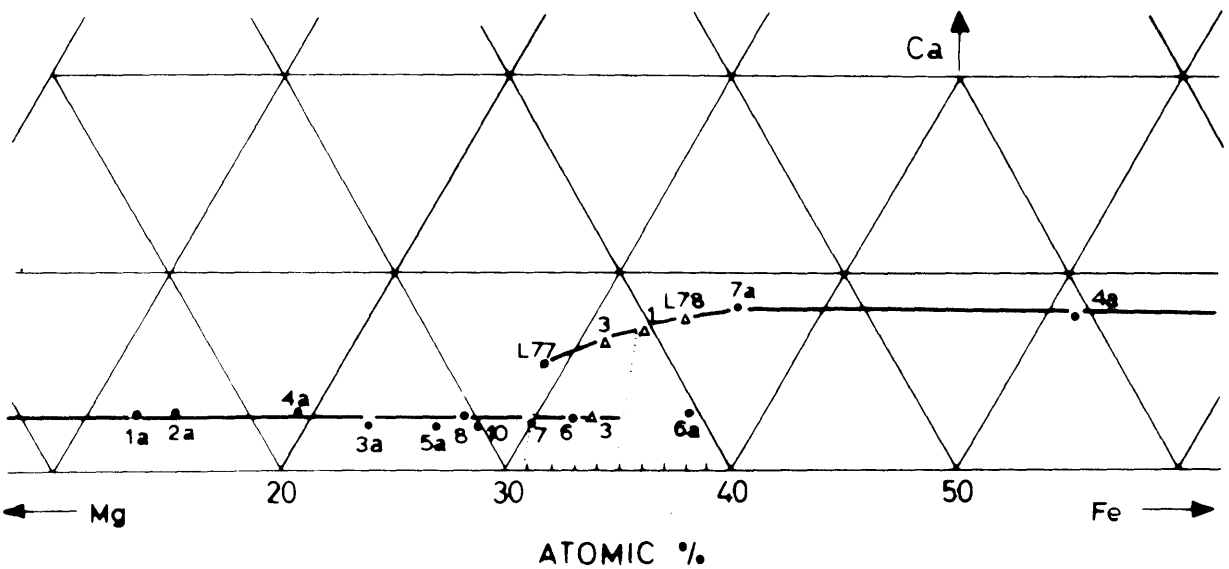

Fig. 43. Trend of Ca-poor pyroxenes from the Bushveld Complex. (Triangles denote that compositions were inferred from optical data.)

p. 2012-2014) have shown from textural relationships and chemical analyses of coexisting pyroxenes that the so-called "inversion interval" (Kuno and Nagashima 1952, p. 1001) between orthopyroxene and pigeonite is actually a hypersthene-pigeonite tie-line of the three-phase triangle augite-hypersthene-pigeonite. With the aid of their diagram (1970b, Fig. 11, p. 2013) reproduced here in a modified version as Fig. 44, it is possible to explain the coexistence of hypersthene and pigeonite in slowly cooled intrusions like the Bushveld.

Fig. 44b is the pyroxene quadrilateral in which the crystallization trends of Bushveld pyroxenes are indicated. The trend for the Ca-rich pyroxenes is after Atkins (1969, Fig. 3, p. 239) whereas the trend for the Ca-poor pyroxenes is based on the chemical analyses by Atkins (1969) and on this investigation (Fig. 43). Tie-lines between coexisting hypersthene, pigeonite and augite are hypothetical, although the positions of the hypersthene points of the triangles are based on the lowest and highest Fe/Mg ratio determined for this mineral where it coexists with pigeonite. Fig. 44a is a temperature-composition diagram along the join $Ca_{8,5}Mg_{91,5}$(A) - $Ca_{8,5}Fe_{91,5}$(B). Two temperature curves ML-ML' and MS-MS' are indicated on Fig. 44a instead of only one on the original diagram by Nakamura and Kushiro. This was done because, with slow cooling of a magma, crystallization takes place over a certain temperature interval. ML and MS do not necessarily refer to the liquidus and solidus temperatures of the magma, but rather to an arbitrary temperature interval between the actual liquidus and solidus temperatures. In this figure pigeonite has a stability field at higher temperatures than augite plus hypersthene. These two fields are separated from each other by a three-pyroxene region, the temperature of which decreases with increasing Fe/Mg ratio (Nakamura and Kushiro, 1970, p. 2012).

To the left of point p in Fig. 44a, hypersthene and augite crystallized from the Bushveld magma. When ML, which may be taken as the crystallization temperature of Ca-poor pyroxene, reached point p, the magma moved into the stability field of hypersthene + augite + pigeonite, with the result that pigeonite (Fe/Mg ratio of x) crystallized. Some of this pigeonite might have formed as a result of the reaction hypersthene + liquid $\rightleftharpoons$ pigeonite (ibid., p. 2014). A slight drop in temperature to MS (at the same Fe/Mg ratio as ML at p) would result in these pigeonite crystals coming into contact with magma which was in the stability field of hypersthene and augite. Immediate inversion of the early

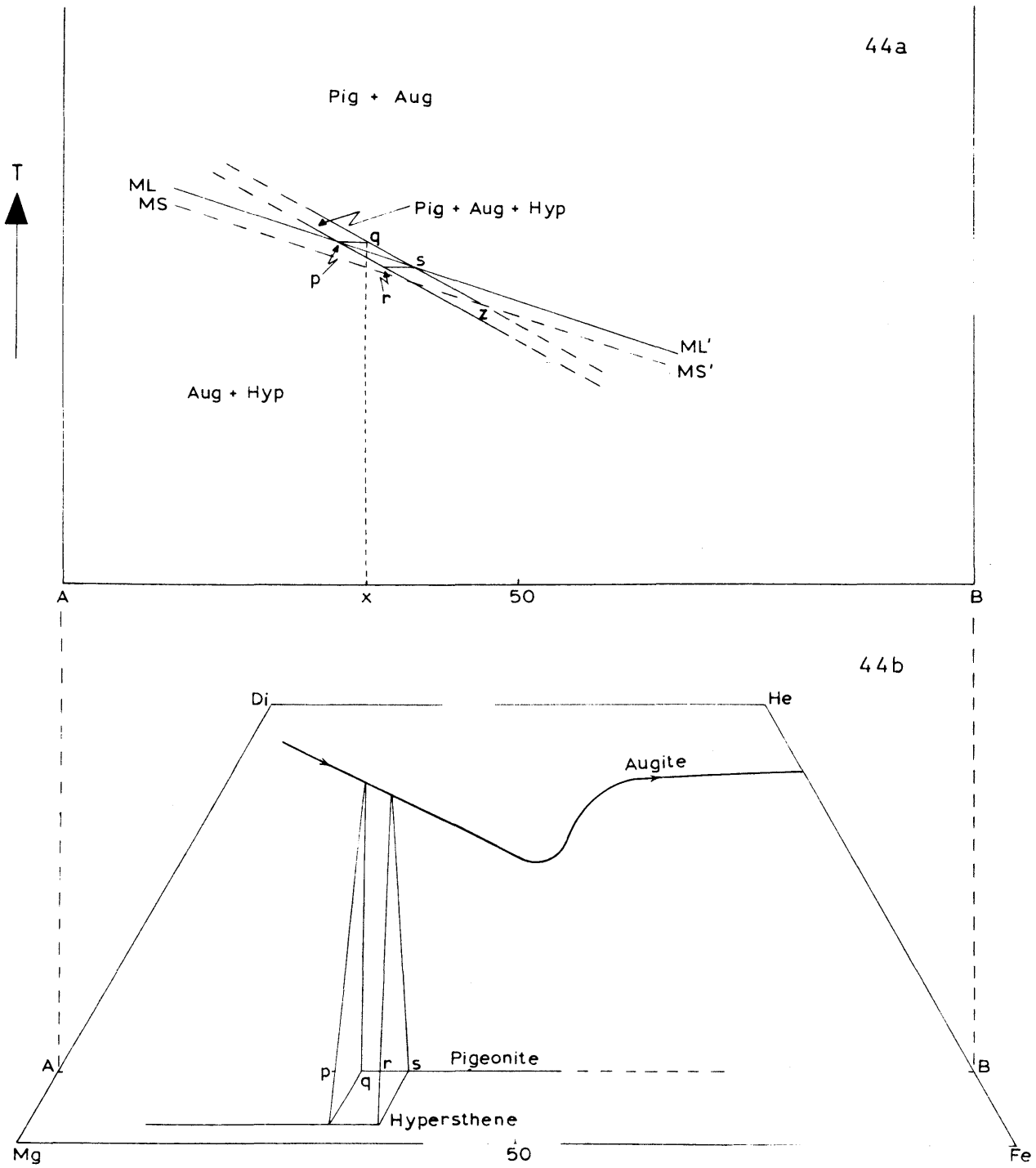

FIG. 44. SCHEMATIC DIAGRAM SHOWING THE CRYSTALLIZATION OF PYROXENES IN THE BUSHVELD COMPLEX. FOR EXPLANATION SEE TEXT. (ADAPTED FROM NAKAMURA AND KUSHIRO 1970, p. 2013)

pigeonite would be the result, but seeing that the Fe/Mg ratio of q is larger than that of the hypersthene and augite crystallizing in equilibrium with the magma, this would effect the dissolution of the early pigeonite. This could bring about the enrichment of the magma in the constituents of hypersthene after a considerable amount of plagioclase and augite had already crystallized, and could cause the large ophitic hypersthene crystals. Small, early pigeonite crystals (now inverted to orthopyroxene) could escape complete dissolution by being enclosed in augite. This is seen by the irregular shape of the former when enclosed in the latter.

As fractional crystallization of the magma continued, the composition of the liquid changed along ML towards s. This resulted in a decrease in the difference between the Fe/Mg ratio of the magma and the early crystallizing pigeonite. Consequently, the temperature interval between MS and the stability field of the augite + hypersthene + pigeonite was gradually reduced, with the result that the time interval available for complete dissolution of the early inverted pigeonite was also reduced. This might have resulted in reaction between magma and pigeonite to form hypersthene. As a result of this reaction, the exsolved augite in the early pigeonite could have been expelled during equilibration of Fe/Mg ratios of the magma and the inverted pigeonite.

As the Fe/Mg ratio of early pigeonite and of the crystallizing magma decreased further, equilibration of early pigeonite by reaction with liquid to form hypersthene continued, but gradually more and more of the augite exsolved from pigeonite was retained owing to a decrease in the reaction time. It seems therefore, that the transition from pigeonite to hypersthene changed from complete dissolution by the magma to reaction with the magma, and hence the texture also changed from ophitic hypersthene to grains, optically continuous over large areas enclosing only a few blebs of exsolved augite. This reaction was replaced by inversion proper as ML moved into the stability field of pigeonite at point s and MS moved into the stability region augite + hypersthene + pigeonite. Where these conditions prevailed, late hypersthene mantles around pigeonite grains could be held responsible for the units of similarly orientated grains of inverted pigeonite as proposed by Maske (1964, p. 61) for the origin of this texture in rocks from the Ingeli Mountains, and also for the lamellae-free rims of inverted pigeonite observed by Brown (1957, p. 528) from Skaergaard. As soon as MS reached point z pigeonite would be the only Ca-poor pyroxene to be precipitated from the magma.

A way in which to determine whether a mechanism as proposed above was operative in giving rise to coexisting inverted pigeonite and primary hypersthene, would be to determine the Fe/Mg ratio of these two, because, according to the above hypothesis, the inverted pigeonite should have a higher Fe/Mg ratio than the coexisting hypersthene. As it is not possible to separate sufficient quantities of the two phases from the same rock, especially inverted pigeonite, electron microbe analysis would be the only way in which to determine the differences in Fe/Mg ratio.

The fine-grained norite directly below the Pyroxenite Marker contains inverted pigeonite only, with composition Fs_{32}, and should according to the above hypothesis contain both Ca-poor phases. A rise in temperature of the magma at this level in the intrusion would have the effect that point s in Fig. 44a would move to lower Fe/Mg ratios. Simultaneously, a change in the composition of the magma was probably brought about by a small influx of fresh magma, prior to larger quantities being added which resulted in the crystallization of primary hypersthene from the Pyroxenite Marker onwards. The composition of the pigeonite in the fine-grained norite L77 from Dsjate (see above) may be explained in a similar way.

B. PLAGIOCLASE

1. Determinative methods

The An content of the plagioclase feldspars was determined by means of X-ray powder data, 2V, Eulerian angles and extinction angles. As a result, several values are given in Appendix I and generally the value which corresponds most closely to the average was used to construct the mineral variation curves of Folder III.

a) X-ray determinations

Desborough and Cameron (1968, p. 117) have established that the plagioclases of the Bushveld Complex are of the low temperature structural variety and consequently X-ray powder diffraction patterns of plagioclases, especially in the range An_{50} - An_{75}, are useful in the determination of the An content (Smith and Gay 1958, p. 760). Various combinations of lines are used by different authors to determine the composition of the plagioclase feldspars. Smith and Gay (1958, p. 744-762) recommend the value $2\Theta_{131} + 2\Theta_{220} - 4\Theta_{1\bar{3}1}$, but Desborough and Cameron (1968, p. 120) have shown that the curve for $2\Theta_{131} + 2\Theta_{220} - 4\Theta_{1\bar{3}1}$ gives values between 2-5 mol. per cent An too high in

the compositional range $An_{60} - An_{80}$. In this study, X-ray powder patterns were obtained by using an AEG Guinier camera developed by Jagodzinski with Cu-$K\alpha_1$ radiation and silicon as internal standard. For the determination of the An content of the plagioclase the values $2\theta_{131} - 2\theta_{1\bar{3}1}$ and $2\theta_{\bar{2}41} - 2\theta_{\bar{2}\bar{4}1}$ were used, as recommended by Tröger (1965, p. 744). The An content of the plagioclases was obtained from the curves of Bambauer et al. (1965) as reproduced in Tröger (1965, p. 748 and 749, Figs. 249 and 250). A potassium content of more than 1 mol. per cent orthoclase apparently lowers the $2\theta_{131} - 2\theta_{1\bar{3}1}$ value considerably, but does not seem to affect the $2\theta_{\bar{2}41} - 2\theta_{\bar{2}\bar{4}1}$ values (Tröger, p. 746 and 749).

In the compositional range $An_{76} - An_{65}$, there is a close agreement in the An values obtained from $2\theta_{131} - 2\theta_{1\bar{3}1}$ and $2\theta_{\bar{2}41} - 2\theta_{\bar{2}\bar{4}1}$. Below An_{65}, the An value determined from $2\theta_{\bar{2}41} - 2\theta_{\bar{2}\bar{4}1}$ is mostly 2-3 mol. per cent higher than that determined from the $2\theta_{131} - 2\theta_{1\bar{3}1}$ value. The reason for this may be due to the K-feldspar which is present in amounts greater than 1 mol. per cent orthoclase (Table V). In specimens where the anorthite content was determined from X-ray data as well as from Eulerian and extinction angles, it was found that the An values obtained from the last two methods agree more closely with the values deduced from $2\theta_{131} - 2\theta_{1\bar{3}1}$, than those deduced from $2\theta_{\bar{2}41} - 2\theta_{\bar{2}\bar{4}1}$.

b) Universal stage determinations

i) 2V measurements

Although the determination of the An content of plagioclase by means of optic axial angles is generally considered to be the least accurate of all the various universal stage methods of determination, the degree of accuracy is increased to some extent by the use of conoscopic illumination (Burri, Parker and Wenk, 1967, p. 203-205).

Grain mounts were made of all samples which were also used for X-ray diffraction determinations, and the 2V was measured under conoscopic illumination on 8 to 10 grains per sample. Only such grains were used which allowed direct measurement of both optical axes of the indicatrix. All the readings on the universal stage were corrected, using an approximated n_y value and the curves provided by Tröger (1959, p. 124).

In most of the samples the 2V measurements fluctuate between $\pm$ 2 and 3^o from the averaged value, but in some samples, fluctuations of up to $\pm 4^o$ were measured. The An values for the averaged 2V were read off from the curves

of J. R. Smith (1960, Plate XII) and these values are listed in Appendix I. The An values thus obtained differ, for most samples, not more than 2 mol. per cent from the values obtained by other methods and only rarely is the difference more than 4 mol. per cent. No An values were determined by this method for measured 2V's of less than 78^{o} because of the uncertainty of the deduced composition from these angles in the range An_{57}-An_{47}.

Of interest is, that the An values obtained from the curves of Smith (1960, Plate XII) agree much more closely with the values determined from X-ray and other methods, than the values obtained from the curve supplied by Burri, Parker and Wenk (1967, Plate XII) which gives An values of 3 mol. per cent too low for plagioclases which contain more than 50 mol. per cent anorthite.

ii) Extinction angles

Extinction angles were measured on albite and on combined albite-Carlsbad twins. When albite twinning alone was used, the stage was tilted so that the extinction angle $[n_x']$ (010)⊥[100] was measured. The An content was then read off the curve supplied by Burri, Parker and Wenk (1967, Plate XI). Wherever possible, extinction angles were measured on grains which exhibited combined albite and Carlsbad twinning. This type of twinning has the advantage that any combination of $[n_x']$ ^(010) angles can be measured, and that several sets of measurements can be made on the same grain. The An content was then determined from the curves given in Tröger (1959, p. 102). Extinction angles were measured on at least five different crystals per thin section and the An values listed in Appendix I are the average values obtained by these methods. These methods were used, together with the Eulerian angles for plagioclases of Subzones B, C and D of the Upper Zone, most of which fall in a compositional range where the composition cannot be determined by either 2V measurements or X-ray powder techniques or both. Extinction angles were also used to some extent for plagioclases of the Main Zone where there was some discrepancy in the An values as determined by X-rays and 2V measurements.

iii) Eulerian angles

Burri, Parker and Wenk (1967, p. 186) consider the determination of the composition of plagioclases with the aid of Eulerian angles as being "die exakte Typisierung eines Plagioklases für mineralogische Spezialstudien". In this study, only Eulerian angles of the first order (ibid., p. 41-43 and 117-133) were measured on Roc-Tourné (combined albite-Carlsbad) twins, and the composition

TABLE V CHEMICAL ANALYSES, STRUCTURAL FORMULAE AND MOLECULAR PERCENTAGES OF PLAGIOCLASE

		PB4389	G491	G422	G277
SiO_2		48, 61	51, 36	53, 62	56, 36
Al_2O_3		31, 54	29, 83	28, 84	26, 61
Fe_2O_3		0, 39	0, 52	0, 24	0, 26
FeO		0, 14	0, 22	0, 36	0, 50
MgO		0, 12	0, 12	0, 09	0, 05
CaO		15, 78	14, 16	11, 89	9, 69
Na_2O		2, 64	3, 22	3, 92	5, 60
K_2O		0, 22	0, 21	0, 36	0, 49
H_2O^+		0, 25	0, 22	0, 35	0, 50
H_2O^-		0, 05	0, 08	0, 08	-
		99, 74	99, 94	99, 75	100, 06
Number of ions on the basis of 32(O)					
Z	Si	8, 972	9, 407	9, 773	10, 211
Z	Al	6, 861	6, 430	6, 185	5, 683
Z	Fe^{+3}	0, 064	0, 070	0, 031	0, 035
X	Fe^{+2}	0, 020	0, 035	0, 057	0, 076
X	Mg	0, 029	0, 029	0, 020	0, 011
X	Ca	3, 122	2, 774	2, 320	1, 881
X	Na	0, 949	1, 148	1, 389	1, 959
X	K	0, 049	0, 046	0, 079	0, 107
Z		15, 90	15, 91	15, 99	15, 93
X		4, 16	4, 03	3, 87	4, 03
Mol.%	An	75, 8	69, 9	61, 2	47, 7
Mol.%	Ab	23, 0	28, 9	36, 7	49, 6
Mol.%	Or	1, 2	1, 2	2, 1	2, 7

PB 4389 from norite, bore-hole PB1, Pietersburg 44JT.
6491 from fine-grained norite below the Pyroxenite Marker, Mapochsgronde 500 JT.
6422 from magnetite gabbro, Vlaklaagte 146 JS
6277 from magnetite anorthosite above Magnetite Seam 17 Onverwacht 148 JS.
Analyst: National Institute for Metallurgy, Johannesburg.

of the plagioclase was obtained from the chart given by Burri, et al. (1967, Plate I). Eulerian angles were usually obtained from only one grain per thin section. For most sections two sets of three angles (i.e. one set per twin) were measured on the stereographic projection and the composition given in Appendix I is therefore an average of six values.

2. Chemical analyses

Four samples of separated plagioclase were chemically analysed by the National Institute for Metallurgy. The object of these analyses was to give an indication of the accuracy of the composition as determined by optical means. Care was taken to ensure that the plagioclases were free of impurities by investigating this mineral in thin section prior to separation. This was necessary because, especially the plagioclases of the Upper Zone and those from rocks below the Pyroxenite Marker, contain tiny needles of magnetite. Comparison of these analyses (Table V) with those listed by Deer et al. (1963, Vol. 4, Tables 15 to 17, p. 115-118) shows them to have a slightly higher iron content, which may be ascribed to submicroscopic needles of magnetite.

From these analyses it would seem that optical determinations give An values of a few mole per cent lower than those calculated from chemical analyses (Table VI). Reverse zoning (Wager and Brown, 1968, p. 386) could be the cause of these differences, although special care was taken to ensure that plagioclase was separated from specimens which showed little or no zoning.

TABLE VI COMPARISON OF MOLECULAR ANORTHITE CONTENT OF PLAGIOCLASE AS DETERMINED BY DIFFERENT METHODS

Sample No.	PB4389	G491	G422	G277
Chemical analysis	76	70	61	48
Eulerian angles I	77	64	56	43
Extinction angles	76	65	56	44
2V	76	63	57	-
X-rays ($2\theta_{131}$-$2\theta_{\bar{1}31}$)	74	n. d.	57	-
n glass*	77	66	57	43

* Determined by A. Kleyenstüber and W. Dohmen.
n. d. - not determined.

3. Compositional variations

In general, the compositional trend, as indicated in Folder III resembles that of orthopyroxene very closely. The compositional breaks recorded in the orthopyroxene trend are also borne out by the plagioclase. The scatter of points in the plagioclase curve is however less, owing to the averaging of the An content as determined by several methods, and consequently the compositional trend as displayed by this mineral is considered to be more accurate than that of the orthopyroxene.

The An content of plagioclase is in the vicinity of 76 directly above the Merensky Reef and corresponds to the composition of this mineral in the reef (Wager and Brown, 1968, Fig. 192, p. 351; Molyneux, 1970, p. 33). Roux (1968, p. 70) on the other hand, recorded values varying between An_{73} - An_{85} for the Merensky Reef in the area a few kilometres to the east. At the first compositional break, 100m above the reef, the An content drops to 68, with a corresponding change in the Fs content of the coexisting inverted pigeonite. It is noteworthy that the change in composition of the Ca-poor pyroxene is much greater (14 mole per cent) than that of the plagioclase (9 mole per cent). Above this break, the composition of the plagioclase returns to above An_{70} for only a short distance, and then gradually drops to An_{64} at the bottom of the next compositional break at 1120m. Higher An values are only maintained for 100m above the break and from here onwards the composition changes progressively to An_{56} below the fine-grained norite which forms the top of Subzone B of the Main Zone.

In the fine-grained norite the composition of the plagioclase rises sharply to about An_{65} and this is analogous to the trend observed in the orthopyroxene. A possible explanation for this change is offered in the previous section on the orthopyroxene (p. 88). Above the Pyroxenite Marker, values of above An_{70} are maintained for about 350m before dropping rapidly to An_{60} at the top of the Main Zone.

The composition of the plagioclase fluctuates between An_{56} and An_{59} in the first 400m of the Upper Zone and drops to a fairly constant An_{53-55} for the greater part of Subzone C. In the top 100m of this subzone, the An content decreases to 50. Noteworthy is the change to An_{45} where cumulus apatite appears in the olivine diorites of Subzone D. The change in composition of the plagioclase at this level is not solely ascribed to a decrease in the Ca-content of the magma, but is considered to be partially due to the fact that fractionation led to the gradual

enrichment in the phosphorus content which reached saturation at this horizon and resulted in the crystallization of apatite. This caused a depletion of Ca in the magma and a consequent drop in the An content of the coexisting plagioclase.

In the lower 550m of Subzone D, cumulus apatite and plagioclase crystallized together, and owing to fractionation the composition drops gradually to An_{42}. The rocks between Magnetitite Seams 17 and 21, contain no apatite and as a result, the An content rises rapidly from 42 to 52, but where apatite appears again above the 21st Seam, the composition of the plagioclase drops to An_{45}, which is also the value obtained for the highest rock in this sequence where the composition could be determined. In the samples of the remaining 30m of the succession, the plagioclase feldspar is highly saussuritized, but in less altered samples, Atkins (1969, Fig. 1, p. 227) and Groeneveld (1970, Fig. 3, p. 40) found the composition to drop to An_{30} at the top of the intrusion.

4. Textural features

Not much attention was given to the textural features displayed by the plagioclase, as this necessitates a detailed study on its own, but the more important textures which were observed during the course of the investigation are briefly discussed below. Twinning is not included in the following discussions as no systematic evaluation was made of the frequency of types present. Molyneux (1970, p. 34) however, states that albite twinning is the most common in the Bushveld plagioclase.

a) Zoning

Zoning is present to some extent in practically all the thin sections investigated. During routine optical determinations of the composition of the plagioclase, the zoning of a few crystals was also determined and the observed values are given in Table VII. The zoning may be reversed, normal or oscillatory and is mostly confined to the outermost, usually narrow, rims of the crystals, but occasionally, especially when the zoning is oscillatory, the rims are wider. In the two specimens where oscillatory zoning was measured, the sequence is normal - reversed in the one and reversed - normal in the other. Specimen G351 (Table VII) requires special comment. The rock is an olivine gabbro from the base of Subzone C of the Upper Zone, and is characterized by the presence of a few small inclusions of anorthosite. The cumulus plagioclase of the rock exhibits reversed zoning from An_{53}-An_{63} whereas the plagioclase of the inclusion has a higher anorthite content and displays normal zoning from

An_{63}-An_{56}. Although the origin of the inclusions is uncertain, the observed zoning is probably inherent in the two rock types.

The recorded zoning in Table VII represents only a few routine determinations with the Universal Stage and much more detailed work is necessary to determine differences in An content between core and mantle of the plagioclase to deduce crystallization trends of the intercumulus liquid.

The presence of reversed zoning of the plagioclases in the rocks of the Bushveld Complex was remarked on by Wager and Brown (1968, p. 385-387) who found it to be unique to this intrusion. They reject the possibility of increased pressure on the confined pore spaces, as this mechanism would also have been operative in other intrusions. The alternative of an increase in pH_2O in the interstitial melt is favoured by them, as this would have the effect of lowering the liquidus - solidus temperatures in the anorthite - albite system. The outer parts of the cumulus crystals would attain equilibrium with this residual liquid by reaction and give rise to the more calcic rims. Simultaneously, SiO_2 would be released and result in the myrmekitic intergrowths commonly observed in plagioclases of the Bushveld Complex. However, myrmekite is not always present where plagioclase displays reversed zoning, as also noted by Ferguson and Wright (1970, p. 65) from rocks of the Critical Zone.

b) Bent crystals of plagioclase and interpenetration

Textural features indicative of deformation after deposition of the cumulus crystals are commonly observed in the plagioclase of the Bushveld Complex. Among these textures are bent crystals of plagioclase, interpenetration of two adjoining crystals and myrmekite. The last of these apparently only develops under certain conditions and is therefore discussed separately in the next section.

Bent crystals of plagioclase were observed in practically all the thin sections investigated from the Main and Upper Zones. Only in the top 400m or so of the intrusion is this texture rarely observed. The bending of the crystals is indicated by the wedge-shaped and curved polysynthetic twins in the plagioclase (Fig. 45). Fracturing of the crystal at the point of maximum stress can sometimes be seen.

The number of bent plagioclase crystals varies considerably from specimen to specimen and no specific trend could be observed in the sequence.

TABLE VII ZONING IN PLAGIOCLASE FROM THE MAIN AND UPPER ZONES OF THE BUSHVELD COMPLEX

Sample No.	Height in m above MR	Mol. % An core	Mol. % An mantle	Type of Zoning
PB4388	4	75-76	79-82	Reversed
PB4284	35	77	68	Normal
PB4254	44,5	77	75-77	Oscillatory N-R*
PB1101	1005	65	68-65	Oscillatory R-N
PB601	1150	70	65	Normal
G573	1425	65	61	Normal
G577	1515	63	68	Reversed
G583	1740	61	68	Reversed
G584	1880	61	58	Normal
G587A	2065	63	70	Reversed
G435	2580	58	68	Reversed
G515	3200	64	68	Reversed
G365	4625	54	62	Reversed
G351	4637	53	63	Reversed) see
		63	56	Normal) Text
G228	5835	44	48	Reversed
G252	5950	50	42	Normal
G285	6073	43	30	Normal
G208	6140	45	39	Normal
G215	6180	45	40	Normal

*N - Normal
R – Reversed

However, certain horizons do contain more deformed plagioclase crystals than others, especially between 1200 - 1500m and also for short intervals at about 3300 and 3750m above the Merensky Reef.

Interpenetration of two plagioclase crystals (Fig. 46) is a texture fairly commonly observed in the investigated rocks. The term "interpenetrated" was

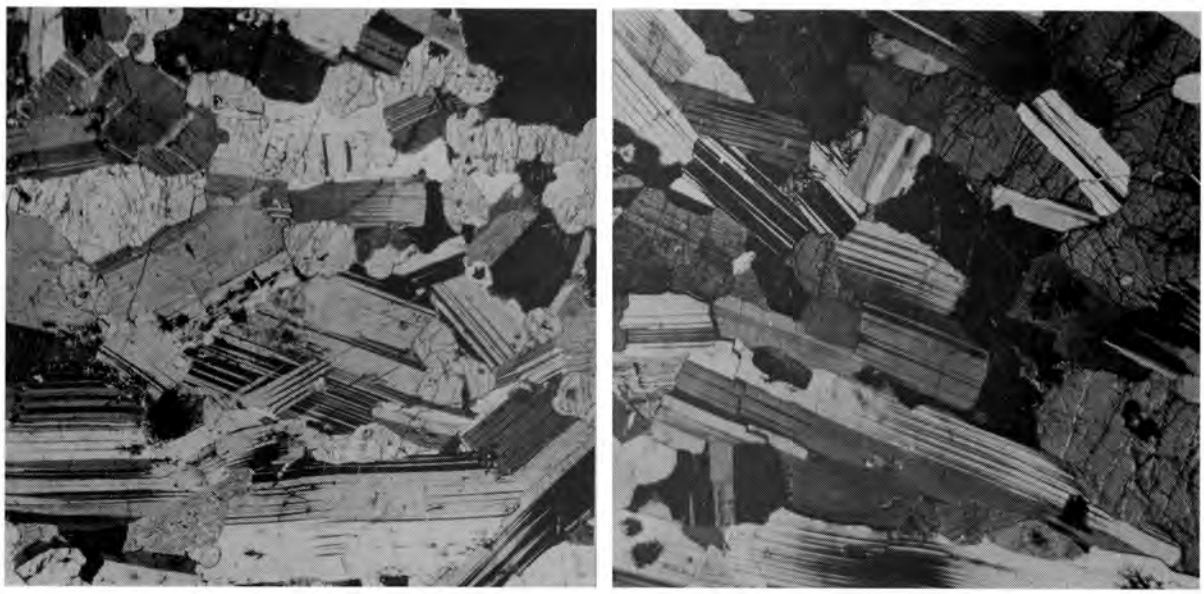

Fig. 45. Numerous bent crystals of plagioclase in plagioclase pyroxene cumulates. G488 (left) and G603 (right). Crossed nicols, x25.

Fig. 46. Interpenetrated crystals of plagioclase. Note the bent, penetrated plagioclase crystal (right), PB2015 (left) PB4076 (right). Crossed nicols, x50

used by Raal (1965, p. 24-25, and Photograph 5) for plagioclase grains which protrude into adjoining grains. He considers the textures to have originated where two settled crystals are in contact with each other in such a way that the corner of the one meets a plane surface of the other. It is suggested by him (p. 55) that partial melting of one feldspar could have taken place at the point of contact if the temperature of the crystals was still close to the temperature of crystallization and if an increase in pressure occurred.

In some cases this texture may be due to crystal settling and adcumulus growth. This is illustrated in Fig. 47A where two cumulus crystals are in contact with each other. Adcumulus overgrowth (solid line) will result in interpenetrating crystals, because each crystal face must compete for space during growth, thus causing an irregular contact between the two (dotted line). Relationships as outlined in Fig. 47B (see also Fig. 47C, points A, B, C, D and E, as well as Fig. 46) cannot be explained in this way. It is highly unlikely that only one crystal will be enlarged by adcumulus growth and not the other. If it is assumed that the solid outlines (Fig. 47B) represent the sizes of the crystals during accumulation then an increase in the pressure would cause a more calcic plagioclase to be stable at the prevailing temperatures. This would result in resolution at the point of stress (the shaded area in Fig. 47B) and in redeposition in the interstices.

A reasonable explanation for the presence of bent plagioclase crystals and interpenetrated relationships between adjoining crystals therefore seems to be compaction owing to an increase in pressure caused by the accumulation of the superincumbent crystal mass.

c) Myrmekite

Myrmekite, by definition an intergrowth of vermicular quartz in plagioclase, is a common constituent of acid plutonic and metamorphic rocks but is extremely rare in calcic plagioclases of mafic intrusions (Barker, 1970, p. 3344). This texture is however present in practically all the gabbroic rocks of the Main Zone of the Bushveld Complex. Its shape and appearance closely resembles that described from granitic rocks and differs only in that it is developed along the grain boundaries of coexisting cumulus plagioclases instead of being associated with alkali feldspars.

The complexity of the myrmekite of the gabbroic rocks in the Main Zone depends largely on the amount of myrmekite present. In all cases, however, it

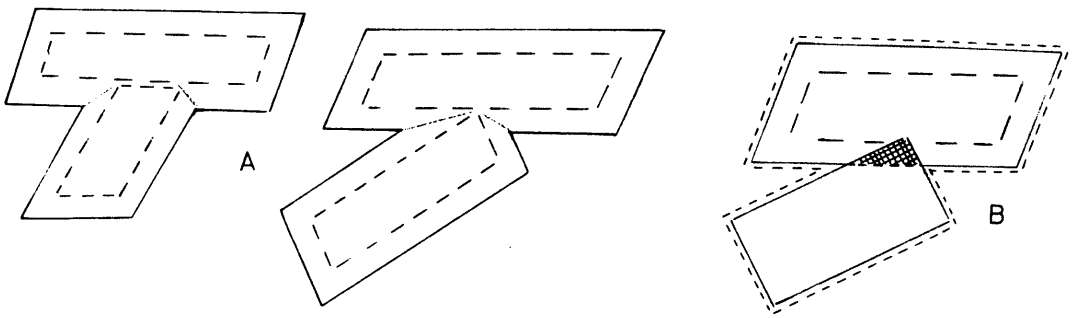

FIG. 47 A AND B. RELATIONS TO ILLUSTRATE DIFFERENCES BETWEEN SIMULTANEOUS CRYSTALLIZATION AND INTERPENETRATION

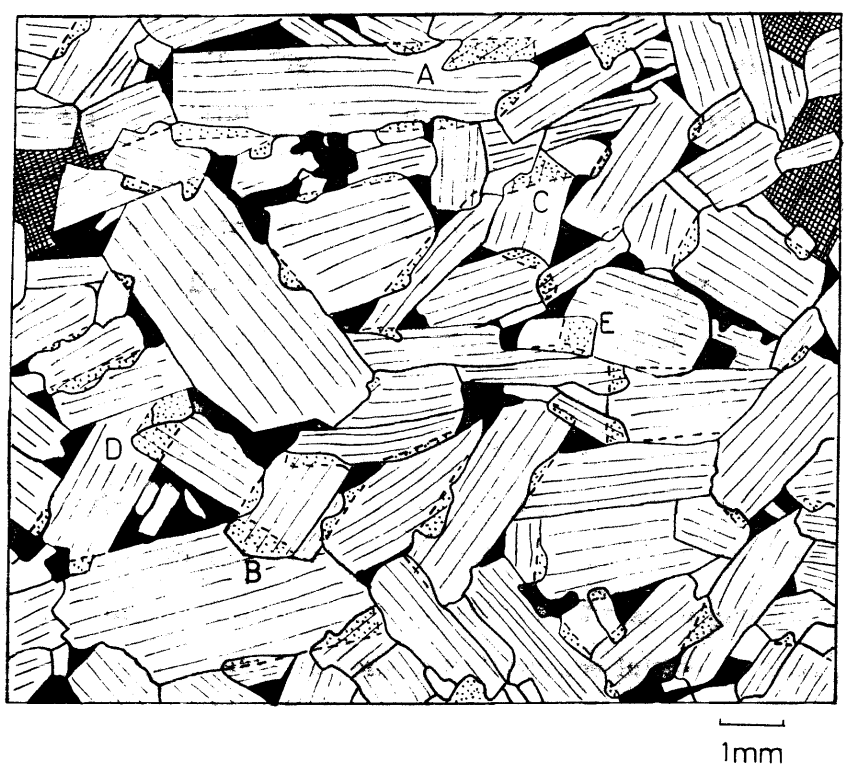

FIG. 47C. MICROGRAPH OF SPECIMEN PB3801 ILLUSTRATING AMOUNT OF INTERPENETRATION (STIPPLED) OF PLAGIOCLASE CRYSTALS. INTERCUMULUS MINERALS: QUARTZ (BLACK), CLINOPYROXENE (HATCHED)

seems to be developed where one plagioclase crystal interpenetrates an adjoining crystal and in many cases, the crystal outline and twinning of the "penetrator" is preserved in the "penetrated", whereas the twinning lamellae of the latter are destroyed (Wager and Brown, Fig. 213, p. 387). The intergrowth seems to advance convexly outwards, and the worms of quartz are orientated perpendicularly to the outer boundary (Fig. 48). At the margin of this intergrowth, the worms tend to be thin and long, and coalesce to form thick, elongated, drop-like inclusions in the central portion. This seems to indicate that the growth has originated at the expense of the penetrated crystal, causing an enrichment of calcium in the penetrator with resultant exsolution of worms of silica.

As the amount of myrmekite increases, the textural relationships also become more complex. This is especially apparent where the two adjoining plagioclases both interpenetrate each other (Fig. 48) and often, relics of the one may be observed in the other. In extreme cases, crystals may be transformed completely to myrmekite (Fig. 49) and often original outlines of the cumulus plagioclase are completely destroyed especially where three or more individuals are involved.

Various theories to explain the myrmekitic textures in granitic rocks have been advanced. Drescher-Kaden (1948, p. 14-104) gives a lengthy discussion of this texture and concludes (p. 102) that it may be due to replacement or corrosion of plagioclase by quartz. However, most authors, who have recently published results of their investigations, favour the theory of unmixing of plagioclase from K-feldspar, because the texture is usually developed between coexisting grains of two alkali-feldspars or between alkali-feldspar and plagioclase. Where this texture is found at grain boundaries of alkali–feldspar and plagioclase, the intergrowth is convex towards the latter. Hubbard (1966, p. 770) explains the texture as being due to exsolution of both the quartz and the plagioclase from the alkali-feldspar, both of which were present as solid solution in the latter at high temperatures. In these cases, the orientation of the more calcic plagioclase of the myrmekite is continuous with that of the primary plagioclase. Shelly (1964, p. 50) on the other hand, believes that the quartz is derived from the interstitial liquid and that the myrmekitic textures resulted from simultaneous crystallization of this quartz and exsolved plagioclase from the alkali-feldspar.

As early as 1909, Schwantke (Barker, 1970, p. 3344), postulated the

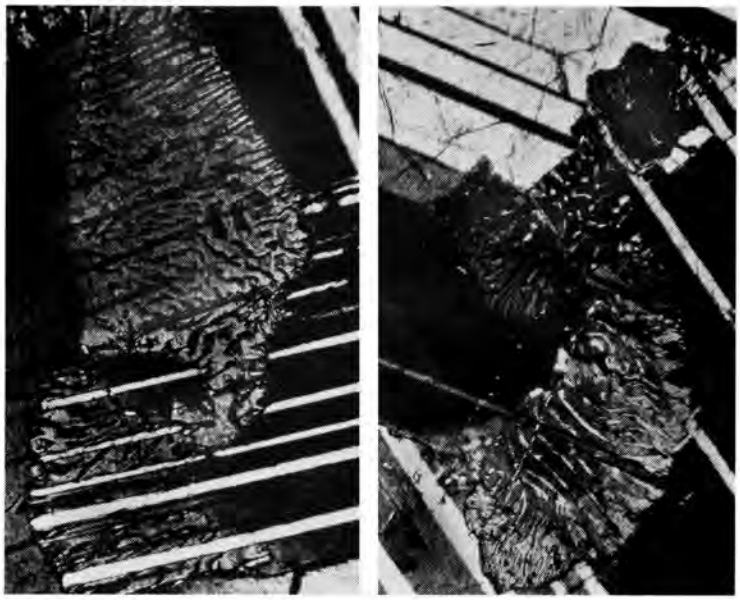

Fig. 48. Complex interpenetration of plagioclase crystals associated with myrmekite. G607. Crossed nicols. x150

Fig. 49. Crystal of plagioclase completely transformed to myrmekite (centre). G609. Crossed nicols, x75

existence of $CaAl_2Si_6O_{16}$ as a compound in solid solution in alkali-feldspar at high temperatures. This has been corroborated by the more recent work of Phillips (1964, p. 58). The amount of $CaAl_2Si_6O_{16}$ exsolved together with albite from the alkali-feldspar would therefore firstly determine the anorthite content of the plagioclase and the amount of quartz in the intergrowth, because these two are apparently controlled by the reaction:

$$CaAl_2Si_6O_{16} \longrightarrow CaAl_2Si_2O_8 + 4SiO_2$$

A close to linear relationship therefore seems to exist between the mole per cent An and the volume per cent quartz in the myrmekite and from volumetric analyses of exsolved quartz, this relationship seems to hold true (Phillips and Ransom, 1968, p. 1412, Barker, 1970, p. 3344).

It is obvious that the above explanation cannot be applied to the gabbroic rocks of the Bushveld Complex, hence Barker's statement (ibid., p. 3339) that "the occurrence of rare calcic myrmekite in mafic rocks remains unexplained", but because of the striking similarities, the mechanism by which these textures originated must be very closely related.

Wager and Brown (1968, p. 387) have pointed out the association of myrmekite with reversed zoning in the Bushveld plagioclases, but as far as could be established during the brief investigation of the textures, reversed zoning can be developed without the presence of myrmekite. During investigation of the thin sections of the sequence, an effort was made to assess the relative abundance of this intergrowth at various levels in the intrusion. The following pattern has emerged from this study:

i) In rocks of Subzone A and the lower half of Subzone B, up to about 2300m above the Merensky Reef, myrmekite is only present in very small amounts. The rocks in this part of the sequence contain fair amounts of intercumulus material (see chapter on modal analyses and Folder IV) and this sequence also includes the orthopyroxene-pigeonite transition zone.

ii) Large quantities of myrmekite are present in the upper half of Subzone B, i.e. where inverted pigeonite proper is developed. Another characteristic of these rocks is the low amount or absence of intercumulus material (Folder IV).

iii) Myrmekite is conspicuously absent in the rocks where primary

cumulus orthopyroxene occurs in Subzone C, but is found in small amounts where ophitic orthopyroxene makes its appearance. Shortly after inverted pigeonite proper appears at the top of this subzone, myrmekite is again abundant, up to the Main Magnetitite Seam.

iv) Above the Main Magnetitite Seam, myrmekite is found in small quantitites, but where symplektitic textures appear about 420m above this seam, myrmekite gradually disappears.

In general, therefore, myrmekite is only developed in abundance where pigeonite proper is present in the rocks and where there is no or very little intercumulus material. Its presence does not seem to be controlled by the composition of the plagioclase, because it is found in plagioclase (An_{63-65}) in the fine-grained norite below the Pyroxenite Marker, whereas plagioclase of similar composition lower down in the sequence, contains hardly any myrmekite.

Other features sometimes observed in the presence of myrmekite are bent crystals of plagioclase. The texture is then often developed where the most deformation of the crystal has taken place, i.e. at the points where the pressure must have been highest to cause bending.

This would seem to indicate that the myrmekite is due to increased load pressure, which would also explain this texture to be associated with interpenetrated plagioclase crystals. On the other hand, rocks which do contain intercumulus material often exhibit interpenetration phenomena, bent plagioclase crystals as well as reversed zoning, but very little or no myrmekite.

From the observed textural relations, it seems as though the development of calcic myrmekite in plagioclase is related to a specific stage in the post-cumulus history of the rock. The abundance of intercumulus material, as well as post-cumulus changes of other mineral phases, for instance the pigeonite-orthopyroxene inversion, seems to affect the change in the feldspar framework.

Deformation of the plagioclase framework owing to load pressure at high temperatures may result in re-solution or recrystallization (interpenetration) at contact points, but owing to equilibration with surrounding intercumulus liquid, the recrystallized or interpenetrated portions will not be more calcic than the rest of the crystal. Deformation at slightly lower temperatures, owing to load pressure and perhaps also owing to a slight shift of the whole cumulus pile during structural rearrangement at the time of the pigeonite-orthopyroxene inversion, and consequently also less intercumulus liquid, may result in non-

equilibration of the recrystallizing plagioclase and cause the calcic myrmekitic intergrowths.

Owing to the interpenetration and bending of the plagioclase crystals, a shortening of the cumulus pile must have taken place, which would suggest the presence of intercumulus liquid prior to and at the time of deformation. Any sodium released during the recrystallization process could have been added to the intercumulus liquid which was continuously pressed out of the pore spaces during compaction.

More detailed information on textural relationships, zoning and the amount of exsolved vermicular quartz is however necessary to determine whether the processes as outlined above may be held responsible for the presence or absence of myrmekite.

d) Orientated inclusions

Long before magnetite appears as a major constituent in rocks of Subzone A of the Upper Zone, the enrichment of iron owing to fractionation is borne out by the presence of tiny rods and "dust" of magnetite in the plagioclase. These inclusions appear at about 2450m above the Merensky Reef and persist up to the base of the fine-grained norite at the top of Subzone B of the Main Zone. They reappear some 250m before the base of the Upper Zone, and continue to be present in plagioclase of Subzones A, B and C, but are practically absent in rocks of Subzone D.

The magnetite inclusions increase southwards in rocks of Subzone B of the Main Zone, so much so that the plagioclase is dark grey to black in hand specimen, forming the well known "black granite" which is quarried at various localities some 40-50km south of the area (Groeneveld, 1970, p. 39).

Where the magnetite needles are well developed, they usually occur in three or more distinct sets in the plagioclase. Their orientation with respect to crystallographic directions of the plagioclase was not determined, as a study of these black gabbroic rocks is at present being undertaken by Mr J. A. van Graan. As far as could be ascertained, none of these sets is orientated parallel to a cleavage direction. Groeneveld (1970, p. 39) mentions that they tend to be orientated parallel to the c-axis of the plagioclase.

Where large amounts of these magnetite rods exist, they are concentrated in the central (cumulus) portion of the plagioclase grains (G409 and G609). This texture is especially well developed in the area under study by Mr J. A.

van Graan, and it is hoped that it will be possible to evaluate the size of the original cumulus crystals, initial porosity prior to adcumulus growth and the post-cumulus enlargement of the plagioclase.

Biotite is often present as tiny flakes embedded in cleavage planes of the plagioclase. This mineral is not considered as an original inclusion, but has probably crystallized at a later stage owing to exsolution of some potassium from the plagioclase at decreasing temperatures.

Fairly common is a mineral which occurs in tiny square or rectangular patches (about 0.02 x 0.03mm) in the central portions of the plagioclase grains. The patches are orientated in such a way that their sides are parallel to cleavage directions of the plagioclase. The refractive index and birefringence of the mineral in these patches seems to be lower than that of the host. The general impression gained is that these inclusions consist of either K-feldspar or quartz.

C. OTHER SILICATES

1. Olivine

Olivine appears in the sequence about 4600m above the Merensky Reef, i.e. at the base of Subzone C of the Upper Zone, although some is also present in rocks at the top of Subzone B (G658, Folder II). Its composition was determined by means of X-ray diffraction, using Co-$K\alpha_1$ radiation and backward reflections in a 114,6mm AEG-Guinier camera as developed by Jagodzinski. The reflection d_{174} and the curve provided by Jambor and Smith (1964, p. 736) were utilized to obtain the molecular percentage of fayalite in the olivine. These values, as well as the composition determined from 2Vx (Tröger, 1959, p. 37) by averaging between 8 and 10 measurements on grain mounts are given in Appendix I. The accuracy of the X-ray determinations is considered by Jambor and Smith (1964, p. 737) to be greater than $\pm$ 1,16 per cent for olivines with composition of Fa_{60} or less, whereas the accuracy decreases slightly for higher Fa values.

In the compositional range Fa_{50}-Fa_{70}, the composition as determined from 2V measurements does not differ much from that derived at from X-ray diffraction, but there are significant differences as the fayalite content increases, the 2V determinations generally giving values of between 8 and 10 mol. per cent Fa too high (Appendix I). Compositions as determined from the X-ray powder data were used in Folder III except the highest Fa value which is based on 2V measurements.

The olivine at the base of Subzone C has a composition of Fa_{49-52} and rises to Fa_{54} in the olivine gabbro associated with the Magnetitite Seam 11. In the olivine diorite below Seam 17, the composition of the olivine is Fa_{69-70}, but rises to Fa_{73} in the rocks directly over and underlying this magnetitite seam. The drop in composition to Fa_{70} directly above Seam 21 is similar, but less, than the reversal in the compositional trend of the plagioclase (Folder III).

Above this magnetitite seam the most iron-rich olivine determined by means of X-ray diffraction has a composition of Fa_{79} 220m below the roof. The composition of olivine, from a sample 175m below the roof was determined as being Fa_{89} by 2V measurements. From reports by Wager and Brown (1968, p. 388) and Molyneux (1970, p. 39) the fayalite content increases to Fa_{100} directly below the roof.

Orthopyroxene and iron-rich olivine frequently coexist as separate cumulus phases especially in rocks of Subzone C of the Upper Zone. In the olivine diorites below Seam 17 in Subzone D, orthopyroxene is however, conspicuously absent, but above this seam it is only present as intercumulus material which is often seen to surround the olivine crystals and a reaction between olivine and the intercumulus liquid to form orthopyroxene cannot be excluded.

Olivine also seems to be a constituent of some of the symplektite which is frequently observed in rocks of the Upper Zone. As several other minerals are involved in these complex intergrowths, they are discussed separately in the section dealing with the postcumulus changes of the rocks.

2. Clinopyroxene

Apart from some observations on the exsolution textures, no work was done on the clinopyroxene of the gabbroic rocks of the Layered Sequence. The reason for this was that determination, by refractive index methods, of the composition of this mineral in the large number of samples which were investigated would have been very time-consuming and the result would probably have been similar to the compositional trend observed for the plagioclase and the orthopyroxene. For the determination of the composition of orthopyroxene and plagioclase, clinopyroxene was also separated. An investigation of the compositional variations of this mineral is intended at a later stage. Recently, Atkins (1969, p. 239) published several analyses of Ca-rich pyroxene from the Bushveld and determined, among other things, their trend of crystallization (ibid., Fig. 3).

Of interest are the observed exsolution textures in the augite. Hess and Poldervaart (1951, p. 481) pointed out that exsolution-lamellae of orthorhombic pyroxene in monoclinic pyroxene or vice versa are parallel to the (100) plane, whereas monoclinic pyroxene exsolves parallel to (001) in another monoclinic pyroxene. Hypersthene therefore exsolves parallel to the (100) plane and pigeonite parallel to the (001) plane of augite. Brown, (1957, p. 527) states that it is to be expected that the type of pyroxene exsolved from the augite would be the same as the coexisting cumulus pyroxene. Augite in the majority of rocks investigated, however, contains two sets of exsolution-lamellae irrespective of whether the coexisting cumulus phase is hypersthene or inverted pigeonite.

In Subzone A and B of the Main Zone, exsolution-lamellae parallel to the (100) plane of augite are the most abundant, and although lamellae parallel to (001) are present and increase upwards in the sequence, they remain subordinate. The (100) lamellae are usually thin, well developed and traverse the whole grain, whereas the (001) lamellae are short and usually thicker. At the base of Subzone C only (100) lamellae are present, but towards the top (001) lamellae are also developed.

In Subzone A of the Upper Zone, thin, well developed (100) lamellae still predominate over the short and thick (001) lamellae, although the latter are more numerous than at the top of the Main Zone. A reversal in the abundance of the two types of exsolution-lamellae takes place in Subzone B of the Upper Zone. At the base of this subzone the two types seem to be developed in equal amounts, but the (001) lamellae increase and predominate towards the top. In Subzone C only a few (100) lamellae are present at the base but are absent at the top. The (001) lamellae are now thin and traverse the whole grain whereas the few (100) lamellae are short and usually slightly thicker. The augite in the predominantly olivine-bearing rocks of Subzone D contains hardly any exsolved lamellae of clinopyroxene, but where they are developed, they are extremely thin and orientated parallel to the (001) plane of the host.

The observed exsolution textures are, for the greater part of the succession not difficult to explain, but the presence of two sets of exsolution-lamellae in Subzone A of the Main Zone where the coexisting Ca-poor pyroxene is primary hypersthene, presents a problem. In these rocks only (100) exsolution-lamellae are expected as this is the direction parallel to which the orthorhombic substance exsolves in the augite. The presence of a few (001) exsolution-lamellae

would seem to indicate that, perhaps at high temperatures, some of the orthopyroxene was exsolved parallel to that direction.

Higher in the sequence, i.e. in the orthopyroxene-pigeonite transition zone, the coexistence of two sets of lamellae can be explained in conjunction with the hypothesis concerning the coexistence of inverted pigeonite and primary hypersthene. As postulated, when the magma entered the stability field of three pyroxenes (Fig. 44a point p) pigeonite would crystallize and consequently is also the phase which exsolved parallel to the (001) plane in coexisting cumulus augite. Slight cooling of the crystallizing magma at constant Fe/Mg ratio would result in hypersthene becoming the stable Ca-poor pyroxene and any further exsolution in augite would be parallel to the (100) plane. The presence of exsolution-lamellae parallel to (001) and (100) of augite in certain rocks of the Skaergaard Intrusion led Brown (1957, p. 528) to suggest that both orthopyroxene and pigeonite could have been in equilibrium with the augite during crystallization of these rocks.

Where inverted pigeonite is the only Ca-poor phase in the rocks, two sets of exsolution-lamellae are usually developed in the augite, i.e. at the top of Subzones B and C of the Main Zone as well as in Subzones A and B of the Upper Zone. In the augite of these rocks, pigeonite was exsolved parallel to the (001) plane above the inversion temperature and hypersthene parallel to the (100) plane below the inversion temperature. As the temperature interval between crystallization of pigeonite and inversion to hypersthene increased, more and more of the monoclinic phase would be exsolved from the augite before the inversion, to such an extent that in the lower half of Subzone B of the Upper Zone, the two exsolution sets are equally abundant, but at higher levels the (100) exsolution-lamellae decrease and are absent at the top of Subzone C. Where orthopyroxene makes way for olivine in Subzone D of the Upper Zone the augite contains hardly any exsolution-lamellae and those which are present are extremely thin and orientated parallel to the (001) plane.

3. Biotite

During the separation of the minerals from specimens of the Main and Upper Zones, it was possible to separate relatively pure biotite where this mineral was present in fairly large quantities. One of these specimens is from Subzone A of the Main Zone and the others are from the Upper Zone. X-ray powder diagrams were obtained from these on an AEG-Guinier camera with

Co-Kα_1 radiation. The purpose of this study was to determine whether there are any variations in the value of the 060 reflection, which, according to Wones (1963, p. 1305) shows the greatest shift with changes in the Fe/(Fe + Mg) ratio in the annite-phlogopite solid solution series. The results are given in Table VIII and are diagrammatically presented in Fig. 50.

Wones (1963, p. 1307) has shown that there is a systematic increase in d_{060} with increase of the Fe/(Fe + Mg) ratio for a given oxygen fugacity and a systematic decrease in d_{060} at constant Fe/(Fe + Mg) as the oxygen fugacity increases. From Fig. 50 it may be seen that the d_{060} of biotite from the specimen of the Main Zone is lower than all those of the Upper Zone, which may be due to an increase in the Fe/(Fe + Mg) ratio. The d_{060} values of biotite from the Upper Zone fluctuate considerably even over short intervals (G620, G621, G310, Table VIII), so much so that the difference in Fe/(Fe + Mg) between samples G620 and G310 at any given constant oxygen fugacity (ibid., Fig. 3) is as much as 0,3. Differences in the Fe/(Fe + Mg) ratios of the other ferromagnesian silicates never show such variations over short distances as this and it follows that different oxygen fugacities may be held responsible for some of the observed fluctuations.

TABLE VIII d_{060} VALUES OF BIOTITE FROM ELEVEN SAMPLES OF THE MAIN AND UPPER ZONES

Sample No.	Height in m above M.R.	$2\theta(\pm 0,025)$ $CoK\alpha_1$	d_{060} (Å)
PB2015	720	70,94	1,5414
G400	4083	70,53	1,5490
G510	4110	70,50	1,5498
G568	4275	70,62	1,5479
G617	4804	70,43	1,5509
G620	4828	70,38	1,5521
G621	4849	70,59	1,5482
G310	4865	70,77	1,5448
G253	5960	70,63	1,5479
G368	5990	70,47	1,5505
G285	6075	70,31	1,5536

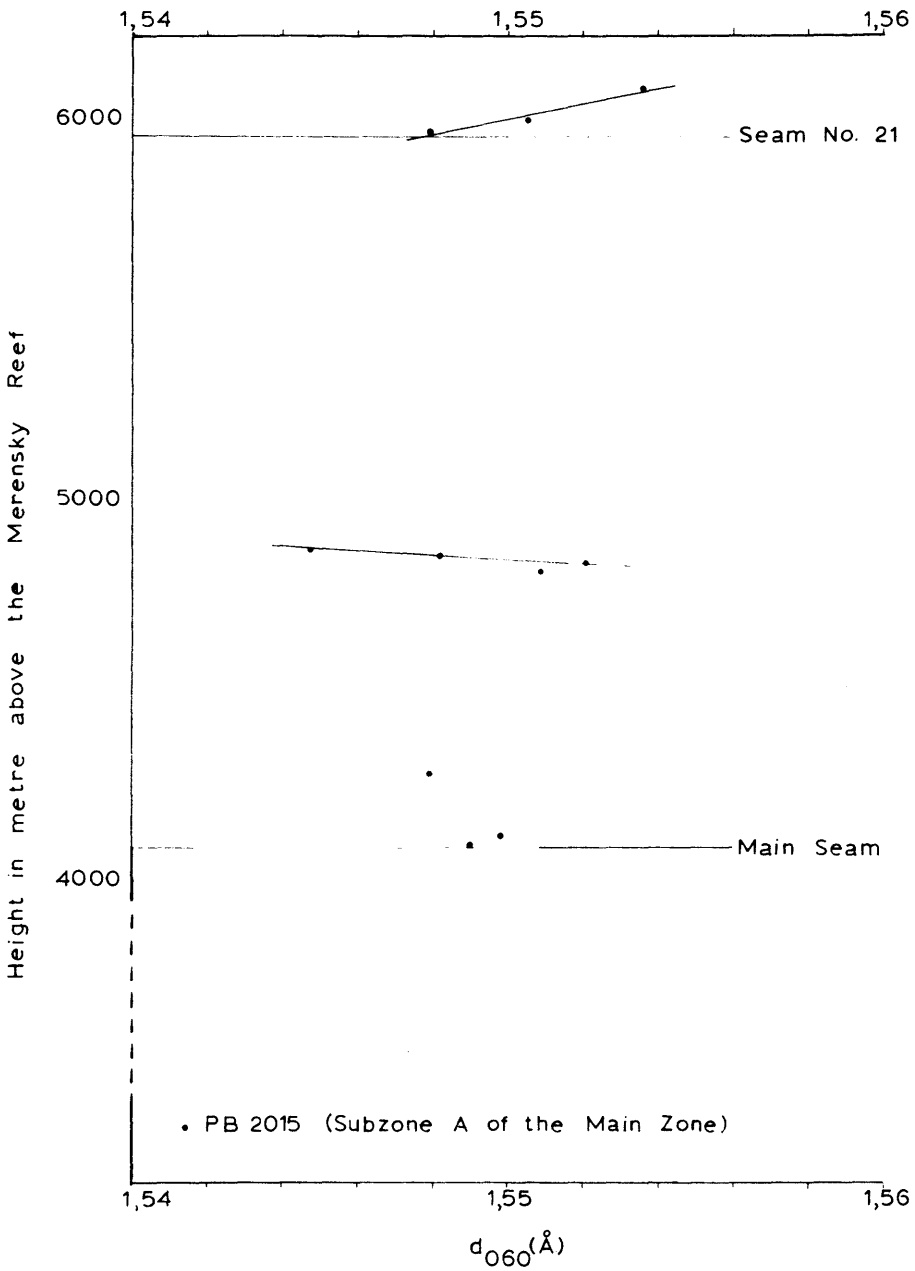

FIG. 50. VARIATION OF d_{060} OF BIOTITE IN THE UPPER ZONE

Seeing that biotite in all these rocks is intercumulus and in some rocks also a product of reaction (see description of symplektite in the section on postcumulus changes) it follows, from the fluctuating d_{060} values, that the oxygen fugacity in the intercumulus liquid changed considerably from one level in the intrusion to the next during crystallization. This may in part be due to changes in load pressure on the water-enriched intercumulus liquid, which is to some extent indicated by bent plagioclase crystals, reversed zoning of this mineral and the presence of various types of pegmatoids.

D. APATITE

1. Introduction

Apatite is an important constituent of the late differentiates in many layered intrusions throughout the world (Wager and Brown, 1968) and is known to be present in the rocks of the Upper Zone of the Bushveld Complex from many reports (Daly, 1928, p. 738; Boshoff, 1942, p. 28; Wager and Brown, 1968, p. 380; Willemse, 1969a, p. 13; Grobler and Whitfield, 1970, p. 208). Very little is, however, known about apatite in gabbroic rocks, and although various analyses exist (Taborszky, 1962, p. 368-369; Cruft, 1966, p. 382-383) the behaviour of this mineral with differentiation in a layered intrusion has not yet been studied.

It is commonly known that magmatic apatite may contain F, OH and Cl in various amounts, the relative abundances of which may give some indication of the environment of crystallization (Taborszky, 1962, p. 373-375). Apatite can also accommodate a large variety of trace elements which are also to some extent indicative of the magma from which the apatite has crystallized (ibid., p. 376; Cruft, 1966, p. 384). If this is borne in mind, as well as the fact that the rocks in layered intrusions are characterized by a gradual change in composition from bottom to top, small changes in abundance of certain elements in apatite from various heights in layered intrusions are to be expected.

Consequently, considerable time was spent on separating sufficient amounts of apatite from rocks of Subzone D of the Upper Zone where it occurs as cumulus crystals, generally in abundance of more than 3 per cent by volume (Folder IV). These samples were submitted to Dr P. J. Fourie of the Atomic Energy Board for analyses of the main and trace elements, but the results are unfortunately not yet available.

2. Microscopic investigation

a) General

Cumulus apatite is present as small idiomorphic crystals throughout the olivine-bearing rocks of Subzone D, and although mostly concentrated along grain boundaries between the silicates, it is also common as inclusions in the silicates and in magnetite (Fig. 51). Apatite occurring as inclusions is usually small, whereas that between the grain boundaries is larger. From this it is reasonable to assume that it started to crystallize early, and judging from the intercumulus nature of some of the grains, it probably crystallized until the final stages of consolidation. The small crystals were therefore trapped in the faster growing silicates, whereas others were pushed out of the way. For this reason, the larger apatite grains are often found to be intimately associated with the products of late crystallization (intercumulus material) such as titanomagnetite and biotite. For the modal distribution of apatite see the chapter on Modal Analyses, Folder IV and Appendix I.

b) Grain size

The size of the apatite crystals depends to a certain extent on the abundance of this mineral in the rock. For instance, in G200 and G201, where the apatite content is only about 0,5 per cent, the average dimensions of the crystals are 0,18 x 0,05mm, whereas in G253 where the apatite constitutes 8,5 per cent by volume of the rock, the average dimensions are 0,75 x 0,14mm. The largest apatite crystals were however found in a pegmatoidal rock (DDH2-248) some 30m below the Magnetitite Seam 21 in the bore-hole on Doornpoort 171 JS. Although crystals measuring up to 1,42 x 0,25mm and 1,25 x 0,55mm are present, the apatite content of this rock does not exceed 4 per cent.

c) Orientated inclusions

Many of the apatite crystals in the separated samples contain small rod-like inclusions usually orientated parallel to the c-axis of the apatite (Fig. 52). These inclusions consist either of biotite or of a green pleochroic mineral. In a few grains small specks of ore, probably magnetite, are also present as inclusions. Taborszky (1962, p. 365) mentions hornblende as inclusions in apatite from the Odenwald and it is possible that the green pleochroic mineral in the apatite of the Bushveld Complex is also hornblende. These inclusions are however, difficult to explain for the following reasons:

i) Biotite is always present in these rocks as intercumulus material and its presence in the centre of the apatite crystals, which are considered to be products of early crystallization, is therefore problematic.

ii) Hornblende is a primary intercumulus constituent only in rocks of the top 100m of the intrusion.

Some of the apatite crystals contain biotite and the green pleochroic mineral in one and the same inclusion and for this reason the latter mineral may also be considered as an alteration product of the biotite, possibly chlorite.

The biotite in the apatite is elongated parallel to its c-axis and the impression gained is that there seems to be an epitaxial relationship between these two minerals. From microscopic observations (Fig. 52) it seems as though the (010) and (110) planes of the biotite coincide with the prism faces of apatite. If these are the lattice planes in the two minerals on which the orientated overgrowth has taken place, then it follows that a_o of apatite must correspond to $2a_o$ of biotite and the c_o of apatite, or a multiple thereof, to c_o of biotite.

Deer et al. (1962, v. 3 p. 55 and v. 5 p. 324) give the following cell parameters for biotite and fluorapatite.

Biotite:	$a_o = 5,3$ Å	Apatite:	$a_o = 9,35$ Å
	$b_o = 9,2$ Å		$c_o = 6,87$ Å
	$c_o = 20,2$ Å		

There is a good correlation between $2a_o$ of biotite and a_o of fluorapatite, as well as between c_o of biotite and $3c_o$ of fluorapatite (20,61 Å). The differences between the cell parameters fall well within the 10-15 per cent permissible tolerance (Neuhaus, 1951, p. 156). Although there is a better correlation between b_o of biotite and a_o of fluorapatite, such an overgrowth would necessitate a morphological (100) plane of biotite, conditions under which the prism faces of biotite would not be parallel to those of apatite and would therefore not agree with the observed relationships (Fig. 52, bottom row).

Neuhaus (1951) gives a detailed review of researches on apitaxy whereas Von Vultée (1951) lists numerous examples of natural occurences of orientated intergrowths recorded in the literature prior to 1951. From Von Vultee's compilation, not much seems to be known about orientated inclusions in apatite.

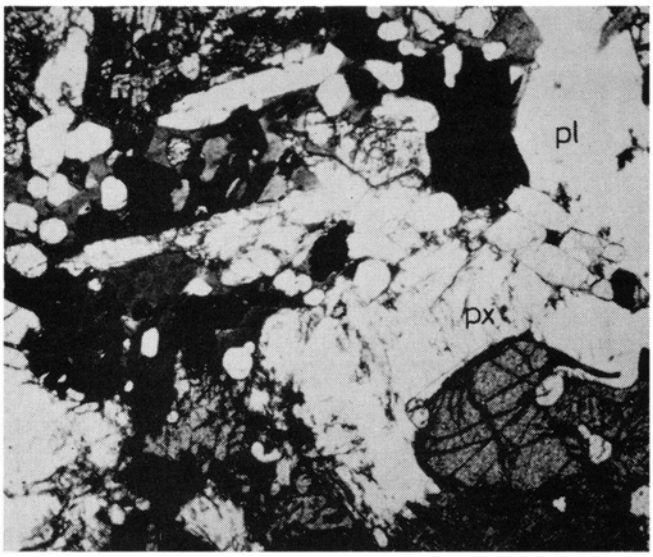

Fig. 51 Apatite-rich olivine diorite directly overlying Magnetitite Seam 21. Note small inclusions in olivine (bottom right) and larger crystals between pyroxene (px) and plagioclase (pl). G253, Duikerkrans 173 JS. x50.

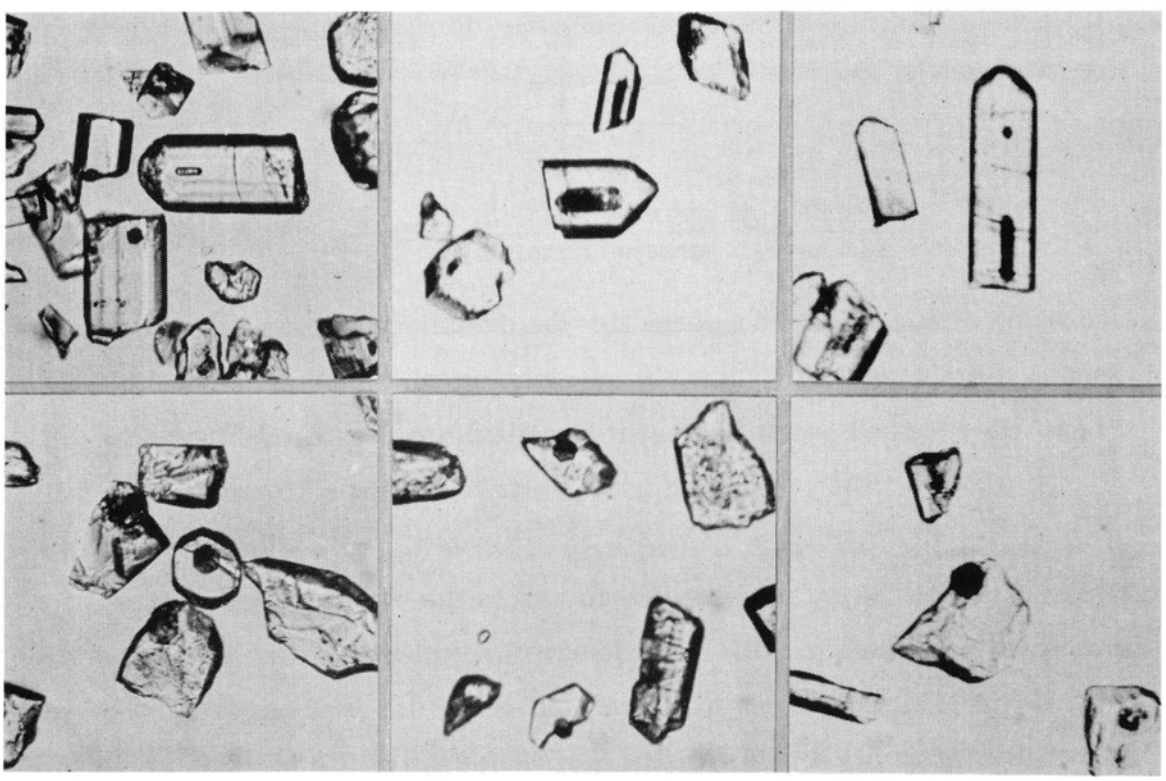

Fig. 52 Inclusions orientated parallel to the c-axis of apatite (top row). The inclusions have hexagonal outlines when viewed in (0001) cleavage fragments (bottom row). Apatite concentrates from various specimens, x100.

He mentions (ibid., p. 337) monazite and opaque ore parallel to the c-axis of apatite and ilmenite parallel as well as perpendicular to the c-axis of apatite. Orientated intergrowth of muscovite (host) and apatite is however recorded (p. 344) but none of the cited directions coincide with the observed ones.

3. Determinative methods

a) X-ray investigations

i) Method

X-ray powder data were obtained by using an AEG Guinier camera developed by Jagodzinski, with Cu-$K\alpha_1$ radiation and silicon as internal standard. The minerals were indexed with the aid of the Powder Data File, card No. 15-876. Cell dimensions c_o and a_o were calculated by using the reflections 00.4 and 41.0 respectively. The observed $\sin^2\theta$ values were compared with the $\sin^2\theta$ values which were calculated by using the determined cell parameters. Seeing that the differences are less than 0,00015, an accuracy of $\pm$ 0,003Å for the cell dimensions is indicated. The c/a ratio was also calculated after the method of Brasseur as modified by Förtsch (1970, p. 224), namely,

$$c/a = \sqrt{\frac{4 + 2m}{4m + 7}}$$

$$\text{where } m = \frac{\text{distance between 41.0 and 00.4}}{\text{distance between 21.3 and 32.1}}$$

The value of m is obtained by direct reading of the distances between the pairs of lines on the film. In most cases, the values obtained by this method differed only in the fourth decimal from those calculated from the 41.0 and 00.4 reflections. The results of this investigation are given in Table IX.

ii) Results

The most striking result of this investigation is borne out by the variation of the a_o value with height in the intrusion (Fig. 53). Apatite from the lowest horizon (G271) has an a_o of 9,388 Å. This value increases gradually to 9,417 Å, 70m below the roof of the intrusion from where it drops abruptly to 9,374 Å directly below the roof (G200).

Comparison of these results (Table IX) with the unit cell dimensions of the end-members of apatite, reproduced here from Deer et al. (1962, v. 5, p. 324) leads to the following conclusions:

TABLE IX PHYSICAL PROPERTIES OF APATITE FROM THE UPPER ZONE OF THE BUSHVELD COMPLEX

Sample No.	G271	G264	G257	G253	G368	G285	G208	G216	G215	G214	G201	G200
Height in m above M. R.	5350	5650	5735	5960	5990	6075	6140	6165	6180	6200	6207	6209
n_o (±0,002)	1,638	1,637	1,637	1,638	1,639	1,639	1,640	1,639	1,638	-	1,638	1,638
n_E (±0,002)	1,634	1,633	1,633	1,635	1,636	1,635	1,636	1,635	1,634	-	1,634	1,634
$(n_o - n_E)$	0,004	0,004	0,004	0,003	0,003	0,004	0,004	0,004	0,004	-	0,004	0,004
D (±0,01)	3,23	3,22	3,23	3,23	3,22	-	3,24	3,26	3,25	-	-	-
a_o (Å) (±0,003)	9,388	9,394	9,396	9,406	9,405	9,405	9,417	9,408	9,400	9,378	9,379	9,374
c_o (Å) (±0,003)	6,873	6,872	6,885	6,873	6,882	6,878	6,881	6,870	6,872	6,885	6,881	6,881
c/a calc.	0,732	0,732	0,733	0,731	0,732	0,731	0,731	0,731	0,731	0,734	0,734	0,734
c/a meas.	0,732	0,732	0,733	0,731	0,732	0,732	0,731	0,731	0,732	0,734	0,734	0,734

Unit cell dimensions of end-members of apatite

	a(Å)	c(Å)	c/a
Fluorapatite	9, 35	6, 87	0, 735
Chlorapatite	9, 61	6, 76	0, 704
Hydroxyapatite	9, 41	6, 87	0, 731

The a_o value of the first cumulus apatite is 9, 388 Å and is intermediate between that of fluorapatite and hydroxyapatite, whereas the c_o value corresponds closely to these two. This would seem to indicate that this apatite contains appreciable amounts of F and OH. The increase in a_o to 9, 417 Å points to a decrease in the F and an increase in the OH content of the apatite and specimen G208 therefore seems to be a relatively pure hydroxyapatite. The sudden drop in a_o from 9, 417 Å to 9, 374 Å in the top 70m of the intrusion is probably due to a sharp increase in the F component of the apatite.

The calculated unit cell dimensions would not favour any large amounts of Cl in the apatite, as these values differ considerably from those of chlorapatite. The ionic radius of Cl is 36 per cent and that of OH 5 per cent larger than that of F. An isomorphous series therefore exists between fluorapatite and hydroxyapatite, and these apatites are only able to accommodate limited amounts of Cl in their structure (Taborszky, 1962, p. 384). Taborszky (1962, p. 308) who studied apatites from the Odenwald, found that they are essentially fluorapatites with fair amounts of OH but very little Cl. He also found that the F/OH ratio in apatite is high in acid rocks and decreases in mafic rocks (p. 373 and 375). From this it is to be expected that the F/OH ratio should gradually increase with differentiation, but unit cell dimensions of apatite from the Upper Zone of the Bushveld Complex point to a considerable decrease in this ratio prior to an increase in the top 70m of the intrusion.

Stormer and Carmichael (1971, p. 130) came to the conclusion that in apatite and phlogopite (biotite) which are in exchange equilibrium with fluorine and hydroxyl at magmatic temperatures, there is a tendency for the F to occupy approximately 75 per cent of the halogen sites in the former and between 60 and 75 per cent in the latter. They point out that there was either a shortage of fluor, or late stage exchange at low temperatures where natural assemblages do

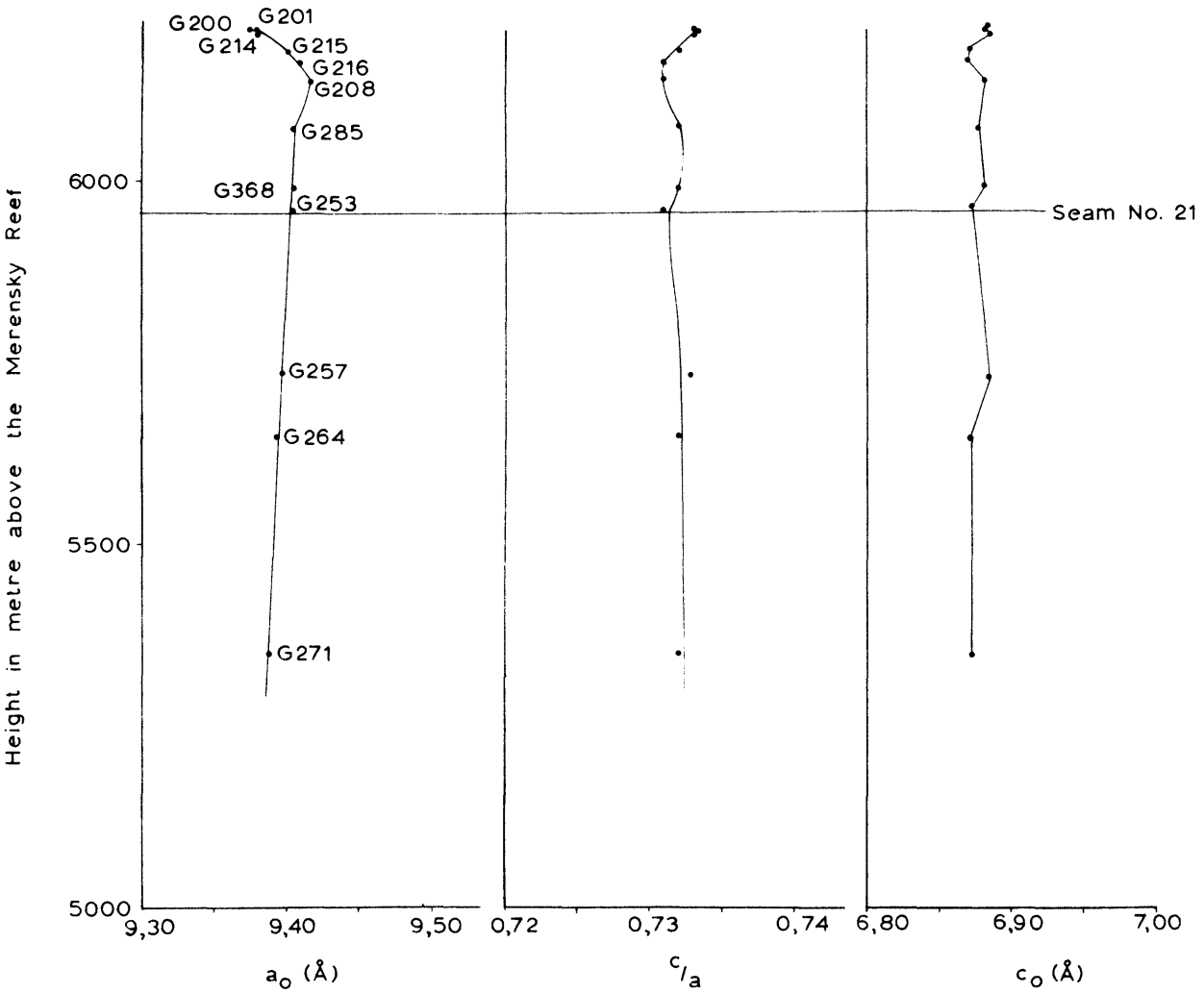

FIG. 53. VARIATION OF UNIT CELL PARAMETERS OF CUMULUS APATITE IN SUBZONE D OF THE UPPER ZONE

not show this relationship. Their results indicate that F has an affinity for apatite and that a F-rich apatite will crystallize from a magma if sufficient F is present.

It may therefore be concluded that at the beginning of crystallization of apatite, fluorine was present in fair amounts in the magma but that due to crystallization of the apatite its concentration in the magma decreased gradually. This probably resulted in more and more of the hydroxyl being incorporated in the apatite structure. The reversal in the top 70m of the intrusion is not ascribed to an increase in the fluorine content of the magma but to a decrease in its phosphorus content which resulted in a decrease in the amount of apatite in these rocks (Folder IV). Larger amounts of fluorine were therefore available for the smaller amounts of apatite which crystallized at the top, thus causing this reversal.

b) Refractive index and density

Routine refractive index determinations were made by means of the immersion method, the results of which are given in Table IX. It is evident that no conclusions can be drawn regarding the relative abundance of the F, OH and Cl content of the apatite, because the method used only allows for an accuracy of $\pm$ 0,002. These determinations do, however, show an increase in the refractive index with an increase in the a_o value.

The few density determinations, made according to the method outlined by Jahns (1939, p. 119-120), also show an increase with higher a_o values. Refractive index and density of the apatite therefore seem to increase with higher hydroxyl content.

4. Petrogenesis

Apatite is present in minute amounts as intercumulus material in many of the rocks of the Main and Upper Zones (Folder IV; Appendix I). It appears abruptly as a cumulus phase at the base of Subzone D in the Upper Zone and generally constitutes between 4 and 6 per cent by volume of the rocks. This would seem to indicate that most of the phosphorus remained in the magma during crystallization of the greater part of the Layered Sequence. Enrichment of this element in the remaining magma would be enhanced by adcumulus growth. Any phosphorus in rocks below Subzone D therefore seems to be present in intercumulus apatite and since cumulus minerals such as plagioclase, olivine and pyroxene are essentially devoid of this element, Wager (1963, p. 6)

concluded that the amount of P_2O_5 in analysed cumulates is an indication of the amount of trapped liquid. Henderson (1968, p. 907) has, however, shown that, although of a low order, phosphorus enters cumulus minerals and may, in some instances, comprise most of the phosphorus in certain adcumulates.

Wager (1960, p. 378-381) calculated the amount of P_2O_5 in successive residual liquids of the Skaergaard Intrusion and concluded that cumulus apatite began to crystallize when the concentration of phosphorus in the magma was 7500ppm (1,75 per cent P_2O_5) (Wager and Brown, 1968, p. 201). Peck et al. (1966, p. 653) also found that P_2O_5 is concentrated in the differentiated liquids (oozes) confined to the interstices of crystallizing tholeiitic basalt in the Alae Lava lake of Hawaii and it was even possible for them to plot this increase in P_2O_5 in the liquids as a function of the temperature of formation of the oozes (ibid., Fig. 11, p. 652). They found that apatite appears as tiny needles in the interstitial glas at 1000°C, and extrapolation of their Fig. 11 reveals that this necessitates a P_2O_5 concentration of about 1,8 per cent (7700ppm P), a value which agrees closely with that determined by Wager and Brown (1968, p. 201). From this it may be concluded that apatite started to crystallize when the phosphorus content of the Bushveld magma was in the vicinity of 7500-7700ppm.

The association of cumulus apatite with olivine and its absence in the olivine-free rocks associated with Magnetitite Seams 17 to 21 (Folder IV; Appendix I) is difficult to explain, but is probably governed by conditions in the magma chamber leading to the precipitation of magnetitite seams. If it is assumed, as proposed by Roeder and Osborn (1966, p. 452-455), that fractionation of magma during the crystallization of the Fe-rich olivines took place at low oxygen pressures i. e. in a closed system where the oxygen content of the crystallizing mixture remains constant, then the associated cumulus apatite would seem to favour similar conditions for crystallization. A constant pO_2 during fractional crystallization causes a change in the oxygen content of the mixture and an increase in the oxygen content of the condensed phases (ibid., p. 454; Hamilton and Anderson, 1967, p. 464). If the oxygen pressure is sufficiently high, it favours crystallization of magnetite. The presence of cumulus magnetite in the apatite-bearing olivine diorites of the Upper Zones would therefore indicate fairly high, constant pO_2 conditions. A slight rise in the pO_2 would probably augment crystallization of magnetite to form magnetitite seams and cessation of crystallization of olivine, conditions under which apatite also did not crystallize.

During the formation of the magnetitite seams of Subzone D, the phosphorus content of the magma therefore increased with the result that when conditions returned to "normal" (i. e. slightly lower oxygen pressure) the crystallizing rocks were enriched in apatite. The highest percentage of apatite (8, 5 per cent by volume) is in rocks directly overlying Magnetitite Seam 21.

Simultaneous crystallization of olivine and magnetite, as indicated in Seam 21, would point to an extreme iron enrichment in the magma, so much so that only a slight increase in oxygen pressure was sufficient to cause abundant crystallization of magnetite but not sufficient to stop crystallization of olivine. The olivine-apatite magnetitites in the Villa Nora area, which contain up to 30 per cent apatite (Grobler and Whitfield, 1970, p. 219), on the other hand, would indicate a simultaneous oversaturation of phosphorus in this locality, so much so that crystallization of large quantities of magnetite did not influence the crystallization of the apatite. Grobler and Whitfield (1970, p. 225) are however of the opinion that these lenticular magnetitite bodies could possibly have formed by a process of residual liquid accumulation and immiscible liquid segregation. This immiscible liquid was then injected concordantly into the host rocks. The available evidence, as cited by these authors indicates that the conditions of formation of these bodies were different from those of the normal apatite-bearing rocks in the area mapped, as well as in other areas of the complex.

E. THE SULPHIDES IN THE UPPER ZONE

1. Introduction

The various sulphides which are present in the Layered Sequence of the Bushveld Complex have already been described in detail by Liebenberg (1970, p. 115-141). Therefore, the purpose of this study is not to describe the various sulphide minerals again, but rather to describe their occurrence in the various horizons present in the area examined. Three mineralized horizons were described by Liebenberg in the sequence dealt with in this investigation: the mineralized anorthosite below the Main Seam, that below the uppermost magnetitite seam, and a mineralized magnetite gabbro some distance above the Main Magnetite Seam in the vicinity of Magnet Heights. This last horizon was not found to be mineralized in the area investigated, although it must be mentioned that outcrops at this particular horizon are not very good. Two additional horizons were found to be mineralized in this area, namely, a mineralized

anorthosite below Lower Magnetitite Seam 2, and concentrations of sulphides in the uppermost magnetitite seam.

In Table X the volumetric composition of the sulphide phase in the various rock groups and mineralized horizons are presented. The values given by Liebenberg (1970, p. 163) for the mineralized horizons of the Upper Zone, have been included for comparison. The following methods were used to attain the values in this table:

a) Conventional point count analyses were made on various polished sections of the mineralized horizons with the aid of a Swift Automatic point counter. (1, 3, 11 and 12, Table X).

b) The ordinary gabbroic rocks usually contain 0,5 vol. per cent or less sulphides. To obtain reasonable values for the various sulphide phases, the cross-hair in the ocular was replaced by a glass disc with a grid engraved on it. The polished sections were placed on a mechanical stage and the sulphide phases at the intersections of the grid lines were counted. Because of the low sulphide content of these rocks, the values given in columns 6, 7, 8, 9, 13 and 14 of Table X do not represent specific horizons in the intrusion, but the average sulphide content of several specimens from characteristic rock units.

2. Variation of the minerals in the sulphide phase

In his description of the sulphides of the Bushveld Complex, Liebenberg (1970, p. 141-147) found certain variations in the mineral composition of the sulphide phase with height in the intrusion. He found (p. 146) that pyrrhotite increases with height in the Upper Zone and attains a maximum value in the mineralized anorthosite below the Magnetitite Seam 21. Chalcopyrite attains its maximum value in the ordinary magnetite-bearing gabbroic rocks but makes way for pyrrhotite in the olivine-bearing rocks. Pentlandite decreases gradually with height in the intrusion whereas pyrite is the most abundant sulphide in the uppermost differentiates (diorites) of the Complex.

The results of this investigation generally confirm Liebenberg's findings but as a larger number of samples from this sequence has been examined, more information concerning the sulphide phase has been obtained.

In the magnetite-bearing anorthosites and gabbros, pyrrhotite increases from 31,2 per cent (Table X; Fig. 54a) in the mineralized anorthosite below Lower Magnetitite Seam 2 to 75,3 per cent (7, Table X) in magnetite gabbros of Subzone C. In all the olivine-bearing rocks above the magnetite gabbros of

TABLE X VOLUMETRIC COMPOSITION OF THE SULPHIDE PHASE IN VARIOUS HORIZONS OF THE UPPER ZONE

	1	2*	3	4*	5*	6	7	8	9	10*	11	12	13	14
Pyrrhotite	31,2	51,0	55,6	57,3	55,1	54,7	75,3	96,7	95,4	85,6	81,6	95,1	95,7	15,4
Pentlandite	5,9	5,4	5,5	4,8	5,1	1,8	1,2	0,5	0,4	7,6	-	0,3	0,2	tr.
Chalcopyrite	55,0	34,9	35,6	35,7	38,2	37,4	22,6	2,7	4,0	6,4	6,6	2,6	3,1	2,6
Pyrite	7,9	8,3	3,3	1,6	0,8	3,1	0,9	-	tr.	-	2,0	1,9	0,7	81,5
Sphalerite	tr,	0,2	tr.	0,2	0,4	-	tr.	tr.	0,2	0,4	9,6	0,1	0,25	0,5
Cubanite	-	-	-	-	-	3,0	-	0,1	-	-	-	-	-	-
Mackinawite	-	0,1	-	-	0,2	tr.	-	tr.	-	-	-	-	-	-
Galena	-	-	-	-	-	-	-	-	tr.	-	0,2	-	0,05	-
Gersdorffite	-	-	-	-	0,3	-	-	-	-	-	-	-	-	-
No. of points counted	4874	-	2155	-	-	3561	3113	4818	4276	-	4932	2224	6259	1976
No. of sections averaged	4	-	2	-	-	6	4	4	6	-	3	4	5	5

*Values taken from Liebenberg 1970, p. 193.

For sample localities see Table XI.

Subzone C, pyrrhotite constitutes more than 95 per cent of the minerals in the suphide phase. The mineralized anorthosite below Magnetitite Seam 21 however, contains less pyrrhotite (No. 11, Table X). In the diorites at the top of the intrusion, pyrrhotite decreases sharply to 15, 4 per cent of the sulphides (No. 14, Table X).

Chalcopyrite attains its maximum value of 55, 0 per cent in the mineralized anorthosite below Lower Seam 2. It gradually decreases upwards in the intrusion to 22, 6 per cent in the ordinary gabbroic rocks of Subzone C. Above this horizon, the chalcopyrite drops to less than 4 per cent and remains fairly constant in all the olivine-bearing rocks. There is a slight increase in this mineral in the mineralized anorthosite below Magnetitite Seam 21.

Pentlandite decreases gradually with height, irrespective of whether olivine is present or not. Of interest is the high pentlandite content recorded by Liebenberg in the mineralized anorthosite below the uppermost magnetitite seam. An increase in the pentlandite content at this horizon is to be expected if the general reversal of the trend of the other sulphides at this horizon is considered (Table X). The sections investigated in this study did not contain any pentlandite in measurable quantities, and one section in particular was found to contain 36 per cent sphalerite (DDH2-243). No explanation for this anomaly can be offered.

Pyrite is present in small quantities in the gabbroic rocks below the olivine-bearing rocks of Subzone D. It is conspicuously absent in the olivine-bearing rocks below the uppermost magnetitite seam, but appears again in this seam and in the overlying olivine-bearing rocks. It is the most common sulphide in the topmost differentiates (diorites) of the intrusion.

The association of pyrite and cubanite in the magnetite gabbros of Subzone B (column 6, Table X) is anomalous. Pyrite is present in two of the six sections from this subzone (G569 and G510), whereas cubanite was found to be developed in four of these six sections (G351, G422, G510 and G652). Only in one of these sections does cubanite occur together with pyrite. The textural relations suggest that the cubanite is a primary mineral of the early separated sulphide phase, whereas pyrite, seems to have replaced pyrrhotite at a very late stage. This association will be discussed in more detail further on.

In Table XI the proportions of the major elements in the sulphide phase have been calculated from the values given in Table X, and by using densities

TABLE XI WEIGHT PER CENT OF THE MAJOR ELEMENTS IN THE SULPHIDE PHASE OF THE VARIOUS HORIZONS. (Calculated from the values given in Table X).

Element	1	2	3	4	5	6	7	8	9	10	11	12	13	14
Fe	41,6	47,5	48,1	48,3	47,5	48,1	53,6	59,5	59,0	56,0	53,1	58,4	59,2	48,0
Ni	2,2	2,0	2,0	1,8	1,9	0,7	0,4	0,2	0,1	2,7	–	0,1	0,1	–
Cu	18,0	11,3	11,6	11,6	12,5	13,0	7,3	0,7	1,3	2,0	2,1	0,7	1,0	0,7
Zn	–	0,1	–	0,1	0,3	–	–	–	0,1	0,2	5,7	–	0,3	0,1
S	38,2	39,1	38,3	38,2	37,8	38,2	38,7	39,5	39,5	39,1	39,1	39,8	39,6	51,0

1. Mineralized anorthosite below Lower Magnetitite Seam 2, Zwartkop 142 JS.
2. Mineralized anorthosite below the Main Magnetitite Seam, Zwartkop 142 JS (Liebenberg, 1970, p. 193).
3. Mineralized anorthosite below the Main Magnetitite Seam, Zwartkop 142 JS.
4. Mineralized anorthosite below the Main Magnetitite Seam, Magnet Heights (Liebenberg, 1970, p. 193).
5. Mineralized anorthosite 70m above the Main Magnetitite Seam, Magnet Heights (Liebenberg, 1970, p. 193).
6. Sulphides in the magnetite gabbros of Subzone B. Luipershoek 140 JS and Mapochsgronde 500 JS.
7. Sulphides in the magnetite gabbros of Subzone C. Luipershoek 140 JS.
8. Sulphides in olivine diorites of Subzone D, Luipershoek 140 JS.
9. Sulphides in olivine-bearing dioritic rocks of Subzone D, below Magnetitite Seam 21. Bore-hole DDH2, Doornpoort 171 JS.
10. Mineralized anorthosite below Magnetitite Seam 21, Duikerskrans 173 JS (Liebenberg, 1970, p. 193).
11. Mineralized anorthositic rock, 20m below Magnetitite Seam 21. Bore-hole DDH2, Doornpoort 171 JS.
12. Sulphides in the Magnetitite Seam 21. Bore-hole DDH2, Doornpoort 171 JS.
13. Sulphides in olivine-bearing diorites above Magnetitite Seam 21, Bore-hole DDH2, Doornpoort 171 JS.
14. Sulphides in the uppermost dioritic rocks from Tauteshoogte.

and chemical formulae as given in Dana (Ford, 1955). These results are presented diagrammatically in Fig. 54B. The distribution of the elements in the sulphide phase shows smooth variations with height in the intrusion. There is a very gradual increase in the sulphur content from 38, 2 per cent at the base of the Upper Zone to 39, 6 per cent in the olivine diorite above Magnetitite Seam 21. Above

FIG. 54A. VARIATION OF MINERALS IN THE SULPHIDE PHASE OF THE UPPER ZONE

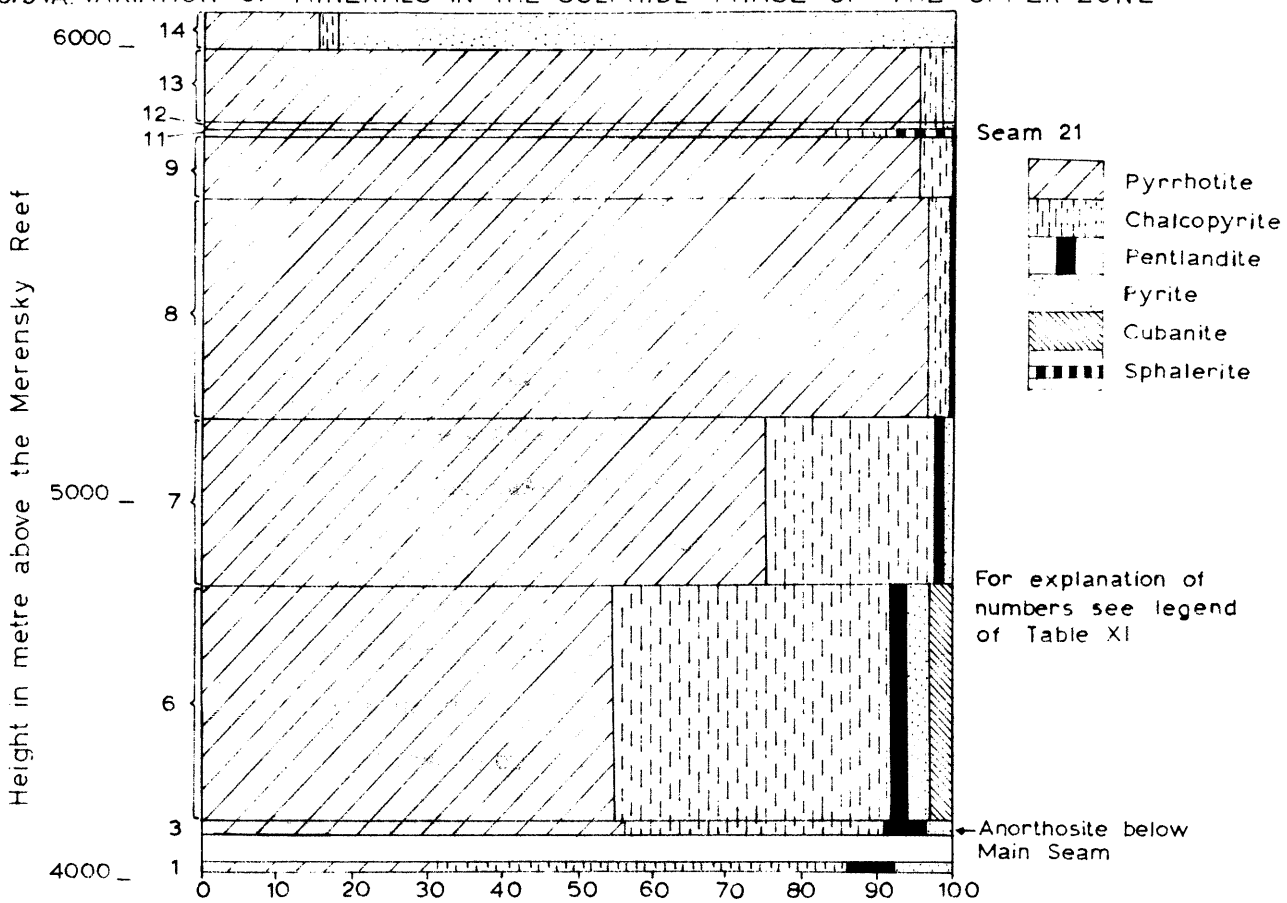

FIG. 54B. VARIATION OF ELEMENTS IN THE SULPHIDE PHASE OF THE UPPER ZONE

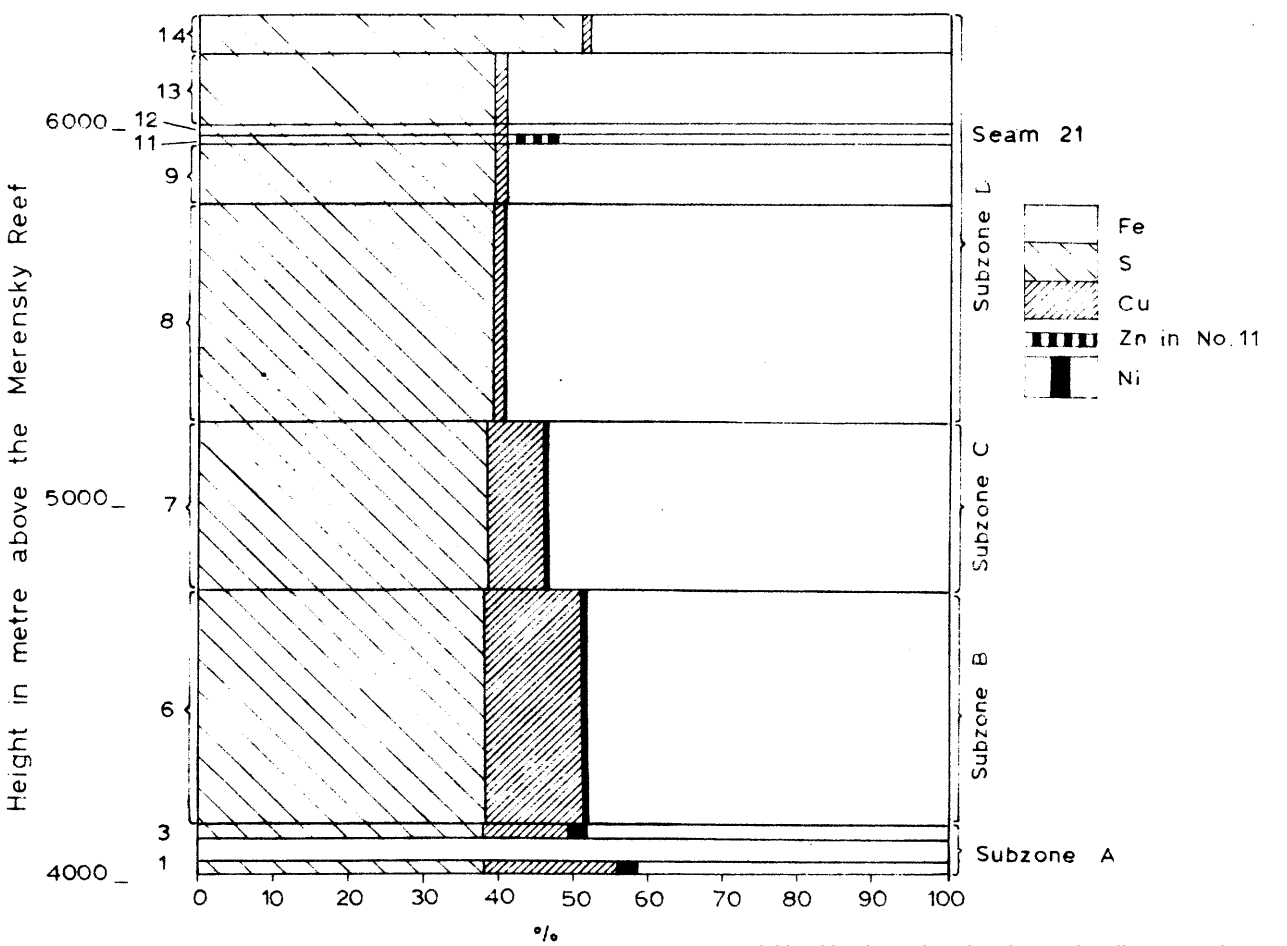

this horizon there is a sharp increase to 51 per cent in the topmost differentiates of the intrusion.

The behaviour of Cu and Ni with height is analogous to that of chalcopyrite and pentlandite (Figs. 54A and B) respectively. The Fe content increases fairly rapidly in the lower half of the Upper Zone, remains fairly constant at its maximum of about 59 per cent in the olivine-bearing rocks in the upper half of the Upper Zone, and drops sharply to 48 per cent at the top of the intrusion.

These modal analyses therefore show:

a) A decrease of chalcopyrite and pentlandite in the normal magnetite (olivine-free) gabbroic rocks in the lower half of the Upper Zone together with a concomitant increase in the pyrrhotite content.

b) A relatively constant pyrrhotite-chalcopyrite ratio in the olivine-bearing dioritic rocks in the upper half of the Upper Zone.

c) An abrupt increase of pyrite and a decrease of pyrrhotite in the top 100m of the intrusion.

Before the significance of these trends is discussed any further with the aid of published phase diagrams, it is necessary to describe briefly the textures of the sulphide minerals in the various horizons.

3. Description and textural features of the sulphides

a) The sulphides in the anorthosite below Lower Seam 2 (1, Table X)

Underlying the Lower Magnetitite Seam 2 is a mottled anorthosite, 1,5m thick, which contains disseminated sulphides at its top. In the riverbed on the farm, Zwartkop, 142 JS, 0,5km to the north of the area investigated, there is a concentration of sulphides at this horizon, with the result that sulphides are present throughout the anorthosite, a few specks also being found in the underlying magnetite gabbro. This enrichment in sulphides was observed for about 10m along strike on both sides of the riverbed.

Five polished sections of this occurrence were examined and the sulphides identified are chalcopyrite, pyrrhotite, pentlandite and pyrite, as well as the alteration products of pyrrhotite and pentlandite, namely, melnikowite-pyrite and bravoite, respectively. In addition to these, a small amount of sphalerite was found in association with the chalcopyrite. The chalcopyrite also contains a few very small specks of blueish-white, probably platinum-bearing, minerals.

Point count analyses were carried out on four of the polished sections and the result is given in Table XII. According to this modal analysis, the anortho-

TABLE XII POINT COUNT ANALYSIS OF THE MINERALIZED ANORTHOSITE BELOW LOWER MAGNETITITE SEAM 2

Mineral	Points counted	Vol. %	Wt. %
Chalcopyrite	2636	1, 96	3, 00
Pyrrhotite	1488	1, 11	1, 86
Pentlandite	275	0, 21	0, 37
Pyrite	380	0, 28	0, 50
Ilmenite	95	0, 07	0, 12
Silicates (more than 99% plag.)	129 441	96, 37	94, 15
	134 315	100, 00	100, 00

Total area counted: 21, 2 sq. cm.

site contains 1, 04% Cu, 0, 12% Ni and 2, 9% S. This may therefore be considered as a comparatively rich mineralized horizon, and consequently two samples were sent for chemical analyses to the Anglo American Corporation of S. A. Ltd., the owners of the mineral rights. Their results are listed in Table XIII.

TABLE XIII PARTIAL CHEMICAL ANALYSES OF THE MINERALIZED ANORTHOSITE BELOW LOWER MAGNETITITE SEAM 2

Element	G562B	$G562B_1$	Average	Reported in
Copper	1, 10	0, 92	1, 01	per cent
Nickel	0, 18	0, 17	0, 175	"
Cobalt	0, 02	0, 02	0, 02	"
Zinc	0, 01	0, 01	0, 01	"
Arsenic	0, 005	0, 002	0, 004	"
Sulphur	2, 23	2, 30	2, 27	"
Platinum	0, 76	0, 83	0, 80	g/ton
Palladium	0, 76	0, 96	0, 86	"
Gold	0, 40	0, 47	0, 44	"
Silver	1, 52	1, 46	1, 49	"
Total precious metals	3, 44	3, 72	3, 59	"

The sulphides, magnetite and ilmenite are intercumulus and from textural relationships it seems as if the sulphides were the last to crystallize because they are moulded around the relic titanomagnetite grains.

Chalcopyrite is the main sulphide mineral. It is present as large grains which contain small blebs of pyrrhotite, and also as lens-like or lamellar exsolution-bodies in pyrrhotite. Sphalerite, in small patches, is intimately associated with the chalcopyrite. In one chalcopyrite grain a small asterisk-like exsolution of sphalerite was observed.

Apart from exsolution blebs and lamellae of chalcopyrite, pyrrhotite also contains flames and lamellae of pentlandite, both exsolved parallel to the (0001) direction. The hexagonal variety of pyrrhotite is the most common and contains only a few lamellae of the low temperature monoclinic variety. The pyrrhotite of this horizon is altered in places to a dull, light grey, lamellar, isotropic mineral, probably melnikowite-pyrite (Liebenberg, 1970, p. 140). Where this mineral is present, alteration was complete and rims around unaltered pyrrhotite were never observed. A certain amount of resorption of pyrrhotite has taken place after exsolution of the pentlandite lamellae and can be seen from pentlandite lamellae which protrude for a small distance into the surrounding silicates. In extreme cases, all the pyrrhotite around such lamellae was resorbed with the result that only pentlandite lamellae which have the same orientation as those in the nearby pyrrhotite remain (Fig. 55).

Pentlandite has a twofold mode of occurrence in this ore, namely, as exsolution-lamellae and flames concentrated along grain boundaries in the pyrrhotite and occasionally in the chalcopyrite (Fig. 56), as well as discrete grains at the margin of larger pyrrhotite grains. Where chalcopyrite is present, the pentlandite is always developed between the chalcopyrite and the pyrrhotite. The granular pentlandite exhibits an octahedral cleavage and fracturing, which is due to its high coefficient of thermal expansion (Morimoto and Kullerud, 1964, p. 205). Pentlandite alters to bravoite which is slightly more red and has a lower reflectivity. Rims of alteration are often found around unaltered pentlandite. Bravoite may be present together with unaltered pyrrhotite but where pyrrhotite has altered to melnikowite-pyrite, all the pentlandite is altered to bravoite.

Pyrite is present as rims around all the other sulphides. It is usually separated from them by a thin rim of late silicates and in most cases is seen to

replace early formed silicates. This seems to indicate that pyrite was the last sulphide to crystallize.

No magnetite was observed in any of the sections investigated, although skeletal ilmenite, typical of the exsolution texture in magnetite, indicates that it was present at an early stage. In many sections from the Upper Zone, the pyrrhotite has either replaced magnetite or filled cavities left by the dissolution of the magnetite (Fig. 57). The exsolved ulvospinel is oxidised to ilmenite, although the delicate exsolution texture is in most cases preserved.

b) Sulphides in the magnetite gabbros of Subzone A

Three polished sections of magnetite gabbros from Subzone A were investigated. The sulphide content in all the sections is very low. From visual estimates, chalcopyrite and pyrrhotite are the most common sulphides and are present in approximately equal amounts. The other sulphides are pentlandite and pyrite.

c) The sulphides in the anorthosite below the Main Magnetitite Seam (3, Table X)

The sulphides in this anorthosite have been described by Liebenberg (1970, p. 193). One of his samples comes from the Roossenekal area, and it is not necessary to repeat the textural relations. One sample (G655) of this anorthosite was collected by the author in Zwartkop 142 JS and point counts on two polished sections were made (Table XIV).

TABLE XIV MODAL ANALYSIS OF THE MINERALIZED ANORTHOSITE (G655) BELOW THE MAIN MAGNETITITE SEAM. ZWARTKOP 142 JS

Mineral	Points counted	Vol. %	Wt. %
Chalcopyrite	767	1, 3	1, 97
Pyrrhotite	1196	2, 0	3, 37
Pentlandite	117	0, 2	0, 35
Pyrite	71	0, 1	0, 21
Ilmenite	4		
Plagioclase	57 353	96, 4	94, 1
	59 508	100, 0	100, 00

Total area counted: ± 10, 0 sq. cm.

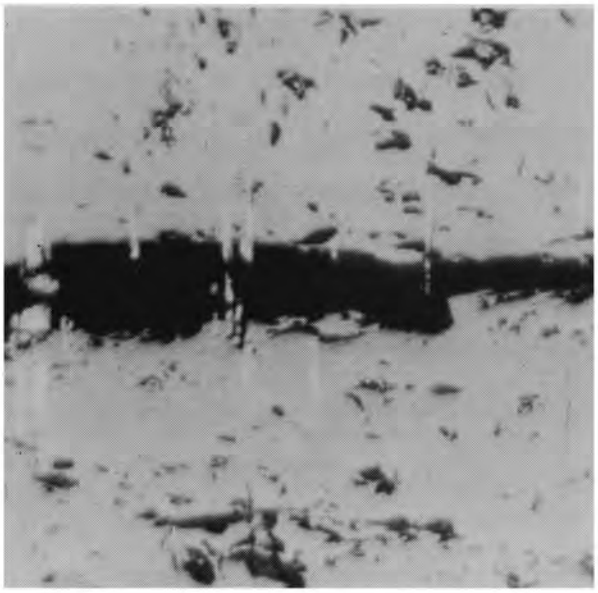

Fig. 55. Exsolution-lamellae of pentlandite protruding into gangue due to replacement of pyrrhotite. Mineralized anorthosite below Lower Seam 2 (G562B). Reflected light, x250.

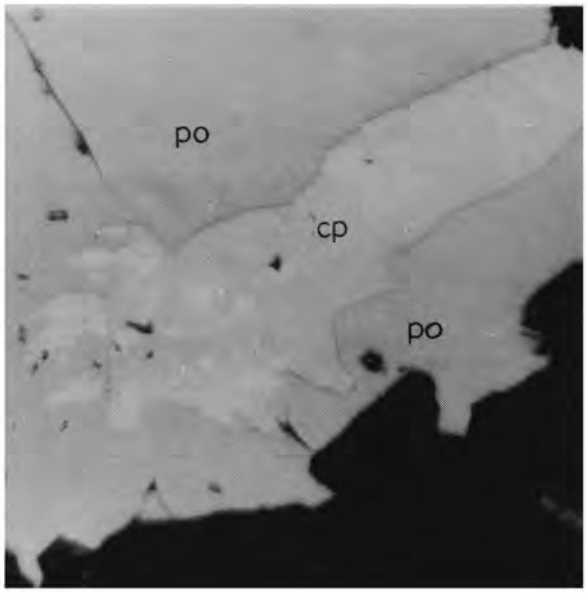

Fig. 56. Pyrrhotite containing exsolved chalcopyrite and pentlandite. Pentlandite (white) is present as exsolution flames in pyrrhotite (po) as well as in chalcopyrite (cp). Mineralized anorthosite below Lower Seam 2 (G562B). Reflected light, x250.

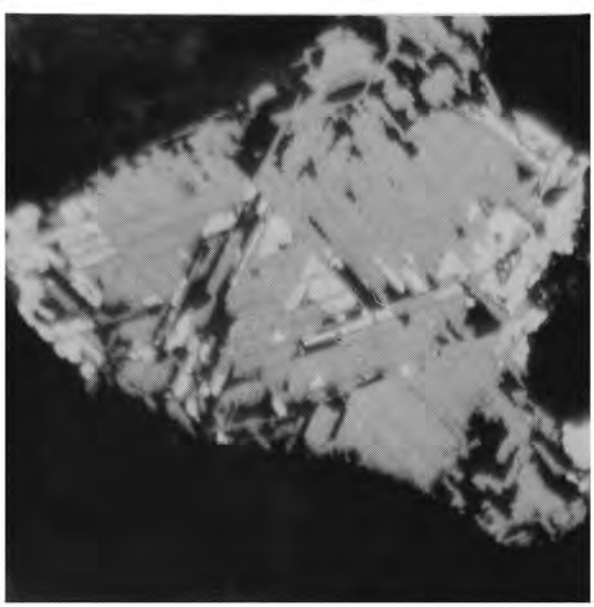

Fig. 57. Pyrrhotite and gangue replacing magnetite but not ilmenite. Olivine diorite (DDH2-229) Reflected light, x250.

According to this volumetric analysis the anorthosite at this locality contains 0,68% Cu, 0,11% Ni and 2,26% S.

The textures of the sulphide minerals are essentially the same as those described in the previous section. The only differences are that the pyrite does not form late rims around the other sulphides, but is present as grains within pyrrhotite. In these sections it can clearly be seen that alteration of pyrrhotite to melnikowite-pyrite starts along the grain boundaries and cracks in the pyrrhotite and advances more rapidly parallel to the (0001) plane of the pyrrhotite.

When the volumetric composition of the sulphides is compared with similar analyses cited by Liebenberg (Table X, Nos 2, 3 and 4) then it is striking how little the composition varies from one locality to the next. Only the pyrrhotite and pyrite content varies which may be explained by small differences in the S content of the sulphide phase.

d) The sulphides in the magnetite gabbros of Subzone B (6, Table X).

The sulphide phase of this horizon is characterized by the presence of cubanite, which occurs as lamellae and blebs in pyrrhotite as well as in chalcopyrite, and is readily distinguishable from chalcopyrite by its paler yellow colour and more lively anisotropism. In one section (G652) thin lamellae of pentlandite were observed in the cubanite. The textures of the other sulphide minerals are similar to those described in the previous chapters.

In certain sections, (G510, G569) pyrrhotite and pentlandite are partially altered to melnikowite-pyrite and bravoite. Wherever these alteration products were encountered in the sequence, they were regarded as the original product. The final alteration product of melnikowite-pyrite seems to be pyrite, but it is often difficult to discern whether the latter has not replaced pyrrhotite at a later stage. The pyrite in the two sections G510 and G569 is however only present where pyrrhotite has been altered to melnikowite-pyrite, and the impression gained is that the pyrite is not part of the primary sulphide minerals.

e) The sulphides in the magnetite gabbros of Subzone C (7, Table X).

The sections investigated of the olvine-bearing rocks of the Sisal Horizon contained very little sulphides and a point count analysis of the few specks encountered would not have been very reliable. Liebenberg (1970, p. 142, Fig. 25) gives an estimate of the composition of the sulphide phase of this horizon and records the absence of chalcopyrite. Sections investigated in this study, however,

showed that chalcopyrite and pyrrhotite are the most abundant sulphides in this horizon. The olivine-bearing rocks from the Sisal Horizon are relatively thin and would not greatly affect the trends observed in the larger rock units.

The sulphide phase in the overlying magnetite gabbro is enriched in pyrrhotite compared to the underlying magnetite gabbros, and also contains considerably less chalcopyrite. Cubanite is absent in these rocks and a small amount of pyrite was observed in one of the four sections investigated. This pyrite is not associated with the other sulphide minerals, but is present as irregular isolated patches and therefore does not seem to be part of the primary sulphide phase.

The textural relationships are similar to those described from lower horizons.

f) The sulphides in the olivine diorites of Subzone D (8, Table X)

A few interesting changes occur at the base of this subzone. The first of these is a sudden increase in the pyrrhotite content from about 75 per cent in the underlying olivine-free gabbroic rocks to more than 95 per cent. This high pyrrhotite content is characteristic of all the olivine-bearing rocks in the upper half of the Upper Zone. The second change, which was already noticed in a section (G642) high up in the previous rock unit, but which is present throughout the olivine-bearing rocks higher up, is that the sulphides occur in small rounded to elongated droplets on an average 0,25 x 0,15mm in size, fairly evenly distributed throughout the rocks. In rocks from lower horizons, the sulphides are essentially interstitial and have very irregular outlines. A further characteristic is that many of the small rounded droplets are either enclosed in or developed at the margins of the titanomagnetite and ilmenite grains. This would seem to indicate that the sulphides crystallized before or simultaneously with the oxide minerals, whereas in lower horizons of the Upper Zone, the sulphides crystallized after the oxide minerals. Another change noticed was that the olivine-bearing rocks in the upper half of the Upper Zone contain a fairly uniform content of 0,5 per cent sulphides, compared to the rather erratic and usually much lower values of the olivine-free gabbros of the lower half of the Upper Zone.

The textural relations of the minerals in the sulphide phase remain essentially the same. The low Ni and Cu content (8, Table XI) of the sulphide phase results in the absence of pentlandite and chalcopyrite as discrete grains. These

two minerals occur as exsolution-lamellae parallel to the basal plane of the pyrrhotite. Small blebs of chalcopyrite are occasionally found to be developed at the margin of the pyrrhotite grains but are also considered to have originated by exsolution of chalcopyrite from pyrrhotite.

A small amount of cubanite and mackinawite was noticed in one section (G634). The latter is present as thin exsolution-lamellae in pyrrhotite and was identified by its strong pleochroism from dark grey to white, and its characteristic black and white anisotropism under crossed nicols.

g) Sulphides in olivine-bearing diorites between Magnetitite Seams 17 and 21

The rock types developed between Seams 17 and 21 either contain very little olivine or are olivine-free. It was also noted (see chapter on lateral variation of facies) that the amount of olivine in this part of the sequence increases gradually in a southerly direction, and also in a westerly direction as indicated by the olivine-bearing rocks intersected below the 21st Seam in bore-hole DDH2 on the farm Doornpoort 171 JS. The sulphides described from this portion of the sequence were studied from material obtained from this bore-hole. Sections of samples from olivine-free rocks in this part of the sequence contain very little sulphides. It must be mentioned that of the six samples investigated, three were taken from above the mineralized anorthosite described in the next section, and that three were taken from below that horizon.

The presence of what may be described as secondary sulphides, is characteristic of the olivine-bearing rocks in this and higher horizons. These secondary sulphides were already noted in small quantities at the top of the previous rock unit, but they contribute quantitatively much more to the modal composition in the higher horizons. They can be distinguished fairly readily from the primary types in that the former do not occur as droplets and in that they are associated with late stage alteration products of olivine and magnetite.

Pyrrhotite is the most common of these secondary sulphides, although some pyrite was observed together with the pyrrhotite in the uppermost magnetitite seam. Where this pyrrhotite occurs together with altered olivine, secondary magnetite, serpentine or ilvaite are invariably present.

A texture that is fairly common in these rocks is magnetite which is dissolved, leaving behind a skeletal texture of exsolved ilmenite. These resorbed areas are usually filled with chloritic material but in some places also by pyrrhotite (Fig. 57) which must necessarily be of a later generation than the

pyrrhotite of the droplets. All the secondary pyrrhotite is of the low temperature monoclinic variety.

h) The mineralized anorthosite 20m below the Uppermost Magnetitite Seam (11, Table X)

Strictly speaking, this is not a pure anorthosite as are those developed below lower magnetite seams, but contains fair amounts of hornblende and biotite. It is some 3m thick and is in places anorthositic. Olivine is conspicuously absent and the rock is considerably coarser grained than the over- and underlying olivine-bearing gabbros. Granophyrically intergrown quartz and K-feldspar is present in places.

The composition of the sulphide phase differs considerably from that of the over- and underlying olivine-bearing rocks (Table X). Although pyrrhotite is by far the most abundant sulphide, it is practically devoid of pentlandite.

Sphalerite is a common constituent of this rock type and comprises about 35 per cent of the sulphides in one section (DDH243). It is intimately associated with chalcopyrite and usually occurs as grains at the margin of, and as small blebs in, chalcopyrite. Exsolved in the sphalerite are numerous small round blebs of chalcopyrite (Fig. 58). Small amounts of galena are associated with the sphalerite. The sulphides are present as roundish blebs, usually about 3mm in diameter, but occasional larger concentrations of up to 1cm in diameter are developed.

The composition of the sulphide phase at this locality differs considerably from that of the correlated mineralized anorthosite described by Liebenberg (1970, p. 193) from Duikerskrans 173 JS (Table X, Nos. 10 and 11). No reasonable explanation for this anomaly can be given, but the possibility cannot be excluded that owing to the change in rock sequence as already explained above, the anorthosite described by Liebenberg is not developed on Doornpoort 171 JS. The coarse-grained nature of the rock under discussion and the presence of hornblende, biotite, quartz and K-feldspar seems to indicate that this rock is a pegmatoid which would explain to some extent the differences in the composition of the sulphide phases recorded in Table X.

i) Sulphides in the Magnetitite Seam 21 (Table X, No. 12)

Fairly large amounts of sulphides are present in the Magnetitite Seam 21 where it was intersected in bore-hole DDH2 on the farm Doornpoort 171 JS. Apart from the numerous small drop-like sulphide concentrations in titanomagnetite grains (Fig. 59) or at the boundaries thereof, larger lens-like concentra-

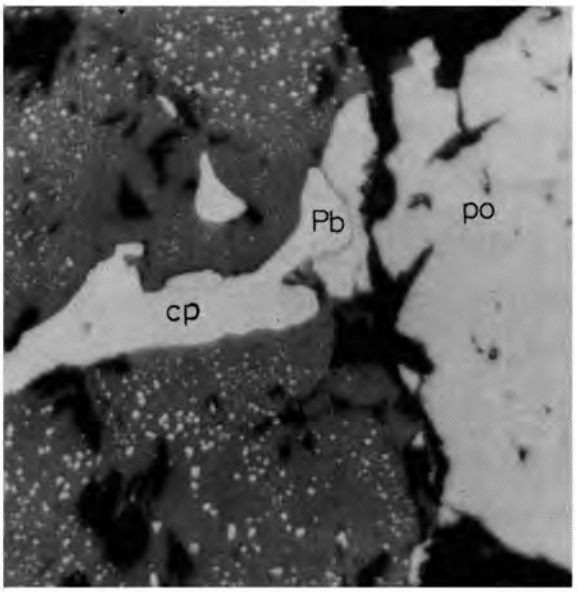

Fig. 58. Sphalerite (dark grey, left) with numerous small exsolved blebs of chalcopyrite, chalcopyrite (cp), pyrrhotite (po) and galena (Pb) in mineralized anorthositic pegmatoidal rock below Seam 21. (DDH2-243). Reflected light, x250.

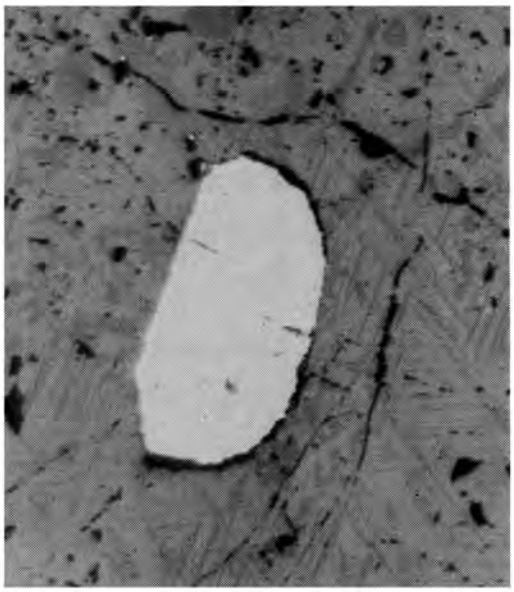

Fig. 59. Typical sulphide droplet (pyrrhotite) in titanomagnetite. Seam 21, (DDH2-160). Reflected light, x250.

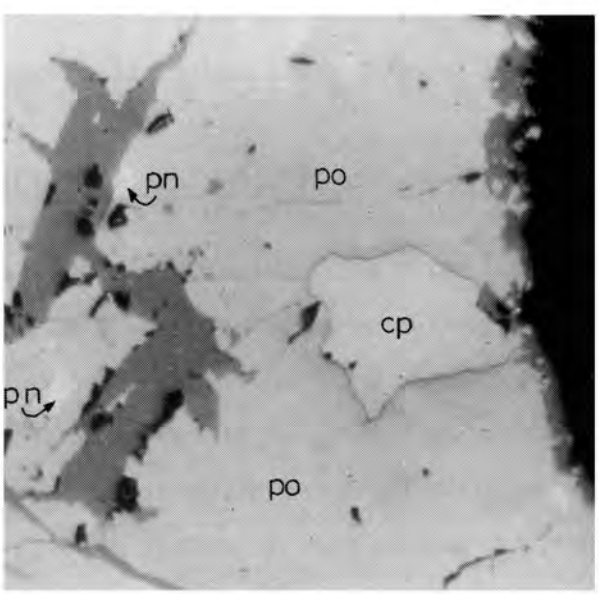

Fig. 60. Magnetite (grey) at the margin of and as stringers in the sulphide phase. Pyrrhotite (po), pentlandite (pn) and chalcopyrite (cp). Seam 21 (DDH2-162). Reflected light, x250.

tions of sulphides are present throughout the whole seam. These concentrations vary in size but are usually 1cm long and a few mm thick, and orientated parallel to the plane of layering.

The composition of the sulphide phase is essentially similar to that of the underlying olivine-bearing gabbro. Some of the pyrite present is associated with the pyrrhotite. Pure magnetite is present as stringers on the borders of, and as patches in, the larger sulphide grains (Fig. 60).

Secondary pyrrhotite is quite common and is associated with the altered olivine grains which are present throughout the seam.

j) Sulphides in the olivine diorites above Seam 21. (Table X, No. 13)

The composition and texture of the sulphides from this horizon are similar to those of the lower-lying olivine-bearing gabbroic rocks and need not be repeated here.

k) Sulphides in the uppermost differentiates (diorites) of the Bushveld Complex (Table X, No. 14)

There is a fairly rapid, but smooth change in the composition of the sulphide phase from the olivine-bearing diorite to the relatively olivine free diorite at the top of the intrusion. Pyrrhotite is still quite common in the lower portion of the diorite (G216, G207), but is very rare at the top of the intrusion where pyrite and chalcopyrite are the most common sulphides (G214, G215). Accompanied by this change is a fairly sharp drop in the sulphide content of the rocks.

4. Interpretation of the textural features and the observed mineral assemblages with the aid of phase diagrams

a) A brief description of the phase relations in the Cu-Ni-Fe-S System

Because many of the Ni-Cu ores of the world are associated with mafic and ultramafic rocks and because the major sulphide minerals in these rocks are essentially combinations of pyrrhotite, chalcopyrite, pentlandite and pyrite (as well as a number of other minor sulphides) much attention has in recent years been given to the Cu-Fe-Ni-S system. A vast amount of literature exists on various components of this system but the most significant recent article is that by Craig and Kullerud (1969, p. 344-358) who, apart from original investigations, have compiled the relevant published data, to give a detailed description of the phase relations in the Cu-Ni-Fe-S system. To interpret the textural and compositional variations in the sulphide phase of the Upper Zone, extensive use has been made of their article, which thus obviated the necessity of having to refer

to many other publications. However, before discussing the various textures observed, it is perhaps advisable to give a brief explanation of the more important reactions which occur in the Cu-Ni-Fe-S system. Only those reactions which involve phases observed are given.

At very high temperatures, well above 1000°C, the Cu-Ni-Fe-S system consists of Cu-Ni-Fe- alloys which coexist with sulphide liquid. This sulphide liquid is separated from the sulphur liquid by a large field of liquid immiscibility (Craig and Kullerud 1969, p. 347). The first sulphide of interest to this study to crystallize is a pyrrhotite-rich Fe-Ni monosulphide solid solution (Mss). This Mss appears as $Fe_{1-x}S$ on the Fe-S join at 1129°C and on cooling rapidly extends across the Fe-Ni-S face and joins $Ni_{1-x}S$ at 992°C to form a region of complete solid solution between $Fe_{1-x}S$ and $Ni_{1-x}S$ (the so-called Mss) (ibid., p. 348). At 743°C the iron-rich portion of the Mss reacts with sulphur liquid to form pyrite and tie lines exist between pyrite and the Fe-rich portion of the Mss. At 826°C the phase $Ni_{3\pm x}S_2$ appears at the Ni-S boundary of the Fe-Ni-S system and tie lines exist between $Ni_{3\pm x}S_2$ and the Mss. The $Ni_{3\pm x}S_2$ phase reacts at 610°C with the Mss to form pentlandite and tie lines between this new phase and Mss are established.

Below 600°C the width of the Mss field in the Fe-Ni-S system decreases gradually as a result of the formation of more pyrite in the more sulphur-rich part of the Mss and the exsolution of Ni as pentlandite in the more metal-rich portion of the Mss. Only below temperatures of 300°C is solid solution between $Fe_{1-x}S$ and $Ni_{1-x}S$ no longer complete and can tie lines between pentlandite and pyrite be established. (Craig and Kullerud, 1969, p. 350-352).

Above 320°C, the pyrrhotite ($Fe_{1-x}S$) of the Mss is of the high temperature hexagonal variety. Below this temperature it inverts to a low temperature hexagonal variety which, in the presence of pyrite, inverts to a monoclinic variety below 310°C (Kullerud 1967, p. 290-291).

The pentlandite which exsolves from pyrrhotite below 610°C has a lower sulphur : metal ratio than the pyrrhotite, with the result that the pyrrhotite is enriched in sulphur. This excess in sulphur will also cause the inversion of some of the hexagonal pyrrhotite to low temperature monoclinic pyrrhotite below 310°C.

From the above it is obvious that at low temperatures, pyrite can coexist with monoclinic pyrrhotite, but not with hexagonal pyrrhotite. Pyrite may however be found in the presence of hexagonal pyrrhotite. This is ascribed by

Naldrett and Kullerud (1967, p. 502) to the stable character of pyrite, which, once formed, does not react rapidly with hexagonal pyrrhotite to form monoclinic pyrrhotite.

The pyrrhotite of the Mss can take approximately 2 wt. per cent Cu into solid solution at high temperatures (Yund and Kullerud, 1966, p. 466) and exsolves as chalcopyrite from the pyrrhotite at temperatures below 450°C (Craig, 1966, p. 335).

A field of chalcopyrite solid solution appears in the Cu-Fe-S system at 970°C (Craig and Kullerud, 1969, p. 348). The chalcopyrite solid solution breaks up at 590°C into two phases, namely chalcopyrite and cubanite. At this temperature tie lines exist between cubanite and pyrite and therefore prevent the coexistence of chalcopyrite and pyrrhotite. At 334°C however, cubanite and pyrite react to form chalcopyrite and pyrrhotite (Yund and Kullerud, 1966, p. 485). Tie lines are again established between pyrrhotite and chalcopyrite below 334°C with the result that the association of cubanite and pyrite is unstable below this temperature.

From the above description of the phase changes on cooling of a sulphide phase with a composition that falls within the Cu-Fe-Ni-S system, it is obvious that the three most common mineral assemblages are (Craig and Kullerud, 1969, p. 352):

i) Chalcopyrite + pyrite + monoclinic pyrrhotite + pentlandite.

ii) Chalcopyrite + monoclinic pyrrhotite + hexagonal pyrrhotite + pentlandite.

iii) Chalcopyrite + cubanite + hexagonal pyrrhotite + pentlandite.

b) Discussion of the mineragraphy in the light of the phase relations in the Cu-Ni-Fe-S system

It is generally believed (Craig and Kullerud, 1969, p. 355) that at high temperatures, liquid immiscibility exists between sulphide liquid and gabbroic melt. Magnetite-pyrrhotite assemblages begin to melt at 1050°C if the pyrrhotite contains 60,5 weight per cent Fe. A rise in the iron content of the pyrrhotite to 62,8 weight per cent Fe has the effect of lowering the melting temperature to a minimum of 934°C (Naldrett, 1969, p. 177 and Fig. 6). The substitution of 2 weight per cent Cu for iron in the pyrrhotite lowers the melting temperature by 15-20°C, whereas the presence of Ni has apparently no effect (ibid., p. 180).

Although no magnetite was observed in the sulphide phase, except in that

from the Magnetitite Seam 21, the nature of the ore is such, that diffusion of oxygen from the separated sulphide liquid to the surrounding magma could have taken place, to prevent the crystallization of magnetite (Naldrett, 1969, p. 192; see below). It therefore seems unlikely that crystallization of the pyrrhotite commenced at temperatures above 1050°C. Where the sulphide phase is interstitial to the silicates, as is the case for the lower half of the Upper Zone, the crystallization temperature of the silicates must have been considerably higher than that of the sulphides. Chalcopyrite is present in large quantities in this ore and apart from the 4-5 per cent of this mineral which has exsolved from pyrrhotite below 450°C, the bulk of the chalcopyrite seems to have crystallized from the residual Cu-rich sulphide liquid at approximately 970°C.

On the grounds of the texture and estimated composition of crystalline sulphide droplets in lava from Hawaii, Skinner and Peck (1969, p. 319) concluded that the sulphide in these droplets crystallized above 1065°C as a Cu and Ni-rich pyrrhotite solid solution which contained as much as 9 weight per cent Cu. Although this does not agree with the experimental studies in the Cu-Fe-S system (Kullerud, 1968, p. 405) the presence of a Cu-rich pyrrhotite ss at high temperatures cannot be disregarded. The sulphide phase in the lower part of the Upper Zone contains more than 11 weight per cent Cu (Table XI) and the texture of the ore does not indicate that the bulk of the chalcopyrite has exsolved from a Cu-rich pyrrhotite ss.

The absence of pyrite associated with pyrrhotite in the mineralized anorthosite below Lower Magnetitite Seam 2 indicates that the sulphide phase was metal-rich. Seeing that these ores contain considerably less than 10 per cent Ni, all the pentlandite (i. e. discrete grains as well as exsolution-lamellae) has probably originated due to exsolution from the monosulfide solid solution at temperatures below 600°C (Naldrett and Kullerud, 1966, p. 322). The presence of pyrite in this anorthosite can be explained by an enrichment in sulphur in the last intercumulus silicate liquids which did not separate from the magma as part of the sulphide phase.

In contrast, the sulphide phase of the mineralized anorthosite below the Main Magnetitite Seam was richer in sulphur than the sulphide phase below the Lower Magnetitite Seam 2. This is seen by the presence of pyrite associated with pyrrhotite and indicates that reaction between pyrrhotite and sulphur took place below 743°C to produce pyrite. In this case, the composition of this ore lies on

the sulphur-rich side of the Mss with the result that all pentlandite probably formed below 300°C. This is similar to the sequence of events at the Strathcona Mine as described by Naldrett and Kullerud (1967, p. 504-505).

The sulphides in the magnetite gabbros of Subzone B are characterized by the presence of cubanite. This is indicative of sulphur deficient ore and the chalcopyrite ss which crystallized at 970°C was probably Fe-rich for cubanite to form at 570°C. The formation of pentlandite therefore resembles the formation of that described in the sulphides in the mineralized anorthosite below Lower Magnetitite Seam 2. As has been mentioned earlier, the pyrite observed in two of the six sections investigated, seems to be secondary, and could have crystallized from the intercumulus liquid owing to an enrichment in sulphur which did not separate as part of the sulphide liquid.

The phase relations in the sulphide phase of the magnetite gabbros of Subzone C are essentially the same as those in the mineralized anorthosite below Lower Magnetitite Seam 2. The only difference is in the lower chalcopyrite and higher pyrrhotite contents.

The sulphides in all the olivine-bearing rocks above the magnetite gabbros of Subzone C can be discussed together.

It was observed by Naldrett (1969, p. 181) that the crystallization temperature of pyrrhotite is not greatly affected by pressure, and it can therefore be assumed that the crystallization temperature of this mineral remained fairly constant throughout crystallization of the Upper Zone. As has been stated previously, one of the major changes observed where large amounts of olivine appear at the base of Subzone D is, that the sulphide changes from an essentially interstitial ore to small droplets, mostly associated with the titanomagnetite but also partially enclosed in other silicates except olivine. This seems to indicate that, owing to a gradual enrichment of S in the magma and owing to a gradual decrease in the crystallization temperature of the silicates, both of which are the direct result of fractional crystallization, the sulphide liquid separated at an early stage to form small globules distributed evenly throughout the crystallizing magma.

The composition of the sulphide phase in this part of the layered intrusion falls practically on the Fe-S boundary of the Cu-Ni-Fe-S system and all the chalcopyrite and pentlandite formed due to exsolution of Cu and Ni in solid solution in the pyrrhotite.

Very small amounts of cubanite are present in the lower olivine-bearing rocks, and some pyrite, which formed from reaction of pyrrhotite with sulphur liquid is present in Seam 21. This indicates that there was a gradual increase in the S content of the sulphide phase.

The sulphide content of the dioritic rocks above Magnetitite Seam 21 drops fairly rapidly, so that the topmost differentiates of the intrusion contain no primary sulphides. The pyrite in these rocks probably originated from magmatic sulphur that remained in solution in the silicate magma and which was concentrated in the residual deuteric fluids. This sulphur which remained in solution in the magma after separation of the sulphide liquid, is probably also responsible for all the secondary pyrite which was observed in the magnetite gabbros of the lower half of the Upper Zone, as well as for the pyrrhotite, and occasionally also pyrite, associated with the deuteric alteration of the olivine in the upper half of the Upper Zone. A similar origin for the pyrite in the felsitic norite of the Sudbury Irruptive was suggested by Naldrett and Kullerud (1967, p. 517).

It has been noted above that the sulphide phase of Magnetitite Seam 21 contains magnetite as small stringers and grains at the borders of the larger sulphide grains (Fig. 60). This magnetite is characterized by the absence of Ti-rich exsolution-bodies and has probably crystallized from the sulphide-rich phase. The presence or absence of magnetite in sulphides has been explained in detail by Naldrett (1969) and depends solely upon equilibrium of oxygen fugacity between sulphide liquid and surrounding silicate liquid. Naldrett has shown that, when oxygen is lost from the sulphide liquid by diffusion to the surrounding silicate melt, pyrrhotite alone will crystallize. On the other hand, if oxygen remains in the sulphide melt, crystallization of pyrrhotite will enrich the remaining sulphide liquid in oxygen, with the result that magnetite will also crystallize. This explains the presence of magnetite in massive sulphide deposits, where effects of diffusion of oxygen to the silicate magma were less, compared with the absence of magnetite in cases where sulphide droplets did not separate from the magma. In the latter instance Naldrett (1969, p. 192) argues that equilibration of oxygen fugacity between droplets and host takes place during crystallization of the pyrrhotite, and in this way may lose all of its oxygen to the surrounding silicate melt. This was probably the case with all the sulphides throughout the crystallization of the Upper Zone, except those in the uppermost magnetitite seam. The oxygen fugacity in the surrounding magma must have been relatively

high during crystallization of this massive magnetitite seam, (although owing to the stabilizing effect of TiO_2 on iron oxides, titanomagnetite crystallizes at a lower oxygen fugacity than that required to crystallize magnetite from a sulphide liquid (ibid., p. 194))and diffusion of oxygen from the residual ore liquid to the surrounding magma must have been very slow. The result was a sufficient enrichment of oxygen in the residual sulphide melt to crystallize pure magnetite from it.

5. Events leading to the crystallization of sulphides in the Upper Zone

Skinner and Peck (1969, p. 311) have shown that, in a tholeiitic basaltic magma from Hawaii with an average S content of 100ppm, the only environment in which the S content can be increased to saturation point is in the interstitial liquids. They found that at between 1060 and 1070^{o}C a sulphide-rich phase separates from the interstitial silicate liquid and that the S concentration in this liquid was 380 $\pm$ 20ppm; the concentration necessary to saturate the magma at that temperature.

Liebenberg (1970, p. 197) has shown that the average S content of the Bushveld magma was in the vicinity of 150ppm and that the average S content of the Main and Upper Zones is 50 and 350ppm respectively. The question that arises is why the sulphur concentration in the Main Zone is so much lower than the average S content of the Bushveld. The only reasonable explanation seems that the nature of the processes responsible for the crystallization of the cumulates never allowed large amounts of intercumulus liquid to become trapped, possibly owing to adcumulus growth and/or filter pressing of the intercumulus liquids into the overlying magma, which consequently became gradually enriched in sulphur. During crystallization of the lower part of the Upper Zone, the S content of the magma was still not high enough for the separation of immiscible sulphide droplets. Only under special conditions did the sulphur concentration rise to saturation point and these conditions were apparently only achieved where sufficiently large amounts of liquid were trapped in the intercumulus spaces. Crystallization of a batch of magma at the bottom of the chamber, to give rise to a cyclic unit would favour enrichment of S in the crystallizing bottom layer and might give rise to sulphides at the top of the cycle as envisaged by Liebenberg (1970, p. 196). He explains the presence of intercumulus sulphides below the magnetitite seams with the aid of the ternary phase diagram FeS - magnetite - gabbroic silicates. The magnetitite seam is considered by him to represent the

beginning of a cycle of crystallization, followed by crystallization of magnetite and silicates. At the ternary eutecticum sulphides, magnetite and gabbroic silicates would crystallize, conditions which would probably prevail in the intercumulus liquids at the end of a cycle. The next cycle would again commence with crystallization of magnetite, to form a seam directly overlying mineralized anorthosite. Absence of sulphides below a magnetitite seam is attributed by Liebenberg to the disturbance of the cycle before its termination (beheaded unit) by a new convection current.

Whatever the origin of the sulphide mineralization in the anorthosites below the Lower Seam 2 and the Main Magnetitite Seam, these sulphides are interstitial and it seems as if the S concentration of the magma during crystallization of these rocks was still fairly low, but apparently considerably higher than during crystallization of the greater part of the Main Zone. As crystallization proceeded, the magma became gradually enriched in S, until, at a level somewhere between Seam 14 and the olivine diorites of Subzone D, crystallization of some plagioclase and olivine was sufficient to saturate the magma in S with the result that numerous small sulphide droplets are found in the overlying rocks. The S concentration in the last 1000 metres of the Bushveld magma must therefore have been very close to saturation, which would correspond to between 350-400ppm.

6. Concluding remarks

Although the olivine-bearing, dioritic rocks of the Upper Zone contain, on the average, more sulphides than the ordinary gabbroic rocks lower down in the sequence, a concentration of sulphides in these rocks would not yield a deposit of economic interest owing to the unfavourable composition of the sulphide phase. Sulphide concentrations in the lower half of the Upper Zone are however of economic importance owing to the favourable composition of the sulphide phase, which, apart from appreciable amounts of chalcopyrite, also contains fair amounts of pentlandite.

More attention should therefore be given to the known sulphide concentrations in the lower part of the Upper Zone. The mineralized anorthosite underlying the Main Magnetitite Seam has been known for quite some time, but this investigation has revealed the existence of a mineralized anorthosite below the Lower Magnetitite Seam 2. The chemical analysis of this anorthosite (Table XIII) shows that concentrations of economic importance are to be found in this horizon.

Although, with our present knowledge, these concentrations seem to be sporadic, it must be borne in mind that outcrops of these mineralized horizons are scarce and restricted to a few river sections in the Eastern Transvaal.

F. POSTCUMULUS CHANGES

The various types of postcumulus changes which are restricted to a particular mineral, such as myrmekite, interpenetration and zoning of plagioclase, as well as the inversion from pigeonite to orthopyroxene, have already been described in the previous sections on the particular minerals. The changes discussed below are therefore those in which two or more minerals are involved, as well as changes in the cumulus pile as such.

1. Symplektite

Complex symplektitic textures characterize most of the rocks of the Upper Zone. Very little is known about these textures in gabbroic rocks and the extremely fine nature of the intergrowths, which closely resemble myrmekite, make identification of the involved phases difficult. Three different types of symplektite seem to be developed and are described separately below. The first two types are probably closely related in origin and occur as an intergrowth surrounding magnetite but seem to have developed at the expense of plagioclase, whereas the third type is an intergrowth of magnetite and pyroxene.

a) Symplektite in gabbroic rocks of Subzone B and C of the Upper Zone often displays a concentric zoning (Fig. 61) which, from magnetite outwards, consists of:

i) an inner zone of flaky biotite which surrounds the magnetite grain;

ii) a central zone of "needles" of biotite projecting radially into

iii) an outer zone of symplektite which advances convexly into the surrounding plagioclase.

Usually only two of these zones are developed, the central zone of biotite needles being mostly absent. It is extremely rare that only needles of biotite are developed (Fig. 62) although flaky biotite often surrounds magnetite grains without the symplektitic outer reaction zone. The white matrix of the biotite "needles" in Fig. 62 has a slightly higher refractive index than the twinned plagioclase and, although it does not exhibit twinning, is considered to be a more calcic plagioclase.

In detail the outer zone of the symplektite resembles myrmekite closely in that the vermicules are thin and orientated perpendicularly to the advancing

Fig. 61. Complex symplektite which consists of an inner zone (dark grey) of biotite, a central zone of "needles" of biotite in plagioclase and an outer zone of myrmekite-like intergrowth of pyroxene and plagioclase.G396. Crossed nicols, x70.

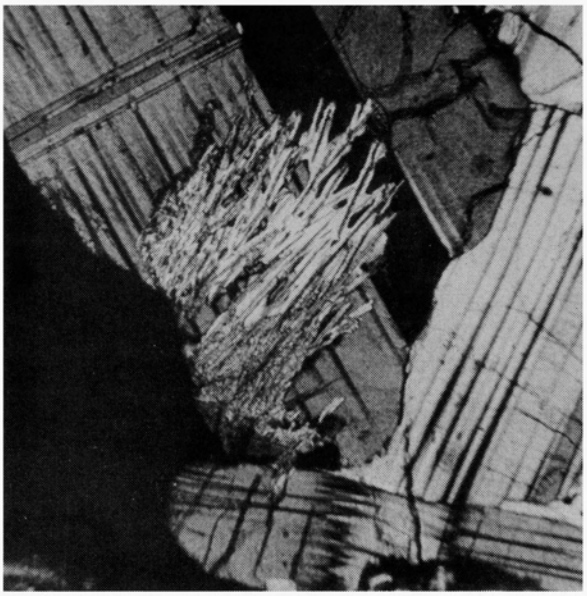

Fig. 62. Needles of biotite protruding into plagioclase. The white matrix between the "needles" is probably more calcic plagioclase. G396. Crossed nicols x70.

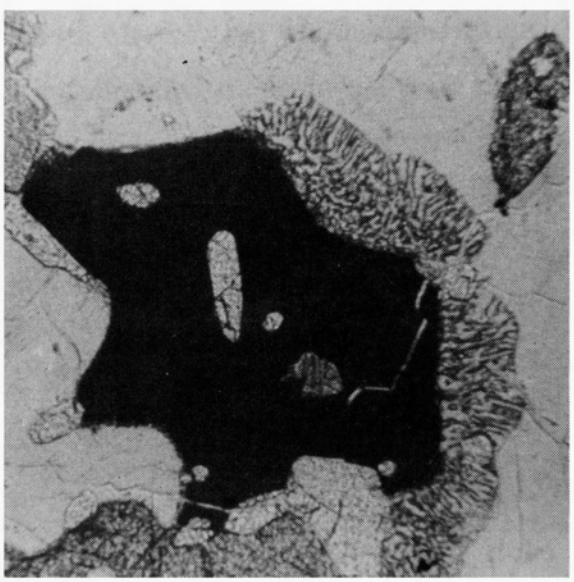

Fig. 63. Relatively coarse symplektite in olivine diorite The intergrowth probably consists of olivine and calcic plagioclase. G271. x70.

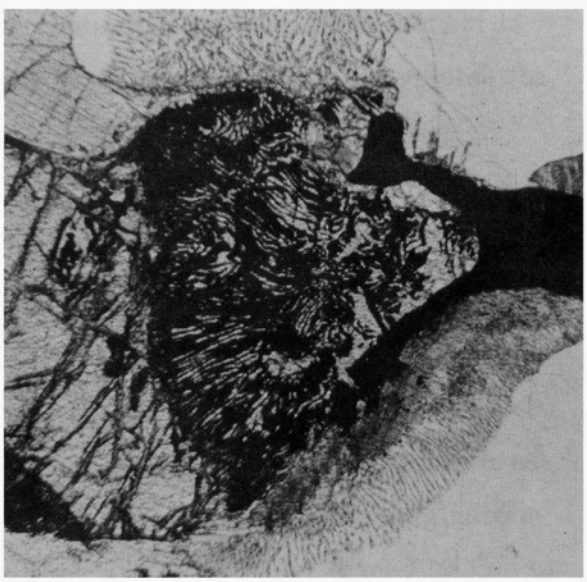

Fig 64 Symplektitic intergrowth of magnetite and pyroxene (centre). Olivine is to the left of the intergrowth. The more common type of symplektite at top and bottom. G621, x70.

"front" but coalesce towards the centre to form small irregular patches. The delicate texture makes it difficult to determine the mineral which constitutes the vermicules, but the higher relief and relatively low birefringence suggests that it may be orthopyroxene.

Symplektitic intergrowth of pyroxene and plagioclase was described by Molyneux (1964, p. 63 and p. 69) from the basal contact of the Main Magnetitite Seam and Seam 11.

b) The symplektite in olivine diorites of Subzone D of the Upper Zone differs from that of the olivine-free gabbroic rocks of the lower subzones in that biotite is scarce, so that the vermicular intergrowth is mostly the only zone present (Fig. 63). Where biotite is present it is always developed between the intergrowth and the magnetite. The intergrowth in these olivine-bearing rocks is slightly coarser than that of lower subzones and the vermicules have a considerably higher birefringence and refractive index than the plagioclase. Sometimes the mineral of these vermicules coalesces to form thin rims around the magnetite where it can be seen to consist of olivine.

c) A third type of symplektite, very seldom seen in thin section, consists of vermicular magnetite in pyroxene (Fig. 64). It is characteristically associated with olivine, but whether the olivine has contributed to the formation thereof is not certain. If, as is the case with myrmekite and the other types of symplektite, the intergrowth advances convexly outwards, then this type seems to have originated at the expense of olivine.

d) Origin of the symplektite

Various authors have described coronas around and reaction rims between certain types of minerals in gabbroic and anorthositic rocks (Buddington, 1939, p. 295-297 ; Huang and Merritt, 1954, p. 555; Murthy, 1958, p. 25-26) but they consider these textures to have originated by later metamorphism of these rocks. Buddington (1939, p. 295) mentions the possibility that coronas may originate by reaction of solid phases with deuteric intergranular fluid or that it may be due to discontinuous reaction between early formed crystals and residual (intercumulus) liquid. Herz (1951, p. 985 and p. 1015) considers that the symplektite in the Baltimore gabbro has originated in such a way. This hypothesis is also favoured by the author for similar intergrowths in the rocks of the Upper Zone.

The presence of either pyroxene or olivine, as well as biotite in these symplektite textures, which appear to be associated with more calcic plagioclase,

seems to suggest that a reaction between the last intercumulus liquid and the plagioclase has taken place. It is envisaged that an increase in the pH_2O would favour the formation of myrmekite, but instead of forming vermicules of quartz, these reacted with the intercumulus liquid to form ferromagnesian minerals, whereas any exsolved alkalis would react with this liquid to form biotite. As noted previously, myrmekite disappears in rocks where symplektite is developed, which may suggest that their origin is somehow related.

No satisfactory explanation can be offered at this stage for the magnetite-pyroxene symplektite.

2. Adcumulus growth and the intercumulus liquid

The initial porosity of the settled crystals in the accumulating mush is estimated as being between 20 and 50 per cent (Hess, 1960, p. 109; Jackson, 1961, p. 62; Wager and Brown, 1968, p. 60) with the result that the mechanism of enlargement of cumulus crystals to form adcumulates or monomineralic rocks with practically no pore material has puzzled many petrologists. As pointed out by Cameron (1969, p. 760) the preferred explanations are: firstly, that settled crystals continued to grow after shallow burial by diffusion of the required constituents into the crystal mush down a slight temperature gradient, a mechanism that was proposed by Hess (1961, p. 113), secondly, by enlargement while still in contact with the supernatant magma (Wager et al., 1960, p. 81 and Jackson, 1961, p. 62) and thirdly, by a combination of both processes mentioned.

As envisaged by Hess (1961, p. 113), the degree of enlargement of cumulus crystals by diffusion may be correlated with the rate of accumulation of crystals, i.e. where the rate of accumulation was slow, diffusion was operative, resulting in overgrowths of almost exactly the same composition as the cumulus crystals, and where accumulation was rapid, the original magma was effectively trapped.

Wager et al. (1960, p. 77) point out that for adcumulus growth, this process of diffusion "must have taken place at the same temperature as that of the formation of the cumulus crystals because of the similarity in the solid solution composition". They do, however, agree that enlargement of the cumulus crystals at constant composition did take place while they formed the uppermost layer of the pile and that thick layers of monomineralic rock must have formed very slowly. More recently, Wager (1963, p. 5 and Wager and Brown, 1968, p. 222)

suggests that adcumulus growth of settled crystals takes place on the top surface of a crystal pile. He argues that for crystal growth, heat has to be removed which, in ordinary circumstances, is lost into the surrounding lower temperature rocks. Conduction of heat from the top layer of accumulated crystals into the underlying crystal mush would not be sufficiently rapid for adcumulus growth to take place and he believes that the loss of heat must be into an overlying supercooled magma which is constantly brought in fresh supplies by convection into contact with the top surface of the cumulus crystals. Adcumulus growth can therefore continue as long as heat can be transferred into the overlying supercooled magma, providing that there is no fresh nucleation. This may be a reasonable explanation for adcumulus growth in the Skaergaard Intrusion where there is ample evidence for convection currents (Wager and Brown, 1968, p. 210-221).

Another mechanism whereby the amount of intercumulus liquid can be reduced, is compaction of the crystal mush prior to cementation, "if this were attended by re-solution of crystals at points of contact and redeposition in interstices" (Cameron, 1969, p. 759). Cameron however, states that owing to lack of evidence, this process has found little favour with students of magmatic sediments.

Compaction of the crystal mush is considered by the author to be one of the most important processes in the Bushveld Complex whereby large amounts of intercumulus liquid were pressed out of the pore spaces into the overlying magma. This is obvious from the various textural features displayed by the plagioclase crystals such as interpenetration, myrmekite, bent crystals and reversed zoning, the presence of all of which cannot, in the light of our present knowledge, be explained by another mechanism. An especially important mechanism whereby adcumulus growth can take place without having to assume large scale diffusion of the required constituents into, and the unwanted constituents out of, the pile of cumulus crystals, seems to be the process of re-solution, causing interpenetration and the redeposition of this material in the interstices. It is by no means suggested that compaction is the only process responsible for adcumulus growth, but that it may be just as important as diffusion after shallow burial or as enlargement of cumulus crystals while still in contact with the supernatant magma.

VII. MODAL ANALYSES. (Folder IV)

1. Introduction

The purpose of this study was to determine, firstly, whether broad trends exist in the variations of components of the more "normal" rock types, secondly, whether there are any noticeable differences in the modal composition of rocks of this area and those of the area mapped by Molyneux farther north, and thirdly, whether changes in the abundance of the minerals are reflected by a change in their composition or texture.

The aim was not to determine exact variations in the mineral composition of the rock types, as the spacing of the rock specimens in the stratigraphical column are too irregular and too far apart. Furthermore, counts of several thin sections of the same sample are necessary for exact determinations of compositions because of the uneven distribution of certain mineral phases like orthopyroxene and clinopyroxene in specimens from Subzone B and parts of Subzone C of the Main Zone. The distribution of the large orphitic orthopyroxene grains in these parts of the sequence is similar to the distribution of intercumulus pyroxene in a mottled anorthosite, and point count analyses on several thin sections of the same rock will therefore result in a variation of the proportions of the components.

One hundred and ninety-two thin sections were "analysed" by means of a Swift Automatic Point Counter (Appendix I). The number of points counted varies between 1500 and 1800 per section over an area of approximately 320 sq mm. The degree of accuracy of the point count can be determined from the IC numbers (i. e. the number of identity changes on a 40mm traverse) and the curves given by Chayes (1956, p. 77).

Although the IC numbers fluctuate considerably from one section to the next (Appendix I), the average IC number lies between 55 and 60. The estimated average analytical error for a particular mineral is therefore between 2, 5 and 3 per cent and thus above the average analytical error of 2, 45 per cent which is considered by Chayes (1956, p. 84) to be a reasonable value for reconnaissance work of this nature. To attain an average mineral analytical error of between 2 and 2, 45 per cent, it is necessary to count two sections of each specimen with IC numbers of between 40 and 60, whereas point counts of three sections are required for specimens with an IC number between 35 and 40. This is essential

because the variation in proportion of the components from one thin section to the next of the same specimen is greater for a coarse-grained rock than for a finer-grained one.

If the variation among thin sections of the same specimen is small, then the accuracy of the analyses is enhanced by an increase in the number of points counted per section, but as the within-specimen variation increases, the influence of the number of points counted diminishes rapidly (ibid., p. 90). The analytical error which is due to the within-specimen variation can therefore only be overcome by increasing the number of thin section counts for each specimen.

2. Main Zone

a) Plagioclase

The plagioclase content of the greater part of the Main Zone is fairly constant, fluctuating between 60 and 70 per cent by volume of the rock. The high values above the Merensky Reef indicate the abundance of anorthositic rocks in the lower 100m of this zone. Only in Subzone C is there a slight tendency for the normal gabbroic rocks to contain less plagioclase.

b) Pyroxene

A striking result of this study is the inverse relationship between orthopyroxene and clinopyroxene in most of the rocks of the Main Zone. The same relationship, although not quite as clear, seems to exist between plagioclase and clinopyroxene. This tendency is only observed in normal gabbroic rocks and not in interlayered anorthosite and pyroxenite. Although speculative, these relationships seem to indicate that some sort of equilibrium existed between the various crystallizing phases and that crystallization of one phase influenced the abundance of the other phases. Where orthopyroxene crystallized early, as in the rocks of Subzone A, it caused an enrichment of Ca but a depletion of Fe and Mg in the magma, resulting in a relatively high plagioclase content and a low clinopyroxene content. Where clinopyroxene crystallized before orthopyroxene, as in Subzone B, it caused a depletion of Ca, Fe and Mg in the magma with the result that the rocks of this subzone contain less orthopyroxene and plagioclase than those of Subzone A. Crystallization of one phase at a higher level in the magma chamber and the settling of this phase to the bottom of the chamber, would disturb this equilibrium of the crystallizing phases and cause the various phases to be present in any proportion.

Nucleation of several phases at the top of the chamber, i.e. in a cool en-

vironment, and transportation of these crystals by convective overturn to the warmer, lower part (bottom) of the chamber would result either in the melting of these phases or in overgrowths of more stable high temperature phases, thus causing the reversed zoning which is frequently observed, especially in the plagioclase of the Main Zone. The latter alternative of overgrowth necessitates extremely slow convection which would cause wide rims of the higher temperature phases. The reversed zoning is, where present, only confined to thin outer rims of the crystals and is probably due to postcumulus overgrowths as described in more detail on p. 94. Small crystals of pigeonite associated with or enclosed in clinopyroxene in the presence of primary orthopyroxene in a large section of the Main Zone would indicate that such a mechanism was operative, but in the section dealing with the mineralogy of the orthopyroxene (p. 83), this association is explained more satisfactorily in another way.

Jackson's concept (1962, p. 96-99) of bottom crystallization and variable depth convection, is a mechanism which explains cyclic units in basal portions of layered intrusions and it is doubtful whether such a mechanism was responsible for the thick accumulation of the relatively homogeneous rocks of Subzone B of the Main Zone. It must, however, be pointed out that a much more detailed investigation of the abundance and composition of coexisting phases is necessary to determine whether variable depth convection was operative during crystallization of the Main Zone or not. Slow continuous convection and crystallization at the bottom of the intrusion, as illustrated by Jackson (1961, p. 94-95) seems the best explanation of the observed relationships against the background of our knowledge at present.

These broad trends in the variation of the pyroxenes can, to some extent, be related to the textural relationships between these coexisting phases. For the greater part of Subzone A, the orthopyroxene is present as cumulus crystals, and predominates over clinopyroxene irrespective of whether the latter is cumulus or intercumulus. The only exception is found for a short distance in the sequence following the appearance of cumulus clinopyroxene at about 350m above the Merensky Reef. The lower half of Subzone B is characterized by large "ophitic" orthopyroxene grains and by the presence of small "inverted" pigeonite grains enclosed in or surrounded by clinopyroxene. In this zone of transition from primary orthopyroxene to inverted pigeonite, clinopyroxene usually predominates over orthopyroxene. Where "inverted" pigeonite proper appears in

the sequence, the orthopyroxene content increases with a decrease in the clinopyroxene content.

In Subzone C, which may be regarded as a repetition of Subzones A and B, similar relationships hold true, except for the first 100m above the Pyroxenite Marker. Where small amounts of pigeonite, now inverted to orthopyroxene, are present as well as "ophitic" primary orthopyroxene, there is a pronounced increase in the clinopyroxene content and where large amounts of orthopyroxene which originated from pigeonite by inversion, appear in the sequence 50m below Subzone A of the Upper Zone, the clinopyroxene content drops considerably. This relationship persists up to the Main Magnetitite Seam, but where magnetite appears in larger quantities in the rocks above this seam, the orthopyroxene and clinopyroxene content of the rocks of the Upper Zone seem to fluctuate sympathetically.

c) Accessory constituents

The accessory constituents of the Main Zone are quartz, biotite, opaque minerals, K-feldspar and apatite. Of these, quartz is by far the most abundant accessory mineral, but it seldom exceeds 1 per cent by volume of the rock. The maximum concentration was found in specimen PB3801 where it constitutes 4, 3 per cent of the rock. It is present as typical intercumulus material occupying isolated patches in the section, but is optically continuous over large areas, indicating that the interstitial spaces are interconnected over large areas even at concentrations below 1 per cent.

Second in abundance is biotite. This mineral is not always a primary product of the intercumulus liquid, but seems to have originated owing to reaction between the liquid and solid phases, mostly interstitial ore. Interstitial ore minerals, K-feldspar and apatite are practically never present in amounts exceeding 0, 2 per cent by volume.

An interesting result of the modal analyses is the distribution of these accessory minerals in the Main Zone. There is a remarkable concentration of these minerals in the lower 2300m of the Main Zone in comparison to the upper half of this zone which is practically devoid of these constituents. It follows that crystallization of the lower half of the Main Zone was of such a nature as to effectively trap the intercumulus liquid, whereas during crystallization of the remainder of the zone very little or no intercumulus liquid was trapped, probably as a result of more effective adcumulus growth of the main constituents.

In the southern part of the mapped area, magnetite appears in small quantities in the rocks directly underlying the Pyroxenite Marker. Ten km farther to the south, Groeneveld (1970, p. 39), found similar rocks in the Main Zone, and although the Pyroxenite Marker seems to be absent in this area, there is a distinct compositional break above this horizon (ibid., Fig. 1, p. 38). Groeneveld also noted the predominance of orthopyroxene over clinopyroxene in these magnetite-bearing rocks, a characteristic which also prevails in the correlated magnetite-free rocks of the succession under discussion, and he also pointed out that this is in contrast with the magnetite-bearing rocks of the Upper Zone where clinopyroxene usually exceeds orthopyroxene.

3. Upper Zone

a) Plagioclase

The plagioclase content of the "normal" gabbroic rocks of this zone is generally slightly lower than that of similar rocks in the Main Zone, namely, ± 55 per cent, compared with between 55 and 70 per cent for the Main Zone. This difference may be due to the large amount of anorthosite and anorthositic rocks, the crystallization of which could be held responsible for a general depletion in the constituents of plagioclase during formation of the more normal rock types. This is also borne out by a trend which occurs repeatedly in the Upper Zone, namely, thick accumulation of plagioclase-rich rocks followed by relatively plagioclase-poor rocks (less than 50 per cent by volume), e. g.:

i) Anorthositic rocks of the lower part of Subzone B (4080-4150m) followed by the feldspathic pyroxenite below Seam 6 (4200m).

ii) Anorthositic rocks between 4700 and 4800m are followed by relatively feldspar-poor rocks between 4825 and 5025m.

iii) Anorthosites over and underlying Seam 15 are followed by feldspar-poor olivine-bearing rocks between 5550 and 5600m.

iv) Feldspar-rich rocks between Seams 17 and 21 are followed by feldspar-poor rocks directly above Seam 21.

Although the reverse of this trend may also be observed, as for instance at 4250 and 5050m, the above trend is much more pronounced. More detailed modal analyses are however necessary to verify this observation, and may reveal several more of these cycles.

Another feature worthy of mention, is the association of anorthosites and anorthositic rocks with the magnetitite seams. This was previously observed by

Molyneux (1964 and 1970). Apart from this association, the more normal olivine-free gabbroic rocks which occur between the magnetitite seams tend to have a relatively high feldspar content (4000-4300m, 4700-5125m, 5400-5500m and 5800-5950m). This is often difficult to discern in the field as a few per cent of magnetite, distributed evenly throughout an anorthositic rock imparts a deceptively dark colour to that rock.

b) Orthopyroxene

Although the rocks of the Upper Zone may contain up to 35 per cent orthopyroxene, they usually contain less of this mineral than do those of the Main Zone, a tendency which was also noted by Groeneveld (1970, p. 39) in the area to the south. That this may in part be due to the presence of magnetite is borne out by the absence of magnetite in specimens G649 and G625, both of which contain more than 20 per cent orthopyroxene. The fine-grained norite (G314) underlying Seam 8, on the other hand, contains appreciable amounts of cumulus magnetite. There is also no indication that the abundance of olivine or clinopyroxene is in any way influenced by the presence of magnetite in the rock.

In contrast to the rocks of the Main Zone where there is an inverse relationship between the orthopyroxene and clinopyroxene content, no such trend was observed in the rocks of the Subzones B, C and D of the Upper Zone. The trend of the Main Zone persists up to the Main Magnetitite Seam, but from here onwards, there is even a tendency for these two minerals to fluctuate sympathetically, which is especially noticeable in Subzone B.

c) Clinopyroxene

Clinopyroxene is the most abundant ferromagnesian mineral in the Upper Zone and normally exceeds orthopyroxene by a few per cent where both are present. In the presence of olivine, however, clinopyroxene tends to be subordinate. It attains its highest concentration of 52 per cent in the feldspathic pyroxenite (G649) of Subzone B, a feature also observed by Molyneux some 40km to the north (1970, Fig. 12, p. 33).

d) Olivine

Olivine makes its first appearance in this area about 4525m above the Merensky Reef, at a height some distance below the Sisal Troctolite Marker of Molyneux (1970, p. 25). No olivine-bearing rocks were found below this horizon and it seems as though the olivine-bearing gabbros of Subzone A, described by Molyneux (1970, p. 24) from Magnet Heights, are not developed in this area.

The olivine content of the olivine-bearing rocks at the base of Subzone C fluctuates considerably. The data for this horizon are, however, not very accurate because of the difficulty to distinguish, in the field, between olivine-bearing and olivine-free rocks at this level in the intrusion. The remainder of Subzone C is practically devoid of olivine except for very small amounts below Seam 11 and a more prominent layer above this seam which is also present in the Magnet Heights area.

Approximately 75 per cent of all the rocks of Subzone D are olivine-bearing. The olivine content in these rocks is for the greater part fairly constant, usually between 15 and 20 per cent except for the topmost 200m of the intrusion where it drops to nil directly below the roof. Where magnetitite seams are present in the sequence (Seam 15 and between Seams 17 and 21) there are very few or no olivine-bearing rocks present.

As mentioned previously, there is a distinct "facies" change in the upper half of Subzone D towards the west and the south, so much so, that the magnetite gabbros below Seam 21 make way for olivine diorites on Doornpoort 171 JS (bore-hole DDH1 and 2) and on Paardekloof 176 JS. The presence of small amounts of olivine in the sequence between Seams 17 and 21 on Duikerskrans 173 JS and Onverwacht 148 JS may already be a manifestation of these changes in a generally southerly direction.

e) Apatite

Small idiomorphic crystals of apatite appear in fairly large quantities at the base of Subzone D. Lower down in the sequence, apatite was observed sporadically in the intercumulus material as small anhedral grains, as low down as 100m above the Merensky Reef. Of interest is that only the olivine-bearing rocks of Subzone D contain large amounts of cumulus apatite, although one sample of the ovicular olivine diorite (G279) contains no apatite at all.

The apatite content of the olivine diorite in the lower half of Subzone D was found to be fairly constant, fluctuating between 4 and 6 per cent (Folder IV). The highest apatite concentration of 8,5 per cent was found in the rocks directly overlying Seam 21. Upwards from here it drops rapidly to about 0,5 per cent in the topmost differentiates of the intrusion.

f) Magnetite

The magnetite content of the normal gabbroic rocks of Subzone A is in the vicinity of 2 per cent or less, compared with the 7 per cent or more of most

rocks higher up in the sequence. The only exception is the extremely fine-grained gabbro (G415) in the middle of this subzone. In Subzones B, C and D the magnetite content remains remarkably constant, irrespective of whether the rock is olivine-bearing or anorthositic. Only the feldspathic pyroxenite and some anorthosite layers were found to have a low magnetite content. This is however only a broad trend. Where anorthosites underly magnetitite seams, they are usually impoverished in magnetite, whereas most of the magnetitite seams have a gradational contact at their top. Positioning of the samples with respect to magnetitite seams therefore influences the magnetite content considerably.

g) Hornblende

Hornblende only becomes a major constituent of the Upper Zone in the dioritic rocks above Seam 21. It increases fairly rapidly above this seam and has an average concentration of about 20 per cent in the top 100m of the intrusion.

h) Accessory minerals

The most common accessory mineral in the Upper Zone is biotite, whereas in the Main Zone it is quartz. The other accessory minerals, K-feldspar and quartz, are only sporadically present in the greater part of the sequence and are developed in larger quantities in the topmost 300m of the intrusion. They may be considered as major constituents only in the top 10m of the intrusion (enlarged portion, Folder IV).

4. Conclusion

Comparison of the modal variation of constituents of the sequence studied, with a similar study by Molyneux (1970, Fig. 12) shows that there is a reasonable agreement in variation of the constituents in rocks of the Upper Zone. The broad trends observed in the rocks of the Main Zone are, on the other hand, not discernable in Molyneux's section. This may in part be due to the wider spacing of specimens.

The following differences between the two sections are however, worth recording:

i) The rocks of Subzone A of the Upper Zone contain more magnetite in the north than in the south.

ii) Olivine-bearing rocks do not seem to be developed below the Main Magnetitite Seam in the south.

iii) Orthopyroxene is more abundant in the Upper Zone in the north, especially in rocks above Seam 21.

VIII. THE CAUSE OF THE DIVERSITY OF THE ROCK TYPES IN THE LAYERED SEQUENCE

It is beyond the scope of this treatise to review in detail the various hypotheses according to which the rock types in the Layered Sequence of the Bushveld Complex could have originated, and only those mechanisms which are considered to be separately or jointly responsible for the diversity of rocks will be summarized briefly below.

1. Convection currents

Wager and Deer (1939, p. 262-266) found ample evidence to suggest significant movement of the magma during solidification and differentiation of the Skaergaard Intrusion. From this evidence they concluded (p. 267-270) that cooling and partial crystallization of the magma took place at the top and walls of the intrusion. This crystal-laden magma was heavier than the rest and would sink to the bottom to give rise to convective circulation.

This hypothesis was further elaborated upon by Wager and Brown (1968, p. 210-227) and they suggest the existence of two types of currents in the Skaergaard Intrusion, namely, a fast turbulent current and a considerably slower current with a laminar flow. The continuous slow currents gave rise to homogeneous cumulates and were periodically interrupted by high velocity currents which were heavily laden with crystals and which gave rise to gravity-stratified layers. Alternation of gravity-stratified layers and homogeneous cumulates gives rise to the rhythmic layering as observed in the Skaergaard Intrusion.

Hess (1960, p. 148-149) also favours convective overturn as a mechanism whereby rhythmic layering can be produced, but points out that there is no evidence for a regular convection-cell system in the Stillwater and Bushveld Complexes in contrast to the Skaergaard Intrusion.

On the grounds of detailed investigations of the textures in the cumulates of the Ultramafic Zone of the Stillwater Complex, Jackson (1961, p. 83-85) rejected convection currents as being the means by which the rhythmically layered sequence in this zone originated. He postulated a theory of crystallization of a stagnant layer of magma at the bottom of the chamber, and variable depth convection to account for the repetitive stratigraphy in the Ultramafic Zone (p. 96-99) and recently (1970, p. 403-419) expanded his hypothesis to

account for cyclic units in the basal zones of other layered intrusions. He is, however, of the opinion (1961, p. 99) that, as the crystal pile above the Ultramafic Zone in the Stillwater Complex thickened and the magma temperatures decreased, crystallization at the top of the intrusion became increasingly more important and would favour continuous convection.

Whether cyclic units of the type described by Jackson are developed in the upper two zones of the Bushveld Complex, seems, at our present knowledge, doubtful, although a more detailed study especially on the rocks of the Main Zone is necessary before this possibility can be excluded. Jackson (1971, p. 420) maintains that there is a general tendency for the cyclic units to decrease in thickness with height in the layered intrusion, and as mentioned above, he is of the opinion that conditions for continuous convection are favoured as the depth of the magma chamber decreases.

It was concluded from modal analyses that continuous bottom crystallization took place during formation of the relatively homogeneous rocks of the Main Zone. Such conditions would prevail during constant, slow convection, a process by which the homogeneous rocks of the Stillwater Intrusion originated (Wager and Brown, 1968, p. 216-217). It is not implied hereby that crystallization started at the top of the intrusion, but that slow convection resulted in a uniform decrease in the temperature of the magma, i.e., the adiabatic gradient was maintained for a long period (Jackson, 1961, p. 94, Fig. 91).

2. Intermittent injection of magma

Hess (1960, p. 154-156) and Jackson (1961, p. 96) are of the opinion that large layered intrusions were emplaced as one surge of magma and that the layering is accounted for by an internal mechanism which controlled the rate of sedimentation of crystals on the floor.

Lombaard (1934, p. 32) proposed a mechanism of intermittent injection of pre-differentiated magma and settling of crystals from each flow to account for the layering of the Bushveld Complex. On the grounds of intrusive relationships between various rock units of the Layered Sequence in the western part of the Bushveld Complex, Coertze, (1970, p. 18-19) came to a similar conclusion and is of the opinion that differential melting of the mantle may be important in generating successive magmas of different composition.

This mechanism has found little support among students of layered intrusions, mainly because it necessitates an elusive, deep-seated, pre-intrusive

differentiation mechanism (Turner and Verhoogen, 1960, p. 300).

Cooper (1936, p. 44-45) postulated repeated injections of original undifferentiated magma to account for the repetitive stratigraphy in the Bay of Islands Complex. Although such a mechanism is rejected by Hess (1960, p. 154) for the Bushveld Igneous Complex, he is of the opinion that the Merensky Reef indicates a quantitatively small addition of undifferentiated basaltic magma. Wager and Brown (1968, p. 353), on the other hand, consider the alternating cumulates of the lower two zones of the Bushveld Complex to have originated in a way similar to that proposed by Cooper for the Bay of Islands Complex.

To account for the disproportionately large amount of ultramafic rocks compared with the basaltic composition of the chilled margin of the Muskox Intrusion, Irvine and Smith (1967, p. 48-49) proposed a mechanism of periodic influx of fresh, undifferentiated magma into the chamber, combined with extrusion of the old, partially differentiated magma to the surface as volcanic fissure eruptions. They are of the opinion that each cyclic unit reflects a major renewal of the composition of the magma brought about by a large influx of fresh liquid in place of that which had partially crystallized. The model proposed by Irvine and Smith for the Muskox Intrusion is essentially the same as that suggested by Brown (1956, p. 44-49) for the cyclic units in the ultramafic complex of Rhum. Although there are no indications of contemporaneous volcanic activity at the surface during crystallization of the Layered Sequence of the Bushveld Complex, periodic injections of undifferentiated magma probably did take place.

Such an influx was postulated by the author (1970, p. 69) at the level of the Pyroxenite Marker in the Main Zone. Owing to the apparent absence of cyclic units or repetitive stratigraphy in the Subzone C of the Main Zone, apart from the reversal at the Pyroxenite Marker, it is possible to calculate the minimum amount of fresh, undifferentiated magma that was added to the magma chamber. When the new influx occurred, the magma of the Bushveld had differentiated to a point where cumulus phases crystallized which are similar in composition to those at the base of Subzone A of the Upper Zone. The differentiated liquid of the old magma (A) and the new influx of fresh magma (B) gave rise to the differentiates of the Upper Zone (C + D) by fractional crystallization.

If A is the thickness of the Layered Sequence below the Pyroxenite Marker, i.e., about 6000m, B is the repetition of the Layered Sequence from the Pyroxenite Marker to the base of Subzone A of the Upper Zone, i.e., about 700m, and

(C + D) is the total thickness of the Upper Zone (2200m) in which C is the result of fractional crystallization of A, and D the result of fractional crystallization of B, then it follows that A/B = C/D and that B + D is the minimum addition of fresh, undifferentiated magma, which according to this calculation amounts to about 930m of the intrusion or to about 10 per cent of the total volume of the Bushveld magma.

If the Merensky Reef also indicates, as is generally believed, the addition of fresh magma, then there is no reason why intermittent injections of fresh, undifferentiated magma did not take place during crystallization of the Basal and Critical Zones. Such a process cannot be excluded as being responsible for the repetitive stratigraphy in these zones.

It may also be concluded that these intermittent additions were partially responsible for the lateral extension of the magma chamber during crystallization, probably in conjunction with Hess's (1960, p. 154) hypothesis that the initial magma chamber was deeper and of smaller extent and that "either gradually or spasmodically the magma chamber extended itself horizontally and diminished in thickness so that the 'sea' of magma transgressed over its 'shore lines' bringing stratigraphically higher and higher horizons in contact with the floor as it progressed farther from the limits of the original magma 'basin'".

3. Effects of pressure and oxygen fugacity

Experimental studies at different oxygen fugacities on silicate systems which are related to basaltic rocks have revealed important information on the differentiation paths with fractional crystallization and the conditions necessary to crystallize certain phases from the magma.

The effect of oxygen pressure on the crystallization and differentiation of basaltic magma was studied by Osborn (1959, and 1962), Roeder and Osborn (1966) and Hamilton and Anderson (1968). They came to the conclusion that under high constant pO_2 conditions, magnetite crystallizes from a basaltic magma, whereas at lower pO_2 crystallization of silicates (olivine) would be favoured and cause enrichment of iron in the liquid.

Ulmer (1969) examined systems which contain spinel and came to similar conclusions, namely, that the oxygen fugacity in the magma is an important control in the precipitation of spinel, and that fluctuations of fO_2 may result in cyclic repetition of layers of chromite and silicates. He found that (p. 129) "spinel crystals would be produced at relatively high oxygen fugacities and silicate

crystals would be produced at comparatively lower oxygen fugacities". Cameron and Desborough (1969, p. 38-39) and Cameron (1970, p. 55) who investigated the chromite of the Bushveld Complex also suggested that cyclic recurrence of chromite as a cumulus phase was controlled by variations in oxygen fugacity.

Crystallization of the Bushveld magma during formation of the Main Zone probably took place at low oxygen pressure resulting in the enrichment of iron in the residual magma. Extreme iron enrichment and a slight rise in fO_2 probably caused titanomagnetite to crystallize together with silicates. Periodic increases in the fO_2 (or pO_2) would have enhanced the crystallization of titanomagnetite, the concentration of which to form seams was probably assisted by its faster settling velocity than the other precipitating silicates.

Irvine (1970, Fig. 16 and p. 466) has shown the pronounced effect of total pressure on the liquidus boundaries in a modelled clinopyroxene-plagioclase-olivine-quartz system. He points out that if liquid crystallizing at a pressure of 4,5 kilobar along the plagioclase-clinopyroxene-orthopyroxene cotectic line is moved to a lower pressure environment it would become isolated in the stability field of plagioclase. He therefore envisaged that the magma, while generally crystallizing near its floor at the relatively high pressures, may, under conditions of convection, also have crystallized periodically near its roof with the result that only plagioclase crystallized, giving rise to anorthosites.

Hess (1961, p. 86) explained the origin of thick sheets of anorthosite in the Stillwater Complex by means of convective overturn. He is of the opinion that pyroxene would settle from a convection current at a faster rate than the plagioclase, causing the magma near the floor to be enriched in the latter. The next convection current would displace the plagioclase-enriched liquid upwards into the central portion of the magma chamber where it would mix with hotter undifferentiated magma which would cause the resorption of the suspended plagioclase crystals. In this way, Hess envisages a mechanism whereby a portion of the magma near the centre of the chamber becomes progressively enriched in the constituents of plagioclase. The composition of this liquid would be in the stability field of plagioclase and plagioclase alone would crystallize to form anorthosite.

Wager and Brown (1968, p. 342) proposed an alternative hypothesis to explain the thick anorthosites in the Stillwater Complex. They suggest that slightly undercooled magma moved downwards during convective overturn and crystallized

both plagioclase and pyroxene near the bottom of the intrusion where pressures were higher. If the velocity of the currents was high enough, only a few plagioclase crystals would settle out, the remainder being carried up by the current (convection-cell) to levels of lower pressure where they may have melted. The magma would become enriched in the plagioclase component and when this magma started to crystallize, only feldspar would settle from it for a long period.

Although no opinion can be expressed as to which of the three hypotheses above would seem most likely for the origin of anorthosite in the Bushveld Complex, it must be pointed out that all three of them rely on a convection mechanism in the magma chamber to produce these monomineralic rocks.

IX. THE MODIFIED DIFFERENTIATION INDEX AND THE MODIFIED CRYSTALLIZATION INDEX AS PARAMETERS OF DIFFERENTIATION IN LAYERED INTRUSIONS

1. Introduction

Several parameters have been proposed by various writers to illustrate differences in chemical composition between various rock types or suites of rocks. Some of these, such as the solidification index (Kuno, et al. 1957), modified Larsen index (Nockolds and Allen, 1953, p. 116), iron and albite ratios (Wagner, 1956), etc. are atomic or oxide proportions calculated directly from the chemical analyses, whereas others, notably the differentiation index (Thornton and Tuttle, 1960) and the crystallization index (Poldervaart and Parker, 1964) are combinations of various normative minerals calculated from the chemical analyses. All these indices were proposed to serve as parameters of igneous differentiation, and were plotted against different oxides to illustrate variation trends by which suites of rocks are characterized. The differentiation index (DI) and crystallization index (CI) have the advantage that they are parameters of igneous differentiation, based on theoretical petrological principles, and are therefore used in this study to illustrate the fractional crystallization of the Bushveld magma. However, when these parameters are used on layered intrusions such as the Bushveld Complex, some complications arise which can be overcome to some extent by making a few modifications. Consequently, a modified differentiation index (MDI) and a modified crystallization index (MCI) are proposed to illustrate the differentiation trends in layered intrusions.

2. The Modified differentiation index (MDI)

The DI was proposed by Thornton and Tuttle (1960, p. 664) and is based on petrogeny's residua system, namely, $SiO_2 - NaAlSiO_4 - KAlSiO_4$, i. e. the goal towards which all magmas will move on fractional crystallization.

$DI = \Sigma$ Qz + Or + Ab + Ne + Lc. (given as normative minerals).

The DI is therefore an indication of the degree of fractionation of a magma, which is reflected by the amount of normative quartz, orthoclase, albite, nepheline and leucite present in the analysed rock. It is obvious that granite, syenite or foyaite will have a very high DI, whereas a pyroxenite or dunite will have a very low DI.

In Fig. 65 the DI of a number of analysed rocks from the Bushveld is plotted against the height in the intrusion. From this figure it is obvious that

the DI as defined by Thornton and Tuttle cannot be used to illustrate the differentiation trend of the Bushveld magma. This is in part due to the variation of rock types caused by variations in the proportions of minerals. Anorthosite has, for example, a much higher DI than an over- or underlying gabbroic rock because of the larger amount of normative albite present in the anorthosite, whereas iron enrichment in the pyroxenes of the gabbroic rocks is not taken into account. This failure to bring out the pronounced iron enrichment which is shown by some basaltic rock series such as the Skaergaard and Bushveld Intrusions is the main criticism against the DI (Poldervaart and Parker, 1964, p. 282 and 1965, p. 279). Diagrammatically this may be seen in Fig. 65 where the DI for anorthosite falls well on the right of the diagram, whereas the DI for pyroxenite falls on the left and in themselves show differentiation trends separate from the more "normal" gabbroic rocks.

For the above reason, it is suggested that the DI should be modified in such a way that the iron enrichment in the minerals is also taken into account. For layered mafic intrusions like the Bushveld Complex, the modified differentiation index (MDI) can therefore be defined as being the sum of the normative quartz, orthoclase, albite, ferroan diopside ($CaFeSi_2O_6$), ferrosilite and fayalite, as well as nepheline and leucite which may be present in small amounts in the norm.

$$MDI = \sum (Qz + Or + Ab + Di' + Fs + Fa + Ne + Lc)$$

where $Di' = 1,88052\ Fs\ (Di)$ (Fs of normative diopside) (See Table XV).

But before the MDI of rocks against height in the intrusion is plotted, another factor which will influence the MDI (or DI) must be taken into account, namely, the various amounts of oxidic ore minerals present in the rock types. Consider, for instance, a magnetite-bearing anorthosite, which, for the sake of simplicity, consists of 50 per cent normative magnetite and 50 per cent normative plagioclase which is composed of 24 per cent normative Ab and 26 per cent normative An. The MDI of this rock will be 24. A rock type directly above or below this magnetite-bearing anorthosite is, for argument's sake, a magnetite-free troctolite which consists of 50 per cent normative olivine (26 per cent Mg_2SiO_4 and 24 per cent Fe_2SiO_4) and 50 per cent normative plagioclase (24 per cent Ab and 26 per cent An). The MDI of this rock will be 48. A magnetite-free anorthosite at the same level in the intrusion will also have an MDI of 48 (48 per cent normative Ab and 52 per cent normative An). The difference in MDI between the first two rock types is considerable although these rocks may occupy nearly the

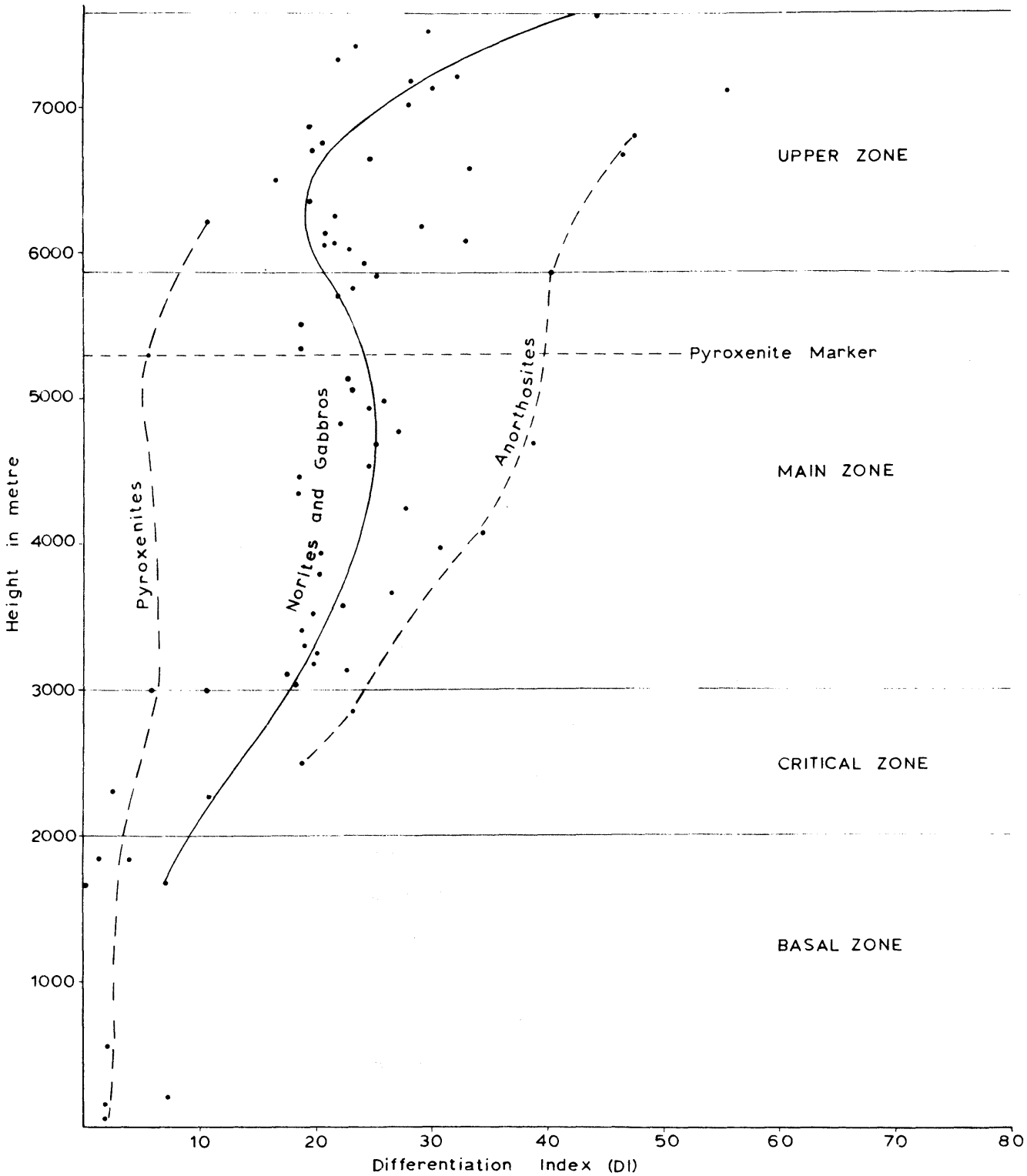

FIG. 65. PLOT OF THE DIFFERENTIATION INDEX OF ROCKS FROM THE BUSHVELD COMPLEX

same height in the intrusion. It follows that all the "inactive" minerals like magnetite, ilmenite, apatite and chromite, (i.e. those normative minerals which do not change in composition with differentiation and which may be present in varying amounts, especially in the Upper, Critical and Basal Zones of the Bushveld Complex) must be subtracted from the norm, the remaining norm must be recalculated to a percentage and the MDI calculated from this recalculated norm. In this way, the magnetite-bearing anorthosite, the troctolite and the magnetite-free anorthosite, which are used as examples above, will all have MDI's of 48. An example of the MDI calculation from the chemical analysis is given in Table XV.

In Fig. 66, a plot of the MDI against height in the intrusion, a fairly good trend in the differentiation is observed. Although the scatter of points is still considerable, the MDI of anorthosites and pyroxenites now fall within the trend of the gabbroic and noritic rocks. The influx of fresh magma at the level of the Pyroxenite Marker of the Main Zone is also clearly indicated.

3. The modified crystallization index (MCI)

The crystallization index was proposed by Poldervaart and Parker (1964, p. 281) and is based on the argument that the great diversity of rock types produced during the late stages of crystallization evolved from very similar source-magmas. The CI is therefore a parameter of differentiation which is based on the onset of magmatic crystallization, i.e. the system $CaAl_2Si_2O_8$ - $CaMgSi_2O_6$ - Mg_2SiO_4. According to Poldervaart and Parker, the CI "measures the progression of partial magmas or igneous rocks from the primitive system anorthite - diopside - forsterite".

CI = normative An + Di' + Fo' + Sp' where

Di' = magnesian diopside ($CaMgSi_2O_6$) calculated from normative diopside.

Fo' = normative forsterite plus normative enstatite converted to forsterite.

Sp' = magnesian spinel ($MgAl_2O_4$) calculated from normative corundum in ultramafic rocks.

Rocks which consist of anorthite, magnesian diopside or forsterite have a CI of 100, whereas rocks which consist of quartz, alkali feldspars or feldspathoids have a CI of 0. Poldervaart and Parker stress that the CI is more useful in indicating trends of differentiation in basaltic magmas, especially where there is a gradual enrichment of iron owing to fractional crystallization. This they illustrated (1965, p. 281, Fig. 2) with the aid of calculated compositions of successive

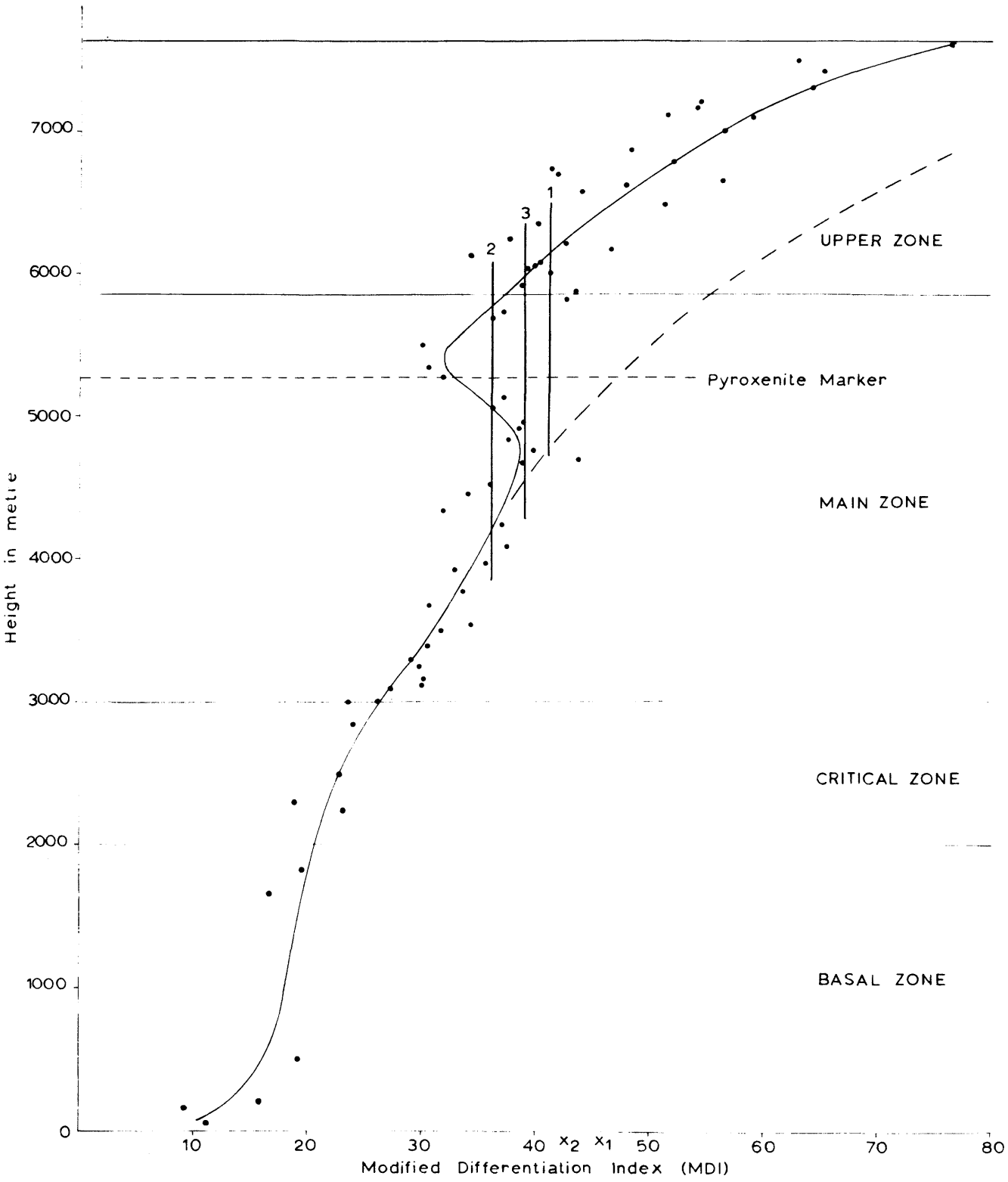

FIG. 66. PLOT OF THE MODIFIED DIFFERENTIATION INDEX OF ROCKS FROM THE BUSHVELD COMPLEX

Skaergaard liquids (Wager 1960, p. 386) which will necessarily give a linear trend as shown. If, however, analyses of rocks are used for the CI calculations and these values plotted against height in the intrusion, as was done with the available analyses of Bushveld rocks (Fig. 67) a sharp reversal in the differentiation trend is observed in the lower zones of the Complex. This may be explained as follows:

A dunite which consists of forsterite has a CI of 100 and an anorthosite which consists of anorthite also has a CI of 100. Dunite and anorthosite are however rock types which do not occur together in layered intrusions. The association pyroxenite and anorthosite is however common, for instance in the Critical Zone of the Bushveld Complex. It follows that an anorthosite with CI 100 may be found in association with a pyroxenite of CI 70. The anorthosites of the top of the Critical Zone and the harzburgites of the Basal Zone have therefore higher CI's than the pyroxenites which occur between these two (Fig. 67). This discrepancy may be overcome if the CI is modified so that the calculations are based on the orthopyroxene content of the norm, in such a way that the CI for both the pyroxenite (enstatite only) and the anorthosite (anorthite only) is 100. Consequently, the CI for a dunite (forsterite only) must be more than 100, namely, 142,68. This figure, based on the amount of SiO_2 necessary to convert all the olivine to orthopyroxene is obtained by multiplying the amount of normative forsterite by

$$\frac{\text{mol. weight } 2MgSiO_3}{\text{mol. weight } Mg_2SiO_4} = 1,4268$$

The maximum value of the CI is therefore 142,68. Recalculation of the CI obtained by this method to 100 is achieved by multiplying by the factor 0,70084. A dunite will now have a MCI of 100, a pyroxenite (enstatite only) will have a MCI of 70,08 and an anorthosite (anorthite only) will also have a MCI of 70,08.

Although Poldervaart and Parker's argument that the "ideal parameter of magmatic differentiation should represent the phases of petrogeny's primitive system" (1964, p. 285) is correct, it must also be borne in mind that the onset of fractional crystallization of a basaltic magma in intrusions such as the Bushveld Complex is not at the ternary eutectic in this system, as implied by Poldervaart and Parker, but usually commences in the olivine field whereupon the

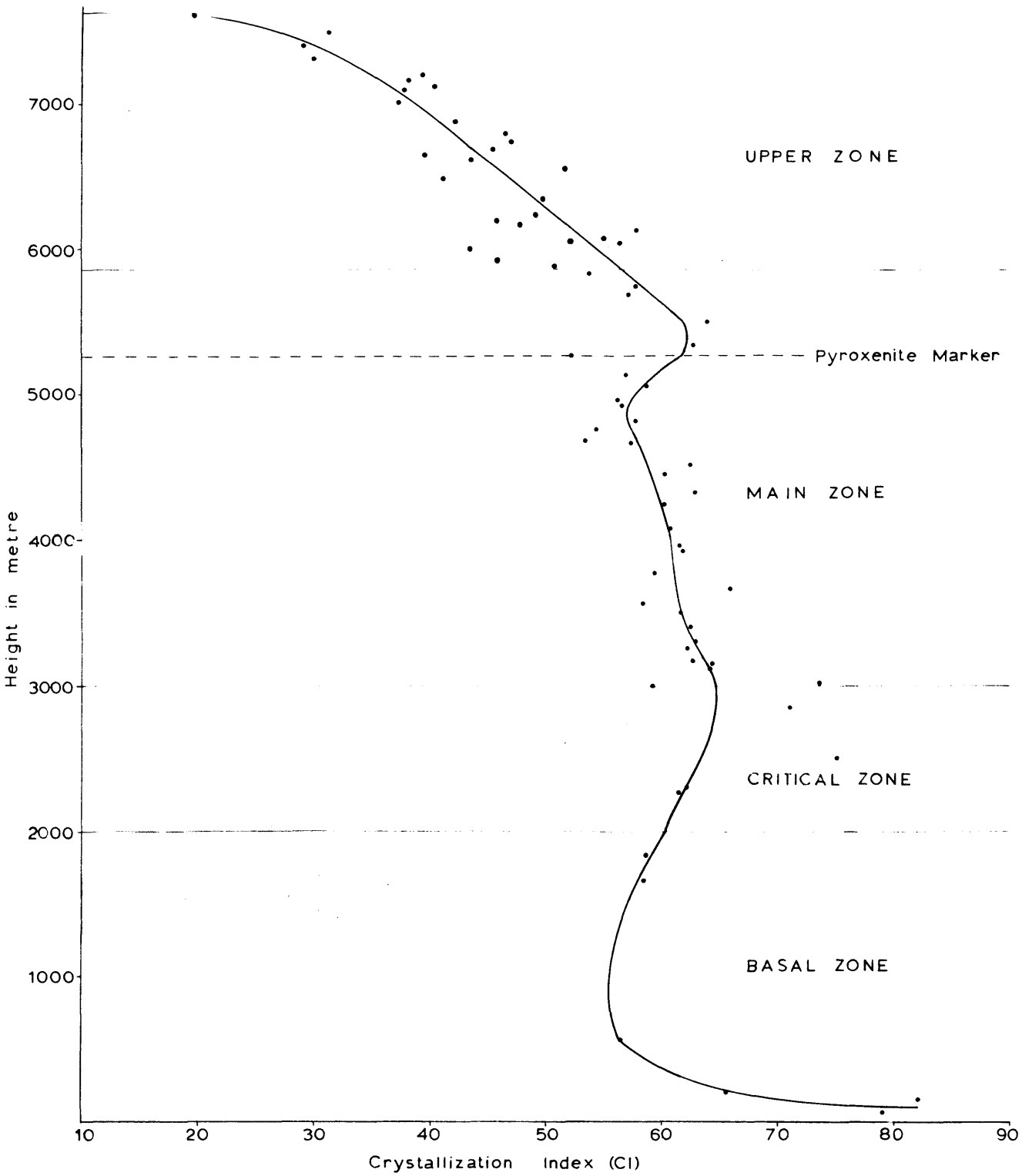

FIG. 67. PLOT OF THE CRYSTALLIZATION INDEX OF ROCKS FROM THE BUSHVELD COMPLEX

TABLE XV EXAMPLE OF MDI AND MCI CALCULATIONS FROM THE CHEMICAL ANALYSIS

Analysis		C. I. P. W. Norm		Recalculated norm		MDI	MCI
SiO_2	48,00	Or	7,39	8,49		8,49	
TiO_2	2,26	Ab	27,04	31,05		31,05	
Al_2O_3	13,00	An	17,54	20,14			20,14
Fe_2O_3	3,03	Di Wo	4,25	5,19			
FeO	16,20	Di En	1,10	1,27			Di' 2,74**
MnO	0,26	Di Fs	3,69	4,23	Di'	7,95*	
MgO	2,88	Hy En	5,63	6,46			6,46
CaO	7,14	Hy Fs	18,84	21,64		21,64	
Na_2O	3,18	Ol Fo	0,28	0,32			Fo' 0,46***
K_2O	1,23	Ol Fa	1,05	1,21		1,21	
P_2O_5	1,06	Mt	4,41	100,00			
H_2O	2,05	Il	4,35				
	100,29	Ap	2,55	Total		70,34	29,80
		H_2O	2,05				x 0,7008
			100,44				= 20,89

* $4,23 \times \frac{\text{mol. wt. } CaFeSi_2O_6}{\text{mol. wt. } FeSiO_3} = 4,23 \times \frac{248,04}{131,90} = 4,23 \times 1,88052 = 7,95$

** $1,27 \times \frac{\text{mol. wt. } CaMgSi_2O_6}{\text{mol. wt. } MgSiO_3} = 1,27 \times \frac{216,52}{100,38} = 1,27 \times 2,15700 = 2,74$

*** $0,32 \times \frac{\text{mol. wt. } 2MgSiO_3}{\text{mol. wt. } Mg_2SiO_4} = 0,32 \times \frac{200,76}{140,70} = 0,32 \times 1,4268 = 0,46$

liquid proceeds towards the ternary eutectic. Pyroxene and plagioclase usually crystallize after olivine, and rocks consisting of magnesian diopside and anorthite should therefore have a lower CI than rocks which consist essentially of olivine.

When the MCI as outlined above is calculated, it is again advisable to subtract mineral phases such as magnetite, ilmenite, apatite and chromite which may be present in variable amounts in the norm and to recalculate the remaining norm to 100. This is necessary because a pyroxenite which, for instance, contains 25 per cent chromite will have a lower MCI than a chromite-free pyroxenite immediately above or below. In norms which do not contain large amounts of magnetite, ilmenite, apatite or chromite, this correction is not necessary as it will not greatly influence the MDI or MCI.

MCI = (An + Di' + En' + Sp') x 0,70084

where An = normative anorthite.

Di' = magnesian diopside, $CaMgSi_2O_6$, calculated from normative diopside.

En' = normative enstatite of normative hypersthene plus normative forsterite converted to enstatite.

Sp' = magnesian spinel, $MgAl_2O_4$, calculated from normative corundum in ultramafic rocks.

An example of the calculation of the MCI is given in Table XV.

In Fig. 68 the MCI of rocks from the Bushveld Complex are plotted against height in the intrusion. If this diagram is compared with Fig. 66 it can be seen that, for the greater part of the intrusion, there is a striking similarity between the observed differentiation trends. This is obvious, because the relationship between the MDI and MCI is to some extent a reciprocal one. The lowest portion of the curve in Fig. 68 flattens out considerably, which is an indication of the relatively few dunitic rocks in the exposed sequence of the Bushveld Intrusion.

4. Binary variation diagrams

The variation diagrams presented in Figs. 69 to 77 are constructed from more than 100 analyses, mostly of rocks from the eastern part of the Bushveld Complex. The majority of the analyses were kindly made available to the author by Dr. D.R. Bowes and Dr. T.G. Molyneux, prior to publication. The rocks for these analyses were collected by Molyneux (1970, Plate III) along traverses across the Main and Upper Zones in the Leolo Mountains and at Magnet Heights

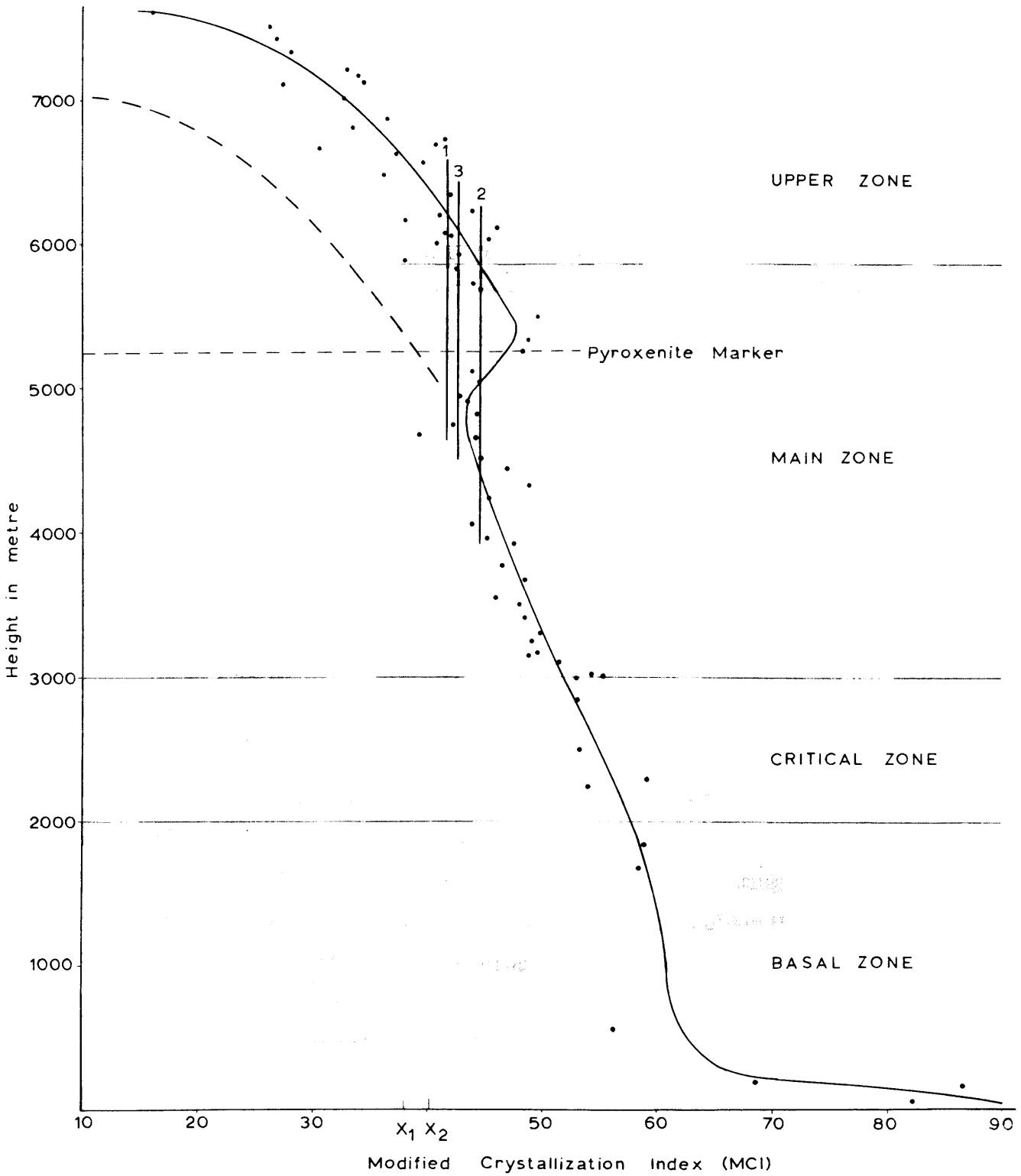

FIG. 68. PLOT OF THE MODIFIED CRYSTALLIZATION INDEX OF ROCKS FROM THE BUSHVELD COMPLEX

respectively, and were analysed by the Department of Geology at the University of Glasgow. Dr. Bowes also kindly supplied the C. I. P. W. norm and the CI of these analyses which were calculated by computer at the University of Glasgow. All the analyses, the C. I. P. W. norms recalculated to 100 (Thornton and Tuttle, 1960, p. 670 and Poldervaart and Parker, 1964, p. 285), CI, DI and the recalculated norms for the MDI and MCI are given in Appendix II, together with a list of the names of the analysed rocks, localities and literature references.

a) Calculated parameters vs. height in the intrusion

For the construction of Figs. 65 to 68 analyses of Molyneux's samples were used for the Main and Upper Zones. The thickness of these two zones is that reported by Molyneux (1970, p. 14) from the area to the north, where the samples were collected, and not the thickness as calculated for these two zones in this study (Folder II). Thicknesses of the lower two zones are rough estimates and the position in the sequence of rocks from these two zones was judged from the description of the localities and are therefore not accurate. Unfortunately, not many analyses of rocks from the Critical and Basal Zones of the eastern part of the Complex are available, and consequently the trends as observed from the few available analyses must be regarded with reservations.

Comparison of Figs. 65, 66, 67 and 68 clearly shows that the MDI and MCI are better parameters to illustrate the differentiation in layered mafic intrusions than the DI and CI, for reasons which are outlined in the sections dealing with the calculation of the MDI and MCI.

The scatter of points in Figs. 66 and 68 is to some extent due to the different degree of fractionation of the coexisting mineral series. Plagioclase usually contains more mol. per cent Ab than the coexisting orthopyroxene contains mol. per cent Fs (Willemse, 1969, p. 8 and Folder III of this study) and consequently, variations in the proportions of coexisting cumulus phases as well as variations in the amount of intercumulus material in the analysed rocks will cause a scatter of points in the diagram.

The MDI and MCI of three available analyses of rocks presumed to be from the chill zone of the Bushveld Complex were also calculated and are shown on Figs. 66 and 68 as vertical lines to indicate where these values intersect the differentiation trend. If the influx of fresh undifferentiated magma at the level of the Pyroxenite Marker of the Main Zone is ignored, and the observed differentiation trend continued (dashed lines Figs. 66 and 68) then the MDI and MCI

of rocks from the chill zone correspond to those of rocks approximately two-thirds up in the Layered Sequence. If the rocks from the chill zone represent the composition of the original magma, then one would expect these to have a MDI or MCI which would correspond to rocks of about half way up in the Layered Sequence, provided that the degree of fractionation of the magma was maintained at a fairly constant rate. Inasmuch as the MDI and MCI may be considered as parameters of fractionation, a constant rate of fractionation would result in a linear variation diagram. The trend, as observed in Figs. 66 and 68 is however, not linear (influence of the addition of fresh magma at the level of the Pyroxenite Marker excluded), but show, owing to a flattening of the curve, an increase in the degree of fractionation during crystallization of the Upper Zone. Consequently, the original magma will have a MDI or MCI which will correspond to that of the rocks in the upper half of the intrusion, as observed in these diagrams. However, the effect of flattening of the curve in the lower portion of the diagram (Basal Zone) will tend to counterbalance the flattening at the top, with the result that the MDI and MCI of the original Bushveld magma would be inclined to correspond to MDI's and MCI's of rocks in the middle of the sequence.

If, on the other hand, the degree of fractionation during crystallization of the Bushveld magma took place at a constant rate, then a steepening of the curve would indicate the presence of cyclic units either due to processes in a single batch of magma, or due to the influx of fresh, undifferentiated magma. Influx of a large volume of fresh magma at the level of the Pyroxenite Marker even resulted in the reversal of the trend in Figs. 66 and 68.

The observed relationship between MDI and MCI of rocks of the Chill Zone and those of the Layered Sequence must, however, be treated with caution as there are several ways in which such a relationship can be explained. These are among others:

i) That these fine-grained rocks are contaminated by assimilation of country-rocks (J. Willemse, 1969, p. 7).

ii) That more acid differentiates (i. e. diorites and granodiorites) existed along the outer, higher levels of the essentially funnel-shaped intrusion, and that the majority of these rocks have since been eroded away.

iii) There are also some indications that the Bushveld magma extended

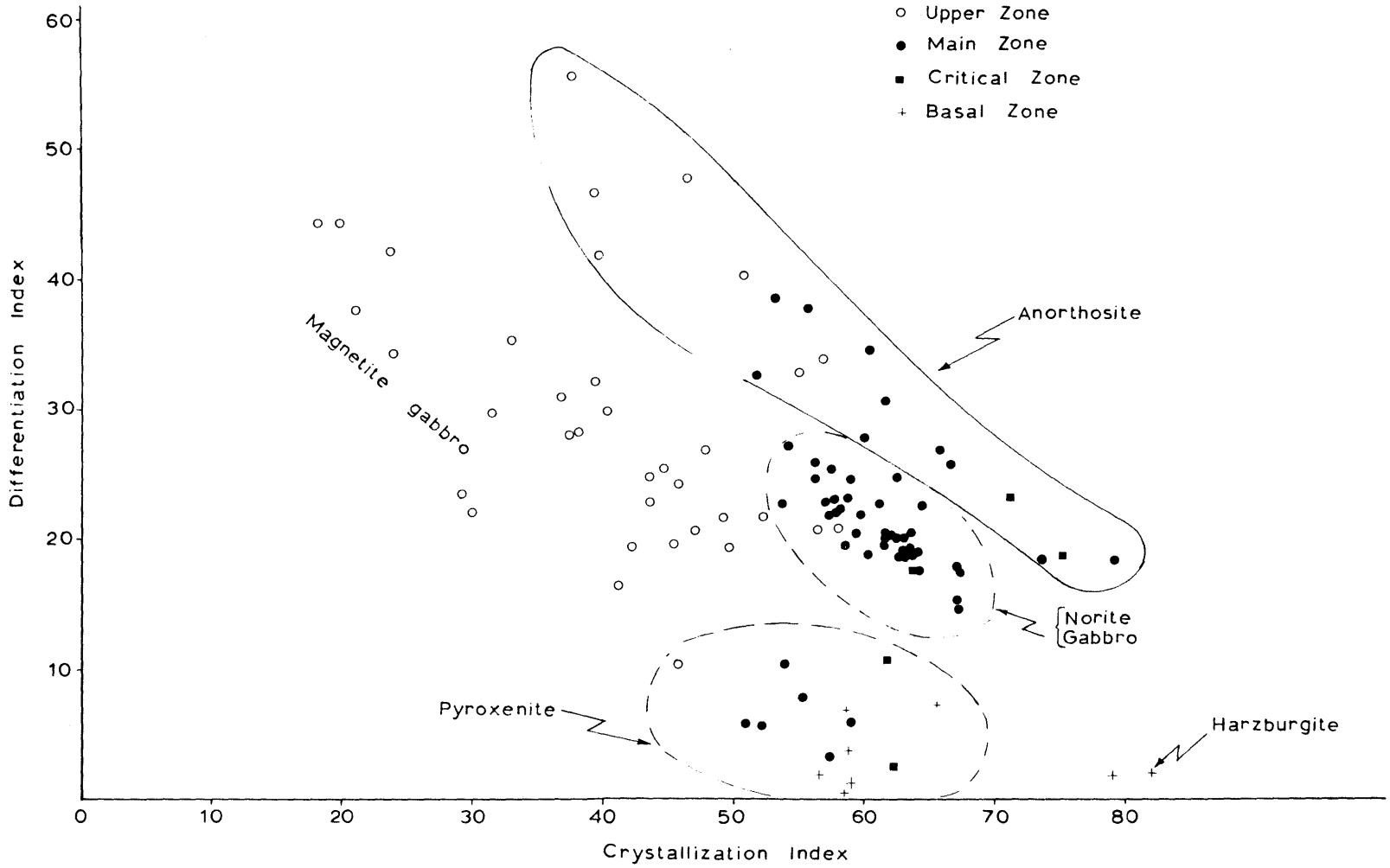

FIG. 69. PLOT OF THE DI VERSUS THE CI FOR ROCKS OF THE BUSHVELD COMPLEX

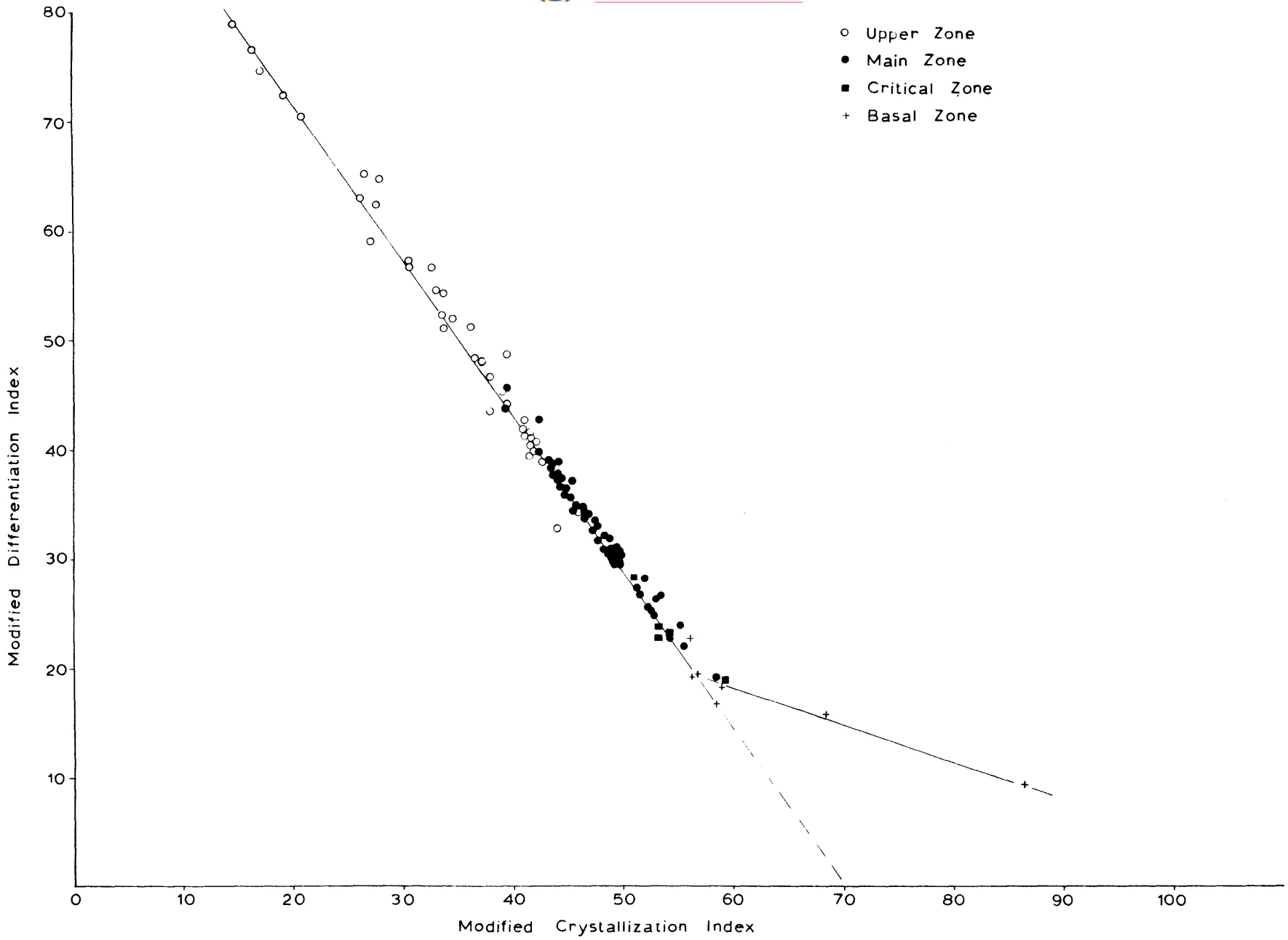

FIG. 70. PLOT OF THE MDI VERSUS THE MCI FOR ROCKS OF THE BUSHVELD COMPLEX

pected because MCI = (100 - MDI) x 0,7008 of rocks which contain no normative forsterite, and consequently all these analyses will fall on the straight line in Fig. 70. Rocks which do contain normative forsterite have, according to the rules of calculation of the MCI, a higher index (see method of calculation of MCI above) with the result that the MCI $\geq$ (100 - MDI) x 0,7008 and will therefore plot to the right of the line. This deviation from the straight line is not pronounced for the olivine-bearing rocks of the Upper Zone, because of the low normative forsterite content, but for rocks of the Basal Zone which contain larger amounts of normative forsterite, the deviation to the right is considerable and thus causes the deflection of the curve at high MCI and low MDI values.

c) DI, CI, MDI and MCI vs. weight per cent oxides

In Figs. 71 to 77 the DI, CI, MDI and MCI of rocks from the Bushveld Complex are plotted against weight per cent of some of the oxides or combinations of oxides. Seeing that layered intrusions consist of crystal cumulates, the composition of the rock is determined by the quantities of settled mineral phases with the result that a specific cumulate may contain a considerably higher or lower percentage of a certain oxide than the magma from which it crystallized. In most of the diagrams (Figs. 71 to 77) separate trends or areas could be deliniated for the major rock types, viz. anorthosite, pyroxenite, norite and gabbro, harzburgite and magnetite-bearing rocks of the Upper Zone.

From the spread of the points in these diagrams, 55 units for the DI, 67 units for the CI, 70 units for the MDI and 72 units for the MCI, it seems as though the last three are the most suitable parameters to illustrate differentiation trends in layered intrusions. In variation diagrams involving the CI, it can again be seen that pyroxenites have a lower CI than gabbros and consequently it is not a suitable parameter to illustrate differentiation trends. The MDI and MCI variation diagrams show very similar trends and seem to be the most suitable parameters. For igneous complexes where many dunites, harzburgites and pyroxenites are developed, the MCI would be the most useful, whereas for the Bushveld Complex where relatively few ultramafic rocks are developed, the MDI seems the more useful parameter (Compare also Figs. 66 and 68).

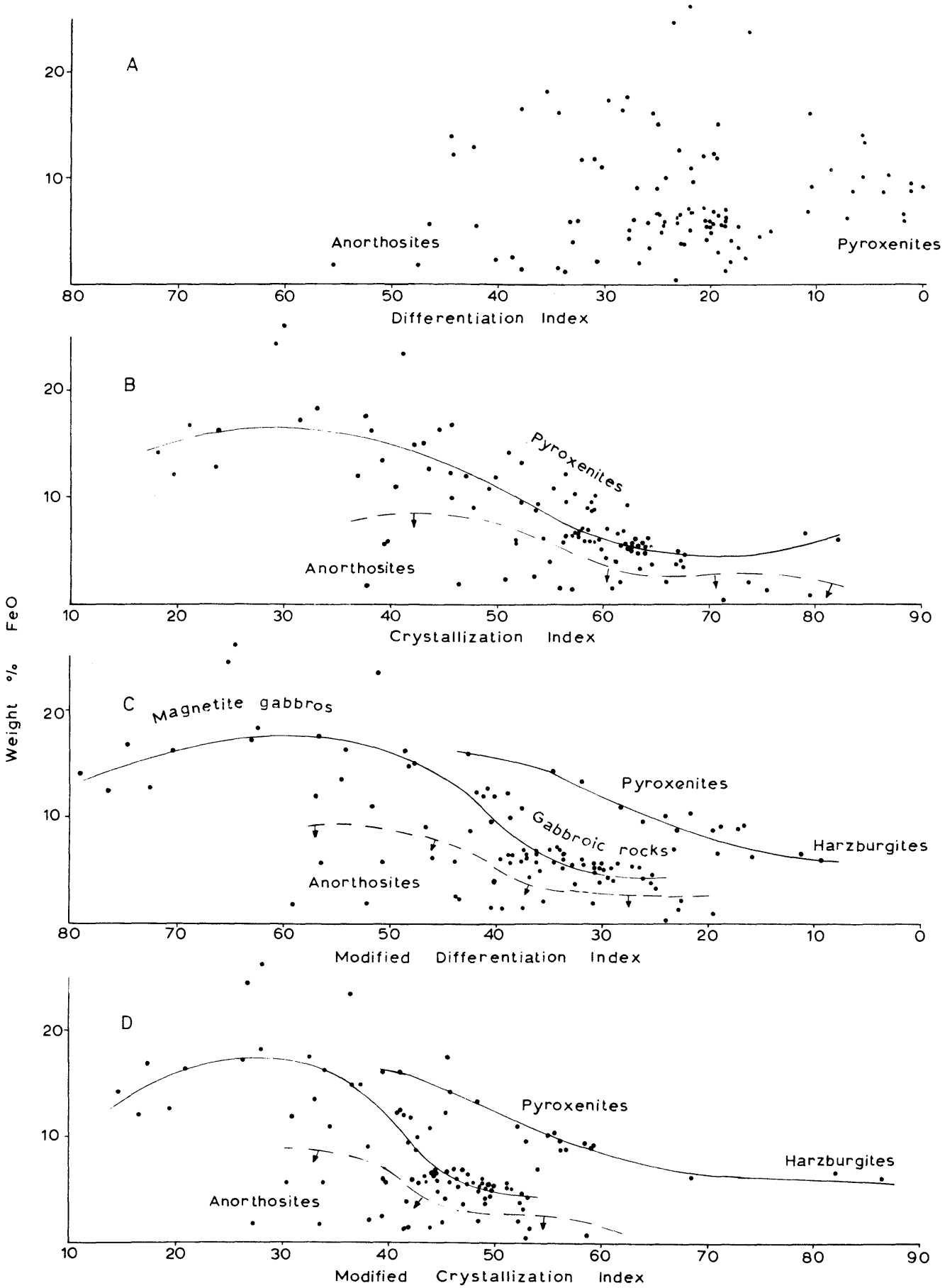

FIG. 71. PLOT OF DI, CI, MDI AND MCI AGAINST WEIGHT % FeO

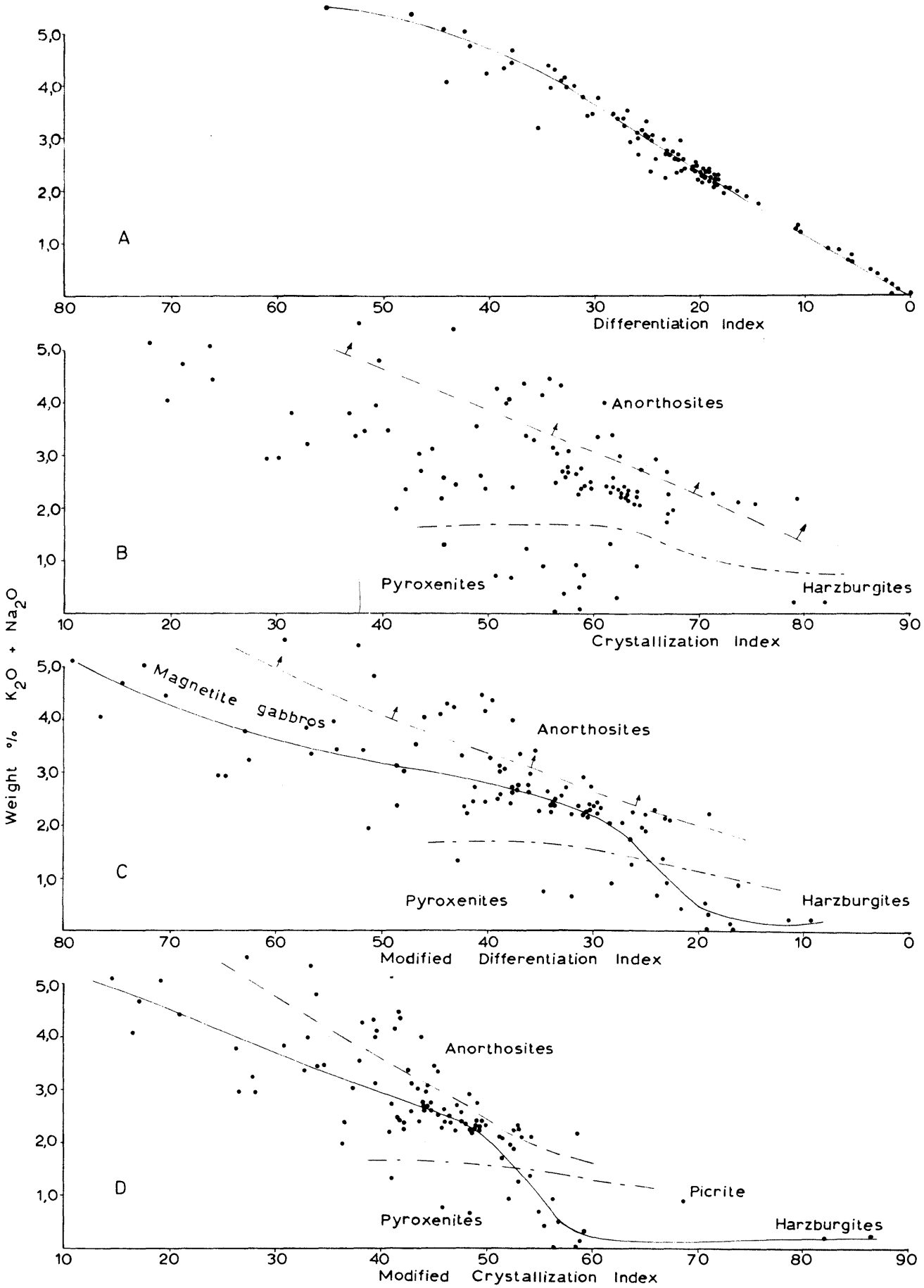

FIG. 72. PLOT OF DI, CI, MDI AND MCI AGAINST WEIGHT % K_2O AND Na_2O

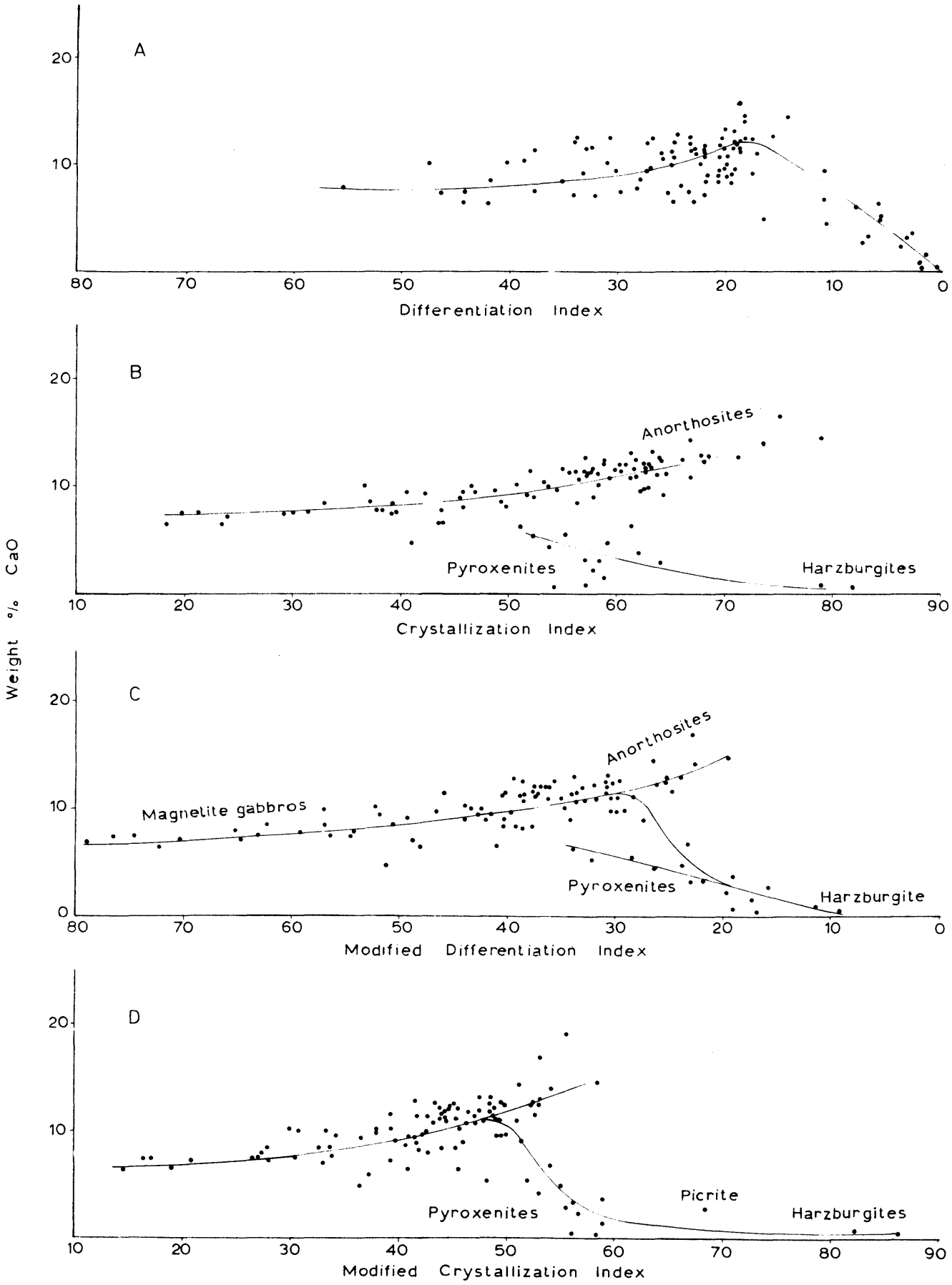

FIG. 73. PLOT OF DI, CI, MDI AND MCI AGAINST WEIGHT % CaO

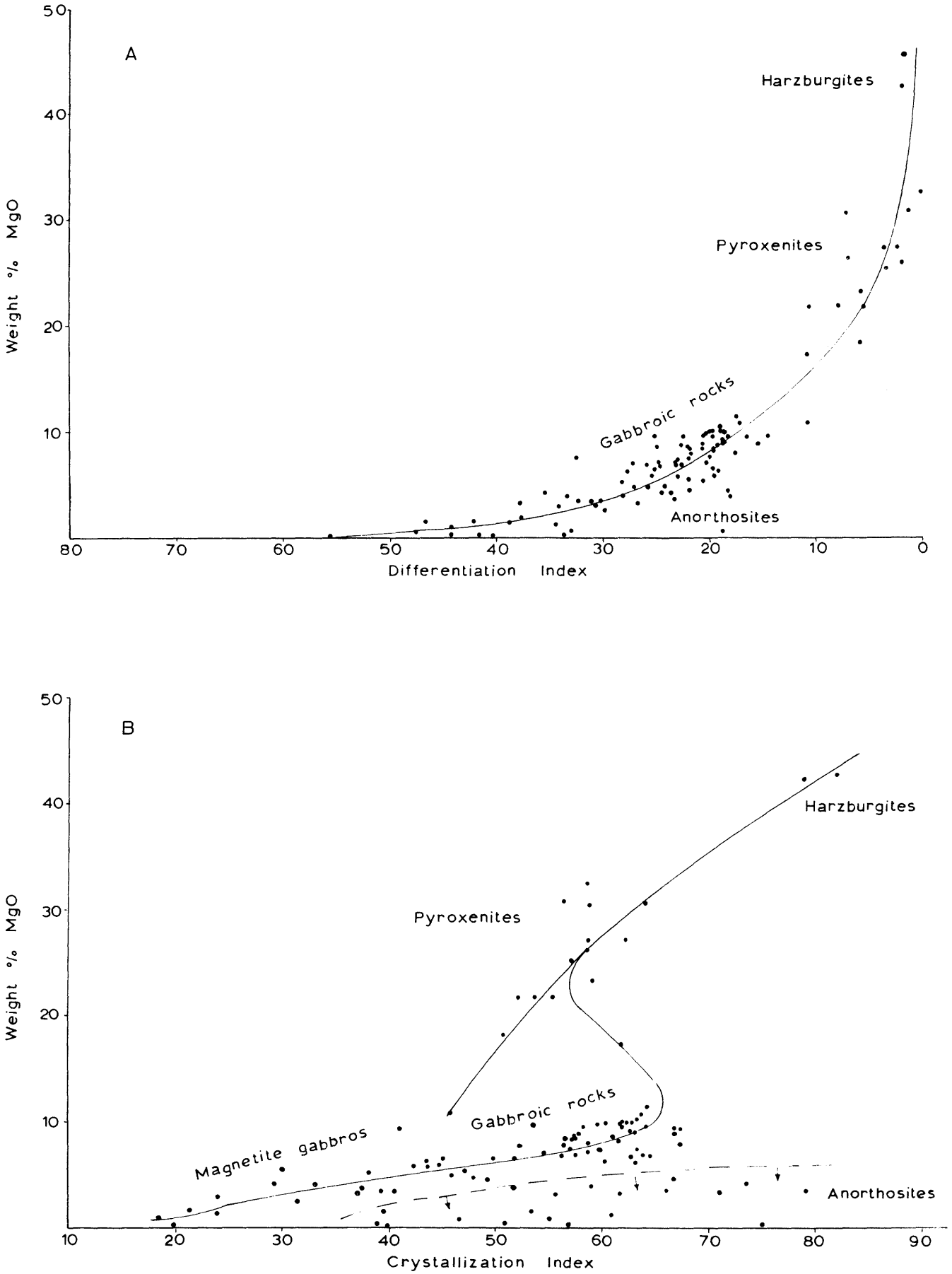

FIG. 74. PLOT OF DI AND CI AGAINST WEIGHT % MgO

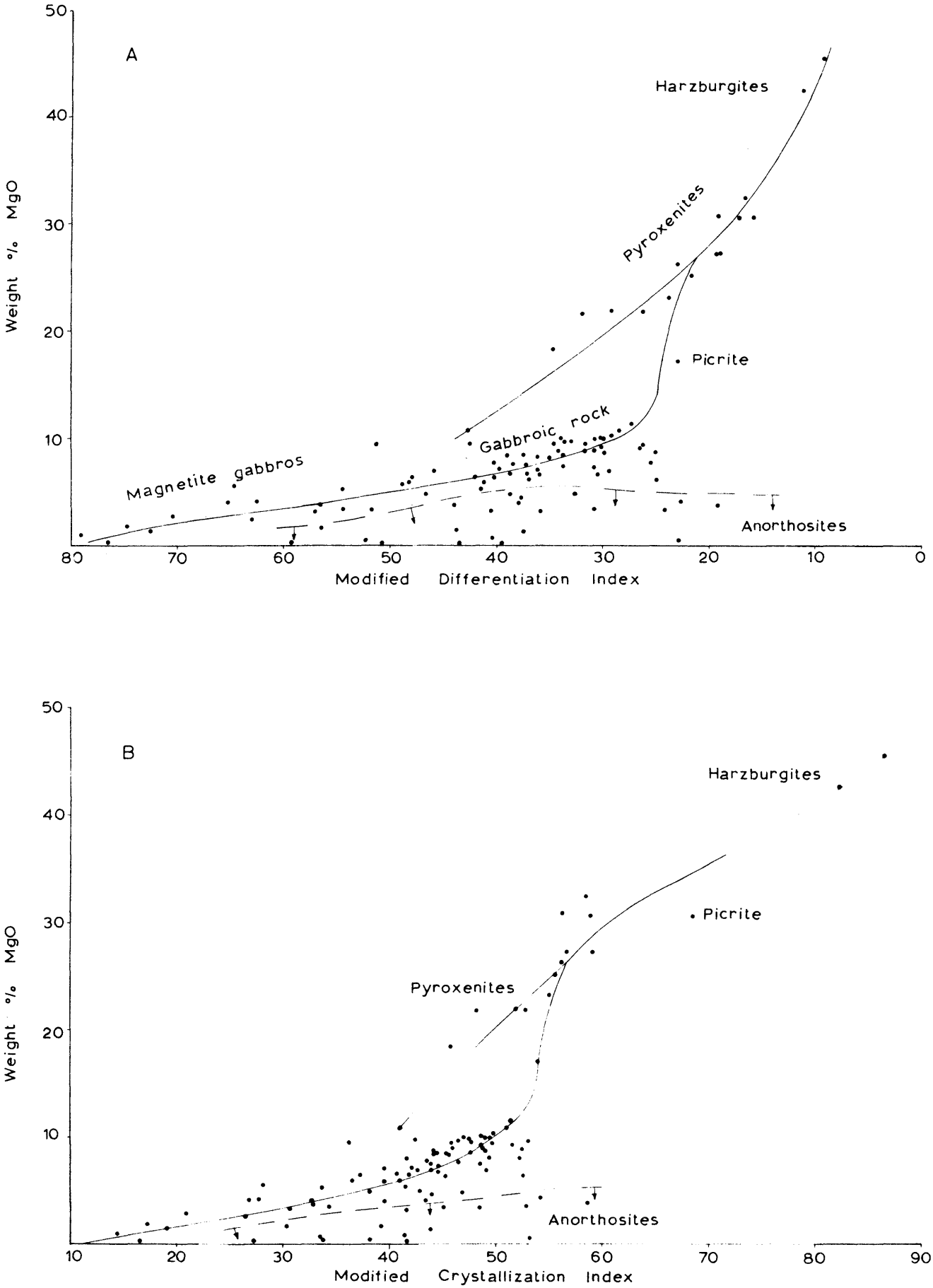

FIG. 75. PLOT OF MDI AND MCI AGAINST WEIGHT % MgO

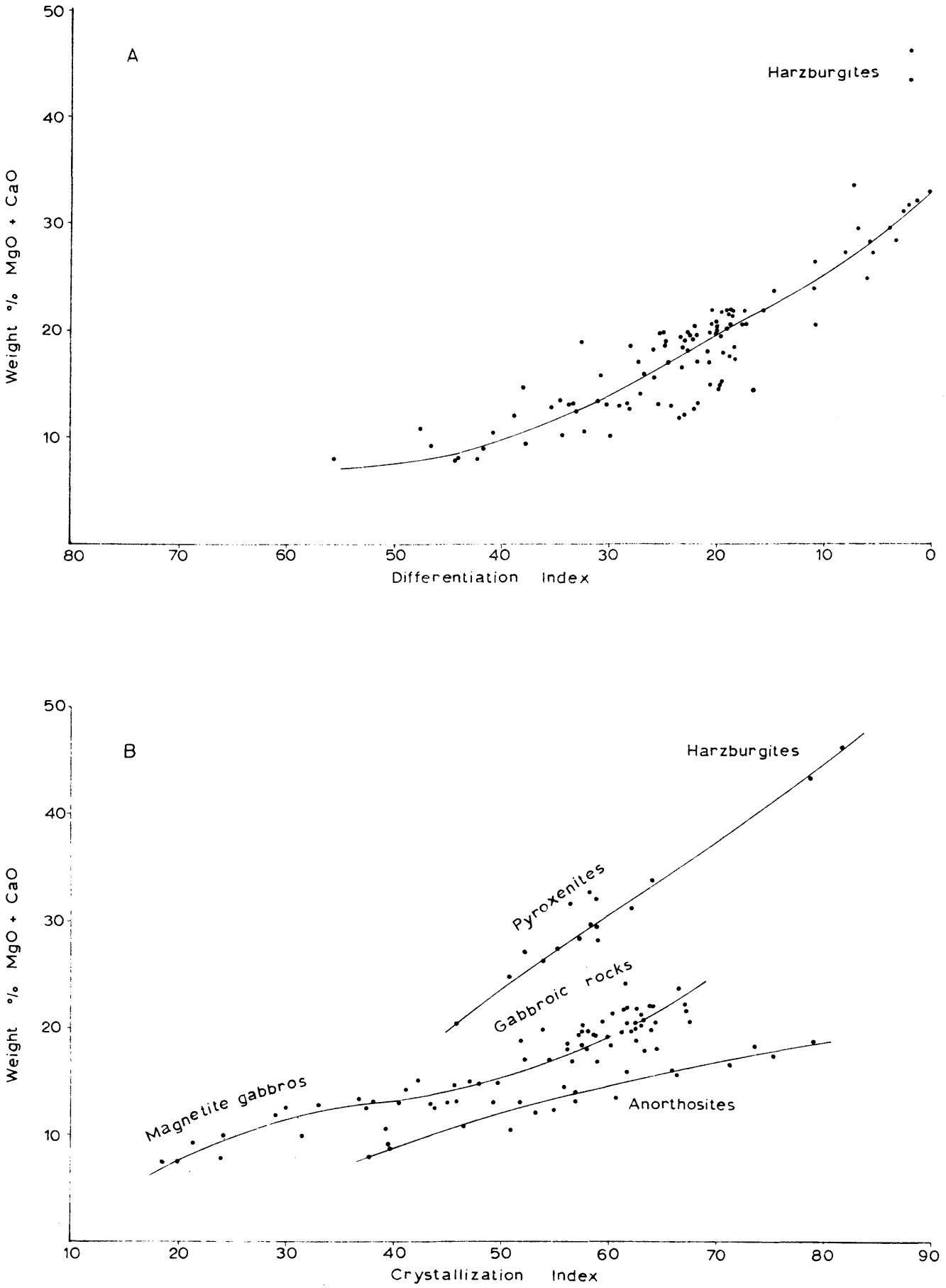

FIG 76. PLOT OF DI AND CI AGAINST WEIGHT % MgO + CaO

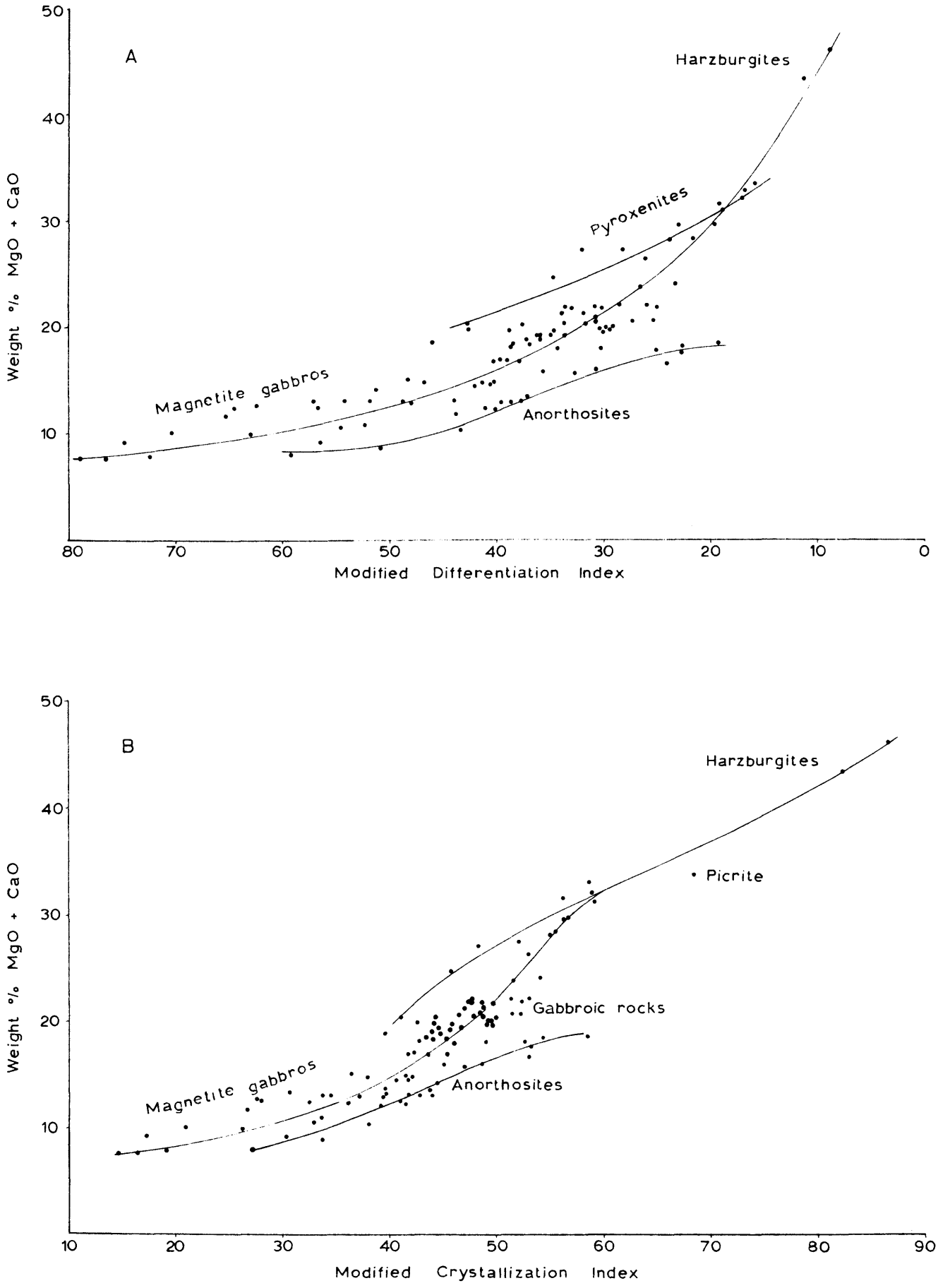

FIG. 77. PLOT OF MDI AND MCI AGAINST WEIGHT % MgO + CaO

X. SUMMARY AND CONCLUSIONS

Emplacement of the basaltic magma took place along an undulating plane near the top of the Pretoria Group. Absence of sediments of the Smelterskop Formation in their normal stratigraphic position at the present level of erosion indicates that they were lifted up vertically by the intrusion and that they have since been removed by erosion, whereas their presence in the roof, as for instance in the Rooiberg area and in the area mapped by Molyneux (1970a, Plate I) points to their absence at the floor.

Cooling of the magma took place primarily as a result of heat loss through the roof causing recrystallization of the felsite to leptite and microgranite as well as the melting of these rocks to give rise to the large amount of granophyre. Intermittent injection of fresh undifferentiated magma may in part be held responsible for the repetitive stratigraphy and also for the lateral extension of the magma chamber causing progressively higher horizons of the Layered Sequence to terminate against the sediments of the floor.

Crystallization of the Main Zone has probably taken place near the floor of the magma chamber under conditions of slow, continuous convection. Intermittent acceleration of the convection currents may have caused crystallization near the top of the intrusion, i.e. at lower pressures, and may have resulted in accumulation of plagioclase crystals only to form anorthosites. Although crystallization of the magma took place at low oxygen pressures causing an enrichment of iron in the residual magma, the appearance of magnetite in the rocks of the Upper Zone is not only considered to be the result of an increase in the oxygen fugacity, but also to be due to enrichment of iron in the liquid. A periodic increase in the oxygen fugacity enhanced the crystallization of magnetite, which, owing to its higher settling velocity could have assisted in the formation of the magnetitite seams. Adcumulus growth of crystals by diffusion or while crystals were still in contact with the supernatant magma probably aided the formation of adcumulates.

Postcumulus changes were to a large extent governed by load pressure which had a pronounced effect on the cumulates of the Layered Sequence. A direct result of this is probably the development of reversed zoning, interpenetration and bending of plagioclase crystals as well as the development of myrmekite, symplektite and units of similarly orienated grains of inverted pigeonite. Simul-

taneous compaction of the cumulus pile probably also resulted in the expulsion of large quantities of the intercumulus liquid which could have been concentrated in places to form transgressive pipe-like or sill-like pegmatoids. It is envisaged that, where their movement to higher levels was hampered by adcumulus growth of the overlying crystal mush, effectively sealing the intercumulus spaces, these liquids spread out laterally, reconstituting the cumulates to form irregularly shaped pegmatoids often displaying gradational as well as sharp contacts with the country-rocks, as described by Cameron and Desborough (1964, p. 200-223). Where confining pressure on these intercumulus liquids was sufficiently high they could have brecciated the overlying rocks on their way upwards, thus forming the occasional breccia pipe, as for instance on Tweefontein (Ferguson and McCarthy, 1970, p. 74) and near Roossenekal.

Towards the outer margins of the complex, the heat loss was probably more effective, causing lower temperature phases to crystallize simultaneously with higher temperature phases in the central portions of the magma chamber. The lower temperature phases of the ferromagnesian minerals extracted more iron from the fractionating magma where the thickness of the chamber was less , as for instance south of Tauteshoogte, with the result that the magma was depleted in iron, relative to that in the central portions, and prevented the formation of the magnetitite seams of Subzone D of the Upper Zone.

Crystallization of apatite and sulphides seems to have been governed by the concentration of phosphorus and sulphur in the magma respectively. The magma reached saturation of both at the base of Subzone D of the Upper Zone, which is indicated by the presence of cumulus apatite crystals and by numerous small droplets of sulphides in the rocks of this subzone.

The appearance of firstly biotite, then cumulus apatite and sulphide droplets and lastly hornblende in the rocks of the Layered Sequence is probably due to a gradual increase of the volatiles in the fractionating magma. Some of the water-rich residual liquids intruded the acid roof rocks and caused additional melting of the leptite to give rise to irregularly transgressive bodies of granodiorite.

The trend of differentiation in layered intrusions can be illustrated graphically by plotting the modified differentiation index or the modified crystallization index against height in the intrusion. Where large amounts of ultramafic rocks are developed, the latter seems to be the more appropriate, whereas the former

is a better parameter to illustrate differentiation of intrusions where not many ultramafic rocks are developed, as in the Bushveld Complex.

REFERENCES

ATKINS, F. B. (1969) Pyroxenes of the Bushveld Intrusion, South Africa. J. Pet., v. 10, 222-249.

BARKER, D. S. (1970) Composition of granophyre, myrmekite, and graphic granite. Bull. geol. Soc. Amer., v. 81, 3339-3350.

BERG, J. J. VAN DEN (1946) Petrofabric analysis of the Bushveld gabbro from Bon Accord. Trans. geol. Soc. S. Afr., v. 49, 155-208.

BOSHOFF, J. C. (1942) The Upper Zone of the Bushveld Complex at Tautes-hoogte. D. Sc. dissertation (unpublished) Univ. of Pretoria, 79p.

BOWEN, N. L. AND SCHAIRER, J. F. (1935) The system MgO-FeO-SiO_2. Amer. J. Sci., 5th Ser., v. 29, 151-217.

BROWN, G. M. (1956) The layered ultrabasic rocks of Rhum, Inner Hebrides. Phil. Trans. Roy. Soc. Lond., Ser. B., v. 240, 1-53.

_____ (1957) Pyroxenes from the early and middle stages of fractionation of the Skaergaard Intrusion, East Greenland. Miner. Mag., v. 31, 511-543.

_____ (1967) Experimental studies on inversion relations in natural pigeonitic pyroxenes. Carnegie Instn. Wash., Yearb. 66, 347-353.

BROWN, G. C. AND FYFE, W. S. (1970) The production of granitic melt during ultrametamorphism. Contr. Miner. Pet., v. 28, 310-318.

BRUYNZEEL, D. (1957) A petrographic study of the Waterfall Gorge profile at Insizwa. Ann. Univ. Stellenbosch, v. 33A, 481-538.

BUDDINGTON, A. F. (1939) Adirondack igneous rocks and their metamorphism. Geol. Soc. Amer., Mem. 7, 354p.

BURRI, C., PARKER, R. L. AND WENK, E. (1967) Die optische Orientierung der Plagioklase. Birkhäuser Verlag, Basel und Stuttgart. 334p.

CAMERON, E. N. (1969) Postcumulus changes in the Eastern Bushveld Complex. Amer. Miner., v. 54, 754-779.

CAMERON, E. N. (1970) Composition of certain coexisting phases in the eastern part of the Bushveld Complex. Geol. Soc. S. Afr., Spec. Publ. 1, 46-58.

_____ AND DESBOROUGH, A. (1964) Origin of certain magnetite-bearing pegmatites in the eastern part of the Bushveld Complex. Econ. Geol., v. 59, 197-225.

_____ AND DESBOROUGH, G. A. (1969) Occurrence and characteristics of chromite deposits - Eastern Bushveld Complex. Econ. Geol., Monogr. 4, 23-40.

CHAYES, F. (1956) Petrographic Modal Analyses. An elementary statistical appraisal. J. Wiley & Sons, Inc., New York, 113p.

COERTZE, F. J. (1962) The Rustenburg fault as a controlling factor of ore deposition south west of Pilanesberg. Trans. geol. Soc. S. Afr., v. 65, 253-257.

_____(1970) The geology of the western part of the Bushveld Igneous Complex. Geol. Soc. S. Afr., Spec. Publ. 1, 5-22.

COETZEE, G. L. (1970) The Rooiberg Felsite Series north of Nylstroom. Geol. Soc. S. Afr., Spec. Publ. 1, 312-325.

COOPER, J. R. (1936) Geology of the southern half of the Bay of Islands Igneous Complex. Newfld. Dep. Nat. Res., Bull, 4, 62p.

COUSINS, C. A. (1964) The platinum deposits of the Merensky Reef. 225-237, In Haughton, S. H. Ed., The geology of some ore deposits of Southern Africa, v. II. Geol. Soc. S. Afr., Johannesburg. 739p.

_____ (1969) The Merensky Reef of the Bushveld Igneous Complex. Econ. Geol., Monogr. 4, 239-251.

CRAIG, J. R. (1966) Appearances of phases during cooling of pyrrhotite-rich Ni-Cu ores. Carnegie Inst. Wash., Yearb. 65, 335-336.

_____ AND KULLERUD, G. (1969) Phase relations in the Cu-Fe-Ni-S System and their application to magmatic ore deposits. Econ. geol., Monogr. 4, 344-358.

CRUFT, E. F. (1966) Minor elements in igneous and metamorphic apatite. Geochim. et Cosmochim. Acta, v. 30, 375-398.

DEER, W. A., HOWIE, R. A. AND ZUSSMAN, J. (1962) Rock-forming minerals. Vol. 2, 371p., Vol. 3, 270p., Vol. 4, 435p., Vol. 5, 370p. Longmans, Green and Co. Ltd., London.

DESBOROUGH, G. A. AND CAMERON, E. N. (1968) Composition and structural state of plagioclases from the lower part of the eastern Bushveld Complex, South Africa. Amer. Miner., v. 53, 116-122.

DRESCHER-KADEN, F. K. (1948) Die Feldspat–Quarz–Reaktionsgefüge der Granite und Gneise. Springer Verlag, Berlin. 259p.

FERGUSON, J. AND WRIGHT, I. H. (1970) Compositional variation of plagioclase in the Critical Series, Bushveld Complex. Geol. Soc. S. Afr., Spec. Publ. 1, 59-66.

FERGUSON, J. AND McCARTHY, T. S. (1970) Origin of an ultramafic pegmatoid in the eastern part of the Bushveld Complex. Geol. Soc. S. Afr., Spec. Publ. 1, 74-79.

FORD, W. E. (1955) Dana's textbook of mineralogy, 4th Ed. John Wiley & Sons, Inc., New York, 851p.

FÖRTSCH, E. (1970) Untersuchungen an Mineralien der Pyromorphit-Gruppe. N. Jb. Miner., Abh., v. 113, 219-250.

GROBLER, N. J. AND WHITFIELD, G. G. (1970) The olivine-apatite-magnetitites and related rocks in the Villa Nora occurrence of the Bushveld Igneous Complex. Geol. Soc. S. Afr., Spec. Publ. 1, 208-227.

GROENEVELD, D. (1968) The Bushveld Igneous Complex in the Stoffberg area, Eastern Transvaal, with special reference to the magnetitite seams. D. Sc. dissertation (unpublished) Univ. of Pretoria. 172p.

_____ (1970) The structural features and the petrography of the Bushveld Complex in the vicinity of Stoffberg, Eastern Transvaal. Geol. Soc. S. Afr., Spec. Publ. 1, 36-45.

GRUENEWALDT, G. VON (1966) The geology of the Bushveld Igneous Complex east of the Kruis River cobalt occurrence, north of Middelburg, Transvaal. M. Sc. thesis (unpublished). Univ. of Pretoria. 104 p.

_____ (1968) The Rooiberg Felsite north of Middelburg and its relation to the layered sequence of the Bushveld Complex. Trans. geol. Soc. S. Afr., v. 71, 153-172.

_____ (1970) On the phase-change orthopyroxene-pigeonite and the resulting textures in the Main and Upper Zones of the Bushveld Complex in the Eastern Transvaal. Geol. Soc. S. Afr., Spec. Publ. 1, 67-73.

HALL, A. L. (1932) The Bushveld Igneous Complex of the Central Transvaal. Geol. Soc. S. Afr., Mem. 28, 560p.

HAMILTON, D. L. AND ANDERSON, G. M. (1967) Effects of water and oxygen pressure on the crystallization of basaltic magmas, 445-482. In, Hess, H. H. and Poldervaart, A., Editors, Basalts, Vol. 1. Interscience Publishers, New York, 482p.

HAMMERBECK, E. C. I. (1970) The Steelpoort Park Granite, eastern part of the Bushveld Complex, and the magnetitites in the gabbroic country rock. Geol. Soc. S. Afr., Spec. Publ. 1, 299-311.

HENDERSON, P. (1968) The distribution of phosphorus in the early and middle stages of fractionation of some basic layered intrusions. Geochim. et Cosmochim. Acta, v. 32, 897-911.

HERZ, N. (1951) Petrology of the Baltimore gabbro, Maryland. Bull. Geol. Soc. Amer., v. 62, p. 979-1016.

HESS, H. H. (1941) Pyroxenes of common mafic magmas. Part 1 and 2. Amer. Miner., v. 26, 515-535 and 573-594.

_____ (1949) Chemical composition and optical properties of common clinopyroxenes, Part. 1. Amer. Miner., v. 34, 621-666.

_____ (1960) Stillwater Igneous Complex, Montana. A quantitative mineralogical study. Geol. Soc. Amer., Mem. 80, 230p.

HUAN, W. T. AND MERRITT, C. A. (1954) Petrography of the troctolite of the Wichita Mountains, Oklahoma. Amer. Miner., v. 39, 549-565.

HUBBARD, F. H. (1966) Myrmekite in charnockite from southwest Nigeria. Amer. Miner., v. 51, 762-773.

HUGHES, C. J. (1970) Lateral cryptic variation in the Great Dyke of Rhodesia. Geol. Mag., v. 107, 319-325.

Index to the Powder Diffraction File 1970. Joint Committee on Powder Diffraction Standards, Publ. PDIS-20i.

IRVINE, T. N. (1970a) Crystallization sequences in the Muskox intrusion and other layered intrusions. Part 1, Olivine-pyroxene-plagioclase relation. Geol. Soc. S. Afr., Spec. Publ. 1, 441-476.

_____ (1970b) Heat transfer during solidification of layered intrusions. I. Sheets and sills. Can. J. Earth Sci., v. 7, 1031-1061.

_____ AND SMITH, C. H. (1967) The ultramafic rocks of the Muskox intrusion. Northwest Territories, Canada, 38-49. In, Wyllie, P. J., Ed. Ultramafic and related rocks. John Wiley & Sons. Inc., New York, 464p.

JACKSON, E. D. (1961) Primary textures and mineral associations in the Ultramafic Zone of the Stillwater Complex, Montana. U. S. Geol. Surv., Prof. Pap. 358, 106p.

_____ (1967) Ultramafic cumulates in the Stillwater, Great Dyke, and Bushveld Intrusions, 20-38. In, P. J. Wyllie Ed., Ultramafic and related rocks. J. Wiley & Sons, New York, 464p.

_____ (1970) The cyclic unit in layered intrusions - a comparison of repetitive stratigraphy in the ultramafic parts of the Stillwater, Muskox, Great Dyke, and Bushveld Complexes. Geol. Soc. S. Afr., Spec. Publ. 1, 391-424.

JAHNS, R. H. (1939) Clerici solution for the specific gravity determination of small mineral grains. Amer. Miner., v. 24, 116-122.

JAMBOR, J. L. AND SMITH, C. H. (1964) Olivine composition determination with small-diameter X-ray powder cameras. Miner. Mag., v. 33, 730-741.

KULLERUD, G. (1967) Sulphide studies, 286-321. In, P. H. Abelson Ed., Researches in geochemistry, Vol. 2. J. Wiley & Sons, New York, 663p.

_____ (1968) High temperature phase relations in the Cu-Fe-S system. Carneg. Inst. Wash., Yearb. 66, 404-409.

KUNO, H. AND NAGASHIMA, K. (1952) Chemical composition of hypersthene and pigeonite in equilibrium in magma. Amer. Miner., v. 37, 1000-1006.

KUNO, H., YAMASAKI, K., IDIA, C. AND NAGASHIMA, K. (1957) Differentiation of Hawaiian magmas. Jap. J. Geol. Geogr., v. 28, 179-218.

LIEBENBERG, C. J. (1961) The trace elements of the rocks of the Bushveld Igneous Complex, Part 2. The different rock types. Publ. Univ. Pretoria, No. 13, 65p.

LIEBENBERG, L. (1970) The sulphides of the Bushveld Complex. Geol. Soc. S. Afr., Spec. Publ. 1, 108-207.

LOMBAARD, A. F. (1949) Die geologie van die Bosveldkompleks langs Bloedrivier. Trans. geol. Soc. S. Afr., v. 52, 343-376.

LOMBAARD, B. V. (1932) The felsites and their relations to the Bushveld Complex. Trans. geol. Soc. S. Afr., v. 35, 125-190.

_____ (1934) On the differentiation and relationships of the rocks of the Bushveld Complex. Trans. geol. Soc. S. Afr., v. 37, 5-52.

MASKE, S. (1966) The petrography of the Ingeli Mountain Range. Ann. Univ. Stellenbosch, v. 41A, 1-109.

MENGE, G. F. W. (1963) The Cassiterite Deposits on Doornhoek 342 KR and vicinity, West of Naboomspruit, Transvaal. M. Sc. thesis (unpublished) Univ. of Pretoria. 56p.

MOLYNEUX, T. G. (1964) The geology and the structure of the area in the vicinity of Magnet Heights, Eastern Transvaal, with special reference to the magnetic iron ore. M. Sc. thesis (unpublished) Univ. of Pretoria, 112p.

_____ (1970a) A geological investigation of the Bushveld Complex in Sekhukhuneland and part of the Steelpoort Valley, Eastern Transvaal, with particular reference to the oxide minerals. D. Sc. thesis (unpublished) Univ. of Pretoria, 123p.

_____ (1970b) The geology of the area in the vicinity of Magnet Heights, Eastern Transvaal, with special reference to the magnetic iron ore. Geol. Soc. S. Afr., Spec. Publ. 1, 228-241.

MORIMOTO, N. AND KULLERUD, G. (1964) Pentlandite: Thermal expansion. Carneg. Inst. Wash., Yearb. 63, 204-205.

MURTHY, M. V. N. (1958) Coronites from India and their bearing on the origin of coronas. Bull. geol. Soc. Amer., v. 68, 23-38.

NAKAMURA, Y. AND KUSHIRO, I. (1970a) Compositional relations of co-existing orthopyroxene, pigeonite and augite in a tholeiitic andesite from Hakone volcano. Contr. Miner. Pet., v. 26, 265-275.

_____ (1970b) Equilibrium relations of hypersthene, pigeonite and augite in crystallizing magmas: Microprobe study of a pigeonite andesite from Weiselberg, Germany. Amer. Miner., v. 55, 1999-2015.

NALDRETT, A. J. (1969) A portion of the system Fe-S-O between 900 and 1080^{o}C and its application to sulfide ore magmas. J. Pet., v. 10, 171-201.

NALDRETT, A. J. AND KULLERUD, G. (1966) Limits of the $Fe_{1-x}S$ - $Ni_{1-x}S$ solid solution between 600^{o} and 250^{o}C. Carneg. Inst. Wash., Yearb. 65, 320-326.

_____ (1967) A study of the Strathcona Mine and its bearing on the origin of the Nickel-Copper Ores of the Sudbury District, Ontario. J. Pet., v. 8, 453-531.

NEL, H. J. (1940) The basal rocks of the Bushveld Igneous Complex, north of Pretoria. Trans. geol. Soc. S. Afr., v. 43, 37-68.

NEUHAUS, A. (1951) Orientierte Substanzabscheidung (Epitaxie). Fortschr. Miner., v. 30, 136-296.

NOCKOLDS, S. R. AND ALLEN, R. (1953) The geochemistry of some igneous rock series. Geochim. et Cosmochim. Acta, v. 4, 105-142.

OSBORN, E. F. (1959) Role of oxygen pressure in the crystallization and differentiation of basaltic magma. Amer. J. Sci., v. 257, 609-647.

_____ (1962) Reaction series for subalkaline igneous rocks based on different oxygen pressure conditions. Amer. Miner. v. 47, 211-226.

PECK, D. L., WRIGHT, T. L. AND MOORE, J. G. (1966) Crystallization of tholeiitic basalt in Alae Lava Lake, Hawaii. Bull. Volc., v. 29, 629-655.

PHILLIPS, E. R. (1964) Myrmekite and albite in some granites of the New England Batholith, New South Wales. J. geol. Soc. Austr., v. 11, 49-50.

_____ AND RANSOM, D. M. (1968) The proportionality of quartz in myrmekite. Amer. Miner., v. 53, 1411-1413.

PLATEN, H. VON (1965) Kristallisation granitischer Schmelzen. Contr. Miner. Pet., v. 11, 334-381.

POLDERVAART, A. AND HESS, H. H. (1951) Pyroxenes in the crystallization of basaltic magma. J. Geol., v. 59, 472-489.

POLDERVAART, A. AND PARKER, A. B. (1964) The crystallization index as a parameter of igneous differentiation in binary variation diagrams. Amer. J. Sci., v. 262, 281-289.

_____ (1965) Reply to discussion by C. P. Thornton and O. F. Tuttle. Amer. J. Sci., v. 263, 279-283.

RAAL, F. (1965) The transition between the Main and Upper Zone of the Bushveld Complex in the Western Transvaal. M. Sc. thesis (unpublished) Univ. of Pretoria, 59p.

REYNOLDS, D. (1947) The granitization controversy. Geol. Mag., v. 84, 209-223.

ROUX, P. (1968) Die Bosveldkompleks op De Kafferskraal 53 JT en omgewing, noord van Dullstroom. M. Sc. thesis (unpublished) Univ. of Pretoria, 100p.

SHELLEY, D. (1964) On myrmekite. Amer. Miner., v. 49, 41-52.

SKINNER, B. J. AND PECK, D. L. (1969) An immiscible sulfide melt from Hawaii. Econ. geol. Monogr. 4, 310-322.

SMITH, J. R. (1960) Optical properties of low-temperature plagioclase. Geol. Soc. Amer., Mem. 80, 191-219.

SMITH, J. V. and GAY, P. (1958) The powder patterns and lattice parameters of plagioclase feldspars. II. Miner. Mag., v. 31, 744-762.

STORMER, J. C. AND CARMICHAEL, I. S. E. (1971) Fluorine-hydroxyl exchange in apatite and biotite: a potential igneous geothermometer. Contr. Miner. Petr., v. 31, 121-131.

TABORSZKY, F. K. (1962) Geochemie des Apatits in Tiefengesteinen am Beispiel des Odenwaldes. Beitr. Miner. Pet., v. 8, 354-392.

THORNTON, C. P. AND TUTTLE, O. F. (1960) Chemistry of igneous rocks, I. Differentiation index. Amer. J. Sci., v. 258, 664-684.

_____ (1965) Discussion of "The crystallization index as a parameter of igneous differentiation in binary variation diagrams" by A. Poldervaart and A. B. Parker. Amer. J. Sci., v. 263, 277-279.

TILLEY, C. E., YODER, H. S. AND SCHAIRER, J. F. (1963) Melting relations of basalts. Carneg. Inst. Wash., Yearb. 62, 77-84.

_____ (1968) Melting relations of igneous rock series. Carneg. Inst. Wash., Yearb. 66, 450-457.

TROGER, W. E. (1959) Optische Bestimmung der gesteinsbildenden Minerale. Teil I, Bestimmungstabellen. E. Schweizerbart'sche Verlagsbuchhandlung, Stuttgart, 147p.

_____ (1967) Optische Bestimmung der gesteinsbildenden Minerale. Teil 2. E. Schweizerbart'sche Verlagsbuchhandlung, Stuttgart, 822p.

TURNER, F. J. AND VERHOOGEN, J. (1960) Igneous and metamorphic petrology, 2nd Ed. McGraw-Hill, New York, 694p.

TUTTLE, O. F. AND BOWEN, N. L. (1958) Origin of granite in the light of experimental studies in the system $NaAlSi_3O_8$-$KAlSi_3O_8$-SiO_2-H_2O. Geol. Soc. Amer. Mem. 74, 153p.

ULMER, G. C. (1969) Experimental investigations of chromite spinels. Econ. Geol., Monogr. 4, 114-131.

VULTEE, J. VON (1951) Die orientierten Verwachsungen der Mineralien. Fortschr. Miner., v. 30, 297-378.

WAGER, L. R. (1956) A chemical definition of fractionation stages as a basis for comparison of Hawaiian, Hebridean and other basic lavas. Geochim. et Cosmochim. Acta, v. 9, 217-248.

_____ (1960) The major element variation of the Layered Series of the Skaergaard Intrusion and a re-estimation of the average composition of the Hidden Layered Series and of the successive residual magmas. J. Pet., v. 1, 364-398.

_____ (1963) The mechanism of adcumulus growth in the layered series of the Skaergaard intrusion. Miner. Soc. Amer., Spec. Pap. 1, 1-9.

WAGER, L. R. AND DEER, W. A. (1939) Geological investigations in East Greenland, Part III. The petrology of the Skaergaard Intrusion, Kangerdlugssuaq, East Greenland. Medd. om Gronland, v. 105, No. 4, 1-352.

WAGER, L. R., BROWN, G. M. AND WADSWORTH, W. J. (1960) Types of igneous cumulates. J. Pet., v. 1, 73-85.

WAGER, L. R. AND BROWN, G. M. (1968) Layered Igneous Rocks. Oliver and Boyd, Edinburgh and London, 588p.

WAGNER, P. A. (1929) The platinum deposits and mines of South Africa. Oliver and Boyd, Edinburgh, 326p.

WILLEMSE, J. (1953) The mineral potentials of the townlands of Roossenekal. Restricted Report, Peri-urban Areas Health Board, Pretoria, 14p.

_____ (1959) The "Floor" of the Bushveld Igneous Complex and its relationships, with special reference to the Eastern Transvaal. Trans. geol. Soc. S. Afr., v. 62, xxi-lxxx.

_____ (1964) A brief outline of the geology of the Bushveld Igneous Complex, 91-128. In, Haughton, S. H., Ed., The geology of some ore deposits of Southern Africa, Vol. II. Geol. Soc. S. Afr., Johannesburg, 739p.

_____ (1969a) The geology of the Bushveld Igneous Complex, the largest repository of magmatic ore deposits in the world. Econ. Geol., Monogr. 4, 1-22.

_____ (1969b) The vanadiferous magnetic iron ore of the Bushveld Igneous Complex. Econ. Geol., Monogr. 4, 187-208.

WILLEMSE, J. AND BENSCH, J.J. (1964) Inclusions of original carbonate rocks in gabbro and norite of the eastern part of the Bushveld Complex. Trans. geol. Soc. S. Afr., v. 67, 1-87.

WILLEMSE, J. AND FRICK, C. (1970) Stroomroof en die invloed van verskuiwings op die geomorfologie in die opvanggebied van die Steelpoortrivier in Oos-Transvaal. Trans. geol. Soc. S. Afr., v. 73, 159-171.

WONES, D.R. (1963) Physical properties of synthetic biotites on the join phlogopite-annite. Amer. Miner., v. 48, 1300-1316.

YODER, H.S. AND TILLEY, C.E. (1962) Origin of basalt magmas. An experimental study of natural and synthetic rock systems. J. Pet., v. 3, 342-532.

_____ AND SCHAIRER, J.F. (1963) Pyroxenes and associated minerals in the crust and mantle. Pyroxene quadrilateral. Carneg. Inst. Wash., Yearb. 62, 84-95.

YUND, R.A. AND KULLERUD, G. (1966) Thermal stability of assemblages in the Cu-Fe-S system. J. Pet., v. 7, 454-488.

ZYL, J.P. VAN (1970) The petrology of the Merensky Reef and associated rocks on Swartkop 988, Rustenburg district. Geol. Soc. S. Afr., Spec. Publ. 1, 80-107.

DALY, R.A. (1928) Bushveld Igneous Complex of the Transvaal. Bull. geol. Soc. Amer., v. 39, 703-768.

FRICK, C. (1967) The margin of the Bushveld Complex in the vicinity of De Berg, north of Dullstroom. M.Sc. thesis (unpublished) Univ. of Pretoria, 127p.

ROEDER, P.L. AND OSBORN, E.F. (1966) Experimental data for the system $MgO - FeO - Fe_2O_3 - CaAl_2Si_2O_8 - SiO_2$ and their petrologic implications. Amer. J. Sci., v. 264, 428-480.

APPENDIX I

MODAL ANALYSES AND COMPOSITION OF CUMULUS PHASES OF ROCKS FROM THE MAIN AND UPPER ZONES OF THE BUSHVELD COMPLEX

M. R. Merensky Reef

I. C. No. Number of identity changes on a 40mm traverse (Chayes, 1956, p. 77).

Cumulus phases are denoted by asterisks following the volumetric percentage.

Values used in the compositional trend of the plagioclase in Folder III are marked by an asterisk. Where only two values are given they were averaged for construction of the trend.

APPENDIX I. MAIN ZONE, Subzone A.

Sample Number	PB4398	PB4389	PB4284	PB4275	PB4271	PB4254	PB4093	PB40895	PB4076	PB4049	PB3883	PB3832	PB3801	PB3701	PB3573
Height in metre above M.R.	1	4	35	38	39	44.5	93.5	94.5	99	107	158	173	182	213	252
Modal analysis (vol.%)															
Plagioclase	84.6*		54.3*	40.6*	88.3*		76.3*	78.8*	80.8*	64.0*	65.8*	69.6*	84.9*	60.9*	74.0*
Orthopyroxene	8.2*		42.1*	40.1*	9.5*		8.5	13.7*	9.2	23.5*	31.7*	27.4*	6.5*	28.4*	21.5*
Clinopyroxene	7.1		2.7	18.8	1.7		14.6	5.4	8.9	10.1*	2.5	3.0	4.1	10.7*	4.4
Biotite	–		0.3	0.2	tr.		tr.	0.2	0.3	1.0	–	–	–	–	–
K-feldspar	–		tr.	–	–		–	0.1	–	–	–	–	–	–	–
Quartz	0.1		0.5	0.2	0.4		0.6	1.6	0.8	1.35	–	–	4.3	–	0.1
Apatite	–		–	–	–		–	tr.	–	–	–	–	tr.	–	–
Opaque	tr.		tr.	0.1	tr.		–	0.2	tr.	tr.	–	–	0.2	–	–
I.C. No.	70		61	73	70		52	51	57	68	115	142	37	98	60
Plagioclase: mol. % An from:															
$2\theta_{131}-2\theta_{1\bar{3}1}$(CuK$\alpha$)	76*	74	76	76		76*		69*		68*	72			72*	73
$2\theta_{\bar{2}41}-2\theta_{2\bar{4}1}$(CuK$\alpha$)	–	73	–	74		71		70		68	71*			72	–
2V	77	76	78	76		81(?)		69		69	70			70	69
Ext. angles	76	76	77*			77	71								
Orthopyroxene: mol. % Fs from:															
2V	25	25	20	20		23		34		30	25			25	26
Name of rock and remarks	Spotted anorthositic hypersthene gabbro		Spotted norite	Feldspathic pyroxenite, Bastard Reef	Spotted anorthosite	Mottled anorthosite	Hypersthene gabbro Inverted pigeonite	Hyperite Inverted pigeonite	Anorthositic hyperite Inverted pigeonite	Hyperite	Fine-grained norite	Finge-grained norite	Spotted anorthosite	Spotted hyperite	Spotted norite

APPENDIX I (Continued). MAIN ZONE, Subzone A

Sample Number	PB3549	PB3521	PB3496	PB3448	PB3372	PB33315	PB3245	PB3166	PB3051	PB2951	PB2829	PB2731	PB2633	PB2461	PB2371
Height in metre above M.R.	259	267	276	291	314	326	352	376	411	441	470	515	538	591	618
Modal analysis (vol. %)															
Plagioclase	36.2*		61.8*		63.8*	67.5*	63.7*	58.3*	57.5*	64.5*	61.1*	55.4*	83.5*	61.7*	63.2*
Orthopyroxene	55.3*		28.3*		22.1*	14.8*	12.9*	21.4*	20.4*	16.9*	11.9*	19.9*	13.1*	20.8*	9.4*
Clinopyroxene	8.5		9.3		13.7*	16.9*	22.8*	20.0*	20.2*	18.4*	26.2*	23.8*	2.8	17.0*	24.3*
Biotite	–		0.3		–	–	–	0.1	0.5	–	0.1	0.1	0.2	0.2	0.8
K-feldspar	–		–		–	–	–	–	–	–	–	–	–	–	0.1
Quartz	–		0.3		0.4	0.8	0.6	0.1	1.4	0.2	0.6	0.8	0.4	0.3	2.1
Apatite	–		–		–	–	–	–	–	–	–	–	–	–	tr.
Opaque	–		–		–	–	–	–	tr.	–	0.1	–	–	–	tr.
I.C. No.	128		92		80	75	68	68	53	62	58	64	56	69	52
Plagioclase: mol. % An from:															
$2\Theta_{131}-2\Theta_{1\bar{3}1}$(CuK α)		70*		69*	69	68*	68*	68*			68*	66	68		67*
$2\Theta_{\bar{2}41}-2\Theta_{\bar{2}\bar{4}1}$(CuKα)		–		70	–	68	68	68			–	–	–		67
2V		69		67	67	68	68	67			66	68	71		67
Extinction angles											68		69*		
Orthopyroxene: mol. % Fs from:															
2V		26		27	27	27	28	27			28	30	29		30
Name of rock and remarks	Finge grained feldspathic pyroxenite		Hyperite, possibly the needle norite		Hyperite Base of so-called "porphyritic norite"	Hypersthene gabbro Large orthopyroxene crystals	Hypersthene gabbro Large orthopyroxene crystals	Hyperite Large orthopyroxene crystals	Hyperite Large orthopyroxene crystals	Hypersthene gabbro Large orthopyroxene crystals	Hypersthene gabbro Large orthopyroxene crystals	Hypersthene gabbro Top of "porphyritic norite"	Norite Banding	Hyperite	Hypersthene gabbro

APPENDIX I (Continued). MAIN ZONE, Subzone A

Sample Number	PB2276	PB2273	PB2127	PB2015	PB1702	PB1677	PB1651	PB1611	PB1572	PB1281	PB1101	PB942	PB837	PB801	PB717
Height in metre above M.R.	640	642	692	727	821	830	835	848	860	948	1005	1045	1080	1095	1115
Modal analysis															
Plagioclase	72.7*		62.4*	62.3*	69.8*	23.1*	63.8*	64.2*	74.8*	60.3*	68.7*	83.7*	34.8*	69.6*	62.9*
Orthopyroxene	22.7*		26.9*	24.2*	18.5*	31.1*	17.0*	9.4*	14.3*	21.7*	7.3	8.3*	35.1	21.3	30.1
Clinopyroxene	3.9		7.7	10.6	10.5*	42.8*	15.1*	24.9*	8.5*	16.7*	23.5*	6.4*	26.6*	7.9*	6.5*
Biotite	0.2		0.5	0.8	0.4	0.9	1.1	0.1	0.5	0.6	tr.	0.4	0.4	0.4	0.2
K-feldspar	–		–	0.2	–	tr.	0.3	–	0.5	0.1	–	–	–	–	–
Quartz	0.4		2.4	1.5	0.6	2.0	2.6	1.2	1.4	0.6	0.5	1.2	3.1	0.8	0.3
Apatite	tr.		tr.	–	0.1	tr.	–	–	–	–	–	–	–	–	–
Opaque	0.1		0.1	0.1	0.1	tr.	0.1	0.2	–	–	–	–	tr.	tr.	–
I.C. No.	65		43	40	58	72	45	65	52	57	60	54	51	60	52
Plagioclase: mol. % An from:															
$2\Theta_{131}-2\Theta_{\bar{1}31}$(CuK$\alpha$)	68	68		68*	67	67	67	67*	66	65		64*	64*		62
$2\Theta_{\bar{2}41}-2\Theta_{\bar{2}41}$(CuK$\alpha$)	–	–		68	68*	68	68	68	67	67		65	65		66
2V	73	71		69	70	67	66	66	68	66*		64	64		65
Extinction angles	70*										65*				64*
Orthopyroxene: mol. % Fs from:															
2V	29	29		32	33	32	32	33	33	30		34	30		33
Name of rock and remarks	Norite	Spotted norite Large orthopyroxene crystals	Hyperite	Hyperite	Feldspathic pyroxenite	Hyperite	Hypersthene gabbro	Hyperite Cumulus bronzite	Hyperite Cumulus bronzite	Hypersthene gabbro "Ophitic" orthopyroxene	Anorthositic hyperite Large ophitic orthopyroxene crystals	Feldspathic pyroxenite Large ophitic orthopyroxene crystals	Norite Large ophitic orthopyroxene crystals	Norite Large ophitic orthopyroxene

APPENDIX I (Continued). MAIN ZONE, Subzone B

Sample Number	G575	G576	G577	G578	G579	G580	G581	G582	G583	G501	G584	G585	G586	G587	G587X
Height in metre above M.R.	1465	1490	1515	1560	1580	1640	1680	1720	1740	1790	1880	1950	1960	1980	2010
Modal analysis (vol. %)															
Plagioclase	67.0*		77.8*	75.0*	61.6*	61.4*	65.4*	77.1*	70.3*	61.0*	61.6*	61.4*	59.7*	47.6*	65.2*
Orthopyroxene	13.6		9.9	8.1	13.1	19.5	13.7	8.7	13.0*	15.6	14.0*	12.5*	18.8*	13.6*	13.4*
Clinopyroxene	18.9*		11.9*	16.2*	24.3*	18.9*	20.1*	13.6*	16.2*	22.0*	21.9*	24.8*	19.7*	35.4*	20.4*
Biotite	tr.		—	—	0.1	—	—	tr.	0.2	0.2	0.6	0.4	0.6	0.2	0.2
K-feldspar	—		—	—	—	—	—	—	—	—	0.4	tr.	—	—	—
Quartz	0.4		0.4	0.7	0.9	0.2	0.8	0.6	0.3	1.2	1.5	0.8	1.2	0.5	0.8
Apatite	—		—	—	—	—	—	—	—	tr.	—	—	—	—	—
Opaque	tr.		—	—	—	tr.	—	—	—	tr.	—	0.1	—	—	—
I.C. No.	59		45	48	45	46	44	43	52	45	46	55	57	65	56
Plagioclase: mol. % An from:															
$2\theta_{131}-2\theta_{\bar{1}31}$ (CuKα)		63	62	62*	62	62				62*	60		61*	62*	
$2\theta_{\bar{2}41}-2\theta_{\bar{2}\bar{4}1}$ (CuKα)		65	64	—	65	64				64	63		64	64	
2V	63	67	64	63	63*	63*			63	62	61		60	62	
Extinction angles			63*	62		64			61		61*				
Orthopyroxene: mol. % Fs from															
2V	33	34	36	34	36	35			38	38	38		37	37	
Name of rock and remarks	Hypersthene gabbro. Inverted pigeonite and primary ophitic orthopyroxene Conspicuous bent plagioclase crystals		Hypersthene gabbro. Inverted pigeonite and primary ophitic orthopyroxene		Hypersthene gabbro. Inverted pigeonite and primary ophitic orthopyroxene	Hyperite. Inverted pigeonite and primary ophitic orthopyroxene			Hypersthene gabbro. Inverted pigeonite and primary ophitic orthopyroxene	Hypersthene gabbro. Inverted pigeonite and primary ophitic orthopyroxene		Hypersthene gabbro. Inverted pigeonite and granular ophitic orthopyroxene.	Hypersthene gabbro. Inverted pigeonite and granular ophitic orthopyroxene	Hypersthene gabbro. Inverted pigeonite and granular ophitic orthopyroxene	Hypersthene gabbro. Inverted pigeonite and granular ophitic orthopyroxene.

APPENDIX I (Continued). MAIN ZONE, Subzone B

Sample Number	G587A	G587B	G587C	G587D	G588	G589	G590	G591	G592	G593	G594	G595	G435	G488	G489
Height in metre above M.R.	2065	2100	2150	2215	2260	2290	2310	2335	2385	2430	2470	2510	2580	2675	2795
Modal analysis (vol. %)															
Plagioclase	59.0*	68.0*	61.5*	68.6*	59.1*	65.4*	68.6*	67.5*	68.2*	56.9*	67.3*	63.7*	77.9*	70.4*	59.6*
Orthopyroxene	17.9*	11.4*	15.7*	13.1*	14.3*	21.7*	22.8*	7.6*	20.5*	21.1*	7.4*	33.4*	8.6*	21.2*	16.8*
Clinopyroxene	23.1*	20.1*	21.7*	18.1*	26.4*	12.8*	7.7*	24.3*	11.3*	22.0*	25.3*	2.9	13.2*	7.3*	23.4*
Biotite	–	tr.	tr.	–	–	tr.	0.2	0.1	–	–	–	–	–	0.3	–
K-feldspar	–	–	tr.	–	–	–	–	–	–	–	–	–	–	–	–
Quartz	–	0.3	1.0	0.2	0.2	tr.	0.6	0.5	–	–	tr.	–	0.3	0.8	0.1
Apatite	–	–	–	–	–	–	–	tr.	–	–	–	–	–	–	–
Opaque	–	0.2	tr.	–	–	tr.	0.1	–	–	–	–	–	–	–	0.1
I.C. No.	74	55	46	57	48	54	49	52	59	48	56	43	46	58	45
Plagioclase: mol. % An from:															
$2\theta_{131}-2\theta_{\bar{1}31}$ (CuKα)	64*	62*	62*	62*	63*	62*		60*	60*	60*	59	58*	57	57*	57*
$2\theta_{\bar{2}41}-2\theta_{2\bar{4}1}$ (CuKα)	65	64	64	64	64	63		62	62	62	61	61	61	61	61
2V	64	61	61	61	61	60		60	60	60	60*	58	58	58	58
Extinction angles	63												58*	57	57
Orthopyroxene: mol. % Fs from															
2V	35	38	38	37	38	38		37	36	36	37	39	39	42	40
Name of rock and remarks	Hypersthene gabbro. Inverted pigeonite and granular ophitic orthopyroxene Conspicuous myrmekite	Hypersthene gabbro. Inverted pigeonite and granular ophitic orthopyroxene Conspicuous bent plagioclase	Hypersthene gabbro. Inverted pigeonite and granular ophitic orthopyroxene	Hypersthene gabbro. Inverted pigeonite and granular ophitic orthopyroxene Conspicuous myrmekite	Hypersthene gabbro. Inverted pigeonite and granular ophitic orthopyroxene Conspicuous bent plagioclase	Hyperite. Inverted pigeonite and granular ophitic orthopyroxene Conspicuous myrmekite and bent plagioclase		Gabbro. Inverted pigeonite and granular ophitic orthopyroxene	Hyperite. Inverted pigeonite only Conspicuous myrmekite	Hypersthene gabbro. Inverted pigeonite only Conspicuous myrmekite	Gabbro. Inverted pigeonite only Conspicuous myrmekite	Norite. Inverted pigeonite only Conspicuous myrmekite and bent plagioclase	Hypersthene gabbro Conspicuous myrmekite	Hyperite Conspicuous bent plagioclase	Hypersthene gabbro Conspicuous bent plagioclase

APPENDIX I (Continued). MAIN ZONE, Subzone B — Subzone C

Sample Number	G490	G512	G513	G514	G515	G517	G518	G426	G520	G522	G523	G524	G525	G526	G527
Height in metre above M.R.	3020	3170	3175	3185	3200	3220	3245	3250	3260	3270	3280	3295	3335	3350	3365
Modal analysis (vol. %)															
Plagioclase	59.3*	60.9*	60.8*	61.5*	61.4*	68.3*	60.5*	15.0*	65.5*	62.3*	69.7*	64.6*	62.1*	59.1*	58.8*
Orthopyroxene	21.0*	30.4*	33.4*	31.4*	24.9*	28.4*	25.7*	58.7*	28.6*	15.2*	5.8*	4.3*	10.8*	20.0*	18.9*
Clinopyroxene	19.6*	8.7*	5.9*	7.1*	13.7*	3.3	13.8*	26.3*	5.9*	22.4*	24.5*	30.9*	26.9*	20.9*	22.3*
Biotite	tr.	–	–	–	–	–	–	–	–	tr.	–	–	–	–	–
K-feldspar	–	–	–	–	–	–	–	–	–	–	–	–	–	–	–
Quartz	tr.	tr.	–	–	tr.	–	–	–	–	0.1	tr.	0.2	0.2	–	–
Opaque	–	–	–	–	–	–	–	–	–	–	–	–	–	–	–
I.C. No.	59	95	85	95	93	70	83	50	48	61	68	70	65	64	95
Plagioclase: mol. % An from:															
$2\theta_{131}-2\theta_{1\bar{3}1}$ (CuKα)		65*	64	64	62	61	64*	65	69*	68	68*	72	70*		72*
$2\theta_{\bar{2}41}-2\theta_{\bar{2}\bar{4}1}$ (CuKα)		68	67	65	65	64	66	–	68	68	68	71			71
2V	55	64		64		63*	65	65	71	69		69	70		72
Extinction angles	56*	65			64*	64	64					71*			
Orthopyroxene: mol. % Fs from:															
2V	44	33		32		33	32	27	28	31		31	31		27
Name of rock and remarks	Hyperite Conspicuous myrmekite and bent plagioclase	Fine-grained norite Conspicuous myrmekite	Fine-grained norite Conspicuous myrmekite	Fine-grained norite Conspicuous myrmekite	Fine-grained hyperite Conspicuous myrmekite	Fine-grained norite Conspicuous myrmekite	Fine-grained hyperite. Inverted pigeonite Conspicuous myrmekite	Feldspathic pyroxenite. Primary orthopyroxene Conspicuous bent plagioclase and orthopyroxene No myrmekite	Norite Conspicuous bent plagioclase and orthopyroxene	Hypersthene gabbro Conspicuous bent plagioclase	Gabbro Conspicuous bent plagioclase	Gabbro Conspicuous bent plagioclase	Hypersthene gabbro Conspicuous bent plagioclase	Hypersthene gabbro. Needles of clinopyroxene Large orthopyroxene crystals Conspicuous bent plagioclase Large orthopyroxene crystals	Hypersthene gabbro. Conspicuous bent plagioclase

APPENDIX I (Continued). MAIN ZONE, Subzone C

Sample Number	G528	G529	G530	G531	G532	G533	G535	G537	G538	G539	G540	G541	G542	G543	G597
Height in metre above M.R.	3380	3395	3410	3435	3445	3450	3475	3505	3535	3565	3585	3600	3620	3650	3715
Modal analysis (vol. %)															
Plagioclase	54.7*	44.2*	55.2*	61.8*	46.5*	79.4*	58.1*	49.1*	53.4*	58.9*	60.0*	81.7*	55.9*	62.7*	68.9*
Orthopyroxene	32.0*	32.6*	30.9*	33.1*	25.2*	6.2*	16.1*	14.8*	23.4*	17.4*	14.3*	12.7*	14.9*	12.1*	9.3
Clinopyroxene	13.2*	23.0*	13.7*	4.9*	28.3*	14.3*	25.8*	36.0*	23.1*	23.5*	24.4*	5.6	28.1*	25.2*	21.4*
Biotite	–	–	–	–	–	tr.	–	–	–	–	0.6	–	0.4	–	0.1
Quartz	0.1	0.2	0.2	0.2	–	tr.	–	0.1	0.1	0.2	0.7	–	0.5	–	0.2
Apatite	–	–	–	–	–	–	–	–	–	–	–	–	0.1	–	–
Opaque	–	–	–	–	–	–	–	–	–	–	tr.	–	0.1	–	0.1
I.C. No.	72	105	94	58	83	63	80	88	62	63	55	63	50	75	46
Plagioclase: mol. % An from:															
$2\Theta_{131}-2\Theta_{1\bar{3}1}$ (CuKα)		70*	72	70	72	72*	73*	72	70		72	69		72	64
$2\Theta_{\bar{2}41}-2\Theta_{\bar{2}\bar{4}1}$ (CuKα)		–	–	70	–	–	–	–	–		70*	–		–	65
2V		71		72		73	73	74		70		71		71	67
Extinction angles				71*					71		69	71*		71*	65*
Orthopyroxene: mol. % Fs from:															
2V		27		28		29	26	28		29		28			36
Name of rock and remarks	Hyperite Large orthopyroxene crystals	Hyperite Large orthopyroxene crystals. Fine-grained plagioclase and clinopyroxene	Hyperite Fine-grained plagioclase and clinopyroxene	Norite Conspicuous bent plagioclase	Hypersthene gabbro	Hypersthene gabbro	Hypersthene gabbro	Hypersthene gabbro	Hyperite	Hypersthene gabbro	Hypersthene gabbro Conspicuous bent plagioclase	Hyperite	Hypersthene gabbro	Hypersthene gabbro Primary orthopyroxene	Hypersthene gabbro. Inverted pigeonite and primary ophitic orthopyroxene Conspicuous bent plagioclase

APPENDIX I (Continued). MAIN ZONE, Subzone C — UPPER ZONE, Subzone A

Sample Number	G598	G412	G599	G600	G601	G602	G413	G603	G411	G605	G410	G607	G608	G609	G611
Height in metre above M.R.	3735	3760	3775	3785	3800	3820	3840	3855	3895	3905	3920	3935	3950	3965	3980
Modal analysis (vol. %)															
Plagioclase	60.8*	66.6*	58.2*	64.6*	56.5*	53.0*	56.0*	56.6*	56.3*	62.9*	72.1*	73.0*	88.9*	77.5*	38.7*
Orthopyroxene	14.8	13.6	4.3	6.3	20.9	21.4	15.8	19.3	16.9	18.9*	26.5*	19.6*	–	18.7*	28.0*
Clinopyroxene	24.4*	19.7*	37.5*	29.0*	22.4*	25.4*	28.2*	24.1*	26.5*	18.2*	1.4	7.2	10.9	3.3	31.0*
Biotite	–	–	–	–	–	–	–	–	–	–	–	–	–	–	–
Quartz	–	0.1	–	0.1	0.1	0.1	–	–	0.2	–	–	–	–	–	–
Apatite	–	–	–	–	–	—	–	–	tr.	–	–	–	–	–	–
Opaque	–	–	–	–	0.1	0.1	–	–	tr.	–	–	0.2	0.2	0.5	2.3*
I.C. No.	64	60	53	63	56	52	57	54	52	53	62	46	48	40	67
Plagioclase: mol. % An from:															
$2\theta_{131}-2\theta_{1\bar{3}1}$ (CuKα)	64*			61		60		60*	60*	60	60*		59	56*	
$2\theta_{\bar{2}41}-2\theta_{\bar{2}\bar{4}1}$ (CuKα)	65			63		62		62	62	62	61		61	58	
2V	64			64		63		60	61	60			60*	57	
Extinction angles				62*		62*								55	
Orthopyroxene: mol. % Fs from:															
2V	33			36		37		37	37	38	37			41	
Name of rock and remarks	Hypersthene gabbro			Norite Conspicuous myrmekite and bent plagioclase					Mottled anorthosite Conspicuous myrmekite		Norite. Inverted pigeonite only		Hyperite Conspicuous myrmekite and bent plagioclase		Hyperite. Inverted pigeonite only Conspicuous myrmekite
	Hypersthene gabbro. Inverted pigeonite and primary ophitic orthopyroxene Conspicuous bent plagioclase			Hypersthene gabbro Primary ophitic orthopyroxene Conspicuous bent plagioclase					Hypersthene gabbro. Inverted pigeonite and primary ophitic orthopyroxene. Conspicuous bent plagioclase		Hypersthene gabbro. Inverted pigeonite and primary ophitic orthopyroxene Conspicuous bent plagioclase		Gabbro. Inverted pigeonite and primary ophitic orthopyroxene Conspicuous bent plagioclase		Gabbro. Inverted pigeonite and primary ophitic orthopyroxene Conspicuous bent plagioclase
	Hypersthene gabbro Primary ophitic orthopyroxene			Gabbro. Inverted pigeonite and primary ophitic orthopyroxene Conspicuous bent plagioclase					Gabbro. Inverted pigeonite and primary ophitic orthopyroxene Conspicuous bent plagioclase		Hypersthene gabbro Primary ophitic orthopyroxene Conspicuous bent plagioclase		Hypersthene gabbro. Inverted pigeonite and primary ophitic orthopyroxene Conspicuous bent plagioclase		Hypersthene gabbro. Inverted pigeonite and primary ophitic orthopyroxene Conspicuous bent plagioclase

APPENDIX I (Continued). UPPER ZONE, Subzone A — Subzone B

Sample Number	G561	G415	G407	G612	G406	G400	G509	G510	G396	G649	G651	G568	G566	G569	G422
Height in metre above M.R.	3990	4005	4030	4050	4070	4083	4087	4110	4175	4200	4205	4275	4286	4290	4375
Modal analysis (vol. %)															
Plagioclase	60.5*	57.5*	65.9*	59.6*	55.4*	88.9*	82.8*	91.4	75.6*	27.5*	34.7*	79.5*	76.7*	59.8*	55.1*
Orthopyroxene	25.6*	14.4*	24.9*	31.7*	30.9*	–	3.9	1.3	4.7*	21.1*	19.2*	5.5*	3.1	6.7*	15.7*
Clinopyroxene	12.8*	17.0*	7.7*	6.3*	13.6*	2.2	0.4	0.9	8.8*	51.1*	41.1*	4.4	10.3*	23.2*	20.4*
Biotite	–	0.6	0.2	–	–	1.3	0.9	1.2	1.1	–	1.2	3.7	0.3	0.8	0.8
K-feldspar	–	–	–	–	–	–	–	–	–	–	–	0.7	–	–	–
Quartz	–	–	–	–	–	0.2	–	0.4	–	–	–	1.5	–	–	0.1
Apatite	–	–	–	–	–	–	–	–	–	–	–	–	–	0.1	–
Opaque	1.1	10.5*	1.3	2.4	0.1	7.4*	12.0*	4.8	9.8*	0.3	3.8	4.7*	9.6*	9.4	7.9*
I.C. No.	41	280	45	43	48	45	40	41	44	55	42	36	55	45	43
Plagioclase: mol. % An from:															
$2\theta_{131}-2\theta_{1\bar{3}1}$ (CuKα)			58	58	57	57	57	57				57	58	57*	57*
$2\theta_{\bar{2}41}-2\theta_{\bar{2}\bar{4}1}$ (CuKα)			60	60	59	59	59	58				59	59	59	59
Eulerian angles I					58			57*	56*	59		57		56	56
Extinction angles	56		59*		58*			57	56	59		58*		56	56
2V			60	60	60	59	58	58				58	59	59	57
Orthopyroxene: mol. % Fs from:															
2V			43	42	43		44						44	42	45
nz													42	42	
Name of rock and remarks	Hyperite Conspicuous myrmekite and bent plagioclase	Very fine-grained hypersthene gabbro	Norite Conspicuous myrmekite	Norite Conspicuous bent plagioclase	Hyperite Conspicuous bent plagioclase	Magnetite anorthosite Conspicuous bent plagioclase	Magnetite anorthosite First symplektite	Magnetite anorthosite Conspicuous bent plagioclase	Magnetite hypersthene gabbro Symplektite present	Feldspathic pyroxenite Inverted pigeonite	Hypersthene gabbro	Magnetite hyperite Conspicuous bent plagioclase	Magnetite gabbro Symplektite present	Magnetite gabbro Conspicuous bent plagioclase Symplektite present	Magnetite hypersthene gabbro

APPENDIX I (Continued). UPPER ZONE, Subzone C

Sample Number	G658	G365	G351	G613	G614	G314	G617	G618	G619	G312	G620	G621	G622	G310	G623
Height in metre above M.R.	4530	4625	4637	4660	4685	4760	4804	4812	4824	4825	4828	4849	4855	4865	4875
Modal analysis (vol.%)															
Plagioclase	60.2*	49.4*	48.0*	63.0*	64.1*	52.7*	87.2*	89.7*	56.9*	57.1*	89.1*	53.7*	56.9*	70.5*	52.6*
Olivine	12.2*	6.4*	4.7*	22.0*	25.9*	3.0*	–	–	–	0.2	–	2.2*	–	12.7*	–
Orthopyroxene	2.8	6.0*	5.3*	–	0.3	32.5*	–	–	33.7*	7.5*	0.2	10.8*	13.9*	4.7	7.9*
Clinopyroxene	15.9*	31.8*	33.2*	0.9	0.9	2.7	–	3.7	3.4	23.3*	0.6	18.0*	20.3*	1.9	30.9*
Biotite	0.9	–	–	0.4	1.4	0.2	3.0	1.5	0.6	0.2	3.6	7.4	0.4	2.8	0.9
K-feldspar	–	–	–	–	–	–	0.2	0.1	–	–	0.3	–	–	–	–
Quartz	–	–	–	–	–	–	3.6	0.1	–	–	1.3	–	–	–	–
Apatite	–	–	–	–	–	–	tr.	0.2	tr.	–	0.2	–	–	–	–
Opaque	8.0*	6.4*	8.8*	13.7*	7.4*	8.9*	6.0*	4.7*	5.4*	11.7*	4.7*	7.9*	8.5*	7.4*	7.7*
I.C. No.	45	69	75	36	53	103	52	43	68	52	38	55	70	47	71
Plagioclase: mol. % An from:															
Eulerian angles I	55	53			54	56	56		56			55			55
Extinction angles	55	54	53		55*	56	56		55			55			55
2V				54	57										
Orthopyroxene: mol. % Fs from:															
2V		44	44			42			46						
nz						41			46				46		
Olivine: mol. % Fa from:															
2V		53		45	50									53	
d_{174}		49		51	52									54	
Name of rock and remarks	Magnetite olivine gabbro Conspicuous symplektite	Magnetite olivine hyperite	Magnetite olivine hypersthene gabbro Clusters of large plagioclase crystals	Magnetite troctolite, Sisal Marker	Magnetite troctolite, Sisal Marker Symplektite present	Magnetite olivine norite Fine-grained	Magnetite anorthosite Conspicuous bent plagioclase	Magnetite anorthosite	Magnetite norite	Magnetite gabbro Symplektite present	Magnetite anorthosite Conspicuous bent plagioclase	Magnetite olivine hypersthene gabbro Conspicuous symplektite	Magnetite hypersthene gabbro Symplektite present	Magnetite Troctolite Conspicuous symplektite	Magnetite gabbro Symplektite present

APPENDIX I (Continued). UPPER ZONE, Subzone C — Subzone D

Sample Number	G309	G624	G307	G625	G626	G630	G642	G641	G271	G640	G639	G636	G635	G279	G634
Height in metre above M.R.	4924	4949	4975	5015	5104	5125	5180	5270	5350	5370	5415	5455	5490	5510	5540
Modal analysis (vol. %)															
Plagioclase	49.3*	53.3*	47.2*	41.6*	65.0*	54.5*	55.8*	55.0*	53.3*	45.8*	63.0*	84.1*	63.9*	52.4*	47.0*
Olivine	–	–	tr.	–	–	–	–	21.2*	16.4*	28.6*	14.7*	–	–	13.4*	18.8*
Orthopyroxene	1.8*	11.9*	6.2*	34.3*	19.0*	5.8*	11.2*	–	–	–	–	–	–	–	tr.
Clinopyroxene	41.1*	27.2*	32.2*	22.2*	5.8*	31.9*	24.7*	13.2*	16.7*	15.0*	11.2*	0.7	28.9*	25.2*	19.0*
Biotite	1.9	0.8	1.1	0.4	0.2	0.4	1.4	tr.	–	tr.	–	0.1	0.7	0.1	0.9
K-feldspar	–	–	–	–	–	0.4	–	–	–	–	–	–	–	–	–
Quartz	0.2	–	–	–	0.1	–	–	–	–	–	–	–	–	–	–
Apatite	–	–	–	–	–	–	–	3.9*	4.4*	4.3*	4.3*	–	tr.	–	6.2*
Opaque	5.7*	6.7*	13.3*	1.5	9.9*	7.0*	6.9*	6.7*	9.2*	6.3*	6.8*	15.1*	6.5*	8.9*	8.1*
I.C. No.	58	61	80	85	45	53	50	45	52	58	74	40	42	73	70
Plagioclase: mol. % An from:															
Eulerian angles I	53		53	54	55	50	51	46		45	46	45	46	45	44
Extinction angles	54		54	56	54	50		47		45	46	46	46	44	45
Orthopyroxene mol. % Fs from:															
2V	38														
nz	39	46		45	49		50								
Olivine: mol. % Fa from															
2V								69		71	70			69	69
d_{174}								69		70	70			70	69
Name of rock and remarks	Magnetite gabbro	Magnetite hypersthene gabbro Symplektite present	Magnetite gabbro	Magnetite hyperite	Magnetite hyperite Conspicuous bent plagioclase Symplektite present	Magnetite gabbro Bent plagioclase Symplektite present	Magnetite hypersthene gabbro	Magnetite olivine diorite Conspicuous symplektite First cumulus apatite	Magnetite olivine diorite Conspicuous symplektite	Magnetite olivine diorite Conspicuous symplektite	Magnetite olivine diorite Conspicuous symplektite	Magnetite anorthosite Conspicuous symplektite	Magnetite gabbro Conspicuous symplektite	Magnetite olivine diorite Conspicuous symplektite Ovicular diorite	Magnetite olivine diorite Symplektite present Ovicular diorite

APPENDIX I (Continued) UPPER ZONE, Subzone D

Sample Number	G633	G632	G631	G263	G257	G242	G276	G277	G228	G247	G505	G231	G252	G253	G368
Height in metre above M.R.	5560	5605	5670	5715	5735	5795	5804	5810	5835	5850	5870	5890	5950	5960	5990
Modal analysis (vol. %)															
Plagioclase	47.9*	50.7*	53.8*	74.9*	53.0*	69.4*	77.9*	85.2*	84.8*	57.0*	65.0*	79.0*	52.5*	41.2*	49.0*
Olivine	22.1*	20.6*	16.3*	–	16.2*	12.2*	17.2*	1.5	1.3	–	5.7*	–	–	24.9*	16.0*
Orthopyroxene	–	–	–	–	–	–	–	–	–	1.3	2.9	–	6.0	8.8	4.1
Clinopyroxene	12.2*	13.9*	14.6*	13.3*	20.2*	14.0*	0.9	1.2	1.0	34.5*	18.6*	–	29.6*	0.6	13.2
Hornblende	–	–	–	–	–	–	–	–	–	–	–	1.9	0.8	tr.	–
Biotite	0.7	–	–	–	0.4	–	0.6	1.0	1.1	tr.	–	7.2	3.1	5.9	5.5
K-feldspar	–	–	–	–	–	–	–	–	–	–	–	0.3	0.3	–	–
Quartz	–	–	–	–	–	–	–	0.1	0.4	0.1	0.1	5.0	1.0	–	0.2
Apatite	6.7*	5.6*	5.5*	–	3.3*	–	tr.	0.1	–	–	tr.	0.4	0.2	8.5*	3.6*
Opaque	10.4*	9.2*	9.8*	11.8*	6.9*	4.4*	3.4*	10.9*	11.4*	7.1*	7.7*	6.2*	6 5*	10.1*	8.4*
I.C. No.	74	73	71	53	60	97	60	65	75	71	61	37	54	56	72
Plagioclase: mol. % An from:															
Eulerian angles I	44	46	45	43		43	42		44	46		50	50	51	49
Extinction angles	46	45	45	43		43	43		44	46		48	50	52	49
Orthopyroxene: mol. % Fs from:															
2V														56	62
nz													53		
Olivine: mol. % Fa from:															
2V	68	71	71			78	74							78	89
d_{174}		69	69			73	73							70	79
Name of rocks and remarks	Magnetite olivine diorite Symplektite present	Magnetite olivine diorite Symplektite present	Magnetite olivine diorite Symplektite present	Magnetite diorite	Magnetite olivine diorite	Magnetite olivine diorite	Magnetite troctolite Conspicuous symplektite	Magnetite anorthosite Intercumulus olivine	Magnetite anorthosite	Magnetite diorite	Magnetite olivine diorite	Magnetite anorthosite	Magnetite diorite	Magnetite olivine diorite	Magnetite olivine diorite

APPENDIX I (Continued). UPPER ZONE, Subzone D

Sample Number	G285	G208	G216	G215	G201	G200
Height in metre above M.R.	6075	6140	6165	6180	6207	6209
Modal analysis (vol. %)						
Plagioclase	56.0*	51.8*	59.4*	49.7	58.1	45.5
Olivine	9.0*	0.4*	2.6*	–	–	–
Orthopyroxene	–	–	–	–	–	–
Clinopyroxene	11.5	9.6	4.8	21.7	7.6	7.7
Hornblende	12.0	24.4	17.1	16.9	12.6	19.9
Biotite	2.3	1.0	2.5	–	–	–
K-feldspar	0.9	0.6	1.8	1.5	6.1	12.5
Quartz	2.1	2.1	3.4	4.9	10.6	12.2
Apatite	2.7*	2.7*	2.2*	1.4	0.3	0.5
Opaque	3.5*	7.4*	6.2*	3.9	4.6	1.7
I.C. No.	76	65	56	65	86	70
Plagioclase: mol.% An from:						
Eulerian angles I	42	45		45		
Extinction angles	43	47		45		
Olivine: mol. % Fa from:						
2V	89					
Name of rock and remarks	Magnetite olivine diorite	Magnetite olivine diorite	Magnetite olivine diorite Partially altered	Diorite Partially altered	Diorite Rock is altered	Diorite Rock is altered

APPENDIX II

Tables of chemical analyses, CIPW norms recalculated to hundred (A), Differentiation Index (DI), Crystallization Index (CI), recalculated norms (B) for the Modified Crystallization Index (MCI) and Modified Differentiation Index (MDI), as well as the names and localities of the samples, and the sources of the chemical analyses.

APPENDIX II. UPPER ZONE

	M55		M282		M281		M280		M279		M278		M51		M276		M274		M272		M63		M269		M268	
SiO_2	52,42		46,16		39,07		37,41		46,29		44,22		45,97		58,62		41,79		45,99		55,40		44,02		45,61	
TiO_2	1,38		2,25		3,29		2,83		2,05		2,36		3,04		0,29		2,49		2,64		0,14		2,80		2,43	
Al_2O_3	13,13		15,34		12,30		11,94		18,30		17,15		16,63		24,14		16,43		13,87		24,37		16,34		14,29	
Fe_2O_3	7,11		2,65		2,70		2,43		3,42		3,13		5,23		0,58		2,61		4,20		0,24		5,80		6,16	
FeO	12,16		17,33		24,51		26,10		13,41		16,27		11,09		1,85		17,59		14,80		1,77		12,01		12,21	
MnO	0,38		0,30		0,36		0,36		0,19		0,21		0,18		0,03		0,24		0,24		0,03		0,18		0,21	
MgO	0,27		2,59		4,13		5,40		3,54		5,35		3,48		0,27		3,94		5,84		0,66		5,35		6,55	
CaO	7,41		7,41		7,52		7,08		7,02		7,73		9,48		7,73		8,48		9,24		10,07		9,48		9,00	
Na_2O	3,14		2,84		2,35		2,32		3,30		3,10		3,24		4,71		3,04		2,13		4,48		2,28		2,13	
K_2O	0,93		0,93		0,59		0,62		0,66		0,33		0,40		0,79		0,33		0,23		0,89		0,17		0,07	
P_2O_5	0,26		0,98		1,85		2,15		0,30		1,64		0,03		0,20		1,71		0,03		0,01		0,00		0,02	
H_2O	1,70		1,19		0,89		1,12		1,12		0,85		0,76		1,06		0,96		0,94		1,94		1,47		1,21	
CO_2	0,10		0,10		0,12		0,11		0,05		0,04		0,06		0,02		0,06		0,04		0,14		0,23		0,16	
	100,39		100,07		99,77		99,87		99,65		100,38		99,59		100,29		99,67		100,19		100,14		100,13		100,05	
	A	B	A	B	A	B	A	B	A	B	A	B	A	B	A	B	A	B	A	B	A	B	A	B	A	B
Qz	11,89	13,78	–	–	–	–	–	–	–	–	–	–	–	–	10,71	10,91	–	–	–	–	3,51	3,53	–	–	1,05	1,22
Or	5,57	6,46	5,55	6,20	3,50	4,11	3,69	4,29	3,96	4,39	1,95	2,24	2,39	2,78	4,71	4,80	1,97	2,26	1,37	1,54	5,39	5,34	1,02	1,19	0,41	0,48
Ab	26,93	31,22	24,27	27,13	20,05	23,55	16,54	19,26	28,34	31,39	26,28	30,18	27,74	32,10	40,13	40,90	25,98	29,75	18,15	20,45	38,63	38,89	99,59	22,76	18,25	21,17
An	19,25	22,31	26,65	29,79	21,43	25,19	20,54	23,92	33,55	37,16	28,76	33,03	30,03	34,75	37,44	38,16	30,53	34,97	27,83	31,36	44,63	44,92	34,39	39,96	29,63	34,36
C or Ne							Ne 0,78	2,07			C 1,18	1,36			C1,94	1,98										
Di Wo	6,87	7,96	1,95	2,18	2,17	2,55	0,90	1,05	–	–	–	–	7,27	8,41	–	–	0,76	0,87	7,59	8,55	2,61	2,63	5,59	6,49	6,47	7,50
Di En	0,33	0,38	0,41	0,46	0,49	0,58	0,23	0,27	–	–	–	–	3,13	3,62	–	–	0,21	0,24	3,23	3,64	0,97	0,98	2,77	3,22	3,41	3,95
Di Fs	7,37	8,54	1,68	1,88	1,82	2,14	0,72	0,84	–	–	–	–	4,12	4,77	–	–	0,58	0,66	4,38	4,94	1,69	1,70	2,70	3,14	2,87	3,33
Hy En	0,34	0,40	4,31	4,82	0,51	0,60	–		4,41	4,88	1,62	1,86	3,48	4,03	0,68	0,69	0,29	0,33	10,11	11,39	0,71	0,71	8,38	9,74	13,11	15,21
Hy Fs	7,72	8,95	17,66	19,74	1,92	2,26	–		9,37	10,38	2,90	3,33	4,56	5,28	2,51	2,56	0,80	0,92	13,76	15,51	1,24	1,25	8,16	9,48	11,02	12,78
Ol Fo			1,26	1,41	6,56	7,70	9,35	10,89	3,19	3,53	8,22	9,44	1,51	1,75	–	–	6,59	7,55	0,93	1,05	–		1,67	1,94	–	
Ol Fa			5,72	6,39	26,67	31,32	32,13	37,41	7,47	8,27	16,16	18,56	2,19	2,53	–	–	19,60	22,45	1,39	1,57	–		1,79	2,08	–	
Mt	10,45		3,88		4,09		3,55		5,04		4,55		7,67		0,85		3,82		6,14		0,36		8,54		9,05	
Ilm	2,66		4,31		6,35		5,43		3,95		4,49		5,84		0,56		4,78		5,05		0,28		5,40		4,68	
Hm																										
Ap	0,62		2,35		4,42		5,14		0,72		3,89		0,07		0,47		4,09		0,07		0,02		–		0,05	
H_2O																										
DI	44,39		29,82		23,55		22,01		32,30		28,23		30,13		55,55		27,95		19,52		47,49		20,61		19,71	
CI	19,87		31,43		29,20		30,05		39,38		38,14		40,44		37,87		37,43		42,38		46,30		47,07		45,60	
MDI		76,47		63,00		65,26		64,61		54,43		54,31		51,66		59,17		56,62		48,36		52,26		41,41		41,91
MCI		16,49		26,36		26,65		28,06		32,99		33,89		34,40		27,23		32,65		36,51		33,43		41,64		40,71

APPENDIX II (Continued) UPPER ZONE

		M465		M48		M47		M46		M255		M253		M45		M44		M43		M3		M37		M40		M288	
SiO_2		51,30		43,81		50,63		39,40		47,19		43,74		45,83		49,14		52,20		48,02		51,79		45,23		41,29	
TiO_2		0,86		1,94		0,26		2,20		1,41		2,16		1,84		1,09		0,08		0,37		0,44		0,37		3,18	
Al_2O_3		22,55		18,37		22,29		15,08		17,52		19,42		8,44		18,60		18,97		25,70		16,86		20,50		18,01	
Fe_2O_3		0,88		4,00		0,51		2,66		3,64		7,54		4,56		2,25		0,62		1,94		1,19		1,33		8,42	
FeO		5,66		14,98		5,78		23,50		11,84		10,77		16,03		9,01		7,07		3,93		9,46		12,23		12,68	
MnO		0,10		0,18		0,10		0,27		0,19		0,16		0,31		0,15		0,18		0,06		0,20		0,16		0,15	
MgO		1,69		6,42		3,94		9,41		6,55		4,56		10,80		4,83		8,97		0,78		7,95		8,45		6,58	
CaO		7,53		6,40		9,17		4,83		8,21		8,42		9,55		9,87		9,00		11,53		9,00		8,35		6,58	
Na_2O		4,18		2,71		3,14		1,88		2,18		2,45		1,03		3,04		2,18		3,60		2,23		2,23		2,58	
K_2O		1,62		0,30		0,96		0,10		0,17		0,17		0,30		0,50		0,21		0,53		0,17		0,27		0,14	
P_2O_5		0,18		0,03		0,01		0,02		0,01		0,01		0,01		0,03		0,00		0,01		0,01		0,02		0,01	
H_2O		3,12		0,95		2,48		0,92		0,93		0,92		1,29		1,50		0,84		2,76		0,80		1,00		0,87	
CO_2		0,28		0,07		0,35		0,01		0,10		0,09		0,11		0,16		0,07		0,12		0,09		0,05		0,08	
		99,95		100,16		99,62		100,28		99,94		100,41		100,10		100,17		100,39		100,12		100,19		100,19		99,83	
		A	B	A	B	A	B	A	B	A	B	A	B	A	B	A	B	A	B	A	B	A	B	A	B	A	B
	Qz	–	–	–	–	–	–	–	–	–	–	–	–	–	–	–	–	1,04	1,05	–	–	1,76	1,81	–	–	–	–
	Or	9,91	10,27	1,79	1,98	5,86	5,94	0,59	0,64	1,01	1,10	1,01	1,19	1,79	2,00	2,99	3,16	1,25	1,26	3,25	3,37	1,01	1,04	1,61	1,65	0,84	1,03
	Ab	36,60	37,91	23,12	25,58	27,43	27,79	16,00	17,42	18,64	20,27	20,85	24,57	8,82	9,83	26,10	27,61	18,53	18,73	29,66	30,79	18,99	19,50	19,02	19,55	22,06	27,06
	An	37,57	38,93	31,85	35,24	45,35	45,94	24,00	26,12	37,93	41,26	41,74	49,19	17,75	19,78	36,17	38,27	41,57	42,01	54,33	56,39	35,75	36,71	41,65	42,80	32,94	40,41
	C	0,64	0,66	2,04	2,25			,3,16	3,44											Ne1,03	1,07			1,42	1,46	1,70	2,09
Di	Wo	–	–	–	–	0,66	0,67	–		1,32	1,44	0,09	0,11	12,60	14,04	5,57	5,89	1,38	1,40	2,04	2,12	3,82	3,92	–	–	–	–
	En	–	–	–	–	0,32	0,32	–		0,65	0,71	0,05	0,06	6,57	7,32	2,63	2,78	0,83	0,84	0,59	0,61	2,04	2,09	–	–	–	–
	Fs	–	–	–	–	0,33	0,33	–		0,66	0,72	0,04	0,05	5,67	6,32	2,87	3,04	0,47	0,47	1,54	1,60	1,65	1,69	–	–	–	–
Hy	En	2,68	2,78	6,09	6,74	7,90	8,00	3,29	3,58	15,08	16,40	10,20	12,02	16,67	18,58	6,14	6,50	21,62	21,85	–	–	17,88	18,36	4,44	4,56	10,08	12,37
	Fs	5,35	5,54	8,13	8,99	8,02	8,13	5,30	5,77	15,50	16,86	9,24	10,89	14,39	16,04	6,72	7,11	12,26	12,39	–	–	14,49	14,88	4,44	4,56	7,87	9,65
Ol	Fo	1,18	1,22	7,03	7,78	1,34	1,36	14,22	15,48	0,53	0,58	0,82	0,97	2,81	3,13	2,42	2,56	–		1,00	1,04	–		11,76	12,09	3,24	3,97
	Fa	2,60	2,69	10,34	11,44	1,50	1,52	25,31	27,55	0,61	0,66	0,81	0,95	2,66	2,96	2,91	3,08	–		2,90	3,01	–		12,97	13,33	2,79	3,42
	Mt	1,33		5,85		0,76		3,88		5,34		11,00		6,70		3,31		0,90		2,91		1,74		1,94		12,35	
	Ilm	1,69		3,69		0,51		4,21		2,71		4,13		3,55		2,10		0,15		0,73		0,85		0,70		6,11	
	Hm																										
	Ap	0,45		0,07		0,02		0,04		0,02		0,02		0,02		0,07		–		0,02		0,02		0,05		0,02	
	H_2O																										
DI		46,51		24,91		33,29		16,59		19,65		21,86		10,61		27,09		20,82		32,91		21,76		20,63		22,90	
CI		39,53		43,43		51,60		41,14		49,95		49,35		45,82		47,82		58,03		55,00		52,25		56,52		43,62	
MDI			56,41		47,99		44,00		51,38		40,24		37,69		42,71		46,68		34,31		40,18		40,41		39,09		41,16
MCI			30,45		37,20		39,64		36,28		42,06		43,95		41,08		38,14		46,02		41,48		41,75		45,28		40,95

APPENDIX II (Continued). UPPER ZONE

		M291		M308		1		2		3		4		5		6		7		8		9		10	
SiO_2		43,56		51,31		46,60		48,00		51,50		49,30		53,2		45,26		46,83		47,14		50,45		53.60	
TiO_2		2,65		0,67		2,52		2,26		1,41		1,80		1,91		1,70		2,50		2,90		0,10		0,22	
Al_2O_3		16,98		27,14		17,52		13,00		14,64		13,87		12,53		13,42		15,55		21,50		27,40		23,87	
Fe_2O_3		9,44		2,98		4,93		3,03		3,22		2,38		3,29		4,63		5,26		7,96		1,10		1,80	
FeO		9,97		2,28		16,25		16,20		12,85		16,78		14,17		18,35		11,90		5,71		1,55		1,54	
MnO		0,16		0,04		0,21		0,26		0,30		0,43		0,12		0,39		0,30		0,05		0,20		0,05	
MgO		4,89		0,27		5,86		2,88		1,49		1,77		1,08		4,19		3,29		0,30		0,15		3,37	
CaO		8,01		10,12		7,10		7,14		6,40		7,49		6,58		8,50		10,01		8,46		12,90		11,29	
Na_2O		2,36		3,84		2,80		3,18		3,23		3,52		2,73		2,97		3,41		4,30		3,85		4,22	
K_2O		0,23		0,40		0,33		1,23		1,80		1,17		2,37		0,25		0,40		0,50		0,50		0,25	
P_2O_5		0,00		0,01		0,08		1,06		0,34		0,45		0,16						0,07		0,05		0,03	
H_2O		1,39		0,96		0,44		2,05		2,40		1,33		1,68		0,79		0,73		0,85		2,65		0,48	
CO_2		0,15		0,13																					
		99,79		100,15		99,64		100,29		99,58		100,29		99,82		100,45		100,18		99,74		100,90		100,72	
		A	B	A	B	A	B	A	B	A	B	A	B	A	B	A	B	A	B	A	B	A	B	A	B
	Qz	2,65	3,27	5,14	5,45	–	–	–	–	4,18	4,68	–		7,25	8,11	–	–	– –	–	2,83	3,43	–	–	0.81	0,84
	Or	1,38	1,70	2,38	2,52	1,84	2,11	7,36	8,49	10,61	11,87	7,09	7,83	13,77	15,39	1,38	1,55	2,21	2,54	2,79	3,39	2,79	2,92	1,38	1,43
	Ab	20,32	25,10	32,79	34,76	23,57	27,00	26,92	31,05	27,54	30,82	29,69	32,80	23,27	26,02	24,90	27,88	28,80	33,13	36,24	46,96	30,91	32,35	35,55	36,88
	An	35,69	44,09	50,61	53,63	34,57	39,61	17,46	20,14	20,14	22,54	18,60	20,55	15,11	16,89	22,44	25,12	25,91	29,80	38,18	46,32	56,26	58,87	45,07	46,76
	C or Ne			C2,04	2,16																				
Di	Wo	1,98	2,45	–	–	0,02	0,02	4,50	5,19	3,99	4,47	6,61	7,30	7,03	7,86	8,21	9,19	9,82	11,30	1,69	2,05	2,32	2,43	4,27	4,43
Di	En	1,22	1,51	–	–	0,01	0,01	1,10	1,27	0,69	0,77	0,10	0,11	0,89	0,99	2,32	2,60	3,65	4,20	0,70	0,85	0,35	0,37	3,37	3,50
Di	Fs	0,64	0,79	–	–	0,01	0,01	3,67	4,23	3,62	4,05	6,18	6,83	6,82	7,62	6,27	7,02	6,36	7,32	–	–	2,18	2,28	0,41	0,43
Hy	En	11,17	13,80	0,68	0,72	–	–	5,60	6,46	3,01	3,37	2,34	2,59	1,77	1,98	1,73	1,94	1,40	1,61	–	–	–	–	4,92	5.10
Hy	Fs	5,90	7,29	0,70	0,74	–	–	18,76	21,64	15,57	17,43	14,17	15,65	13,54	15,14	4,64	5,19	2,43	2,79	–	–	–	–	0,61	0,63
Ol	Fo	–	–	–	–	10,20	11,69	0,28	0,32	–	–	0,75	0,83	–	–	4,39	4,91	2,18	2,51	–	–				
Ol	Fa	–	–	–	–	17,06	19,55	1,05	1,21	–	–	4,99	5,51	–	–	13,04	14,60	4,17	4,80	–	–				
	Mt	13,93		4,36		7,22		4,39		4,71		3,45		4,86		6,71		7,64		10,00		1,62		2,54	
	Ilm	5,12		1,28		4,79		4,33		2,76		3,52		3,67		3,18		4,70		5,48		0,16		0,49	
	Hm																			1,12					
	Ap	–		0,02		0,27		2,54		0,77		1,17		0,34		–		–		–				0.10	
	H_2O					0,44		2,04		2,41		1,34		1,68		0,79		0,73		0,97		2,66		0,48	
DI		24,35		40,31		25,41		34,28		42,33		37,78		44,29		35,28		31,01		41,86		33,70		37,74	
CI		45,51		51,08		44,79		24,03		23,74		21,25		18,27		33,04		36,94		39,69		57,01		55,79	
MDI			38,85		43,47		48,68		70,34		72,41		74,64		78,99		62,42		57,02		50,78		39,56		40,59
MCI			42,85		38,10		39,46		20,89		19,32		17,21		14,73		27,81		30,87		33,75		41,82		41,64

APPENDIX II (Continued). MAIN ZONE

		M306		M305		M303		M299		M296		M294		M226		M224		M221		M219		M216		M213		M94	
SiO_2		50,71		51,60		52,37		50,99		51,34		53,02		51,96		52,40		52,71		52,31		52,28		52,36		52,53	
TiO_2		0,15		0,17		0,21		0,21		0,20		0,23		0,67		0,42		0,13		0,13		0,15		0,07		0,08	
Al_2O_3		15,61		18,73		17,38		17,87		18,60		3,63		17,51		18,50		18,77		18,42		16,79		18,99		25,25	
Fe_2O_3		0,95		0,55		0,72		0,60		0,63		0,84		0,39		0,49		0,86		0,62		0,45		1,12		0,38	
FeO		8,79		6,22		6,67		5,30		5,74		13,38		6,58		5,75		5,72		6,43		6,88		6,07		2,55	
MnO		0,21		0,15		0,17		0,14		0,14		0,31		0,17		0,15		0,16		0,17		0,18		0,15		0,06	
MgO		9,70		6,93		8,46		9,36		9,04		21,72		7,57		7,17		6,85		7,71		8,62		7,17		1,55	
CaO		10,07		11,39		10,90		12,37		11,39		5,36		11,39		12,05		11,31		10,72		11,62		9,76		10,35	
Na_2O		2,08		2,53		2,38		1,98		2,04		0,60		2,46		2,57		2,88		2,71		2,49		3,03		4,01	
K_2O		1,26		0,24		0,22		0,31		0,22		0,07		0,22		0,18		0,24		0,31		0,18		0,22		0,31	
P_2O_5		–		0,01		0,02		0,02		0,02		–		0,01		–		–		0,01		0,01		0,01		0,01	
H_2O		0,83		0,97		0,84		1,17		0,85		1,18		0,90		0,65		0,80		0,73		0,73		0,77		2,28	
CO_2		0,10		0,10		0,05		0,16		0,10		0,14		0,15		0,07		0,07		0,08		0,09		0,11		0,66	
		100,46		99,59		100,39		100,48		100,31		100,47		99,98		100,40		100,50		100,35		100,47		99,83		100,01	
		A	B	A	B	A	B	A	B	A	B	A	B	A	B	A	B	A	B	A	B	A	B	A	B	A	B
Qz		–	–	0,04	0,04	0,36	0,37	–	–	–	–	–	–	0,58	0,59	0,46	0,47	0,12	0,12	–	–	–	–	– –	–	1,95	1,97
Or		7,47	7,60	1,44	1,46	1,31	1,33	1,85	1,87	1,31	1,33	0,41	0,42	1,31	1,34	1,06	1,08	1,42	1,44	1,84	1,86	1,06	1,07	1,31	1,34	1,89	1,90
Ab		17,67	17,97	21,72	21,97	20,23	20,54	16,89	17,12	17,36	17,60	5,11	5,20	21,03	21,43	21,80	22,13	24,45	24,82	23,03	23,30	21,13	21,33	25,90	26,37	34,93	35,19
An		29,68	30,19	39,63	40,09	36,27	36,82	39,29	39,82	41,20	41,76	7,07	7,19	36,47	37,17	38,53	39,12	37,71	38,29	37,35	37,79	34,23	34,56	37,96	38,65	51,50	51,89
Di	Wo	8,56	8,71	7,37	7,46	7,49	7,60	9,38	9,51	6,48	6,57	8,22	8,36	8,59	8,75	8,95	9,09	7,76	7,88	6,68	6,76	9,83	9,93	4,55	4,63	0,53	0,53
	En	4,97	5,05	4,29	4,34	4,56	4,63	6,24	6,32	4,20	4,26	5,30	5,39	5,14	5,24	5,47	5,55	4,66	4,73	3,98	4,03	5,91	5,97	2,73	2,78	0,25	0,25
	Fs	3,19	3,25	2,73	2,76	2,51	2,55	2,45	2,48	1,85	1,88	2,36	2,40	2,99	3,05	2,98	3,03	2,70	2,74	2,36	2,39	3,40	3,43	1,59	1,62	0,28	0,28
Hy	En	8,31	8,45	13,22	13,37	16,61	16,86	13,50	13,68	17,53	17,77	45,98	46,77	13,91	14,18	12,34	12,64	12,46	12,65	13,46	13,62	12,96	13,09	15,19	15,47	3,73	3,76
	Fs	5,33	5,42	8,41	8,51	9,16	9,30	5,30	5,37	7,75	7,85	20,46	20,81	8,10	8,25	6,79	6,89	7,22	7,33	7,99	8,08	7,46	7,53	8,83	8,99	4,20	4,23
Ol	Fo	7,70	7,83	–		–		2,63	2,67	0,65	0,66	2,28	2,32							1,30	1,32	1,87	1,89	0,09	0,09		
	Fa	5,44	5,54	–		–		1,14	1,16	0,32	0,32	1,12	1 14							0,84	0,85	1,19	1,20	0,06	0,06		
	Mt	1,39		0,81		1,05		0,88		0,92		1,23		0.58		0,71		1,25		0,90		0,65		1,64		0,57	
	Ilm	0,29		0,32		0,40		0,40		0,38		0,44		1,28		0,80		0,25		0,25		0,29		0,13		0,15	
	Ap	–		0,02		0,05		0,05		0,05		–		0,02		–				0,02		0,02		0,02		0,02	
DI		25,14		23,20		21,90		18,74		18,67		5,52		22,92		23,32		25,99		24,87		22,19		27,21		38,77	
CI		53,47		57,59		57,26		64,09		62,65		52,39		56,80		58,66		56,05		56,25		57,50		54,16		53,39	
MDI			42,63		37,17		36,34		30,18		30,64		32,08		37,35		36,27		38,86		38,58		37,58		39,81		43,82
MCI			42,54		44,02		44,62		49,71		48,82		48,29		43,91		44,66		42,85		43,44		44,31		42,22		39,38

APPENDIX II (Continued). MAIN ZONE

	M209		M202		M189		M188		M186		M182		M179		M177		M174		M172		M169		M166		M165	
SiO_2	51,95		52,38		51,78		50,09		51,63		51,77		52,18		52,36		52,54		51,45		52,91		52,67		52,69	
TiO_2	0,15		0,17		0,14		0,14		0,13		0,11		0,13		0,18		0,22		0,06		0,21		0,14		0,17	
Al_2O_3	17,72		19,42		16,27		17,49		21,08		27,09		24,15		16,65		16,77		25,97		17,12		18,19		16,59	
Fe_2O_3	0,51		0,64		0,32		0,48		0,44		0,53		0,53		0,33		0,32		0,36		0,44		0,27		0,45	
FeO	6,43		4,89		7,03		6,04		4,26		1,44		2,18		5,54		6,06		2,02		5,82		5,56		5,30	
MnO	0,17		0,13		0,18		0,16		0,11		0,05		0,06		0,14		0,15		0,06		0,14		0,13		0,14	
MgO	8,46		6,70		10,00		9,11		6,22		1,35		3,33		9,83		9,75		3,41		9,61		9,45		10,08	
CaO	11,23		12,12		11,39		12,20		12,05		12,12		12,45		11,96		10,72		12,45		10,07		10,90		11,78	
Na_2O	2,71		2,67		2,08		2,04		3,03		3,53		3,05		2,12		2,04		2,64		2,12		2,04		1,92	
K_2O	0,37		0,31		0,18		0,18		0,34		0,46		0,37		0,43		0,46		0,28		0,52		0,31		0,31	
P_2O_5	0,01		0,02		–		0,01		0,01		0,02		0,01		0,02		0,02		0,01		0,04		0,02		0,02	
H_2O	0,65		0,92		0,90		1,57		0,95		1,01		0,94		0,74		1,06		0,81		0,98		0,68		0,75	
CO_2	0,12		0,13		0,10		0,33		0,03		0,08		0,17		0,12		0,30		0,08		0,28		0,07		0,11	
	100,48		100,50		100,37		99,84		100,28		99,56		99,57		100,42		100,41		99,60		100,24		100,43		100,31	
	A	B	A	B	A	B	A	B	A	B	A	B	A	B	A	B	A	B	A	B	A	B	A	B	A	B
Qz	–	–	0,25	0,25	–	–	–	–	–	–	1,33	1,34	2,07	2,09	–	–	0,43	0,43	2,54	2,56	1,20	1,21	0,81	0,82	0,78	0,79
Or	2,20	2,22	1,84	1,86	1,07	1,08	1,08	1,09	2,02	2,04	2,76	2,79	2,22	2,24	2,55	2,57	2,75	2,78	1,67	1,68	3,10	3,14	1,84	1,85	1,84	1,86
Ab	22,98	23,22	22,70	23,00	17,70	17,83	17,61	17,79	25,82	26,05	30,31	30,63	26,37	26,65	18,01	18,17	17,41	17,58	22,62	22,77	18,11	18,32	17,30	17,42	16,33	16,50
An	35,20	35,57	40,31	40,85	34,75	35,01	38,84	39,24	43,23	43,62	57,60	58,21	51,83	52,38	34,80	35,11	35,58	35,92	58,96	59,35	36,02	36,43	39,68	39,97	35,93	36,30
Di Wo	8,60	8,69	8,36	8,47	9,23	9,30	9,56	9,66	7,06	7,12	1,39	1,40	4,52	4,57	10,30	10,39	7,51	7,58	1,48	1,49	5,92	5,99	6,03	6,07	9,48	9,58
Di En	5,26	5,32	5,22	5,29	5,74	5,78	6,07	6,13	4,47	4,51	0,81	0,82	2,97	3,00	6,81	6,87	4,85	4,89	0,98	0,99	3,86	3,91	3,94	3,97	6,38	6,45
Di Fs	2,86	2,89	2,64	2,68	2,94	2,96	2,88	2,91	2,15	2,17	0,51	0,52	1,24	1,25	2,74	2,76	2,15	2,17	0,40	0,40	1,66	1,68	1,67	1,68	2,37	2,39
Hy En	9,64	9,74	11,55	11,70	16,04	16,16	11,59	11,71	5,95	6,00	2,60	2,63	5,45	5,51	15,19	15,32	19,65	19,84	7,62	7,67	20,30	20,53	19,67	19,81	18,85	19,04
Hy Fs	5,23	5,29	5,82	5,90	8,21	8,27	5,50	5,55	2,86	2,89	1,64	1,66	2,28	2,31	6,12	6,17	8,73	8,81	3,07	3,09	8,69	8,79	8,35	8,41	7,02	7,09
Ol Fo	4,36	4,41			2,29	2,30	3,85	3,89	3,63	3,66					1,81	1,83										
Ol Fa	2,62	2,65			1,30	1,31	2,01	2,03	1,92	1,94					0,80	0,81										
Mt	0,74		0,94		0,46		0,72		0,64		0,78		0,78		0,48		0,47		0,53		0,65		0,39		0,65	
Ilm	0,29		0,32		0,27		0,27		0,25		0,22		0,25		0,34		0,42		0,11		0,40		0,27		0,32	
Ap	0,02		0,05		–		0,02		–		0,05		0,02		0,05		0,05		0,02		0,09		0,05		0,05	
DI	25,18		24,79		18,77		18,69		27,84		34,40		30,66		20,56		20,59		26,83		22,41		19,95		18,95	
CI	57,29		59,12		60,12		62,89		60,08		60,55		61,46		61,49		59,18		65,86		58,01		61,54		62,44	
MDI		38,81		36,05		34,06		31,93		37,00		37,40		35,64		32,91		33,68		30,85		34,62		31,66		30,74
MCI		44,21		44,82		46,90		48,86		45,25		43,88		45,10		47,56		46,47		48,47		45,83		47,89		48,53

APPENDIX II (Continued). MAIN ZONE

	M161		M160		M159		M158		M157		M153		1		2		3		4		5		6		7	
SiO_2	51,74		52,61		51,54		51,65		51,63		51,86		52,10		53,40		51,66		51,65		51,60		50,40		49,96	
TiO_2	0,11		0,13		0,10		0,08		0,08		0,17		0,14		0,18		0,14		0,11		0,16		0,17		0,12	
Al_2O_3	19,20		19,34		19,47		22,95		19,30		6,50		18,05		17,51		17,85		23,97		17,49		15,85		24,66	
Fe_2O_3	0,29		0,39		0,39		0,19		0,32		0,83		3,19		1,17		1,37		1,01		0,89		1,87		1,20	
Cr_2O_3											0,85		0,07				0,09				0,02		0,06		0,05	
FeO	5,27		5,11		5,37		3,72		5,32		10,03		4,02		6,12		5,20		3,69		6,95		5,20		3,23	
MnO	0,13		0,13		0,13		0,09		0,13		0,23		0,12		0,20		0,14		0,11		0,20		0,16		0,10	
MgO	10,33		10,00		10,00		6,85		11,47		23,32		8,75		7,10		7,57		4,83		8,23		9,23		6,23	
CaO	9,76		9,68		9,83		11,15		9,02		4,84		11,10		11,60		11,70		10,75		11,15		14,50		11,60	
Na_2O	2,08		2,12		2,22		2,57		1,98		0,64		2,19		3,79		2,15		2,45		2,12		1,60		2,00	
K_2O	0,24		0,22		0,18		0,16		0,10		0,06		0,21		0,21		0,22		0,25		0,16		0,14		0 21	
P_2O_5	0.01		0,01		0,01		–		–		0,01															
H_2)	0,75		0,85		1,12		0,85		0,74		0,96		0,55		0,60		1,21		0,80		0,81		0,73		0,91	
CO_2	0,13		0,10		0,12		0,10		0,09		0,12															
	100,04		100,49		100,48		100,35		100,18		100,41		100,49		101,88		99,30		99,62		99,78		99,91		100,27	
	A	B	A	B	A	B	A	B	A	B	A	B	A	B	A	B	A	B	A	B	A	B	A	B	A	B
Qz	–	–	0,86	0,87	–	–	–	–	–	–	–	–	3,23	3,42	–	–	2,54	2,63	3,57	3,66	0,84	0,86	–	–	1,34	1,38
Or	1,43	1,44	1,30	1,31	1,07	1,08	0,95	0,95	0,60	0,61	0,35	0,36	1,17	1,24	1,15	1,18	1,23	1,28	1,40	1,43	0,89	0,91	0,78	0,81	1,17	1,21
Ab	17,75	17,87	17,97	18,12	18,92	19,07	21,86	21,95	16,86	16,96	5,37	5,53	18,23	19,27	31,43	32,32	18,24	18,92	20,81	21,33	17,96	18,43	13,66	14,21	16,74	17,26
An	42,70	42,98	42,71	43,07	42,96	43,30	50,92	51,14	43,76	44,03	14,84	15,27	38,93	41,19	29,87	30,71	38,92	40,37	53,66	54,99	37,93	38,92	35,70	37,13	52,46	59,25
Di Wo	2,53	2,55	2,24	2,26	2,55	2,57	1,97	1,98	0,53	0,53	3,87	3,98	6,64	7,03	11,19	11,51	8,21	8,51			7,33	7,52	15,22	15,83		
Di En	1,70	1,71	1,52	1,53	1,70	1,71	1,31	1,32	0,36	0,36	2,74	2,82	4,92	5,21	6,69	6,88	5,31	5,51			4,36	4,47	10,41	10,83		
Di Fs	0,63	0,63	0,55	0,56	0,66	0,66	0,51	0,51	0,12	0,12	0,81	0,83	1.07	1,13	3,90	4,01	2,34	2,43			2,57	2,64	3,59	3,73		
Hy En	22,75	22,90	23,45	23,65	20,66	20,82	15,77	15,84	26,31	26,47	47,59	48,97	16,71	17,68	2,59	2,66	13,60	14,11	11,98	12,28	16,08	16,50	12,35	12,84	15,38	15,86
Hy Fs	8,40	8,45	8,56	8,63	7,98	8,04	6,21	6,24	8,86	8,92	14,05	14,46	3,62	3,83	1,52	1,56	6,02	6,24	6,06	6,21	9,50	9,75	4,26	4,43	4,82	4,97
Ol Fo	1,04	1,05			1,90	1,92	0,05	0,05	1,45	1,46	5,71	5,87			5,64	5,80							0,13	0,14		
Ol Fa	0,42	0,42			0,82	0,83	0,02	0,02	0,54	0,54	1,86	1,91			3,28	3,37							0,05	0,05		
Mt	0,42		0,57		0,57		0,28		0,46		1,21		4,61		1,76		2,03		1,43		1,39		2,72		1,86	
Ilm	0,21		0,25		0,19		0,15		0,15		0,32		0,27		0,39		0,27		0,18		0,33		0,36		0,21	
Chr											1,26		0,05				0,07				0,01		0,04		0,04	
Sp.																			0,10						0,07	0,07
Hz																										
Ap	0,02		0,02		0,02						0,02															
H_2O													0,55		0,59		1,22		0,81		0,81		0,73		0,91	
DI	19,18		20,13		19,99		22,81		17,46		5,71		22,63		32,58		22,01		25,78		19,69		14,44		19,25	
CI	62,89		62,01		62,32		64,30		63,96		59,15		61,25		51,76		59,90		66,83		58,56		66,93		63,31	
MDI		29,36		29,98		30,26		30,12		27,26		23,82		29,89		45,97		33,64		32,63		34,92		26,52		24,89
MCI		49,81		49,07		49,44		48,99		51,41		55,15		49,14		39,58		46,51		47,15		45,60		51,53		52,69

APPENDIX II (Continued). MAIN ZONE

	8		9		10		11		12		13		14		15		16		17		18		19		20	
SiO_2	49,96		49,51		50,20		51,11		52,70		48,85		51,48		50,72		52,25		46,60		50,50		51,50		52,00	
TiO_2	0,17		0,22		0,13		0,16		0,15		0,10		0,26		0,44		0,20		0,06		0,25		0,20		0,20	
Al_2O_3	18,49		18,83		20,05		19,75		21,05		26,45		18,04		16,40		5,35		30,17		6,00		5,40		4,76	
Fe_2O_3	1,86		1,92		1,84		2,14		0,50		0,45		1,82		1,55		1,10		1,12		4,15		2,40		1,59	
Cr_2O_3	0,06		0,04		0,03														0,03		0,55				0,51	
FeO	4,65		4,30		3,80		4,39		5,80		2,15		4,96		6,66		14,25		0,86		9,40		11,00		10,38	
MnO	0,14		0,14		0,13		0,15		–		–		0,04		0,02		0,30		0,04		0,15		0,15		0,24	
MgO	8,95		9,57		7,90		7,05		4,20		4,25		7,40		8,55		18,40		3,81		21,90		21,95		25,20	
CaO	12,83		12,47		12,64		12,64		12,60		14,05		13,35		13,30		6,25		14,60		4,40		5,40		3,03	
Na_2O	1,72		2,00		1,80		2,02		2,10		2,10		1,90		2,20		0,55		2,05		1,25		0,90		0,31	
K_2O	0,17		0,25		0,17		0,20		0,30		–		0,26		0,20		0,20		0,15		–		–		0,10	
P_2O_5							0,04		0,20		0,05		0,03		0,06						0,10		0,10			
H_2O	0,89		0,81		0,84		0,65		0,05		0,25		0,30		0,40		1,05		0,32		0,80		0,85		1,17	
	99,89		100,06		99,53		100,30		99,65		98,70		99,84		100,50		99,90		99,81		99,45		99,85		99,49	
	A	B	A	B	A	B	A	B	A	B	A	B	A	B	A	B	A	B	A	B	A	B	A	B	A	B
Qz	0,16	0,17	–	–	1,40	1,46	2,35	2,45	5,03	5,10	0,24	0,24	2,10	2,18	–	–	–	–	–	–	– –	–	–	– –	–	–
Or	0,95	0,99	1,39	1,45	0,96	1,00	1,11	1,16	1,68	1,70	–	–	1,67	1,73	1,11	1,15	1,11	1,15	0,83	0,85	–	–	– –	–	0,58	0,61
Ab	14,42	15,02	16,79	17,52	15,31	15,91	16,97	17,69	17,90	18,16	18,06	18,29	16,28	16,88	18,29	18,91	4,72	4,87	17,35	17,72	10,57	11,53	7,88	8,31	2,70	2,83
An	42,36	44,12	41,68	43,49	46,34	48,16	44,20	46,08	47,34	48,02	63,54	64,36	39,57	41,02	34,37	35,54	11,40	11,77	72,52	74,08	10,94	11,94	10,59	11,16	11,37	11,91
Di Wo	8,94	9,31	8,43	8,80	6,96	7,23	7 54	7,86	6,13	6,22	2,70	2,74	11,16	11,57	13,18	13,63	8,25	8,52			4,22	4,60	6,40	6,75	1,54	1,61
Di En	6,25	6,51	6,09	6,35	4,96	5,16	5,12	5,34	3,04	3,08	1,88	1,90	7,42	7,69	8,38	8,67	5,00	5,16			3,07	3,35	4,40	4,64	1,09	1,14
Di Fs	1,92	2,00	1,56	1,63	1,38	1,47	1,83	1,91	2,94	2,98	0,61	0,62	2,91	3,03	3,95	4,09	2,77	2,87			0,75	0,82	1,47	1,55	0,30	0,31
Hy En	16,03	16,70	11,21	11,69	14,78	15,36	12,37	12,90	7,40	7,51	8,83	8,94	11,12	11,53	8,38	8,67	41,03	42,36	0,04	0,04	45,65	49,80	42,91	45,23	58,49	61,25
Hy Fs	4,97	5,18	2,88	3,00	4,13	4,29	4,42	4,61	7,13	7,23	2,87	2,91	4,23	4,38	4,21	4,35	22,58	23,31			11,06	12,07	14,25	15,02	16,24	17,01
Ol Fo			4,53	4,73											3,21	3,32			6,51	6,65	4,26	4,65	5,10	5,38	2,47	2,59
Ol Fa			1,28	1,34											1,62	1,67			0,48	0,49	1,14	1,24	1,86	1,96	0,71	0,74
Mt	2,70		2,83		2,66		3,11		0,70		0,70		2,56		2,08		1,62		1,68		6,08		3,49		2,32	
Il	0,36		0,49		0,24		0,33		0,32		0,15		0,61		0,76		0,46		0,09		0,53		0,46		0,46	
Ap									0,34		0,17										0,34		0,34			
Ch	0,04		0,03		0,03														0,01		0,58		–		0,55	
Sp																			0,17	0,17			–			
H_2O	0,89		0,81		0,85		0,65		0,05		0,25		0,37		0,46		1,05		0,32		0,81		0,85		1,18	
DI	15,53		18,18		17,67		20,43		24,61		18,30		20,05		19,40		5,83		18,18		10,57		7,88		3,28	
CI	67,07		67,24		67,40		63,91		59,09		73,79		63,36		61,52		50,94		79,38		53,81		55,25		57,18	
MDI		25,12		26,33		25,35		29,50		37,80		22,61		30,85		33,77		34,71		19,05		26,38		28,21		21,77
MCI		52,45		53,00		52,32		49,41		43,57		54,25		48,46		47,41		45,74		58,60		52,98		51,92		55,59

APPENDIX II (Continued). CRITICAL ZONE BASAL ZONE

	1	2	3	4	5	1	2	3	4	5	6	7	8
SiO_2	49,90	71,70	52,00	50,80	48,90	41,50	53,60	54,50	53,20	55,40	55,40	41,40	45,30
TiO_2	0,12	0,20	0,18	0,10	–	0,08	0,12	0,16	0,21	0,10	0,10	0,07	0,17
Al_2O_3	28,20	13,19	4,82	17,01	30,00	1,16	5,64	1,77	5,05	1,60	2,35	3,16	3,76
Fe_2O_3	1,46	1,48	1,06	2,01	0,50	2,19	0,46	1,01	1,17	–	–	0,60	4,51
Cr_2O_3	0,74	0,24	0,27	0,10	–	1,00	0,23	0,43	0,26	0,65	0,60	0,95	0,25
FeO	0,41	7,00	9,35	5,60	1,30	6,13	8,78	8,90	8,70	9,35	9,65	6,63	6,27
MnO	0,04	0,20	0,22	0,15	–	0,13	0,22	0,22	0,19	0,15	0,15	0,13	0,15
MgO	3,57	17,30	27,25	10,97	0,55	45,50	27,20	30,60	26,22	32,45	30,85	42,50	30,60
CaO	12,98	6,76	3,78	11,10	16,90	0,53	2,26	1,52	3,38	0,45	0,65	0,88	2,98
Na_2O	2,19	1,20	0,27	1,96	1,95	0,22	0,42	0,10	0,61	–	–	0,22	0,62
K_2O	0,09	0,14	0,04	0,11	0,15	0,01	0,08	0,04	0,30	–	–	0,01	0,29
P_2O_5										0,20	0,30		
H_2O	0,18	1,04	1,18	0,53	0,20	1,67	1,42	1,22	1,13	0,15	0,10	2,86	4,86
	99,98	100,45	100,42	100,51	100,45	100,12	100,43	100,47	100,42	100,50	100,15	99,41	99,76

		A	B	A	B	A	B	A	B	A	B	A	B	A	B	A	B	A	B	A	B	A	B	A	B
	Qu	4,45	4,60	–	–	–	–	–	–	1,52	1,53	–	–	–	–	–	–	–	–	–	–	1,96	1,99	–	–	–	–
	Or	0,50	0,52	0,78	0,81	0,22	0,23	0,61	0,63	0,83	0,84	0,05	0,05	0,44	0,45	0,22	0,23	1,67	1,73	–	–	–	–	0,05	0,05	1,70	1,84
	Ab	18,28	18,89	9,95	10,35	2,31	2,39	16,51	17,16	16,46	16,61	1,79	1,91	3,30	3,44	1,05	1,09	5,28	5,48	–	–	–	–	1,81	1,90	5,66	6,12
	An	64,33	66,46	30,14	31,34	11,78	12,19	37,24	38,70	72,34	73,00	2,29	2,42	11,08	11,47	4,25	4,40	10,10	10,48	1,39	1,41	1,54	1,56	4,41	4,64	6,92	7,49
Di	Wo	–	–	1,36	1,41	2,92	3,02	7,36	7,65	3,30	3,33	0,17	0,18	–	–	1,40	1,45	2,80	2,91	–	–	–	–	–	– –	3,60	3,89
	En	–	–	0,97	1,01	2,14	2,21	5,11	5,31	1,35	1,36	0,14	0,15	–	–	1,05	1,08	2,07	2,15	–	–	–	–	–	–	2,89	3,13
	Fs	–	–	0,26	0,27	0,50	0,52	1,61	1,67	1,97	1,99	0,01	0,01	–	–	0,21	0,22	0,47	0,49	–	–	–	– –	–	–	0,27	0,30
Hy	En	7,87	8,13	41,01	42,65	53,40	55,27	18,76	19,49	–	–	10,42	11,09	63,80	65,48	70,46	72,93	54,11	56,16	78,17	79,18	75,25	76,42	13,94	14,66	34,72	37,59
	Fs	–	–	10,88	11,31	12,73	13,18	5,97	6,20	–	–	0,80	0,85	14,85	15,24	14,22	14,72	12,21	12,67	16,25	16,46	17,08	17,34	1,45	1,52	3,45	3,73
Ol	Fo	–	–	0,63	0,66	8,40	8,69	2,27	2,36	–	–	72,19	76,82	2,10	2,16	3,06	3,17	6,11	6,34	1,06	1,07	–	–	64,39	67,69	29,94	32,36
	Fa	–	–	0,18	0,19	2,22	2,30	0,80	0,83	–	–	6,13	6,52	0,53	0,54	0,69	0,71	1,53	1,59	0,25	0,25	–	–	7,39	7,77	3,28	3,55
	Mt	0,05		2,09		1,53		3,01		0,70		3,25		0,70		1,42		1,78		–		–		0,94		6,91	
	Il	0,21		0,46		0,40		0,15				0,12		0,21		0,33		0,47		0,15		0,15		0,10		0,38	
	Hm	2,04	–	–																							
	Ch	0,73	–	0,25		0,27		0,07		–		0,98		0,24		0,42		0,27		0,63		0,60		0,93		0,28	
	Sp	1,36	1,40											0,97	1,00					1,35	1,37	2,19	2,22	1,54	1,62		
	Hz													0,21	0,22					0,26	0,26	0,46	0,47	0,14	0,15		
	Ap																			0,34		0,67					
	H_2O	0,18		1,04		1,18		0,53		0,20		1,68		1,42		1,22		1,13		0,15		0,10		2,90			
DI		23,23		10,73		2,53		17,12		18,81		1,84		3,74		1,27		6,95		0		1,96		1,86		7,36	
CI		71,21		61,60		62,22		63,68		75,25		82,06		58,81		58,95		58,60		58,58		56,47		79,10		65,57	
MDI			24,01		23,17		19,08		28,41		22,72		9,35		19,67		17,16		22,93		16,71		19,33		11,24		15,80
MCI			53,07		54,04		59,31		51,17		53,21		86,51		56,79		59,00		56,30		58,51		56,21		82,35		69,54

APPENDIX II (Continued). CHILL PHASE AND AVERAGE OF SILLS

		1		2		3		4		5	
SiO_2		50,55		51,45		50,30		52,41		55,06	
TiO_2		0,66		0,34		2,13		1,03		0,67	
Al_2O_3		15,23		18,67		15,02		13,07		14,63	
Fe_2O_3		1,04		0,28		2,63		2,55		1,84	
Cr_2O_3		0,01		–							
FeO		10,07		9,04		8,64		8,43		6,75	
MnO		0,23		0,47		0,17		0,16		0,18	
MgO		8,30		6,84		7,43		8,28		9,14	
CaO		11,30		10,95		10,49		9,00		7,67	
Na_2O		2,24		1,58		2,02		2,09		1,96	
K_2O		0,19		0,14		0,28		0,92		0,79	
P_2O_5		0,12		0,09		0,16		0,12		0,22	
H_2O		0,24		0,37		0,33		1,66		0,79	
		A	B	A	B	A	B	A	B	A	B
	Qz	–	–	2,93	2,98	3,92	4,29	4,29	4,65	8,40	8,86
	Or	1,12	1,16	0,83	0,84	1,58	1,73	5,69	6,17	4,41	4,65
	Ab	18,91	19,50	13,34	13,56	17,08	18,68	17,76	19,25	16,64	17,55
	An	30,90	31,86	43,35	44,06	31,32	34,24	23,42	25,39	29,01	30,59
Di	Wo	10,14	10,73	4,29	4,36	8,38	9,16	8,50	9,21	3,42	3,61
	En	5,40	5,57	2,13	2,17	5,04	5,51	5,08	5,51	2,20	2,32
	Fs	4,42	4,56	2,08	2,11	2,88	3,15	2,97	3,22	0,99	1,04
Hy	En	11,28	11,63	14,88	15,12	13,53	14,79	15,53	16,83	20,59	21,71
	Fs	9,25	9,54	14,56	14,80	7,73	8,45	9,01	9,77	9,17	9,67
Ol	Fo	2,77	2,86	–	–	–	–	–	–	–	–
	Fa	2,51	2,59	–	–	–	–	–	–	—	–
	Mt	1,51		0,41		3,80		3,72		2,65	
	Il	1,25		0,65		4,07		2,03		1,33	
	Ch	0,02		–		–					
	Ap	0,28		0,21		0,34		0,34		0,40	
	H_2O	0,24		0,34		0,33		1,66		0,79	
DI		20,03		17,10		22,58		27,74		29,45	
CI		53,23		58,37		51,67		45,26		48,19	
MDI			41,36		36,15		39,08		45,90		42,69
MCI			41,76		44,76		42,70		37,92		40,16

APPENDIX II (continued) Locality of samples and references

UPPER ZONE

Sample No.	Height in m above M.R.	Rock Type
M55	4620	Quartz diorite
M282	4510	Olivine diorite
M281	4420	Olivine magnetite diorite
M280	4330	Olivine diorite
M279	4220	Diorite
M278	4180	Olivine diorite
M51	4130	Magnetite diorite
M276	4115	Anorthosite
M274	4020	Olivine diorite
M272	3870	Hypersthene gabbro
M63	3805	Anorthosite
M269	3740	Magnetite gabbro
M268	3690	Hypersthene gabbro
M465	3670	Anorthosite
M48	3630	Troctolite
M47	3580	Anorthosite
M46	3500	Troctolite
M255	3365	Hyperite
M253	3240	Magnetite gabbro
M45	3205	Pyroxenite (feldspathic)
M44	3180	Magnetite gabbro
M43	3140	Norite
M3	3078	Anorthosite
M37	3070	Magnetite gabbro
M40	3050	Troctolite
M288	3010	Olivine gabbro
M291	2915	Magnetite gabbro
M308	2860	Mangetite anorthosite

APPENDIX II (continued)

All the above samples were collected by Molyneux (1970, Plate III) along a traverse at Magnet Heights and analysed at the Dept. of Geology, University of Glasgow.

1. Troctolite - 1 mile from Magnet Heights on road to Jane Furse (Sisal horizon) C. J. Liebenberg, 1961, LIEB-26.
2. Diorite - First outcrops on old Tauteshoogte road. C. J. Liebenberg, 1961, LIEB-7(a).
3. Diorite - 20 ft. below leptite on old Tauteshoogte road. C. J. Liebenberg, 1961, LIEB-9.
4. Fayalite diorite - Duikerskrans. J. C. Boshoff, 1942, Table 13, No. 85.
5. Syenodiorite - Paardekloof. J. C. Boshoff, 1942, Table 13, No. 10.
6. Olivine diorite - Duikerskrans. J. C. Boshoff, 1942, Table 13, No. 72.
7. Diorite - Duikerskrans. J. C. Boshoff, 1942, Table 13, No. 74.
8. Magnetite bearing anorthositic norite - Luipershoek. B. V. Lombaard, 1934, Table 5, No. 423.
9. Anorthosite, below Main Magnetitite Seam - Mamagalies Kraal. R. A. Daly, 1928, Table 10, No. 6.
10. Anorthositic gabbro - 1 mile from bridge on road to Magnet Heights. C. J. Liebenberg, 1961, LIEB-29.

APPENDIX II (continued)

MAIN ZONE

Sample No.	Height in m above M.R.	Rock type
M306	2830	Hyperite
M305	2740	Hyperite
M303	2700	Hypersthene gabbro
M299	2500	Hypersthene gabbro
M296	2340	Hyperite
M294	2270	Pyroxenite
M226	2130	Hypersthene gabbro
M224	2050	Hypersthene gabbro
M221	1970	Hypersthene gabbro
M219	1920	Hyperite
M216	1820	Hypersthene gabbro
M213	1770	Norite
M94	1695	Anorthosite
M209	1670	Hypersthene gabbro
M202	1520	Hypersthene gabbro
M189	1460	Hyperite
M188	1330	Gabbro
M186	1230	Hyperite
M182	1060	Anorthosite
M179	970	Anorthositic gabbro
M177	930	Hyperite
M174	780	Hypersthene gabbro
M172	660	Anorthosite
M169	560	Hypersthene gabbro
M166	505	Hypersthene gabbro
M165	400	Hypersthene gabbro
M161	305	Hyperite
M160	250	Hyperite
M159	170	Hyperite
M158	140	Hyperite
M157	110	Norite
M153	0	Pyroxenite - Merensky Reef

APPENDIX II (continued)

All the above samples were collected by Molyneux (1970, Plate III) along a traverse across the Leolo Mountains, and analysed at the Dept. of Geology, University of Glasgow.

1. Norite - Maandagshoek Missionhospital.
   C. J. Liebenberg, 1961, LIEB-52.
2. Gabbro - 3 miles from the Steelpoort bridge along the road to Dwars River.
   C. J. Liebenberg, 1961, LIEB-30.

3-11. Norite and gabbro - from unspecified localities in the Leolo Mountains.
   C. J. Liebenberg, 1961, W1-W9.

12. Norite - Bon Accord. A. L. Hall, 1932, Table 28, No. 1.
13. Spotted anorthosite - Forest Hill, hanging wall of Merensky Reef.
   P. A. Wagner, 1929, p. 125.
14. Norite - Uysedoorns. B. V. Lombaard, 1934, Table 5, No. 409.
15. Norite - 0,5 mile east of Roossenekal.
   B. V. Lombaard, 1934, Table 5, No. 410.
16. Pyroxenite - Chieftains Plain. B. V. Lombaard, 1934, Table 5, No. 480.
17. Spotted anorthosite - above Merensky Reef, Maandagshoek.
   C. J. Liebenberg, 1961, LIEB-51.
18. Pyroxenite - Merensky Reef, Dwars River.
   P. A. Wagner, 1929, p. 118.
19. Pyroxenite - Merensky Reef, Winnaarshoek.
   P. A. Wagner, 1929, p. 118.
20. Pyroxenite - Merensky Reef, Forest Hill.
   C. J. Liebenberg, 1961, LIEB-59.

CRITICAL ZONE

1. Anorthosite - Dwars River. C. J. Liebenberg, 1961, LIEB-31.
2. Norite - Mooihoek. C. J. Liebenberg, 1961, LIEB-45.
3. Pyroxenite - Mooihoek. C. J. Liebenberg, 1961, LIEB-46.
4. Norite - East of Mooihoek pipe. C. J. Liebenberg, 1961, LIEB-50.
5. Anorthosite - Driekop, north of Mooihoek.
   A. L. Hall, 1932, Table 38, No. 1.

APPENDIX II (continued)

BASAL ZONE

1. Harzburgite - Aapiesdoringdraai, at Spekboom River bridge.
   C. J. Liebenberg, 1961, LIEB-32.
2. Pyroxenite - 0,5 mile east of Steelpoort on road to Burgersfort.
   C. J. Liebenberg, 1961, LIEB-34.
3. Pyroxenite - Jagdlust on main road.
   C. J. Liebenberg, 1961, LIEB-61.
4. Pyroxenite - above Hendriksplaats norite, Hendriksplaats.
   C. J. Liebenberg, 1961, LIEB-36.
5. Bronzitite - Jagdlust, south of Olifants River.
   A. L. Hall, 1932, Table 32, No. II.
6. Bronzitite - Bronzitite, southeast of Malipsdrift, north of the Olifants River. A. L. Hall, 1932, Table 32, No. I.
7. Harzburgite - Borehole on Aapiesdoorndraai.
   C. J. Liebenberg, 1961, LIEB-32(a).
8. Picrite - Aapiesdoorndraai. C. J. Liebenberg, 1961, LIEB-32.

MARGINAL GROUP

1. Hypersthene gabbro - 4,5 miles east of Klip River along road to Lydenburg. (SA 1087). L. R. Wager and G. M. Brown, 1968, Table 26, No. 1, p. 355.
2. Hypersthene gabbro - south of Sjambock Railway Station, northwest of Pretoria. R. A. Daly, 1928, Table 6, No. 6, p. 727.
3. Gabbro - Chilled floor phase, Zilikaatsnek.
   H. J. Nel, 1940, Table 5(a), p. 53.
4. Average of 5 Lydenburg type mafic sills.
   J. Willemse, 1959, Table 4 and Fig. 5, p. xlv.
5. Average of 9 Maruleng type mafic sills.
   J. Willemse, 1959, Table 4 and Fig. 5, p. xlv.

FOLDER I

THE GEOLOGY OF THE BUSHVELD COMPLEX IN THE VICINITY OF TAUTESHOOGTE AND ROOSSENEKAL.

SCALE 1:50 000

0 1 2 3 4 5 6 7 8 9 10 km

LEGEND

- Alluvium, soil cover, cultivated land, etc.
- Talus
- Dolerite — POST KARROO
- Bushveld Granite.
- Granophyre and associated granite, Granodiorite and Melanogranophyre — Post Rooiberg Felsite pre Bushveld Granite
- Diorite (Fayalite diorite)
- Olivine bearing rocks.
- Magnetite gabbro, Mottled anorthosite, Magnetitite Seam (numbers after Molyneux 1964) — UPPER ZONE
- Main Magnetitite Seam.
- Magnetite gabbro. — MAIN ZONE
- Pyroxenite Marker, Magnetite gabbro, Gabbro and norite, Mottled anorthosite.
- Felsite +/- agglomerate, amygdaloidal, Quartzite, Leptite (metamorphosed felsite) — ROOIBERG FELSITE
- Andesitic lava — DULLSTROOM VOLCANICS(?)

BUSHVELD IGNEOUS COMPLEX

- Quartzite inclusions.
- Magnetitite rubble.
- Magnetitite plugs.
- Pegmatoid
- A,B,C,D. Inclusions of original carbonate rocks.
- F Faults
- 10° Dip of strata
- Prospecting pits: V Vermiculite, Au Gold
- DDH1, DDH2, PB1 Bore-holes

- Railways
- Main Roads
- Secondary Roads.
- Farm Roads
- Homestead
- Rivers and Streams
- Marshes
- Trigonometrical beacons.
- •214 Position and number of specimen referred to in the text

29°45' 25°15' 30°00'

PAARDEKOP 147 · NEBO · DWARS-IN-DE-WEG 137 JS · GROOTHOEK 139 JS · TIGERHOEK 140 JS · GOEDGEDACHT 152 JS · HOLNEK 153 JS · KEEROM 151 JS · STEYNSDRIFT 145 JS · BURGERSFORT · Mapochs Dam · ZWARTKOP 142 JS · Swartkop 1458 · PAARDENFONTEIN 159 JS · VLAKLAAGTE 154 JS · LUIPERSHOEK 149 JS · BANKFONTEIN 158 JS · ZAAIPLAATS 157 JS · ELANDSLAAGTE 155 JS · ONVERWACHT 148 JS · BANKSLOOT 147 JS · VLAKLAAGTE 146 JS · ROOSSENEKAL · MAPOCHS MINE · MAPOCHSGRONDE 500 JS · Galgkop · Hoofstadkop · WALHALLA 1 JT · HERMANSDAL 3 JT · HEBRON 5 JT · JOHANNESBURG 15 JT · CHIEFTAINS PLAIN 46 JT · PIETERSBURG 44 JT · UYSEDOORNS 47 JT · DRAAIKRAAL 48 JT · SHEEPRUN 50 JT · KLIPRIVIER 73 JT · KLIPBANKSPRUIT 76 JT · HAAKDOORNDRAAI 169 JS · BUFFELSVALLEI 170 JS · DOORNPOORT 171 JS · UITKYK 172 JS · DUIKERSKRANS 173 JS · THE WEDGE 175 JS · PAARDEKLOOF 176 JS · ROOIKRAAL 188 JS · DRIEVOET 182 JS · KAFFERSKRAAL 181 JS · GROOTKOP 185 JS · BLAAUWBANK 179 JS · TAUTESHOOGTE

Rooikraal dam · Vlugkraal Dam · Blood River · Steelpoort River · Klip River · Groblersdal · Lydenburg · Stoffberg

F — TAUTESHOOGTE — G
1500m, 1000m; Blood River; Talus; Steelpoort River

D — E
1500m, 1000m; Blood River

A — SEKHUKHUNE PLATEAU — B — C
1500m, 1000m, 500m; Talus; Steelpoort River; 21 17 13 12 11 7 6 M L1

FOLDER II. COLUMNAR SECTION OF THE MAIN AND UPPER ZONES IN THE ROOSSENEKAL AREA

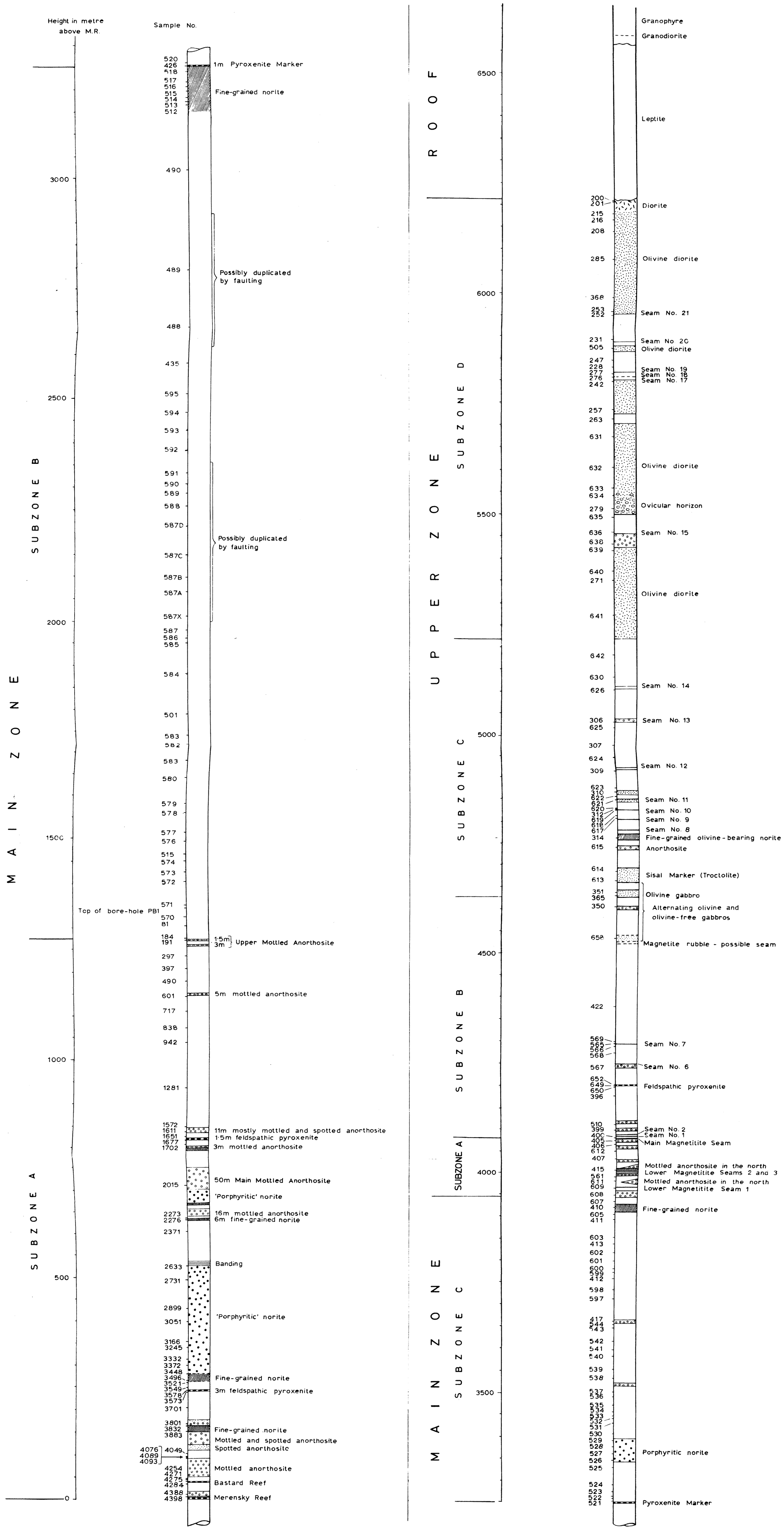

FOLLER III. COMPOSITIONAL VARIATION OF PLAGIOCLASE (MOL. % An), ORTHOPYROXENE (MOL. % Fs) AND OLIVINE (MOL. % Fa) IN ROCKS OF THE MAIN AND UPPER ZONE

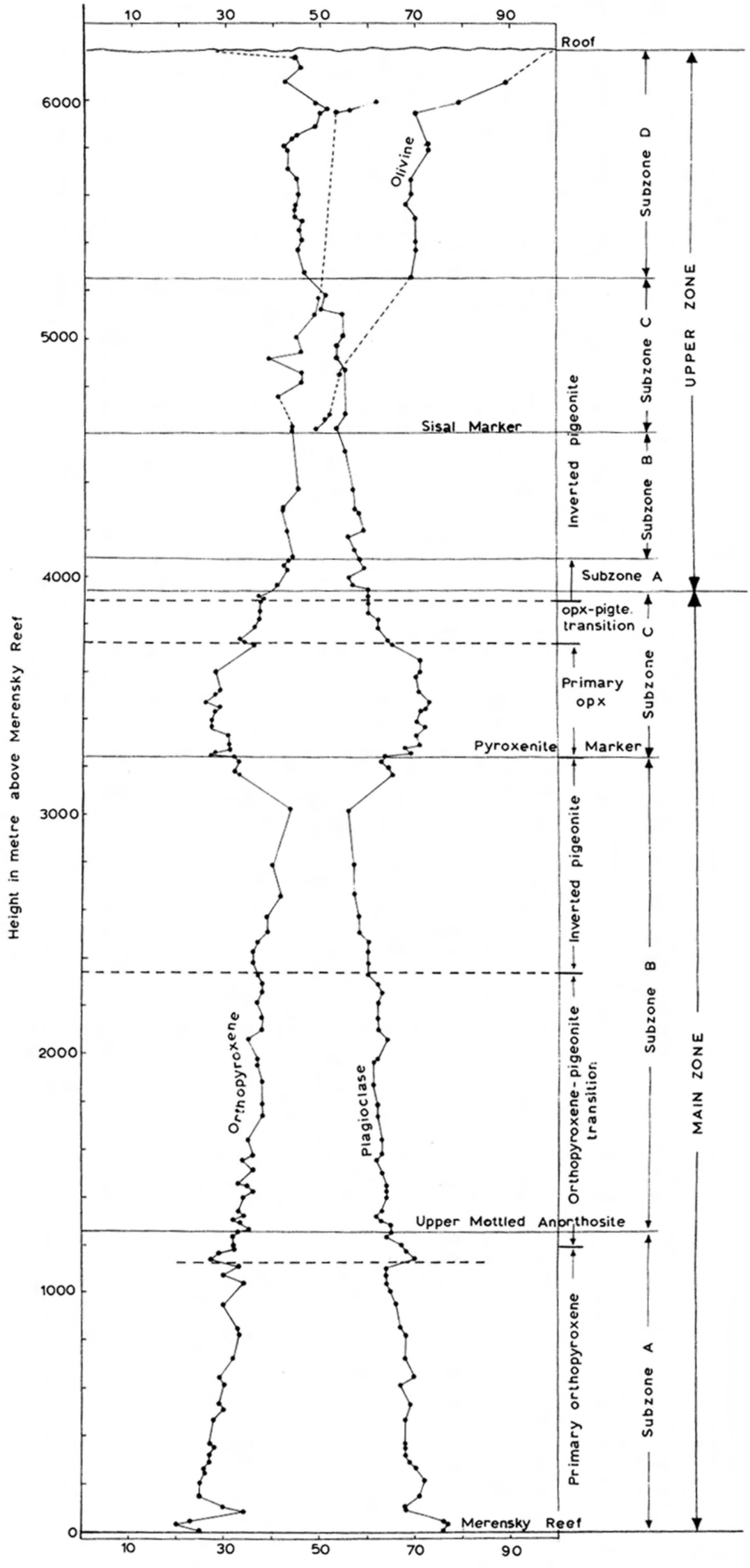

FOLDER IV. MODAL VARIATION OF MINERALS IN THE MAIN AND UPPER ZONES OF THE BUSHVELD COMPLEX IN THE VICINITY OF ROOSSENEKAL

Typed and litographed by:

Hennie's Secretarial Services (Pty.) Ltd.,
120 Vigilans Building,
Pretorius Street,
PRETORIA.